THE DIFFUSION AND SORPTION OF WATER IN HIGH POLYMERS

by

DAVID MACHIN

A thesis presented for the

Diploma of Imperial College

Physical Chemistry Department,

August 1968

ABSTRACT

The sorption, permeation and steady and transient state diffusion of water have been measured (the latter from rates of sorption) in polymethylmethacrylate, polyethylmethacrylate, poly-n-propylmethacrylate, poly-n-butylmethacrylate, poly-n-propylacrylate, in polydimethylsiloxane, polydimethyl-methylphenylsiloxane, poly-3,3,3, trifluoropropylmethylsiloxane and in some salt (NaCl) - and silica - filled samples of polydimethylsiloxane. Except for the silica-filled samples, satisfactory agreement is obtained between steady and transient state results.

At high relative humidities the diffusion coefficient (D) and the activation energy for diffusion of water in each polymer are found to decrease and increase respectively with increasing sorbed water concentration (c). This behaviour is interpreted in terms of sorbed water molecules undergoing rapid association such that an increasing fraction becomes relatively immobile. At low relative humidities D is found to decrease with c for the polymethacrylates and poly-n-propylacrylate, to increase with c for the silica-filled samples of polydimethylsiloxane and to be constant for the unfilled and salt-filled polysiloxanes.

The increase in D with c is interpreted in terms of immobilisation of water on surface sites of the silica filler. The cases where D is initially constant are less clear and possible reasons for this behaviour are discussed.

Shapes of equilibrium sorption isotherms and D vs. c curves are compared at several temperatures with those expected on the basis of a model which treats the polymer as an inert medium and considers association of water to take place by a polycondensation process involving hydrogen bond formation. The model predicts the qualitative features of the results although quantitative agreement is not found.

Theoretical calculations have been made:

a) concerning the determination of D-c relationships from sorption rate measurements.

b) indicating the extra precision required of 'integral' measurements in systems where D decreases with c.

c) illustrating the extent to which measurements can be complicated by water sorption on glass walls of vacuum apparatus.

ACKNOWLEDGEMENTS

I am greatly indebted to Dr. J. A. Barrie for his interest and guidance throughout this research.

I am very grateful to the Ministry of Technology (formerly Aviation) for a bursary and in particular to Dr. B. Hollingsworth, E.R.D.E., Waltham Abbey for his interest and help in the work.

I would like to thank Imperial Chemical Industries Ltd., Midland Silicones Ltd., Dow-Corning Corp. (U.S.A) and Rohm and Haas Co. (U.S.A) for gifts of material samples, and the technical staff of this Department for help with the construction of some parts of the apparatus.

I would like to acknowledge particularly useful discussions with Professor M. Gordon, Chemistry Department, University of Essex, and with Mr. A. G. Thomas and Mr. E. Southern, Natural Rubber Producers Research Association.

Finally, I would like to thank the University of London Institute of Computer Science for the use of their facilities.

CONTENTS

CHAPTER I

INTRODUCTION AND LITERATURE SURVEY

The permeation of a gas or vapour through a polymer membrane can be regarded as a three stage process :

a) Penetrant molecules in the gas phase are sorbed in the ingoing face of the membrane.

b) The sorbed molecules undergo a series of random molecular displacements or diffuse. When a concentration gradient exists across the membrane this process leads to a net flux or transport of penetrant through the membrane.

c) Penetrant molecules in the outgoing face of the membrane are desorbed into the gas phase.

It is assumed that step (b), the diffusion process, is rate controlling. The rate of sorption of a penetrant by a membrane is governed by steps (a) and (b) only.

Transport studies of this kind are of interest as they yield valuable information on the mechanism of the diffusion process and its dependence on variables such as temperature, pressure and concentration of penetrant in the membrane. In addition the effect of factors such as the chemical structure of both the polymer and penetrant, the physical state and

morphology of the polymer has been studied in detail. With this information the penetrant molecule can in turn be used as a probe to investigate the microstructure of the polymer. Much work has been done in this field and several reviews are now available[1-5].

There is also strong interest of a practical nature in this subject. As an example many protective coatings and wrappings are polymer films and it is desirable to know which characteristics of a polymer confer on it relatively low gas or vapour permeabilities, in particular water vapour permeabilities, in addition to other attributes such as physical strength[6,7]. On the other hand it may be desirable to have a polymer exhibiting a high permeability to water, as for example polymer membranes used in the desalination of sea or brackish waters.

The interpretation and analysis of diffusion is generally carried out in terms of Fick's laws[8] which are expressed mathematically in chapter 2. At this stage a diffusion coefficient D may be defined, in the absence of other transport processes, as the amount of material passing across a plane of unit area in unit time under a unit concentration gradient. Units are usually adjusted to express

D in cm^2 sec^{-1}. A solubility coefficient σ is defined as the concentration c of penetrant sorbed per unit volume of dry polymer at unit gas phase pressure and is often expressed in cc. s.t.p. cm^{-3} $(cmHg)^{-1}$. The permeability coefficient P is defined as the amount of material passing through a membrane of unit area and thickness in unit time and with a unit pressure differential applied across the membrane. P is often expressed in cc. s.t.p. cm. $sec.^{-1}$ $cm.^{-2}$ $(cmHg)^{-1}$. When P, D and σ are independent of c or in the limit $c \longrightarrow 0$, then

$$P = D \cdot \sigma \qquad \ldots.(1\text{-}1)$$

when the quantities are expressed in the units given.

For permanent gases in polymers at a given temperature both D and σ are always constant at moderate pressures[9]. This result has generally been explained in terms of the low solubilities of these gases in polymers and the negligible gas-polymer or gas-gas specific interactions.

For organic vapours in polymers D generally increases with increasing c and very often σ also increases with increasing c[10]. This behaviour has been interpreted in terms of plasticisation or loosening of the polymer matrix by the sorbed penetrant since organic vapours are much more soluble than permanent gases in polymers and polymer-penetrant

interactions are generally more important.

On the other hand for water in polymers the concentration dependence of D and σ is more varied depending on the type of polymer used[11]. In particular, for some of the more hydrophobic polymers D decreases with increasing c. This has been explained on the basis of clustering or association of water molecules inside the polymer in such a way that the larger, associated species have relatively small mobilities and are formed in proportionally larger amounts with increasing overall sorbed concentration c of water.

The principal purpose of the present investigation was to examine, in more detail than hitherto, the aspect of water clustering in polymers and the effect of changes in the chemical and physical structure of the polymer on water clustering. Particular effort has therefore been made to determine the concentration dependence of D for water in a number of polymers and to examine the results in terms of proposed specific models or theories of water association in polymers.

1.1 Factors affecting D, σ and P.

Much of the previous work has already been reviewed[1-5] and only brief mention of the effect of each variable on D, σ

and P is made in this section. So many factors and types of experimental conditions are significant that reproducible results on different samples of the same polymer are sometimes difficult to achieve. The method of sample preparation can be very important and this point has been discussed in some detail by Crank and Park[12].

1.1.1 Temperature Dependence

Penetrant diffusion in a polymer is essentially an activated process and the temperature dependence of D can be expressed by an Arrhenius-type equation

$$D = D_o \exp(-E_D/RT) \qquad .....(1\text{-}2)$$

where E_D is the activation energy for diffusion and D_o a pre-exponential factor only weakly dependent on T. For relatively small temperature ranges E_D is constant for many polymer-penetrant systems.

The solubility coefficient varies in a similar manner with temperature, i.e.

$$\sigma = \sigma_o \exp(-\Delta\bar{H}_s/RT) \qquad .....(1\text{-}3)$$

where $\Delta\bar{H}_s$ is the heat of sorption which for condensable vapours is equivalent to the sum of the heat of condensation and heat of dilution. $\Delta\bar{H}_s$ is generally small and positive for permanent

gases but negative for vapours when the heat of condensation is often the predominant quantity in determining the sign of $\Delta\bar{H}_s$.

Combination of equations (1-1), (1-2) and (1-3) yields

$$P = P_o \exp (E_P/RT) \qquad .....(1-4)$$

where E_P, the temperature coefficient of the permeability, is given by $E_P = \Delta\bar{H}_s + E_D$ and $P_o = D_o \sigma_o$. Thus P may increase or decrease with temperature depending on the relative values of $\Delta\bar{H}_s$ and E_D. Generally P increases with increasing temperature but for some silicone rubbers E_D values are especially low and decreases in P with increasing temperature have been observed[13].

1.1.2 The Nature of the Penetrant

The principal differences between the concentration dependences of D and of σ for permanent gases, organic vapours and water vapour in polymers have already been indicated. For water an important consideration is whether water-polymer or water-water interactions predominate, and this is discussed with reference to specific polymers in section 1.2 and to theoretical models in section 2.7.

The sorptive capacity of a polymer is often greater

the higher the boiling point of the penetrant[9], i.e. the more easily a vapour condenses then, in general, the greater is the extent to which it is sorbed.

Important factors in penetrant diffusion are the size and shape of the diffusing molecules. As a rule the larger the molecular diameter of the penetrant the smaller is D and the larger is E_D[9] as more polymer segments are disturbed in the diffusion process. The effect of shape is illustrated by the branched hydrocarbon penetrants which exhibit relatively low values of D compared with their straight-chain isomers[14] and it is considered that the latter diffuse preferentially with the long axes in the diffusion direction. Above a certain size of penetrant diffusion becomes controlled solely by co-operative segmental motion and further increases in penetrant size have little effect on either D or E_D[15].

1.1.3 The Nature of the Polymer

The sorptive capacity of a polymer for a penetrant is governed principally by an extension of the "like dissolves like" principle usually applied to low molecular weight substances. For polymers of varying relative polar group content the uptake of benzene was found to increase with the relative hydrophobic, or hydrocarbon group content[16]. On

the other hand the largest uptakes of water are exhibited by polymers containing high proportions of hydrophilic groups such as hydroxyl, carboxyl or amide[17].

Since diffusion involves the displacement of polymer chain segments values of D are generally decreased when the segmental mobility is decreased. This effect is observed when chain stiffening is brought about by the addition to the main chain of rigid and bulky side groups or when interchain cohesive forces are increased by an increase in the symmetry of the chain or by some types of polar side groups. Although polymers with low segmental mobilities usually offer most resistance to diffusion they are also most amenable to plasticisation by penetrant and as a result exhibit the more marked concentration dependence for penetrant diffusion. This effect is illustrated by benzene in a variety of polymers[18].

1.1.4 The Glass Transition Temperature of the Polymer (T_g)

Below T_g the segmental motion of a polymer is so slow that the rate of transport of the larger, and more appreciably sorbed, penetrant molecules, i.e. organic vapours, is not controlled solely by diffusion but also by segmental relaxation processes. An alternative view is that the diffusion coefficient in these systems becomes time dependent

or the diffusion "Non-Fickian"[19]. For water in the more hydrophobic polymers and for the smaller permanent gases the effect of T_g is not so important[9]. However some of the larger gas penetrants[20] exhibit changes in the slope of log D vs. 1/T at T_g because of the relatively sudden change in segmental mobility.

Values of σ in glassy polymers can depend on the previous history of a sample[2,6] and comparisons below T_g have to be treated with caution.

1.1.5 The Crosslink Density and Molecular Weight of the Polymer

The degree of crosslinking does not appreciably affect the solubility of a penetrant in a polymer unless considerable swelling of the polymer matrix occurs in which case the retractive force exerted by the network tends to reduce σ. Usually, with increasing crosslink density, D decreases and E_D increases. This effect is more marked for larger penetrants[4,14] and is attributed to a decrease in the mobility of polymer chains.

With apparently one exception[2], little effect of the molecular weight of a high polymer on D or σ has been observed.

1.1.6 Crystallinity

Under normal conditions very little sorption or diffusion of a penetrant in crystalline regions of a polymer is to be expected. For gases σ is generally reduced in proportion to the amorphous fraction of the polymer, but D is further reduced because of the increased tortuosity of diffusion paths[22].

Analyses of the concentration and temperature dependences of D in partially crystalline polymers are complicated by the fact that the percentage crystallinity of a sample is often critically dependent on its history. The present investigation is concerned only with polymers which are amorphous in the temperature range of study.

1.1.7 Incorporated Fillers

The presence of filler particles in a polymer is similar in some ways to that of regions of crystallinity if sorption and diffusion through the filler can be considered negligible. However appreciable sorption of penetrant is often possible on surfaces of filler particles which need not be completely wetted by the surrounding polymer. In addition polymer-filler interactions are sometimes relatively weak and the formation of voids or air gaps, for which there

is some evidence from density measurements[22,23], may occur. The latter tend to be facilitated if penetrant-filler surface interactions are significant, when an interfacial diffusive flow of penetrant is encouraged.

Other principal factors affecting D and σ in filled polymers are the size, shape, distribution and degree of dispersion of filler particles[22]. In particular, the largest relative decreases in D occur when lamellar fillers[4] oriented normally to the direction of diffusion are present.

Filled polymers are discussed in more detail in chapter 3.

1.1.8 The Presence of Other Gases or Vapours

Generally the presence of permanent gases in a polymer has a negligible effect on the transport of other penetrant species whereas with a vapour present appreciable interaction of flows may be expected. The diffusion of water in several polymers is enhanced considerably by the presence of small quantities of a plasticiser such as dioctyl phthalate[9-11]. Conversely, in some polymers with large sorptive capacities for water, such as cellophane, the presence of water facilitates the diffusion of other penetrants[11].

1.1.9 Macro-Heterogeneity of Membranes

Membranes which are heterogeneous on a macro-scale can arise, for example, through progressive changes in structure or of concentration of a disperse phase[22]. Membranes of this type have been prepared, some of which exhibited water vapour permeabilities which depended significantly on the direction of flow of water through them[24,25].

1.2 Previous Work on Water-Polymer Systems

Much of this subject was reviewed recently by Barrie[11].

1.2.1 The Nature of Water as a Penetrant

Although the water molecule is relatively small in comparison with most organic penetrants, liquid water is vastly associated through hydrogen bonding and has been the subject of extensive study[26,27]. Since the present work is largely concerned with the association of water inside polymers it seems pertinent to describe briefly the principal models proposed for the associated structure of liquid water.

The "uniformist" structure model[28] postulates a uniform amount of hydrogen bonding and considers water essentially as an unstructured liquid with no local domains

of structure different from that of any other volume element in the water. However, more attention has been given to mixture models for water[26] which require the coexistence of a bulky, structured species of associated water with a dense species such as monomeric water molecules. One of these models proposes a broken-down ice type of structure[29] with relatively few hydrogen bonds broken. Another proposes monomeric water and other small entities contained in cavities or clathrate-like cages[30] inside large, associated structures, and a third requires the existence of monomeric water and relatively large clusters[31]. The last-mentioned model stemmed from the strongly co-operative nature of hydrogen bond formation proposed in liquid water[32]. A resonance stabilisation effect causes the formation of one bond to facilitate the formation of others and "flickering" clusters with a lifetime of $\sim 10^{-11}$ sec. were proposed[32]. This model is most amenable to mathematical treatment and the average cluster size has been calculated as decreasing from 91 to 25 in the range 0-70°C, being ~ 50 at room temperature[31].

Evidence for the existence of higher order transitions in liquid water has been compiled[26] based on "thermal anomalies" or "kinks" in the temperature dependences of

several physical quantities for liquid water and for aqueous solutions. As yet this evidence is neither conclusive nor universally accepted[33]. It has even been suggested[34] that the apparent transition observed at 60°C in a study of the diffusion of water in vinyl acetate-vinyl chloride copolymer[35] is due to a transition in water itself.

In contrast to the liquid state, there is little or no evidence[36] for any appreciable association of water in the vapour phase except possibly close to the saturation point.

1.2.2 Natural Fibres, Synthetic Fibres and other Polymers containing Hydrophilic Groups

The present investigation is not directly concerned with polymers of the type in which water-polymer interactions are predominant. Nevertheless, many studies have been made on this type of polymer and it is of interest to compare the findings with those for polymers exhibiting lower sorptive capacities for water.

Most of the work on natural fibres has been concerned with wool and cellulose[11,16] which exhibit water regains of 20-40% at saturation. Sorption isotherms exhibit hysteresis and diffusion is markedly "non-Fickian".

There are strong interactions between water and polar groups inside the polymer and there appears to be a rapid, initial diffusion of water into the fibre accompanied by an elastic swelling. This stage is followed by slow polymeric relaxation processes which allow further sorption to occur. Values of D, calculated from the first reversible stage, increase markedly with c as diffusion becomes easier in the more swollen polymer.

Nylon is most widely studied of the synthetic fibres[11,37,38]. D increases with c although less markedly than for wool or cellulose as the uptake of water by nylon ($\sim$10% saturation regain), and hence the degree of swelling, are less. Non-Fickian behaviour was also detected as D measured in the transient state of diffusion from rates of sorption increased less with c than did the corresponding steady state D.

The third category of this class of polymers includes polyvinylalcohol and cellulose acetate both of which have been studied in some detail[17,39,40]. Completely amorphous polyvinylalcohol dissolves in water and the polymer swells considerably in water even when the percentage crystallinity is high. Both D and P increase rapidly with c but the

analysis is complicated by marked non-Fickian behaviour as a consequence of the rupture by water of strong interchain bonds. At low relative humidities D is exceptionally low because of the very strong cohesive forces between chains of the dry polymer. Cellulose acetate exhibits saturation water regains of $\sim$ 20% but D does not appear to increase strongly with c (cf. natural fibres). Values of P are exceptionally high and it has been postulated[41] that capillary pores are present in the polymer along which water transport can take place.

1.2.3 Polymers containing no Polar Groups or only moderately Polar Groups

These are considered in rather more detail since water-water interactions are relatively more pronounced in these systems.

i) Polyethylene and Polypropylene[40,42]

In both these polymers P is independent of sorbed water concentration. Despite appreciable experimental errors it was established that sorption follows Henry's law so that σ, and hence D, are also constant. Water uptakes are sufficiently low (less than 0.1% at saturation) to rule out specific water-polymer interactions and the Henry's law behaviour suggests that specific water-water interactions

are not important either.

ii) Polydimethylsiloxane[43]

P was observed to decrease very slightly with c and sorption isotherms appeared to be of the B.E.T. class III type[44], although the accuracy of the sorption measurements was rather low. The steady state D decreases as c is increased and this was interpreted in terms of water clustering inside the polymer.

iii) Natural Rubber[45-7]

P is constant up to ~ 0.8 relative humidity. Sorption isotherms are initially linear but become type III[44] above relative humidities of 0.7-0.8. D is almost constant at low sorbed water concentrations but close to saturation it decreases appreciably with increasing c. Interpretation of the results was complicated, however, by the presence of water-soluble material. In particular, sorption isotherms appeared to be linear up to a vapour pressure corresponding to that of a saturated solution of the water-soluble impurities.

iv) Polymethacrylates, Polyacrylates and Polyvinylacetate

These polymers sorb 1-2% of water at saturation. For polyvinylacetate and polymethylacrylate[48] D is

constant. For polymethylmethacrylate[43] and polyethylmethacrylate[49] the steady state D decreases with increasing c. Again P is constant and sorption isotherms are of type III. However time lag (chapter 2) results for polyethylmethacrylate suggest that D is constant. This discrepancy was tentatively ascribed[49] to the formation of clusters under equilibrium sorption conditions but not under time lag conditions.

v) Ethyl Cellulose[50,51] and Rubber Hydrochloride[42]

Both these polymers exhibit type III sorption isotherms. As for polyethylmethacrylate the steady state D decreases with increasing c but D from time lag measurements is apparently constant. On the other hand sorption rate measurements yield values of D in ethyl cellulose in good agreement with the steady state values. As yet, the discrepancies in the time lag results remain largely unresolved.

vi) Other Polymers

For water in some cellulose acetate/polystyrene graft copolymers[52] both σ and P increase with c while D, as measured from both steady state and time lags, remains constant. These results were interpreted in terms of

relatively low degrees of water clustering in comparison with those in ethyl cellulose. Presumably similar behaviour would result if clustering and plasticisation were to occur concurrently with their effects on the D - c dependence cancelling out to a large extent.

In polyethyleneterephthalate[42] P, σ and D are all constant.

1.3 Clustering of Water in Polymers

As already indicated, in many of the more hydrophobic polymers water-water interactions are preferred to water-polymer interactions, so producing strong tendencies for water clustering.

1.3.1 Evidence for Clustering

Evidence for clustering of water in polymers has come mainly from observed diffusion coefficients which decrease with increasing sorbed water concentration[42,43,49-52]. If clustering occurs such that the proportion of clustered molecules increases with increasing overall water concentration, then a decrease in the overall D with increasing c would be expected since clustered water can be assumed to be relatively immobile compared with monomeric water. The proportion of clustered molecules depends on the relative rates of clustering

and dissociation of water molecules. The former would be expected to increase with c owing to the increasing chance of encounter. The number of molecules dissociating from clusters would also be larger for higher c. However, as clustered water molecules are possibly stabilised to some extent when each is attached by two or more hydrogen bonds, then it may be expected that the rate of dissociation increases less rapidly with c than does the rate of association. The comparative immobility of clustered water has been interpreted on the basis that a water molecule inside a cluster would require additional energy to break free prior to diffusion, although it has been pointed out[42] that apart from energy considerations the probability of a H_2O unit undergoing a successful diffusion jump would be less if the unit were part of a cluster than if it were free as monomeric water. Transport of complete clusters, especially large ones, was considered unlikely[2].

Additional evidence for the presence of clusters has come from the shape and temperature dependence of water sorption isotherms[42]. When water does not interact appreciably with the polymer deviations from Henry's law can be interpreted in terms of clustering[53,54].

Thermodynamic heats of dilution $\Delta\bar{H}_A$ of water in a number of polymers decrease with increasing c[42,55]. This is consistent with clustering of water becoming more predominant with increasing c. Thus decreases in $\Delta\bar{H}_A$ with increasing c could result from corresponding decreases in the degree of mixing of polymer and monomeric water. Clustering of water would tend to decrease this degree of mixing.

The development of opacity[50] in ethyl cellulose films when exposed to high relative humidities was attributed to cluster formation. Presumably the clusters are of sufficient size to create a heterogeneous system having significant fluctuations in refractive index.

Measurements of the dielectric constant ε of water-polystyrene at various sorbed water concentrations[56] showed that the relative increases $\varepsilon - \varepsilon_o / \varepsilon_o$, where ε_o is the value for dry polymer, are greater at high relative humidities than expected on the basis of a mixture with random molecular mixing. Since it is known that ε for liquid (associated) water exceeds ε for monomeric water (80 cf. 29 for the latter), the discrepancy was interpreted in terms of association of water inside the polymer.

In addition to studies of water in polymers, the

properties of water in polar and non-polar organic liquids have been investigated. Gordon et al[57] measured specific volumes, viscosities and heats of mixing of water-benzene and water-toluene mixtures under conditions where the water concentration was insufficient to cause phase separation. They concluded that appreciable clustering of water takes place. On the other hand a more recent investigation[58] in which the amounts of water present in organic liquids were measured directly by an analytical procedure indicated that little if any clustering of water takes place in benzene but that some clustering occurs in the polar liquids chloroform and 1,2-dichloroethane.

1.3.2 Clustering of Methanol

Short chain aliphatic alcohols, particularly methanol, are also capable of association through hydrogen bonding and might be expected to cluster inside polymers. However most hydrophobic polymers have much higher sorptive capacities for methanol than for water and plasticisation of polymer would normally mask any observable effect of clustering on diffusion coefficients. In the case of polydimethylsiloxane the segmental mobility is sufficiently high at room temperature to minimise any plasticisation effect and the steady state D for methanol in this polymer decreases with increasing c[59].

There is also some indirect evidence that the constant D obtained for methanol in ethyl cellulose[50] is a result of cancelling concentration dependences arising from plasticisation of polymer and clustering of penetrant.

Clustering of methanol in benzene has also been reported[60].

1.3.3 Sizes of Clusters

The mean cluster size of penetrant molecules in a polymer-penetrant mixture can be calculated from the shape of the sorption isotherm by the use of equations based on cluster integrals[53,54] which are discussed in chapter 2. Mean cluster sizes of water and of methanol in relatively hydrophobic polymers have been calculated in this way[42,59,61] and are generally in the range from 1 (i.e. no association) at low relative humidity to 2 - 3 at relative humidity 0.8 - 0.9.

Although mean cluster sizes can be established there is relatively little information on the distribution of cluster sizes. The development of opacity in ethyl cellulose[50], already mentioned, indicates that some clusters of water molecules are very large in this polymer at close to saturation.

Gordon et al.[57] derived a model which postulates water association by hydrogen bonding in an inert medium as a random polycondensation with H_2O as a tetrafunctional A_4 type monomer. This type of model yields an exact distribution of cluster sizes. Gordon et al.[57] interpreted their results for water-benzene and water-toluene as consistent with this model. Barrie and Platt[43] applied the same model to the water-polydimethylsiloxane system and, with a number of assumptions, they found the observed D-c dependence to agree with that predicted by the model, although the experimental error was rather large. The model was found to be inadequate to describe the observed D-c dependence of the water-polymethylmethacrylate system and it was assumed[43] that this polymer does not match the criterion of an inert medium to water.

An analogous polymerisation model for methanol gives reasonable agreement[59] with the experimentally determined sorption isotherm and D-c relation for the methanol-polydimethylsiloxane system although a somewhat arbitrary adjustable parameter was used in the comparison.

On the other hand results for water in chloroform and in 1,2-dichloroethane[58] are consistent with water

association involving dimer formation only.

1.3.4 The effect of Polymer Structure on Cluster Formation

Barrer and Barrie[50] pointed out that the ultimate size of clusters would be controlled by the amount of free space in the polymer, i.e. the physical presence of polymer segments would restrict further cluster expansion after a certain point in their growth. As a consequence of this they suggested that, in the case of ethyl cellulose and other polymers which are glassy at room temperature and contain voids in their structures, formation of clusters would occur preferentially in voids since less disturbance of the polymer matrix as a whole would be required.

Yasuda and Stannett[42] suggested that the formation of water clusters might be initiated by the presence of polar groups in the polymer. They proposed that results obtained previously by Rouse[62] for water in polyethylene, which indicated considerable clustering of water, were a consequence of cluster initiation by polar impurities resulting from oxidation of the polymer. Barrie and Platt[43] considered that water clustering in polydimethylsiloxane might possibly be initiated by the presence of trace catalyst or the Si-O-Si linkage. If the initiation process were relatively slow in

comparison with diffusion the anomalous time lag results, described in the last section, might be a consequence[51] of the setting up of a quasi-steady state in permeation.

The effect of polar groups on the sorption and clustering of water, and the comparative immobility of clustered water were clearly illustrated by the addition of 5% of an ionic emulsifier to a styrene-ethyl acrylate copolymer latex[42]. Values of σ for water increase markedly, particularly at higher relative humidities, but P is very little altered.

1.3.5 The effect of Clusters on the Bulk Properties of the Polymer

Rogers[6] pointed out that local concentrations of a clustered penetrant inside a polymer might be as great as an equivalent overall concentration of a penetrant which is a strong swelling agent for the polymer. This could lead to localised swelling and possibly stress-cracking of the polymer. Analysis of sorption isotherms for methanol, ethanol and propanol in polyethylene indicates[6] that clustering of alcohols takes place only at higher relative vapour pressures. Polyethylene films containing sorbed alcohol crack readily under applied stress[6] only in the regions of the isotherms where clustering is indicated. At lower vapour pressures

stress-cracking either takes a long time to occur or is not exhibited at all.

1.4 The Present Investigation

The principal aim of the work presented in this thesis is the investigation of the properties of water in a number of amorphous high polymers by sorption and diffusion studies. The polymers used are relatively hydrophobic in the sense that water uptakes close to saturation do not generally exceed 2% by weight of dry polymer, and emphasis is placed throughout on the study of clustering or association of water in these polymers. For this reason particular attention is given to the concentration dependences of P, σ , D, E_D and $\Delta \bar{H}_A$ of water in the polymers, as well as to their absolute magnitudes.

Effects of structural changes in a polymer on the properties of imbibed water are investigated by making measurements on series of polymer samples which differ only slightly in the chemical constitutions of their monomer units. Polymer samples containing various proportions of incorporated fillers, which sorb relatively large amounts of water in comparison with the bulk polymer, are also examined briefly. Filler particles then constitute, in a sense, large local concentrations of relatively hydrophilic groups inside a polymer.

A few measurements with methanol as penetrant vapour are also made to compare concentration dependences of D, σ and P in some of the polymers with those for water. This is done with a view to comparing the relative degrees, and possible mechanism, of clustering of the two penetrants.

Previous theories of water (and methanol) clustering in polymers, in particular that of Gordon et al.[57] already described in section 1.3.3 and discussed in more detail in chapter 2, are examined critically on the basis of the experimental results.

1.4.1 Polymers used in the Present Investigation

i) Series of Polyalkylmethacrylates

Polymethyl-, ethyl-, n-propyl- and n-butyl-methacrylates (PMMA, PEMA, PPMA and PBMA respectively) were used, i.e. the polymer structure was modified by varying the size of the alkyl group in the side chain. A similar investigation has been carried out previously using benzene as penetrant[16]. Although PMMA and PEMA have been studied previously in connection with water[43,49], the polymers are all around or below their T_g at room temperature and some discrepancies might be expected between values of P, σ and D obtained from different polymer samples. In this investigation the polymers were prepared at the same

time and in the same manner, and were subjected to similar solvent and thermal treatments in order that a serious comparison of sorption and diffusion of water in each is justified. Hence, despite the previous work, it was considered worthwhile to make a more comprehensive study of these systems, particularly with respect to an analysis of concentration and temperature dependence of P, σ and D. In addition a few comparative measurements were made on poly-n-propylacrylate (PPA) which is well above its T_g at room temperature.

Diffusion measurements were generally made under steady state conditions although some values of D for the PBMA- and PPA- water systems were also calculated from sorption rate measurements to compare steady and transient state values. It was thus hoped to obtain information on the relative rates of the diffusion and clustering processes.

ii) Polysiloxanes

As previously indicated in section 1.2.3 the polydimethylsiloxane (DMS) - water system was studied by Barrie and Platt[43] who applied to it a specific polymerisation model for water association. However, the accuracy of their sorption measurements was not high, and

in the present work a more detailed investigation of this system is carried out using a more sensitive weighing procedure. In addition the effect on P, σ and D of structural variations in silicone rubbers, by the introduction of bulky or polar substituents, was examined by a study of a polymethylphenylsiloxane (PMS) containing 5.4% of phenyl groups and of poly 3,3,3, trifluoropropylmethylsiloxane (FMS).

A few sorption rate measurements were also made to compare values of D obtained from the steady and transient states of diffusion.

iii) Filled Samples

DMS was chosen as the bulk polymer since it sorbs relatively little water[43] and since a number of fillers can be incorporated rather readily into it. Two different types of filler were used: a fine powder of silica and finely ground crystals of sodium chloride. The former sorbs large amounts of water[44] compared with DMS and the latter dissolves completely if the activity of water is above ~ 0.75. The effect on P of incorporated fillers could conceivably be of some technical interest since P for water in DMS is relatively high[11] compared with most polymers at room temperature, and any increase in P due to the presence of a filler could possibly be utilised in membrane separation

processes involving water.

A few sorption rate measurements enabled comparisons to be made of values of D obtained from the steady and transient states of diffusion.

iv) Polymers used with Methanol

Some equilibrium sorption and steady state diffusion measurements for methanol in FMS and in PEMA were made, together with some sorption rate measurements in the latter. FMS was chosen principally for comparison with an earlier study of the DMS-methanol system[58]. PEMA was chosen to investigate the effect of the increased amenability of the polymer to plasticisation on the concentration dependence of D.

CHAPTER 2

THEORY

2.1 Basic Diffusion Equations

For an isotropic medium the rate of transfer of material by unidirectional diffusion under a concentration gradient is expressed mathematically in terms of Fick's first law of diffusion[8],

i.e. $$J = -D\frac{\partial c}{\partial x} \qquad \ldots.(2\text{-}1)$$

where J is the rate of transfer across unit area of a section normal to the direction of flow, c is the concentration of diffusing material at a distance x along the direction of flow and D is the diffusion coefficient. The quantity of material is usually given the same units in c and in J so that D has the dimensions length^2 time^{-1}.

From equation (2-1) the fundamental differential equation for unidirectional diffusion can be derived by considering the rate of accumulation of material in a volume element having faces of unit area normal to the direction of diffusion at x - dx and x + dx. Diffusing material enters and leaves the element at rates given by $J_x - \frac{\partial J_x}{\partial x} \cdot dx$ and $J_x + \frac{\partial J_x}{\partial x} \cdot dx$ respectively where J_x is the rate of transfer across the plane at x, i.e. the plane at the centre of the

element. The rate of accumulation inside the element is then given by

$$-2\frac{\partial J_x}{\partial x}\cdot dx = 2\cdot dx\cdot\frac{\partial c}{\partial t}$$

or

$$\frac{\partial c}{\partial t}+\frac{\partial J_x}{\partial x}=0$$

J_x may be substituted for using equation (2-1) so that for D constant

$$\frac{\partial c}{\partial t} = D\cdot\frac{\partial^2 c}{\partial x^2} \qquad \ldots.(2\text{-}2)$$

When D varies with c equation (2-2) becomes

$$\frac{\partial c}{\partial t} = \frac{\partial}{\partial x}\left(D(c)\cdot\frac{\partial c}{\partial x}\right) \qquad \ldots.(2\text{-}3)$$

Equations (2-2) and (2-3) are often called Fick's second law of diffusion.

2.2 Alternative Diffusion Coefficients

Equation (2-1) refers to diffusion across an arbitrarily chosen plane, or frame of reference. To define a diffusion coefficient completely in a two component system the frame of reference must be specified precisely. This section describes the more common and useful frames of reference and their respective diffusion coefficients[63].

2.2.1 Total Volume of the System remains Constant

The interdiffusion in a closed vessel of two components

A and B of constant volumes V_A and V_B, respectively, per unit amount of component can be expressed by

$$J_A = - D_A^V \frac{\partial c_A^V}{\partial x} \quad \text{and} \quad J_B = - D_B^V \frac{\partial c_B^V}{\partial x}$$

where superscript V refers to a volume-fixed frame and subscripts A and B to the components A and B respectively. c^V is expressed as the amount of component per unit volume, the amount of material having the same units as in J. J_A and J_B refer to a section such that the total volume on either side of it remains constant as diffusion proceeds, i.e. fixed with respect to the closed vessel.

The volume transfers of A and B across unit area of this section are -

$$- D_A^V V_A \frac{\partial c_A^V}{\partial x} \quad \text{and} \quad - D_B^V V_B \frac{\partial c_B^V}{\partial x} \quad \text{respectively and}$$

since there is no net transfer of volume

$$D_A^V V_A \cdot \frac{\partial c_A^V}{\partial x} + D_B^V V_B \frac{\partial c_B^V}{\partial x} = 0 \qquad \ldots.(2\text{-}4).$$

An overall mass balance for the system gives $V_A c_A^V + V_B c_B^V = 1$, which on differentiation with respect to x becomes

$$V_A \frac{\partial c_A^V}{\partial x} + V_B \frac{\partial c_B^V}{\partial x} = 0 \qquad \ldots.(2\text{-}5)$$

For non-zero V_A and V_B equations (2-4) and (2-5) require $D_A^V \equiv D_B^V \equiv D^V$ so that a two component system, in which the volume change on mixing is zero, can be described by a single diffusion coefficient D^V often referred to as the mutual diffusion coefficient.

2.2.2 Total Mass of the System remains Constant

When volume changes take place in a system an alternative frame of reference is used in which the mass of the system on either side of the reference section remains constant. By modification of the scale of length from x to ϵ_M, where equal increments in ϵ_M correspond to equal increments in the total mass of the components, and by using a procedure analogous to that in 2.2.1 it can be shown that a single diffusion coefficient D^M is again sufficient to describe interdiffusion. The superscript M refers to a total mass-fixed reference frame.

2.2.3 Mass of One Component remains Constant

The diffusion of a penetrant in a polymer is usually most conveniently described by a frame of reference in which the mass of one component (polymer) remains constant on either side of the reference section. By choosing ϵ_B as the scale of length, where equal increments in ϵ_B contain increments

in the mass of component B (polymer), theequation

$$D_A^B \cdot \frac{\partial c_A^B}{\partial \epsilon_B} + D_B^B \cdot \frac{\partial c_B^B}{\partial \epsilon_B} = 0 \qquad \ldots.(2\text{-}6)$$

is obtained by analogy with equation (2-4) where the superscript B refers to a component B-fixed frame.

However, D_B^B must be zero so that interdiffusion is again described by one diffusion coefficient D_A^B with which most of the work in this thesis is concerned.

2.2.4 Intrinsic Diffusion Coefficients

If the two components diffuse independently of each other then in general they may be expected to do so at different rates. To reconcile this deduction with the fact that equal amounts of both components are transferred across a volume-fixed section it has been postulated[64] that a compensating mass flow of both components occurs so as to equalise the total rates of transfer of each component. In order to correlate diffusion coefficients more closely with random molecular motions, intrinsic diffusion coefficients $\mathfrak{D}_A$ and $\mathfrak{D}_B$ were defined with respect to a reference section across which no mass flow occurs[64]. For a volume-fixed reference section the rate of transfer of A is then given by

$$J_A = -D^V \frac{\partial c_A}{\partial x} = -\mathfrak{D}_A \frac{\partial c_A}{\partial x} + c_A \cdot \frac{dV}{dt} \qquad \ldots.(2\text{-}7)$$

where dV/dt is the rate of change of total volume due to mass flow.

The use of intrinsic diffusion coefficients has been criticised on the grounds that, in condensed phases at least, the diffusion of one component is linked or correlated with the diffusion of the other and cannot be regarded as independent processes[65,66].

2.2.5 Relationships between Diffusion Coefficients

Diffusion coefficients from any two chosen frames of reference (X and Y say) can be related since

$$J_A^X = J_A^Y + c_A \; U_{YX}$$

where U_{YX} is the relative velocity of Y with respect to X. Taking the three frames considered above and considering the flux of A across a B-fixed section,

$$-D_A^B \cdot \frac{\partial c_A^B}{\partial \epsilon_B} = -D^M \frac{\partial c_A^M}{\partial \epsilon_M} + D^M \cdot \frac{c_A}{c_B^M} \cdot \frac{\partial c_B^M}{\partial \epsilon_M}$$

$$= -D^V \frac{\partial c_A^V}{\partial x} + D^V \frac{c_A^V}{c_B^V} \cdot \frac{\partial c_B^V}{\partial x} \qquad \ldots.(2\text{-}8)$$

from which it can be deduced that

$$D_A^B = D^M \cdot \frac{(c_B^M)^2}{(c_A^M + c_B^M)^2} = D^V \phi_B^2 \qquad \ldots.(2\text{-}9)$$

where ϕ_B is the volume fraction of B.

It can also be shown that, provided the partial volumes of the components are constant, then

$$D^V = V_A c_A^V (\mathfrak{D}_B - \mathfrak{D}_A) + \mathfrak{D}_A \qquad \ldots.(2\text{-}10)$$

$\mathfrak{D}_B$ is usually considered to be zero for polymer-penetrant systems so that

$$\mathfrak{D}_A = \frac{D^V}{\phi_B} = \frac{D_A^B}{\phi_B^3} \qquad \ldots.(2\text{-}11)$$

Although most diffusion coefficients considered in the present work are D_A^B, ϕ_A is less than 0.02 in most cases so that to a good approximation $\mathfrak{D}_A = D^V = D_A^B$. For this reason diffusion coefficients will henceforth be simply referred to by the symbol D unless otherwise indicated.

2.3 Solution of the Diffusion Equations[12,67]

Solutions to equations (2-1) and (2-2) depend on the initial and boundary conditions imposed. The two most important cases for a plane sheet of polymer are:-

i) Permeation through a sheet with fixed, but different penetrant concentrations in the ingoing and outgoing faces and no penetrant initially in the sheet.

ii) Sorption into or desorption from a sheet,

with uniform initial concentration of penetrant and with the concentrations in each face equal and fixed at a value different from that initially in the interior of the sheet.

2.3.1 Steady State Permeation

i) Diffusion Coefficient Constant

If the concentrations of penetrant in the ingoing and outgoing faces ($x=0$, $x=\ell$) of a plane sheet of polymer of thickness ℓ are maintained at c_0 and c_ℓ respectively ($c_0 > c_\ell$), then when steady state conditions hold equation (2-2) gives $\partial^2 c/\partial x^2 = 0$.

Integrating twice gives $c = Ax + B$ where A and B are constants. Introduction of the conditions at $x = 0$ and $x = \ell$ gives $c_0 = B$, $c = A\ell + B$ so that

$$c = \frac{x\,(c_\ell - c_0)}{\ell} + c_0 \qquad \ldots. \text{(2-11a)}$$

or

$$x/\ell = \frac{c_0 - c}{c_0 - c_\ell} \qquad \ldots. \text{(2-11b)}$$

showing that a linear concentration gradient exists across the sheet. From equation (2-1) the diffusion coefficient may be calculated since

$$J = -D\,\partial c/\partial x = \frac{D(c_0 - c_\ell)}{\ell} \qquad \ldots. \text{(2-12)}.$$

ii) Diffusion Coefficient a function of Concentration

When D varies with c equation (2-1) is still valid and can be integrated to yield an average value $\bar{D}$ of the diffusion coefficient.

Thus $$J = -\frac{1}{\ell}\int_{c_0}^{c_\ell} D(c)\,dc = \frac{\bar{D}\,(c_0 - c_\ell)}{\ell} \qquad \ldots.(2\text{-}13a)$$

where $\bar{D}$ is given by

$$\bar{D} = \frac{1}{c_0 - c_\ell}\int_{c_\ell}^{c_0} D(c)\,dc \qquad \ldots.(2\text{-}13b)$$

Comparison of equations (2-12) and (2-13a) shows that $\bar{D}$ is the "effective" diffusion coefficient for steady state permeation when D varies with c.

2.3.2 Transient State Permeation

i) Time Lag

In most experimental arrangements the concentration of penetrant in the outgoing face of a polymer sheet is kept small enough to be considered negligible compared with the concentration in the ingoing face. If, in addition, the sheet contains no penetrant at zero time the boundary conditions are

$$c = c_0, \qquad x = 0, \qquad t \geq 0$$

$$c = 0, \qquad 0 < x < \ell, \qquad t = 0$$

$$c = 0, \qquad x = \ell, \qquad t \geq 0$$

and the solution of equation (2-2) takes the form

$$\frac{Q_t}{\ell c_0} = \frac{D.t}{\ell^2} - \frac{1}{6} - \frac{2}{\pi^2} \sum_{n=1}^{\infty} \frac{(-1)^n}{n^2} \exp\left(\frac{-D\, n^2 \pi^2\, t}{\ell^2}\right) \quad \ldots.(2\text{-}14)$$

where Q_t is the total amount of penetrant which has passed through unit area of sheet in time t. As $t \to \infty$ equation (2-14) tends to the steady state straight line

$$Q_t = \frac{D.c_0}{\ell} \left(t - \frac{\ell^2}{6D}\right)$$

so that if a graph of Q_t vs. t is drawn, the intercept L of this line on the time axis is given by[68]

$$L = \frac{\ell^2}{6D} \quad \ldots.(2\text{-}15)$$

L is known as the time lag and a knowledge of this will thus enable D to be calculated. Equations (2-14) and (2-15) are valid only for a constant D.

When D varies with c Frisch[69] has shown that L may be obtained from

$$L = \frac{\int_0^{\ell} x\, c_s\,(x)\, dx}{\int_0^{c_0} D\,(c)\, dc} \quad \ldots.(2\text{-}16)$$

where $c_s\,(x)$ is the steady state concentration distribution of penetrant in the sheet.

ii) Permeation at Small Times

An alternative equation to (2-14) for constant D[70] is

$$\frac{dQ_t}{dt} = c_0 \left(\frac{4D}{\pi}\right)^{\frac{1}{2}} \sum_{m=0}^{\infty} \exp\left(-\frac{\ell^2(2m+1)^2}{4Dt}\right)$$

which, for small t, reduces to

$$\ln\left(t^{\frac{1}{2}} \frac{dQ_t}{dt}\right) = \ln\left(\frac{4c_0^2 D}{\pi}\right)^{\frac{1}{2}} - \frac{\ell^2}{4Dt} \qquad \ldots.(2\text{-}17)$$

D may be obtained from the slope of $\ln\left(t^{\frac{1}{2}} \frac{dQ_t}{dt}\right)$ vs. $1/t$.

2.3.3 Rates of Sorption or Desorption

For a constant D system with the following boundary conditions for sorption into a plane sheet,

$$c = c_0, \quad x = 0, \quad x = \ell, \quad t \geqslant 0$$

$$c = 0, \quad 0 < x < \ell, \quad t = 0$$

the solution of equation (2-2) can take either the form

$$\frac{M_t}{M_\infty} = 4\left(\frac{D.t}{\ell^2}\right)^{\frac{1}{2}} \left[\frac{1}{\pi^{\frac{1}{2}}} - 2\sum_{n=0}^{\infty} (-1)^n \operatorname{ierfc}\left(\frac{n\ell}{4Dt^{\frac{1}{2}}}\right)\right] \qquad \ldots.(2\text{-}18)$$

or $$\frac{M_t}{M_\infty} = 1 - \frac{8}{\pi^2} \sum_{m=0}^{\infty} \frac{1}{(2m+1)^2} \exp\left(\frac{-D(2m+1)^2 \pi^2 t}{\ell^2}\right) \qquad \ldots.(2\text{-}19)$$

where M_t is the uptake of penetrant by the sheet at time t and

M_∞ is the equilibrium uptake. Equation (2-18) is useful at small times when the summation term tends to zero and D can be obtained from

$$D = \pi l^2/16 \qquad \ldots\ldots(2\text{-}20)$$

where I is the initial slope of the reduced sorption curve, i.e. a plot of M_t/M_∞ vs. $t^{\frac{1}{2}}/l$.

Equation (2-19) is more useful at longer times for which it approximates to

$$\ln (1 - M_t/M_\infty) = \ln (8/\pi^2) - \frac{D.\pi^2 t}{l^2} \qquad \ldots\ldots(2\text{-}21)$$

D may be obtained from the slope of a plot of $\ln (1 - M_t/M_\infty)$ vs. t.

In the case of desorption from a sheet with boundary conditions

$$c = 0, \quad x = 0, \quad x = l, \quad t \geqslant 0$$

$$c = c_0, \quad 0 < x < l, \quad t = 0$$

equations (2-18) to (2-21) still apply with M_t the amount of penetrant lost from the sheet at time t.

When D varies with c equations (2-20) and (2-21) give an average value $\bar{D}$ over the concentration range 0 - c_0. This average is not the same as that for permeation (equation (2-13b)) and is discussed in the following section (2.4).

2.3.4 Numerical Solutions of Diffusion Equations[71]

When D varies with c analytical solutions of equation (2-3) exist only in a few specific cases and numerical methods generally have to be used. It is often desirable, for example, to be able to calculate expected reduced sorption curves from a known, steady state D-c dependence. This can be done by approximating the derivatives in equation (2-3) to finite difference expressions. It is usually convenient to make the variables dimensionless by the transformations

$$C = c/c_0, \qquad X = x/\ell, \qquad T = \frac{D_{c=0} \cdot t}{\ell^2} \qquad D^1 = D/D_{c=0}$$

where c_0 is the final or initial concentration of penetrant in the sheet and $D_{c=0}$ is the limiting value of D at zero penetrant concentration. Equation (2-3) then becomes

$$\frac{\partial C}{\partial T} = \frac{\partial}{\partial X}\left(D^1(C)\,\frac{\partial C}{\partial X}\right) \qquad \ldots.(2\text{-}22)$$

At this stage it is convenient to introduce a variable s such that

$$s = \frac{\int_0^C D^1(C)\,dC}{\int_0^1 D^1(C)\,dC} \qquad \ldots.(2\text{-}23)$$

when (2-22) may be expressed as

$$\frac{\partial C}{\partial T} = \int_0^1 D^1(C)\,dC \cdot \frac{\partial^2 s}{\partial X^2} \qquad \ldots.(2\text{-}24)$$

The ranges in X and in T are now divided into a number of equal intervals ΔX and ΔT respectively. If penetrant concentrations at the points (m-1) ΔX, m ΔX, (m+1) ΔX are denoted by C_{m-1}, C_m, C_{m+1} respectively at time n ΔT, and at m ΔX by C_m^+, C_m^- at times (n+1) ΔT and (n-1) ΔT respectively, then from Taylor's expansion the derivatives in equation (2-24) may be replaced, to first approximations, by

$$\left(\frac{\partial C}{\partial T}\right)_m = \frac{C_m^+ - C_m}{\Delta T}$$

and $$\left(\frac{\partial^2 s}{\partial X^2}\right)_m = \frac{(s_{m+1} - 2s_m + s_{m-1})}{(\Delta X)^2}$$

where s values are computed from corresponding C values using equation (2-23). The boundary conditions at the face and centre of the sheet are $C_{m=0} = 1$ and $C_{m+1} = C_{m-1}$ respectively. Only half the sheet need be considered due to symmetry. Hence equation (2-24) enables values of C at time (n+1)ΔT to be computed for various positions in the sheet from known values of C at time nΔT. Since values of C are known for zero time the concentration distribution in the sheet can therefore be calculated at any time. A suitable integrating procedure then gives $M_t/M_\infty = \int_0^1 C \, dX$ at any instant in time.

The above explicit procedure is usually sufficiently accurate as long as the ratio $\Delta T/(\Delta X)^2$ and the value of ΔX are kept small. In particular $\Delta T/(\Delta X)^2$ should be less than $\frac{1}{2\int_0^1 D^1(C)\,dC}$. More accurate procedures involving implicit, iterative procedures are discussed by Crank[71].

2.4 Determination of Concentration-Dependent Diffusion Coefficients[63]

2.4.1 From Steady State Measurements

For steady state permeation of penetrant through a sheet with the concentration in the outgoing face effectively zero, equation (2-13) becomes

$$J = 1/\ell \int_0^{c_0} D(c)\,dc \qquad \ldots.(2\text{-}25)$$

In practice values of the flux J are measured for a series of ingoing vapour pressures p and the relationship between J and p obtained. The equilibrium sorption isotherm for the penetrant, measured in a separate experiment, gives c_0 as a function of p. A combination of permeation and sorption measurements yields J as a function of c_0. Graphical or analytical differentiation of the $J\ell - c_0$ curve then gives the required D-c relationship since from (2-25)

$$D_{c=c_0} = \ell\,(dJ/dc)_{c=c_0} \qquad \ldots.(2\text{-}26)$$

2.4.2 From Transient Permeation Measurements

i) Time Lag

Equation (2-16) can be modified since under steady state conditions the flux of penetrant is the same at all points in a sheet so that

$$\int_{c_s}^{c_0} D(c)\,dc = \frac{x}{\ell}\int_{0}^{c_0} D(c)\,dc \qquad \ldots.(2\text{-}27)$$

where $c_s(x)$ is the steady state concentration at a distance x inside the sheet. Eliminating x in equation (2-16) then yields[69]

$$L = \frac{\ell^2 \int_0^{c_0} c_s D(c_s) \int_{c_s}^{c_0} D(u)\,du\,dc_s}{\left(\int_0^{c_0} D(u)\,du\right)^3} \qquad \ldots.(2\text{-}28)$$

where u is a dummy variable. On the other hand equation (2-27) can be rewritten in terms of fluxes at differing ingoing concentrations as

$$\ell J_{c_0} - J_{c_s} = x J_{c_0}, \text{ or } x = \ell (1 - J_{c_s}/J_{c_0}) .$$

Elimination of x in equation (2-16) now gives[72]

$$L = \frac{\ell \int_0^{J_{c_0}} c_s (J_{c_0} - J_{c_s})\,d J_{c_s}}{J_{c_0}^3} \qquad \ldots.(2\text{-}29)$$

It is not usually possible to obtain the D-c relationship with a high degree of accuracy from a known L-c relationship but equations (2-28) and (2-29) serve as useful checks if D-c is already known from steady state measurements. If the J-c relationship is a smooth curve which can be fitted accurately by some mathematical function then (2-28) and (2-29) are simply alternative, equivalent expressions. On the other hand if discontinuities or particularly sharp curvatures arise in the J-c plot then equation (2-29) is preferable since only quantities which are actually measured are involved and the integration may be performed graphically or numerically.

ii) Permeation at Small Times

If the mathematical form, but not the numerical parameters of a D-c relationship is known then Meares[73] has shown that the exact D-c relationship may be determined. First equation (2-17) is applied for very small t when $D = D_{c=0}$ to a very good approximation. A knowledge of $D_{c=0}$ together with the mathematical form of D-c can then be utilised to fit the L-c results using equation (2-16) or (2-28). Hence the best values for the unknown parameters of the D-c relationship can be determined.

2.4.3 From Sorption and Desorption Kinetic Measurements

When D varies with c equations (2-20) and (2-21) become

$$\bar{D} = \pi l^2/16 \qquad \ldots.(2\text{-}30)$$

and

$$\ln (1 - M_t/M_\infty) = \ln(8/\pi^2) - \frac{\bar{D}\pi^2 t}{l^2} \qquad \ldots.(2\text{-}31)$$

If measurements very close to equilibrium can be made then $\bar{D}$ in equation (2-31) refers, to a good approximation, to the actual value of D at the equilibrium concentration c_0 in the case of sorption and to $D_{c=0}$ in the case of desorption. However it is often difficult to make accurate kinetic measurements sufficiently close to equilibrium and although some workers[74,75] have utilised equation (2-31), most have calculated D vs. c from a knowledge of the $\bar{D}$ - c_0 relationship obtained by applying equation (2-30) for a series of different equilibrium concentrations.

i) Successive Approximations Procedure

A first approximation to $\bar{D}$ can be taken as[76]

$$\bar{D} = \frac{1}{c_0} \int_0^{c_0} D(c)\, dc \qquad \ldots.(2\text{-}32)$$

so that the first approximation to D(c) is

$$D(c) = \bar{D}(c) + c_0 \frac{d\bar{D}}{dc_0} \qquad \ldots.(2\text{-}33)$$

This first approximation can be used to construct sorption-time curves for various values of c_0 by a method such as that described in section 2.3.4. From these, $\bar{D}$ values are obtained from equation (2-30) and compared with the original values of $1/c_0 \int_0^{c_0} D(c)\,dc$. From a graph of calculated $\bar{D}$ vs. $1/c_0 \int_0^{c_0} D(c)\,dc$ improved values of the latter are obtained corresponding to the experimentally observed values of $\bar{D}$. These improved values are then differentiated to give a second approximation to D(c) and the whole process is repeated until the observed and calculated values of $\bar{D}$ are in agreement[77].

This method tends to be exceedingly laborious, although in the specific cases when D depends linearly or exponentially on c correction curves giving percentage differences between $\bar{D}$ and $1/c_0 \int_0^{c_0} D(c)\,dc$ have been constructed[77]. The principal advantage of the method is that its use can be extended to cases where the initial penetrant concentration in the sheet is non-zero, i.e. cases of "interval" sorption.

ii) From Mean Diffusion Coefficients for Sorption and Desorption

If values of $\bar{D}_s$ and $\bar{D}_d$ are obtained from conjugate reduced sorption and desorption curves respectively using equation (2-30), then for several D-c relationships it is established that $1/2\ (\bar{D}_s + \bar{D}_d)$ is an accurate approximation to $1/c_0 \int_0^{c_0} D(c)dc$

so that

$$D(c) = \frac{1}{2} \frac{d\left[c_0 (\bar{D}_s + \bar{D}_d)\right]}{d\, c_0}$$

This approximation can be improved in cases of D with a linear or exponential concentration dependence by correction curves[77] showing the percentage differences between $1/2\ (\bar{D}_s + \bar{D}_d)$ and $1/c_0 \int_0^{c_0} D\,(c)\, dc$.

iii) The use of Weighted Mean Diffusion Coefficients

Calculations carried out by Crank[77] show that $\bar{D}$ obtained from equation (2-30) is much more accurately expressed as a weighted mean diffusion coefficient than by equation (2-32), i.e. for sorption

$$\bar{D}_s = p\, c_0^{-p} \int_0^{c_0} c^{p-1}\, D\,(c)\, dc \qquad ....(2\text{-}34)$$

and for desorption

$$\bar{D}_d = q\, c_0^{-q} \int_0^{c_0} (c_0 - c)^{q-1}\, D(c)\, dc \qquad ....(2\text{-}35)$$

where p and q represent the weighting values for sorption and desorption respectively.

These equations are particularly useful when D increases strongly with increasing c. For a large variety of different algebraic D-c relationships in which D increases with increasing c, Crank[77] has established that equations

(2-34) and (2-35) hold accurately over large concentration ranges with p = 1.67 and q = 1.85.

Equation (2-34) can be differentiated directly to obtain

$$D(c) = \bar{D}_s(c) + \frac{c_0}{p} \cdot \frac{d\bar{D}_s}{dc_0} \qquad \ldots\ldots(2\text{-}36)$$

so that D(c) follows from a knowledge of $\bar{D}_s$ vs. c_0. D(c) may also be obtained from equation (2-35) in certain cases. Kishimoto and Enda[78] illustrated the use of this when D(c) is assumed to be of the form

$$D(c) = D_{c=0}(1 + \alpha c + \beta c^2 + \ldots)$$

which gives $\bar{D}_d = D_{c=0}\left(1 + \frac{\alpha}{1+q} \cdot c_0 + \frac{2\beta}{(1+q)(2+q)} \cdot c_0^2 + \ldots\right)$

Hence by curve-fitting the $\bar{D}_d - c_0$ relationship, D vs. c follows.

When D decreases with increasing c it can be considered to increase by the same function of $(c_0 - c)$ so that it is to be expected that p = 1.85 and q = 1.67 for these cases. That this is so is confirmed for a number of functions in the appendix (9.1)

iv) Polynomial Expression for D.

When D can be expressed in the form $D(c) = D_{c=0}(1 + \alpha c + \beta c^2 + \ldots.)$ a procedure derived by

Lin Hwang[79] may be used. This depends on the assumption that the concentration of penetrant in a sheet at any point and at any time can be expressed as a series of ascending powers of the equilibrium concentration c_0

i.e. $$c(\eta) = c_0\,\theta_1(\eta) + c_0^2\,\theta_2(\eta) + c_0^3 \cdot \theta_3(\eta) \quad \ldots.(2\text{-}37)$$

where η is the reduced variable $(x^2/4D_{c=0}.t)^{\frac{1}{2}}$ and θ_1, θ_2, θ_3 etc. are functions of η which contain the polynomial coefficients α, β etc. Assuming the sheet to act as a semi-infinite medium at small times gives

$$I_s.c_0 = 4\,D_{c=0}^{\frac{1}{2}} \int_0^\infty c\,(\eta)\,d\eta \quad \ldots.(2\text{-}38)$$

where I_s is the initial slope of the reduced sorption curve corresponding to the equilibrium concentration c_0.

Lin Hwang solved equation (2-37) and showed[79] that when equation (2-38) is applied I_s is given by

$$\begin{aligned} I_s = 4D_{c=0}^{\frac{1}{2}} \Big[& A + (B\alpha)\,c_0 + (C_1\alpha^2 + C_2\beta)\,c_0^2 \\ & + (D_1\alpha^3 + D_2\alpha\beta + D_3\gamma)\,c_0^3 \\ & + (E_1\alpha^4 + E_2\alpha^2\beta + E_3\alpha\gamma + E_4\beta^2 + E_5\delta).c_0^4 \\ & + \ldots\ldots \Big] \end{aligned} \quad \ldots.(2\text{-}39)$$

where A, B, C_1 etc. are universal constants obtained by numerical integration with respect to η of various functions

which make up θ_1, θ_2, θ_3 etc. The actual functions involved, together with their graphs are presented in the appendix (9.2.1), where the calculated values of the first twelve constants A-E_5 are also given.

Practically, equation (2-39) is used as a series of simultaneous equations, into which are fed pairs of values of I_s and c_0. The solution of the equations yields $D_{c=0}$, α, β etc. It is generally advisable, if a high degree of accuracy is required, to feed in more I_s, c_0 pairs than the minimum necessary and to solve the simultaneous equations (2-39) by a matrix technique invólving minimum mean squares deviations (appendix 9.2.2).

This procedure is very suitable for automatic computation but breaks down if the concentration dependence of D is too great for the series in equation (2-37) to converge sufficiently rapidly. If $f(c_0) = \alpha c_0 + \beta c_0^2 + \ldots$, then it is found (appendix 9.2.3) that for accurate work $f(c_0)$, (αc_0), (βc_0^2) etc. must all be numerically less than unity. This means that the method is more likely to be applicable when D is a decreasing function of c since f(c) cannot then exceed unity (numerically).

When D takes the form of a polynomial in c equation

(2-34) becomes

$$\bar{D}_s = D_{c=0}\left[1 + \frac{p}{1+p}(\alpha c_0) + \frac{p}{2+p}(\beta c_0^2) + \frac{p}{3+p}(\gamma c_0^3) + ...\right] \quad ....(2\text{-}40)$$

Equation (2-40) may be compared with equations (2-39) and (2-30) and values of p calculated when D varies but slightly with c. The calculations and results for a number of D-c relationships are given in detail in the appendix (9.2.4). Generally, p is found to lie between 1.75 and 1.85 when D decreases slightly with c and between 1.75 and 1.67 when D increases slightly with c. In a sense therefore, this procedure may be considered complementary to the more general weighted mean procedure of Crank[77] in that it is particularly useful for small ranges in c whereas the latter is useful over larger ranges.

v) Other Procedures

Although several other procedures exist for the determination of D(c) from sorption kinetic data[63] methods i) to iii) have been used most widely. One other alternative which is convenient for automatic computation is due to Prager[80]. It consists of approximating D(c) to a step function in c by a successive approximations procedure, followed by a smoothing or averaging process. Although its

accuracy is limited to a small number of steps, it is used occasionally in the present work for comparison with other methods.

2.5 Molecular Interpretations of Diffusion in Polymers

2.5.1 Hydrodynamic Theories

One interpretation of diffusion is that diffusive flow can be regarded as a balance between a driving force supplied by a gradient in the chemical potential of the diffusing species, and a resistance to flow which leads to a constant average diffusion velocity[81].

For spherical molecules of radius r diffusing in a continuous medium of viscosity η Stokes calculated the viscous resistance per molecule to be

$$6\pi\eta r \frac{1 + 2\eta/\beta r}{1 + 3\eta/\beta r}$$

where β is the coefficient of sliding friction between the diffusing molecule and its surroundings. For an ideal system and for $\beta = \infty$ the Stokes-Einstein equation

$$D = \frac{kT}{6\pi\eta r} \qquad \ldots.(2\text{-}41)$$

can be derived. Other theories of viscosity[81] replace the factor 6 in equation (2-41) by different constants (K).

An "apparent viscosity" η of a medium defined[82] as $kT/K\pi\eta Dr$ is approximately constant for many liquids. However for crosslinked rubbery polymers η increases with the molecular size of the penetrant and with the degree of crosslinking. For glassy polymers η increases extremely rapidly with penetrant size for penetrants larger than neon.

It is obvious therefore that simple hydrodynamic models such as those leading to the Stokes-Einstein and related equations, which refer to diffusion in continuous media, are not suitable to describe diffusion in polymers. More refined treatments which take into account interactions between diffusing molecules and their environment by means of phenomenological resistance coefficients have been considered by Tyrrell[81].

2.5.2 Transition State Theory

When investigations are carried out over a wide range of temperature it is quite often found that the energy of activation for diffusion E_D varies appreciably with temperature. Two principal theories take account of this, both depending on the existence of an activated state. Thus a unimolecular reaction A → B can be represented in a stepwise manner as

$$\underset{\text{I}}{A} \longrightarrow \underset{\text{II}}{A^1} \longrightarrow \underset{\text{III}}{A^*} \longrightarrow B \qquad \ldots.(2\text{-}42)$$

where A and B are initial and final states. Step I corresponds to the acquisition of the necessary activation energy, step II to the distribution of this energy within the system to give state A^* and step III to the actual passage over the energy barrier down to the equilibrium state B.

Step I is generally assumed to be relatively rapid. The transition state theory[83] requires step III to be rate controlling and leads to the expression

$$D = \varkappa \left(\frac{kT}{h}\right) \lambda^2 \exp\left(-\Delta G^{\neq}/RT\right) \qquad \ldots.(2\text{-}43)$$

where k and h are the Boltzmann and Planck constants, $\varkappa$ is a probability or "transmission" coefficient and λ is the average distance of a unit diffusion jump. $\Delta G^{\neq}$ is the free energy of activation given by $\Delta H^{\neq} - T\Delta S^{\neq}$ where $\Delta H^{\neq}$ and $\Delta S^{\neq}$ are the enthalpy and entropy of activation. A comparison of equation (2-43) with

$$D = D_o \exp\left(-E_D/RT\right) \text{ yields}$$

$$E_D = \Delta H^{\neq} + RT \qquad \ldots.(2\text{-}44)$$

and

$$D_o = e \cdot \left(\frac{kT}{h}\right) \cdot \lambda^2 \exp\left(\Delta S^{\neq}/R\right) \qquad \ldots.(2\text{-}45)$$

since $\varkappa$ is generally close to unity. Equation (2-44) thus predicts variations in E_D with temperature.

$\Delta S^{\neq}$ can be evaluated from experimental determinations

of D_o if reasonable values for λ are assumed. Large and positive values of $\Delta S^{\neq}$ found by Barrer were attributed by Glasstone et al.[83] to breaking of chemical bonds in the diffusion process.

2.5.3 Kinetic Statistical or Activated Zone Theory

As an alternative explanation for the observed large values of $\Delta S^{\neq}$ Barrer[84,85] proposed that a considerable disturbance of the polymer matrix occurs in the formation of the transition state. He postulated that penetrant diffusion in polymers takes place due to the prior formation of activated zones and that step II in (2-42) is rate controlling. The activation energy is distributed among all the degrees of freedom, i.e. of both the chain segments and the diffusing molecule, in a particular zone, and co-operation of several chain segments is considered necessary to promote a unit diffusion jump.

An activated zone containing n degrees of freedom has to acquire an energy $\geq$ some value E before a diffusion jump can occur. The probability W that an energy $\geq$ E is distributed among the n degrees of freedom is

$$W = \sum_{f=1}^{n} \left[(E/RT)^{f-1} / (f-1)! \right] \exp(-E/RT) \qquad \ldots.(2\text{-}46)$$

and from this the expression

$$D = \frac{\nu\lambda^2}{2} \sum_{f=1}^{f=f'} \rho_f \frac{(E/RT)^{f-1}}{(f-1)!} \exp(-E/RT) \quad \ldots(2\text{-}47)$$

can be derived for the diffusion coefficient where ν is the penetrant vibration frequency and ρ_f is the probability that f degrees of freedom will co-operate with sufficient synchronisation to promote a unit diffusion jump. f' is the is the value of f corresponding to the maximum value of the term inside the summation and it replaces n in equation (2-47) as Barrer showed that the significant activated zones are those having f between 1 and f'. Further, it was proposed[84] that the summation can be replaced by its maximum term, to a reasonable approximation, so that equation (2-47) becomes

$$D = \frac{\nu\lambda^2}{2} \cdot \rho_f \cdot \frac{(E/RT)^{f'-1}}{(f'-1)!} \exp(-E/RT) \quad \ldots.(2\text{-}48)$$

A comparison of equation (2-48) with $D = D_o \exp(-E_D/RT)$ gives

$$E = E_D + (f'-1)\,RT \quad \ldots.(2\text{-}49a)$$

or

$$\frac{dE_D}{dT} = -(f'-1)\,R \quad \ldots.(2\text{-}49b)$$

assuming that f' does not vary with temperature.

The value of f' may thus be estimated from the temperature dependence of E_D although this estimate would

be an upper limiting value as some variation of f' with temperature is to be expected. Values for f' have also been calculated from measurements of D_o assuming reasonable values for λ and ν. Values between 10 and 25 were found[85] for diffusion of simple gases in rubbers.

2.5.4 Free Volume Theory[86].

Not all the volume of a polymer is occupied physically by its segments due to steric restrictions and random thermal motions. Free volume or holes, created by local fluctuations of thermal energy, exist in a polymer. The free volume theory for diffusion of small molecules in polymers postulates that the principal energy barrier to diffusion is that of hole formation and that the probability of the occurrence of a successful unit diffusion jump is proportional to the probability that a hole of sufficient size is adjacent to the molecule. If the critical hole size for diffusion to occur is $V^{\neq}$, the jump frequency is proportional to the total number of holes multiplied by the fraction having a volume $\geq V^{\neq}$. In the simplest possible model for a liquid, where holes are assumed to be discrete entities, the latter quantity is given by

$$\frac{\int_{V^{\neq}}^{\infty} \exp\left(-E_h/kT\right) dV_h}{\int_{0}^{\infty} \exp\left(-E_h/kT\right) dV_h}$$

where E_h refers to the energy associated with the creation of a hole of size V_h.

In reality however, and particularly in the case of polymers, the co-operative motion of several segments may allow two or more holes to come together to form one hole large enough for a diffusion jump to take place even if the individual holes are not large enough. This feature of co-operative participation of several segments is thus common to both the activated zone and free volume theories.

Free volume and other postulated theories[86] are not considered in detail in the present work as water is such a small penetrant molecule that diffusion of water in polymers can be considered, to a first approximation, to be independent of the proportion of free volume present in a polymer.

2.6 Thermodynamics of Vapour Sorption by Polymers.

2.6.1 Free Energy, Heat and Entropy of Dilution

Information regarding a sorption process can often be obtained from the magnitudes of the heat and entropy of dilution together with their dependence on concentration and temperature. The free energy of dilution $\Delta\bar{G}_A$ is defined as the change in free energy on transferring, isothermally and

reversibly, one mole of penetrant from pure liquid to an infinite amount of polymer-penetrant mixture at a given composition. If the vapour pressure in equilibrium with the mixture is p and the saturation vapour pressure at the same temperature is p_0 then $\Delta\bar{G}_A$ is given by

$$\Delta\bar{G}_A = RT \ln (p/p_0) \qquad \ldots.(2\text{-}50)$$

The corresponding heat of dilution $\Delta\bar{H}_A$ and entropy of dilution $\Delta\bar{S}_A$ are given respectively by

$$\Delta\bar{H}_A = \left[\frac{\partial(\Delta\bar{G}_A/T)}{\partial(1/T)}\right]_{P,c} = R\left[\frac{\partial \ln(p/p_0)}{\partial(1/T)}\right]_{P,c} \qquad \ldots(2\text{-}51)$$

and

$$\Delta\bar{S}_A = -\left[\partial(\Delta\bar{G}_A)/\partial T\right]_{P,c}$$

$$= -R\left[\ln (p/p_0) + \frac{\partial \ln (p/p_0)}{\partial \ln (T)}\right]_{P,c} \qquad \ldots.(2\text{-}52)$$

P is the hydrostatic pressure in the mixture phase. In our experiments P = p, the pressure of vapour in equilibrium with the mixture which will vary with temperature if c is constant. However, the effect of this variation in P on the activity of the sorbed component is negligible as large changes in P

are required to change significantly the activities of components in condensed phases.

Variations in $\Delta\bar{H}_A$ and $\Delta\bar{S}_A$ with sorbed penetrant concentration c are thus sensitive measures of changes in isotherm shape with temperature.

2.6.2 Polymer Solution Theory

By postulating a lattice theory in which a cell of a lattice network is occupied by a polymer segment or by a solvent molecule, Flory[87] deduced that

$$\Delta S_m = -k\,(n_A \ln \phi_A + n_B \ln \phi_B) \qquad \ldots.(2\text{-}53)$$

where ΔS_m is the entropy of mixing of n_A molecules of solvent and n_B molecules of polymer, k is the Boltzmann constant and ϕ_A and ϕ_B are the volume fractions of solvent and polymer respectively. If each polymer molecule contains x segments then from equation (2-53) the entropy of dilution can be calculated as

$$\Delta\bar{S}_A = -R\left[\ln (1-\phi_B) + (1-\tfrac{1}{x})\,\phi_B\right] \qquad \ldots.(2\text{-}54)$$

Huggins[88] using a similar lattice model to Flory obtained

$$\Delta\bar{S}_A = -R\left[\ln (1-\phi_B) - \tfrac{z}{2}\,(1-\tfrac{1}{x})\ln\left(1-\frac{2\phi_B}{z}\right)\right] \qquad \ldots(2\text{-}55)$$

where z is the coordination number of the lattice.

Further refinements[89,90] using the same lattice model lead to considerably more complicated expressions but for many systems the improvement in the agreement with experiment is not greatly marked.

For the heat of mixing of polymer and solvent Flory[91] deduced that

$$\Delta H_m = kT\, n_A\, \phi_B\, \chi \qquad \ldots.(2\text{-}56)$$

where χ, the interaction parameter, is a dimensionless quantity given by

$$\chi = \frac{z \cdot \Delta w_{AB}}{kT} \qquad \ldots.(2\text{-}57)$$

where $\Delta w_{AB} = w_{AB} - 1/2(w_{AA} + w_{BB})$ ....(2-58)

Values of w refer to energies associated with particular types of bond e.g. w_{AB} refers to a solvent-polymer bond. If the total entropy change on mixing is given by equation (2-53) then the free energy of mixing is given by

$$\Delta G_m = kT\,(n_A \ln \phi_A + n_B \ln \phi_B + \chi n_A \phi_B) \qquad \ldots.(2\text{-}59)$$

In addition, contributions to the entropy of mixing arising from polymer-solvent interactions may have to be considered[90]. In this case equation (2-59) still holds

but χ is now a free energy parameter rather than an interaction parameter. ΔH_m and ΔS_m are obtained from $\Delta H_m = \frac{\partial (\Delta G_m/T)}{\partial (1/T)}$ and $\Delta S_m = - \partial(\Delta G_m)/\partial T$, and are given by

$$\Delta H_m = - kT^2 \, (\partial\chi/\partial T) \cdot n_A \, \phi_B \qquad \ldots.(2\text{-}60)$$

and $$\Delta S_m = -k \left[n_A \ln \phi_A + n_B \ln \phi_B + \frac{\partial(T\chi)}{\partial T} \cdot n_A \, \phi_B \right] \qquad \ldots.(2\text{-}61)$$

$\Delta \bar{G}_A$, $\Delta \bar{H}_A$ and $\Delta \bar{S}_A$ are obtained by differentiating ΔG_m, ΔH_m and ΔS_m with respect to n_A and multiplying by the Avogadro number. $\Delta \bar{G}_A$ is given by

$$\Delta \bar{G}_A = RT \left[\ln (1-\phi_B) + (1- \tfrac{1}{x}) \, \phi_B + \chi \phi_B^2 \right] \qquad \ldots.(2\text{-}62)$$

When χ is considered simply as an interaction parameter

then $$\Delta \bar{H}_A = RT \, \phi_B^2 \, \chi \qquad (2\text{-}63)$$

and $$\Delta \bar{S}_A = -R \left[\ln (1-\phi_B) + (1- \tfrac{1}{x}) \, \phi_B \right] \qquad (2\text{-}64)$$

When χ is a free energy parameter then

$$\Delta \bar{H}_A = -RT \, (\partial \chi / \partial T) \cdot \phi_B^2 \qquad \ldots.(2\text{-}65)$$

and $$\Delta \bar{S}_A = -R \left[\ln (1-\phi_B) + (1- \tfrac{1}{x}) \, \phi_B + \frac{\partial(\chi T)}{\partial T} \right] \qquad \ldots.(2\text{-}66)$$

In theory an isotherm can be predicted from a knowledge of χ by comparing equations (2-50) and (2-62), but in practice it is found that χ has to be treated as a somewhat arbitrary adjustable parameter in order to match experimental data. With the exception of benzene in natural rubber marked deviations from the lattice theory have generally been observed for polymer solutions, although the free energy expressions are sometimes reasonable models in that errors arising in expressions for ΔH_m and ΔS_m tend to cancel to a large extent.

2.6.3 Swelling of Crosslinked Polymers on Sorption of Vapour

In the case of a crosslinked polymer the driving force for sorption of penetrant vapour from the free energy of dilution is opposed by the retractive force exerted by the polymer network. When equilibrium sorption is attained, a state of swelling is reached at which these two forces are in balance. An expression for the elastic contribution to the free energy was derived by Flory and Rehner[92] and the overall expression for the resultant free energy ΔG_c is

$$\Delta G_c = RT \left[\ln (1-\phi_B) + \phi_B + \chi \phi_B^2 + \left(\frac{\rho V_A}{M_c}\right) \phi_B^{1/3} \right] \quad \ldots(2\text{-}67)$$

where subscript c refers to a crosslinked system. M_c is the

average molecular weight between crosslinks, ρ is the density of swollen polymer and V_A is the molar volume of the solvent. At equilibrium ΔG_c is zero and equation (2-67) is often used to calculate a value for M_c. On the other hand, if M_c can be measured or estimated in some other manner, then equation (2-67) can be used in conjunction with equations (2-50) and (2-62) to predict a sorption isotherm.

2.6.4 Clustering Theory of Vapour Sorption

The Flory-Huggins lattice theory is reasonable for hydrocarbon vapour-polymer systems but breaks down for more polar components and particularly so in the case of water vapour. An alternative, more exact treatment was proposed by Zimm and Lundberg[54]. This is based on the statistical mechanics of fluctuations and does not predict isotherms, as does the lattice theory, but interprets their shapes in terms of molecular distributions in the mixture.

The molecular pair distribution function $F_2(i,j)$ is defined by the statement that

$$(1/V^2)\ F_2\ (i,j)\ d(i)\ d(j)$$

is the probability that the molecules i and j are each at the positions specified by the co-ordinates (i,j) in the ranges d(i) and d(j), where V is the total volume of the mixture.

The penetrant cluster integral G_{AA} is defined by

$$G_{AA} = (1/V) \iint \left[F_2 (i,j) - 1 \right] d(i)\, d(j) \qquad \ldots.(2\text{-}68)$$

where i and j now refer to penetrant molecules.

G_{AA}/v_A can be taken as a measure of the tendency of the penetrant to cluster in a given mixture and $\phi_A\, G_{AA}/v_A$ is the mean number of penetrant molecules, in the neighbourhood of a given penetrant molecule. ϕ_A and v_A are the volume fraction and partial molecular volume respectively of penetrant.

Zimm[53] derived the expression

$$G_{AA}/v_A = -(1 - \phi_A) \left[\frac{\partial (a_A/\phi_A)}{\partial a_A} \right]_{P,T} - 1 \qquad \ldots.(2\text{-}69)$$

where a_A is the activity of the penetrant vapour and P is the hydrostatic pressure in the mixture phase (see section 2.6.1). Equation (2-69) actually neglects a small term involving the isothermal compressibility of the system, i.e. it is exact for an incompressible system. Since for a vapour a_A is given by (p/p_o), G_{AA}/v_A may be calculated at various points on a sorption isotherm from equation (2-69).

If sorption is governed by Henry's law so that a_A is proportional to ϕ_A then G_{AA} is minus one molecular volume

so that any particular penetrant molecule excludes its own volume to other molecules but does not otherwise affect their distribution i.e. the behaviour expected of an ideal solution. Equation (2-69) can be re-arranged to read

$$\phi_A \, G_{AA}/v_A = (1 - \phi_A) \left[\frac{\partial \ln (\phi_A)}{\partial \ln (a_A)} \right]_{P,T} - 1 \qquad \ldots.(2\text{-}70)$$

Starkweather[61] obtained a similar expression for the mean number of penetrant molecules in the neighbourhood of a polymer molecule in excess of the mean concentration of penetrant molecules, namely

$$\frac{\phi_A G_{AB}}{v_A} = - \phi_A \left[\frac{\partial \ln (\phi_A)}{\partial \ln (a_A)} \right]_{P,T} \qquad \ldots.(2\text{-}71)$$

A tendency for penetrant molecules to cluster is indicated by $G_{AA}/v_A > - 1$. From equation (2-69) this is expected of any system where sorption isotherms are continuously convex towards the pressure axis. Equations (2-69) and (2-70) are thus useful for comparisons of the overall degrees of penetrant clustering in different polymers. Equation (2-71) is correspondingly useful when polymer-penetrant interactions are relatively important such as in cases of specific site sorption. These three equations can also be considered to be complementary to equations (2-51)

and (2-52) in an analysis of the temperature dependence of polymer-penetrant sorption isotherms as the clustering functions G_{AA}/v_A, $\phi_A G_{AA}/v_A$ and $\phi_A G_{AB}/v_A$ can be determined for a given activity or sorbed concentration of penetrant at a number of different temperatures.

Completely random mixing of polymer segments and penetrant molecules cannot generally be obtained since segments are necessarily attached to one another, i.e. some degree of clustering is inherent in the system.

Starkweather[61] applied equations (2-69), (2-70) and (2-71) to several water-polymer systems. For cellulose and proteins $\phi_A G_{AA}/v_A$ at low relative humidities is about - 0.5 and half the volume of a water molecule is excluded from water in the neighbourhood of a point occupied by a polymer segment. These results imply that water-polymer contacts are favoured at low relative humidities. On increasing the relative humidity above ~ 0.85, $\phi_A G_{AA}/v_A$ increases very rapidly, becoming positive, showing that water clustering is dominant at close to saturation.

For nylon, polymethylmethacrylate and polyvinylacetate water clustering was also found to be very important at close to saturation. $\phi_A G_{AA}/v_A$ for water in the latter two polymers appeared to exhibit minima close to 0.5 relative humidity.

2.7 Models for the Concentration Dependence of D, and P for water in Polymers

The diffusion coefficient of water can follow a variety of types of concentration dependence depending on the polymer under consideration and it is this aspect which tends to distinguish the diffusion behaviour of water from that of most other penetrants in polymers[11].

The thermodynamic formulation of the diffusion equation is

$$J = -Bc \cdot \partial\mu/\partial x \qquad \ldots.(2\text{-}72)$$

where c is the concentration and μ the chemical potential of the penetrant at the point x. B is termed the intrinsic mobility of the sorbed penetrant. Equation (2-72) may be rewritten as

$$J = - BRT \left(\partial \ln a/\partial \ln c\right). \partial c/\partial x \qquad \ldots.(2\text{-}73)$$

where a is the activity of sorbed penetrant. Comparison of equation (2-73) with Fick's first law, equation (2-1), gives

$$D(c) = BRT \left(\partial \ln a/\partial \ln c\right) \qquad \ldots.(2\text{-}74)$$

so that the concentration dependence of D can arise through that of the intrinsic mobility B or that of the term $\left(\partial \ln a/\partial \ln c\right)$ which is a measure of the thermodynamic non-ideality of the system.

Some of the models which lead to various types of D-c relationships for water are considered in the following sections.

2.7.1 Plasticisation of Polymer

Concentration dependences of D arising from penetrant plasticising action are contained in the term B in equation (2-74) which increases with increasing c due to a loosening of the polymer structure. The resultant increase in segmental mobility increases the ease of hole formation which, in accord with free volume theories[86], increases the diffusion flow. One free volume model due to Wilkens and Long[93] postulates that the amount of free volume in a system depends linearly on the mole fraction of each component, and fluctuation theory has been used to derive

$$\log D = \log D_{c=0} + A' \phi_A - B' \phi_A^2 \qquad \ldots.(2\text{-}75)$$

where ϕ_A is the sorbed volume fraction of penetrant and A' and B' are constants characteristic of a particular system. Equation (2-75) often agrees well with experimental results[93] for organic vapours in rubbery polymers.

It is not proposed to discuss free volume theories in any detail because the diffusion of small molecules such

as water requires co-operative motion of only two or three polymer segments and the probability of this event, to a first approximation, is independent of the free volume of a system. For this reason the main factor contributing to the concentration dependence of D for water in polymers is in general not that of a simple plasticising action, as is often the case for organic vapours. One principal exception appears to be that of polyvinylalcohol for which there is little evidence[11] for localised water sorption on specific sites. This polymer has a very compact structure with strong interchain interactions and plasticisation is significant even for a small penetrant such as water. D increases rapidly with c in this system but as bond scission also tends to take place[17], the concentration dependence of D is complicated by non-Fickian behaviour.

2.7.2 Immobilisation of Water Molecules

In several water-polymer systems some of the sorbed water molecules become either immobile or at least suffer a decrease in mobility[11]. In polymers containing strongly polar groups, water molecules may exhibit such strong interactions with these groups that they become relatively "fixed" after sorption, i.e. a specific site mechanism is operative. On the other hand, in some of the more hydrophobic

polymers, water molecules prefer. to cluster together which also results in a decrease in mobility.

The simplest case to consider is that where only two forms of water, mobile and immobile, are present in a system. These forms are given subscripts f and b denoting "free" and "bound" water respectively. The diffusion flux of water can then be written

$$J = - B_f c_f \cdot \frac{\partial \mu_f}{\partial x}$$

$$= - B_f RT \left(\partial \ln a_f / \partial \ln c_f\right) \cdot \partial c_f / \partial c \qquad \ldots.(2\text{-}76)$$

since B_b, the intrinsic mobility of bound water is zero. Equation (2-76) can be rewritten as

$$J = - B_f RT \left(\frac{\partial \ln a_f}{\partial \ln c_f}\right) \cdot \left(\frac{\partial c_f}{\partial c}\right) \cdot \partial c / \partial x \qquad \ldots.(2\text{-}77)$$

which on comparison with equation (2-1) yields

$$D(c) = B_f RT \cdot \left(\partial \ln a_f / \partial \ln c_f\right) \cdot \partial c_f / \partial c \qquad \ldots.(2\text{-}78)$$

where c refers to the total water concentration, i.e. $c_f + c_b$.

From equation (2-78) it can be seen that there may be three separate contributions to the concentration dependence of D, i.e. from the terms B_f, $\left(\partial \ln a_f / \partial \ln c_f\right)$

and $(\partial c_f / \partial c)$. To study the concentration dependence due solely to immobilisation, either the concentration dependence of B_f must be known, or B_f must be independent of c as in a system where negligible plasticisation or swelling of the polymer takes place.

An alternative view of immobilisation is that it may be regarded as a case of diffusion with simultaneous chemical reaction[94]. The simplest case arises when the product (immobilised molecules) is in equilibrium with the diffusing species at any instant in time i.e. the "reaction" or immobilisation is considered instantaneous in comparison with the diffusion process. The diffusion equation becomes

$$\frac{\partial c_f}{\partial t} = \frac{\partial}{\partial x} \left(D_f \frac{\partial c_f}{\partial x} \right) - \partial c_b / \partial t \qquad \ldots.(2\text{-}79)$$

or $$\partial c / \partial t = \partial / \partial x \, (D_f \cdot \partial c_f / \partial x) \qquad \ldots.(2\text{-}80)$$

A comparison of equations (2-80) and (2-3) yields

$$D(c) \cdot \partial c / \partial x = D_f \cdot \partial c_f / \partial x \qquad \ldots.(2\text{-}81)$$

or $$D(c) = D_f \cdot \partial c_f / \partial c \qquad \ldots.(2\text{-}82)$$

Equations (2-78) and (2-82) are identical since from equation (2-74) $D_f = B_f \, RT \, (\partial \ln a_f / \partial \ln c_f)$.

2.7.3 Immobilisation on Specific Sites in a Polymer

The D-c dependence may be predicted by the use of simple models. For example, if it is assumed that immobilised molecules are sorbed according to a Langmuir isotherm and mobile molecules according to Henry's law[95] then

$$c_b = \frac{c_f}{(\alpha + \beta c_f)} \qquad \ldots.(2\text{-}83)$$

where α and β are constants. Again if $c_b \gg c_f$ then c_b may be replaced by c and

$$\partial c_f / \partial c = \frac{\alpha}{(1 - \beta c)^2} .$$

Hence from equation (2-82)

$$D(c) = D_f \cdot \frac{\alpha}{(1 - \beta c)^2} \qquad \ldots.(2\text{-}84)$$

If D_f is independent of c equation (2-84) shows that D will increase with c. This type of equation has been used satisfactorily[11] to describe D-c for water in some of the more polar polymers such as wool or cellulose, with D_f equated to $D_{c=0}$. In this case equation (2-84) is of the form for which an explicit solution of equation (2-3) was found by Fujita[95].

If specific site sorption occurs together with some degree of plasticisation of polymer then D_f itself increases with c and the overall concentration dependence of D is

correspondingly greater.

2.7.4 Random Polycondensation of Water in an Inert Medium

This treatment considers an idealised situation where no specific polymer-water interactions exist. The model was derived and applied to the water-benzene and water-toluene systems by Gordon et al.[57], and later applied to the water-polydimethylsiloxane system by Barrie and Platt[43].

The water molecule is treated as a tetrafunctional monomer of the A_4 type and hydrogen bond formation between water molecules is considered as a random polycondensation process with the formation of any hydrogen bond being independent of the formation of any other. The gel point of the system is identified with the saturation point, i.e. unit relative humidity. The weight fraction distribution formula for such a system was derived by Flory[96] and is

$$\frac{c_n}{c} = \frac{4\alpha^{n-1}(1-\alpha)^{2n+2}(3n)!}{(n-1)!\ (2n+2)!} \qquad \ldots.(2\text{-}85)$$

where c_n/c is the weight fraction of n-mer and α is the overall fraction of hydrogen bonds formed. The equilibrium constant K for the breaking of a hydrogen bond is given by

$$K = \frac{c(1-\alpha)^2}{\alpha} \qquad \ldots.(2\text{-}86)$$

where c is the total water concentration. The value of

at the gel point[96], α_s, is 1/3 and so

$$K = \frac{4\ c_s}{3} \qquad \ldots.(2\text{-}87)$$

where c_s is the total concentration of sorbed water at saturation. A combination of equations (2-85) and (2-86) gives

$$c_n = \frac{(3n)!}{(n-1)!\ (2n+2)!} \cdot \frac{(2c + K - k)^{n-1}\ (k-K)^{2n+2}}{2^{3n-1} \cdot c^{3n}} \qquad \ldots.(2\text{-}88)$$

where $k = (K^2 + 4\ Kc)^{\frac{1}{2}}$

The concentration of monomeric water c_1 is therefore given by

$$c_1 = \frac{(k - K)^4}{16\ c^3} \qquad \ldots.(2\text{-}89)$$

Since no water-polymer interactions exist, it is reasonable to assume that sorption of monomeric water follows Henry's law i.e.

$$p = \frac{(k-K)^4}{16\ \sigma_1\ c^3} \qquad \ldots.(2\text{-}90)$$

where σ_1 is the solubility coefficient for monomeric water and p is the external vapour pressure. At the saturation point $p_0 = \frac{(k-K)^4}{16\ \sigma_1\ c_s^3}$ which with equation (2-87) reduces to

$$p_0 = \frac{16\ c_s}{81\ \sigma_1} = \frac{4K}{27\ \sigma_1} \qquad \ldots.(2\text{-}91)$$

Division of equation (2-90) by equation (2-91) yields the equilibrium sorption isotherm equation for the random polycondensation model which is

$$(p/p_0) = \frac{27\ (k-K)^4}{64\ K\ c^3} \qquad \ldots.(2\text{-}92)$$

The concentration dependence of the overall diffusion coefficient for water is obtained if to a first approximation it is assumed that monomeric water is the only mobile species so that, from equation (2-82),

$$D(c) = D_1 \cdot \frac{\partial c_1}{\partial c} \qquad \ldots.(2\text{-}93)$$

The term $\partial c_1 / \partial c$ can be obtained from equation (2-89) and equation (2-93) becomes

$$D(c) = D_1 \cdot \frac{(k-K)^3}{16\ c^3} \left[\frac{8K}{k} - \frac{3(k-K)}{c}\right] \qquad \ldots.(2\text{-}94)$$

Barrie and Platt[43] assumed D_1 the diffusion coefficient of monomeric water to be constant and equal to $D_{c=0}$. This is in fact justified because the application of L'Hôpital's rule shows that

$$\lim_{c \to 0} \frac{(k-K)^3}{16\ c^3} \left[\frac{8K}{k} - \frac{3(k-K)}{c}\right] = 1.$$

The D-c relationship given by equation (2-94) can then be calculated for a given value of K.

If dimer and higher polymeric species of water contribute appreciably to the overall diffusion flux, and if interaction of flows between species is neglected, then equation (2-93) can be generalised to

$$D(c) = D_1 \cdot \frac{\partial c_1}{\partial c} + D_2 \cdot \frac{\partial c_2}{\partial c} + D_3 \cdot \frac{\partial c_3}{\partial c} + \ldots . \quad \ldots .(2\text{-}95)$$

where subscript 2 refers to dimer, etc. The terms $\partial c_2/\partial c$, $\partial c_3/\partial c$ etc. are obtained from equation (2-88) and the D-c relationship calculated for given values of D_2, D_3 etc. Barrie and Platt[43] used a simple analogy with results obtained[97] for relative values of D for methane, ethane and propane diffusion in natural rubber to estimate values for D_2 and D_3. However their experimental data were not sufficiently accurate to establish whether or not polymeric water species do contribute significantly to the diffusion process.

Rogers[2] pointed out that when the activation energy for the diffusion of a cluster of water molecules exceeds the energy required for a water molecule to break free from the cluster then cluster diffusion is unlikely to occur to any appreciable extent. This would seem to suggest that only the smallest associated water species contribute

appreciably to the transport process. It appears reasonable therefore, to extend the simplest situation considered in 2.7.2 of this section to one where three forms of water are considered i.e. mobile, less mobile (lower diffusion coefficient) and immobile.

The case of diffusion with instantaneous chemical reaction was extended by Standing et al.[98] to include the case where the product diffuses concurrently with the reactant but has a different diffusion coefficient. They derived the equation

$$D = (D_1 - D_2) \cdot \frac{\partial c_1}{\partial c} + D_2 \qquad \ldots.(2\text{-}96)$$

where subscript 1 refers to reactant and subscript 2 refers to product. If this treatment is applied to the case of the three forms of water mentioned above then equation (2-96) is equivalent to equation (2-95) with D_3, D_4 etc. equal to zero and with D_2 an average diffusion coefficient describing the diffusion of all the clustered species which are mobile.

One immediate limitation of this simple polycondensation model arises since at the gel point $\frac{\partial c_n}{\partial c}$ is zero for all finite values of n. The model therefore predicts a zero overall diffusion coefficient at the saturation point (e.g. Figure 2-2) whether or not polymeric water species

contribute to diffusion. In a practical sense, however, this does not constitute a serious drawback because although D becomes zero, the corresponding diffusive flux $J = -D \frac{\partial c}{\partial x}$ is non-zero as $\frac{\partial c}{\partial x}$ goes to infinity at the saturation point.

Since the unassociated water molecule contains two hydrogen atoms and two lone pairs of electrons it is strictly a monomer of the A_2B_2 type, where A-B bond formation only is possible, rather than of the A_4 type as exemplified by pentaerithrytol. However the probabilities that a lone pair of electrons and a hydrogen atom have undergone reaction at any time are identical because of the stoichiometry of the reaction so that all the four "functionalities" of a water molecule may be considered identical in this sense. The equilibrium constant K considered above would be changed in the case of a A_2 B_2 type monomer, but the weight fraction distribution and the <u>shapes</u> of the sorption isotherm and D-c curve remain identical to those expressed above (M. Gordon, private communication).

2.7.5 <u>Non-Random Polycondensation of Water</u>

The random case discussed above neglects two main effects. Firstly ring formation may occur during the polycondensation process. It is assumed that the effect of

this is small except at close to the gel point, and so is neglected in the present analysis. The other possibility is the co-operative effect whereby formation of one hydrogen bond facilitates the formation of others. This effect is extremely important in liquid water and is perhaps unlikely to be negligible for water sorbed in a polymer. Since the effect is a consequence of the resonance stabilisation of associated species due to the partial covalent character of the hydrogen bond[32], the chance of a particular species growing by further hydrogen bond formation will depend on the number of hydrogen bonds already present in the whole of that species. However as a first approximation, the chance of further hydrogen bond formation can be considered to depend only on the number of hydrogen bonded links already present on the monomer unit of water to which the new bond is to be attached. This is termed a first shell substitution effect.

Gordon and Scantlebury[99] have treated mathematically the particular case of a linear first shell substitution effect i.e. when the free energy of hydrogen bond formation is a linear function of the total degree of substitution of the two monomer units to be bonded or

$$\Delta G^{\circ} = \Delta G^{\circ *} + i \Delta G^{\neq} \qquad \ldots.(2\text{-}97)$$

where ΔG^{o} is the standard free energy for the formation of one mole of hydrogen bonds of a particular type, ΔG^{o*} is the corresponding standard free energy in the case of the random reaction, $\Delta G^{\neq}$ is the change in free energy brought about by each link that the two participating units already carry and i is the degree of substitution of the pair of participating units.

When $\Delta G^{\neq}$ is small in comparison with ΔG^{o*} i.e. the system is given a small perturbation from the equilibrium situation for the random polycondensation, an average free energy $\overline{\Delta G}^{o}$ is given by

$$\overline{\Delta G}^{o} = \Delta G^{o*} + 6 \alpha . \Delta G^{\neq} \qquad ....(2\text{-}98)$$

since 6α is the average degree of substitution of all pairs of bondable units throughout the system.

A quantity ϵ may be defined[99] by the relation

$$\exp (- \Delta G^{\neq}/2 RT) = 1 + \epsilon \qquad ....(2\text{-}99)$$

where ϵ, which must remain small in comparison with unity, is a convenient measure of the free energy change due to the substitution effect and is expressed in units of -2RT (if higher terms in ϵ are neglected). For random hydrogen bond formation ϵ is zero. Rewriting equations (2-98) and (2-99) in terms of the equilibrium constants for hydrogen bond breaking

gives

$$+ RT \ln \bar{K} = + RT \ln K - 12\alpha \cdot RT \ln (1+\varepsilon)$$

where $\bar{K}$ is an average equilibrium constant for the system at fractional conversion α and K is the equilibrium constant in the random case. Substitution for K using equation (2-86) gives

$$\bar{K} = \frac{c\,(1-\alpha)^2}{\alpha(1+12\alpha\varepsilon)} \qquad \ldots.(2\text{-}100)$$

again neglecting higher powers of ε.

The weight fraction distribution equation was derived by Gordon and Scantlebury[99] and is

$$\frac{c_n}{c} = \mathcal{N} \cdot \frac{4(3n)!\,(1-\alpha)^{2n+2}\,\alpha^{n-1}}{(n-1)!\,(2n+2)!} \left[1 + \varepsilon \left\{ \frac{(n-1)(14n-18)}{(3n-1)} + (n-1)(12\alpha^2 - 12\alpha - 2) + 12\alpha \right\} \right] \qquad \ldots.(2\text{-}101)$$

where $\mathcal{N}$ is a normalisation factor $\cong 1$.

Hence for the concentration of monomeric water

$$c_1 = c(1-\alpha)^4 (1 + 12\alpha\varepsilon) \qquad \ldots.(2\text{-}102)$$

Gordon and Scantlebury[99] also computed α_s the value of α at saturation as functions of ε. From their

curve for a tetrafunctional monomer, when ε is small the relation

$$\alpha_s = \frac{1}{3}(1 - \varepsilon) \qquad \ldots.(2\text{-}103)$$

appears to hold a good approximation. A combination of equations (2-100) and (2-103) yields

$$\bar{K}_s = \frac{4c_s}{3}(1 - 2\varepsilon) \qquad \ldots.(2\text{-}104)$$

again neglecting powers of ε higher than the first.

Assuming that monomer sorption follows Henry's law, the relations

$$p = \frac{c}{\sigma_1}(1-\alpha)^4(1+12\alpha\varepsilon) \text{ and } p_0 = \frac{16c_s}{81\sigma_1}(1 + 6\varepsilon)$$

hold, the latter resulting from substitution for α_s using equation (2-103). The equilibrium sorption isotherm equation is then given by

$$(p/p_0) = \frac{81}{16}\cdot\left(\frac{c}{c_s}\right)\cdot\frac{(1-\alpha)^4(1 + 12\alpha\varepsilon)}{(1 + 6\varepsilon)} \qquad \ldots.(2\text{-}105)$$

From equation (2-98), $\overline{\Delta G}^o$ and hence $\bar{K}$ are strictly functions of α. However, to enable equilibrium sorption isotherms to be constructed, it is assumed as a further approximation that $\bar{K}$ remains constant. As for the

the previous assumptions this is a reasonable approximation only if ε remains small.

Equations (2-100), (2-104) and (2-105) can then be combined to yield

$$(p/p_0) = \frac{27}{4} \cdot \alpha (1-\alpha)^2 (1-8\varepsilon) (1 + 24\alpha\varepsilon) . \quad \ldots.(2\text{-}106)$$

Sorption isotherms can be constructed for given values of ε by first calculating values for α using equations (2-100) and (2-104) for particular values of c and then substituting into equation (2-106). Some isotherms plotted for various values of ε are illustrated in Figure 2.1.

The D-c relation can also be obtained assuming monomeric water diffusion only, since from equations (2-100) and (2-102)

$$\frac{\partial c_1}{\partial c} = \frac{(1-\alpha)^4 (1-3\alpha + 48\alpha\varepsilon - 96\alpha^2\varepsilon)}{(1 + \alpha + 24\alpha\varepsilon)} \quad \ldots.(2\text{-}107)$$

The D-c relationship follows from equations (2-100), (2-104), (2-107) and (2-93). D-c curves for various values of ε are illustrated in Figure 2.2.

As $c \rightarrow 0$, $\alpha \rightarrow 0$ and $\frac{\partial c_1}{\partial c} \rightarrow 1$ so that D_1 is again identified with $D_{c=0}$.

FIG. 2·1

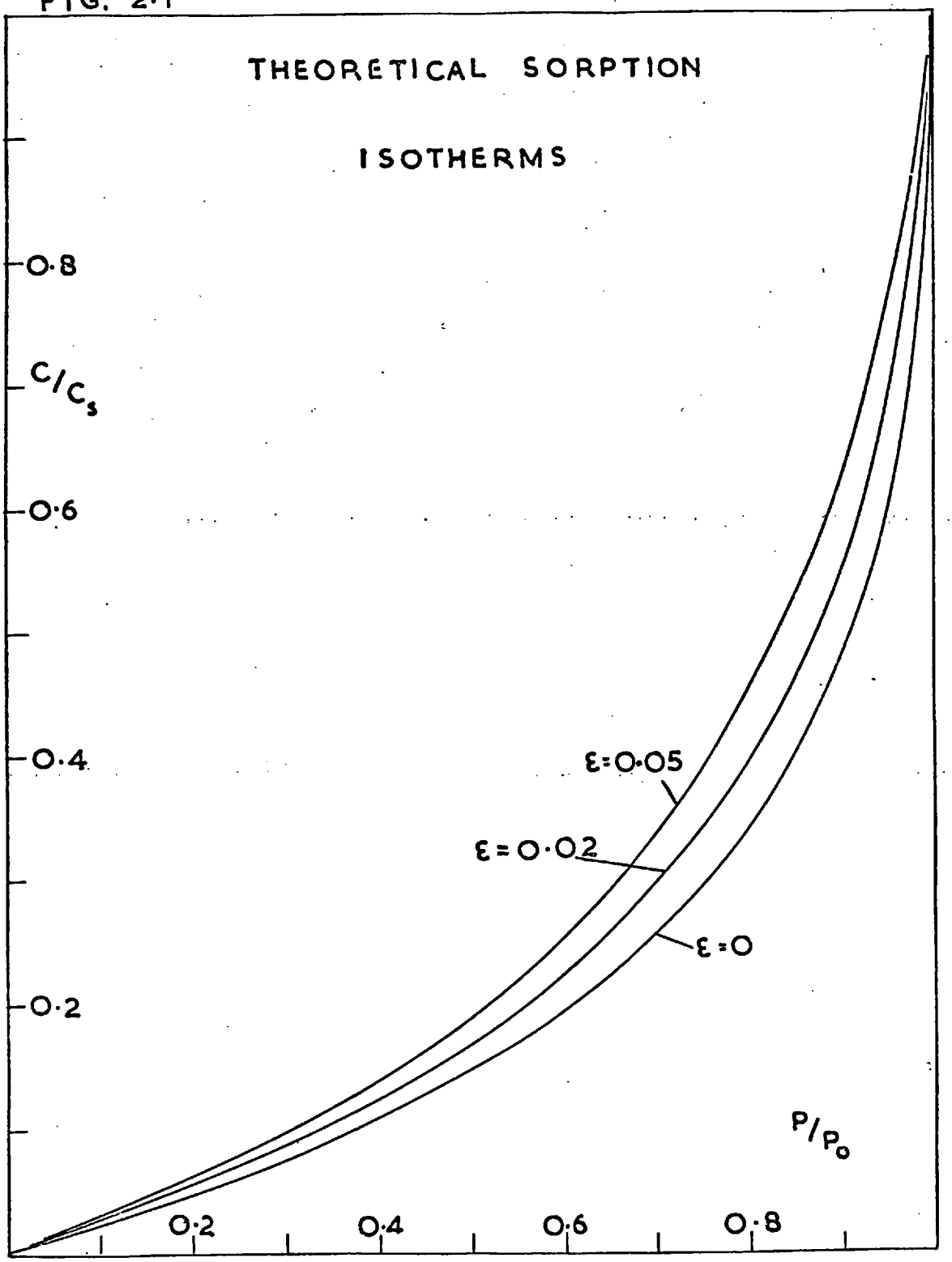
THEORETICAL SORPTION
ISOTHERMS
0·8
C/Cs
0·6
0·4
0·2
ε=0·05
ε=0·02
ε=0
P/Po
0·2
0·4
0·6
0·8

FIG. 2·2

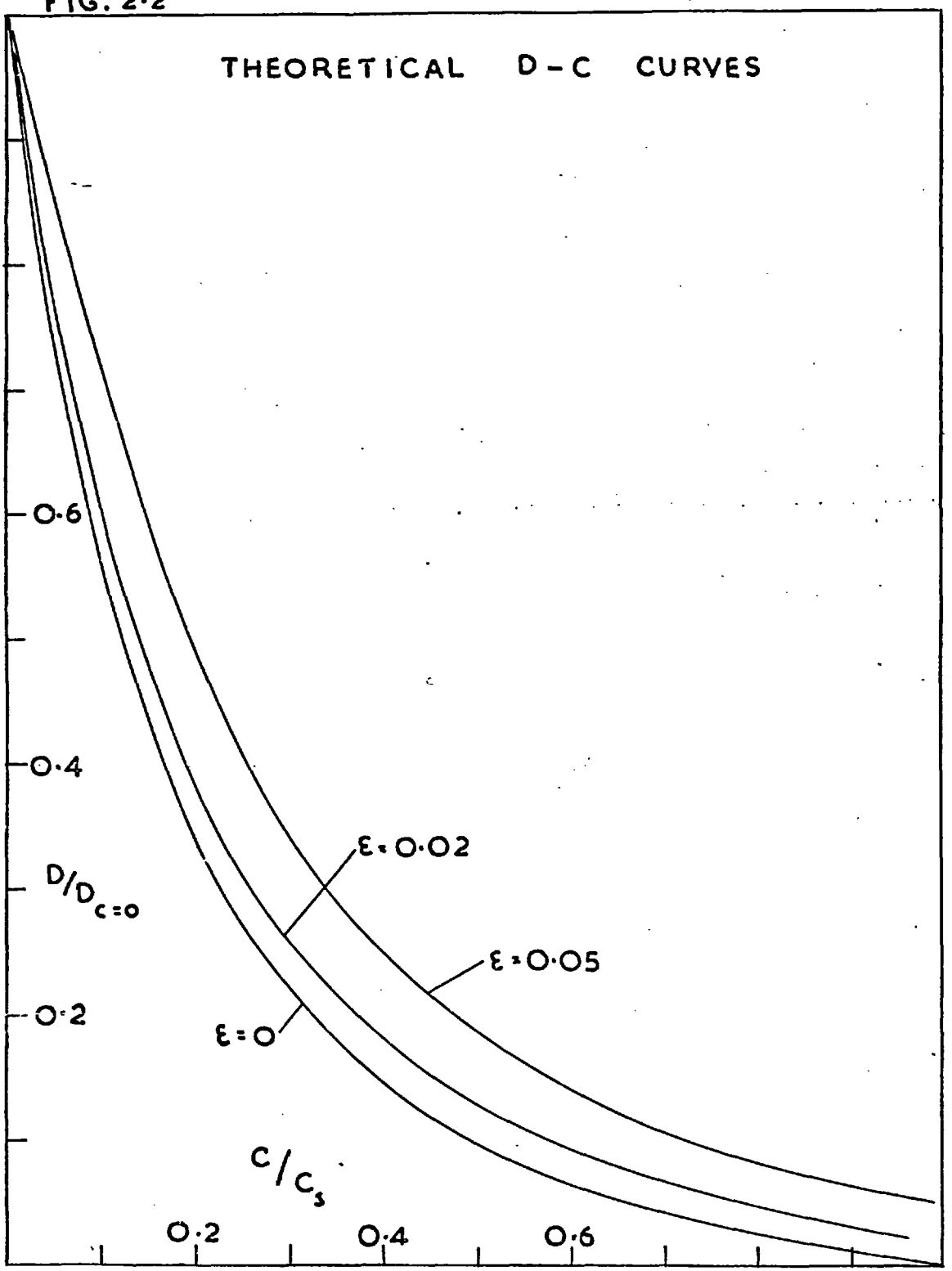

Although the above treatment is only very approximate it is useful in the sense that it provides a limiting, ideal model which can be compared with the corresponding model for random polycondensation and used to predict qualitatively the effect on water sorption and diffusion of a stronger co-operative effect in hydrogen bonding.

2.7.6 Influence of Polymer Structure and total Water Concentration

Parts 2.7.4 and 2.7.5 of this section were concerned with situations where no specific interactions between water and polymer exist, and part 2.7.3 with situations where very strong water-polymer interactions are present. In intermediate cases where a polymer contains moderately polar groups such as ester linkages, water clustering may still be the predominant factor in determining the D-c relationship but smaller contributions might also occur from mechanisms involving specific site interactions e.g. equation (2-84) with α close to unity and β very small. In addition the overall sorbed water concentration might be sufficient to cause slight plasticisation, especially in the more glassy polymers. Under these circumstances equations (2-94) and (2-95) would tend to

overestimate the decrease in D with increasing c as was found for the water-polymethylmethacrylate system[43].

If the polymer structure is a significant factor in initiating or in physically terminating the growth of clusters then further deviation from the simple models is to be expected.

The rate of water migration inside a cluster may be very rapid[2] but in general is virtually random in direction owing to the absence of a concentration gradient inside a cluster. However small differences in chemical potential must still exist between different water molecules in a cluster if these are in equilibrium with free water molecules. Although an isolated cluster might not diffuse it would be unlikely to act as a significant geometric impedance to the diffusion of free water molecules. If the total water concentration inside a polymer is sufficiently high an effective "continuum of clusters" through a membrane may exist resulting in very rapid transport of water. This appears to be the case for water in certain polyelectrolyte membranes[100].

2.7.7 Methanol as a comparative monomer for Random Polycondensation in an Inert Medium

Methanol has been considered[59] as a polycondensation monomer of type AB_2 corresponding to one hydrogen atom and two lone pairs of electrons available for hydrogen bonding. The equation for the weight fraction of n-mer is[96]

$$\frac{c_n}{c} = \frac{(1-2\alpha) \cdot \alpha^{n-1} \cdot (1-\alpha)^{n+1} \cdot (2n)!}{(n-1)! \ (n+1)!} \quad \ldots.(2\text{-}108)$$

and the equilibrium constant for the breaking of a hydrogen bond is given by

$$K = \frac{c(1-\alpha)(1-2\alpha)}{\alpha} \quad \ldots.(2\text{-}109)$$

However in this type of polycondensation gelation does not occur until the polymerisation is complete when $\alpha_s = 1/2$, and so K cannot be determined independently.

For monomeric methanol equation (2-108) yields

$$c_1 = c(1-\alpha)^2 (1-2\alpha) \quad \ldots.(2\text{-}110)$$

Assuming that the sorption of monomeric methanol follows Henry's law the isotherm equation is

$$p = \frac{c}{\sigma_1} (1-\alpha)^2 (1-2\alpha) \quad \ldots.(2\text{-}111)$$

Barrie[59] adopted the practical procedure of

calculating σ_1 from the initial slope ($\alpha \rightarrow 0$) of the experimental isotherm for polydimethylsiloxane-methanol and choosing a suitable value of the parameter K for the best fit to the experimental curve. The overall isotherm shape was then in quite good agreement with that obtained from equation (2-111).

From equations (2-109), (2-110) and (2-93)

$$D = D_1 \left[\cdot \frac{K}{2c} \cdot \frac{\alpha\left[(1-\alpha)^2+(1-2\alpha)(1-\alpha)\right]}{\alpha - 1/4\ (3 + K/c)} +(1-\alpha)^2(1-2\alpha) \right] \quad \ldots.(2\text{-}112)$$

As for the water polycondensation scheme when $c \rightarrow 0$, $\alpha \rightarrow 0$ and $D_1 \rightarrow D_{c=0}$ so that the D-c relation can be obtained from equation (2-112) if a suitable value for K is selected. This treatment, as that for water, assumes monomer diffusion only. For the polydimethylsiloxane-methanol system permeation rates depend linearly on the ingoing pressure[59], and so because of equation (2-26), the experimental D-c curves for this system are well represented by equation (2-112) assuming the same value for K as in the isotherm fit.

2.7.8 The Concentration Dependence of the Permeability Coefficient

The permeability coefficient for water in the more

hydrophilic polymers such as polyvinylalcohol[39] increases markedly with sorbed water concentration since both D and σ increase with c. However for water in several relatively hydrophobic polymers[42,43,49] P is constant even though D and σ each vary with c. This behaviour was also observed for methanol in polydimethylsiloxane[59]. Three main explanations have been put forward to account for these observations[51,59, 101-3].

i) Stannett et al.[42,49,51] proposed that association of water takes place under equilibrium sorption but not under permeation conditions, and further that monomeric water has constant D_1 and σ_1. The physical reason for the different behaviour under sorption and permeation conditions was assumed to be a slow nucleation time for cluster growth leading to the establishment of a quasi-steady state in permeation.

ii) Barrie[59] pointed out that if the monomeric water sorption obeyed Henry's law and if the diffusion coefficient for monomeric water were constant then provided that only this species

contributes to the total flux the permeability coefficient would be constant whether or not association takes place. This explanation could possibly be extended to cover the case where small polymeric water species also diffuse, each having a constant value of D.

For example, if only monomer and dimer diffusion is considered then the flux J is given by

$$J = -\left(D_1 \frac{\partial c_1}{\partial c} + D_2 \frac{\partial c_2}{\partial c}\right) \cdot \frac{\partial c}{\partial x} \qquad \ldots.(2\text{-}113)$$

assuming negligible interaction of flows. Figure 2-3 shows J plotted vs. p/p_0 for various values of D_2/D_1. The random polycondensation model, as outlined in part 2.7.4 of this section, was used together with equation (2-113). For the J - p/p_0 plot to appear linear within a normal experimental scatter it would seem that D_2/D_1 should be less than ~ 0.2.

iii) Some authors have proposed[101-3] that diffusion is dependent on a gradient of activity rather than of concentration of the diffusing species.

FIG. 2·3

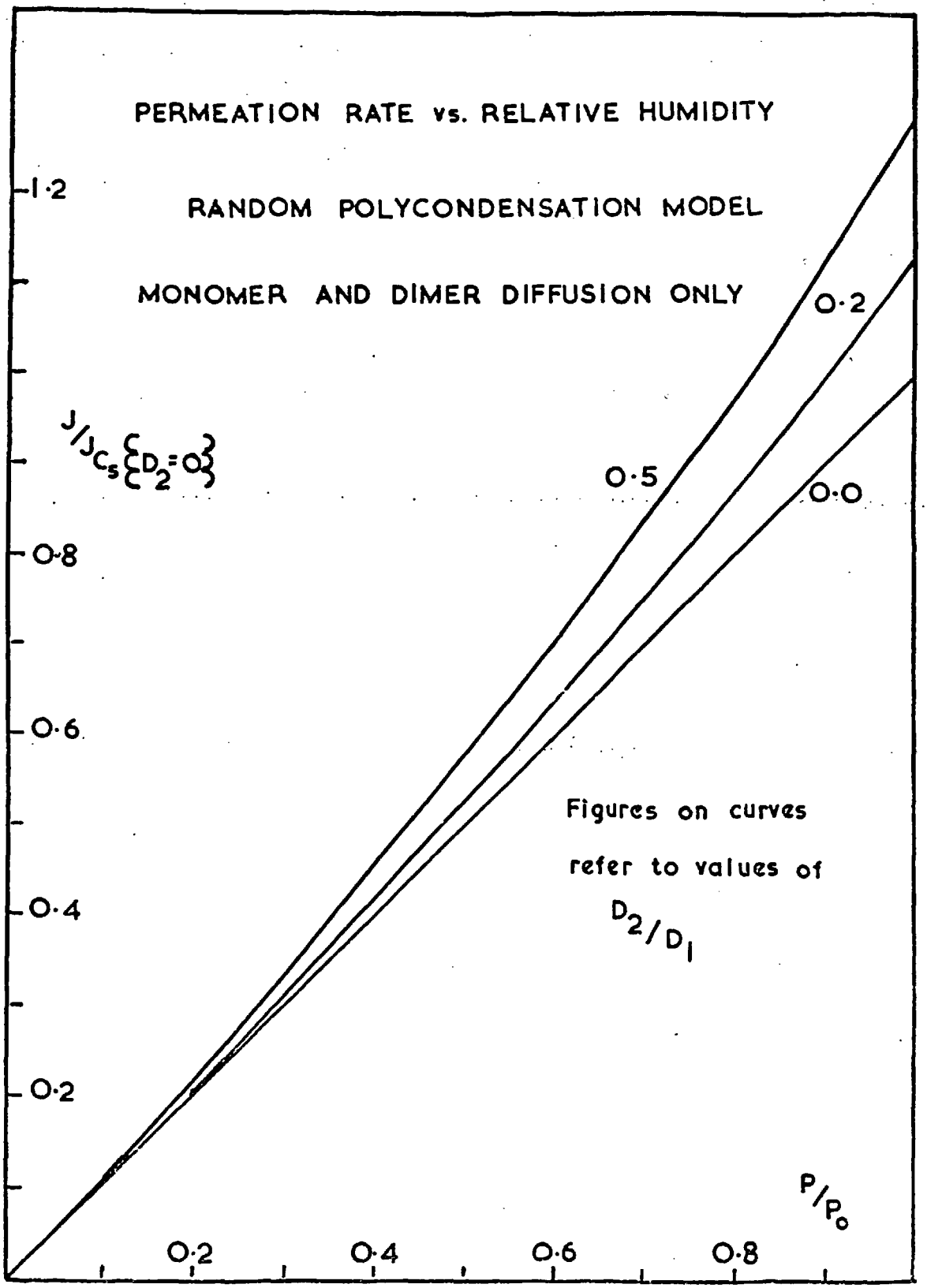
PERMEATION RATE vs. RELATIVE HUMIDITY
RANDOM POLYCONDENSATION MODEL
MONOMER AND DIMER DIFFUSION ONLY
J/J_Cs {D_2=0}
1·2
0·8
0·6
0·4
0·2
0·2
0·4
0·6
0·8
P/P_o
0·2
0·5
0·0
Figures on curves refer to values of D_2/D_1

If this is expressed mathematically as

$$J = - BRT \cdot (\partial a / \partial x) \qquad \ldots.(2\text{-}114)$$

then this is equivalent to

$$J = - B \cdot a \cdot (\partial \mu / \partial x) \qquad \ldots.(2\text{-}115)$$

i.e. to equation (2-72) with concentration replaced by activity. Since the relative humidity (p/p_0) is a measure of activity it follows that J vs. p would be linear, and hence P constant, for constant B.

Equation (2-114) has been proposed in general when osmotic mechanisms were being considered[101,102]. Kuppers and Reid[103], however, proposed it as an expedient to maintain a constant diffusion coefficient, i.e.

$$J = - D(c) \cdot \frac{\partial c}{\partial x} \quad \text{becomes}$$

$$J = - D' \cdot \frac{\partial a}{\partial x} \qquad \ldots.(2\text{-}118)$$

where D' is constant and a was defined as a "diffusive activity" not necessarily equal to the thermodynamic activity. This procedure is in fact rather similar to that discussed in ii) above since "diffusive activity" could be termed "effective concentration for diffusion" - i.e. monomer concentration in the simplest case.

There is little evidence for hydrogen bonding in the vapour phase for water. However, if dimers are postulated then two separate Henry's law sorptions may occur

$$\left.\begin{aligned} c_1 &= \sigma_1 p_1 \\ c_2 &= \sigma_2 p_2 \end{aligned}\right\} \qquad \ldots.(2\text{-}119)$$

where subscript 2 refers to dimer and $p_1 + p_2 = p$ the ingoing pressure. If now it is assumed that $D_2 \sigma_2$ is close in magnitude to $D_1 \sigma_1$ then a linear J-p dependence, i.e. constant P, results from the equations (2-119).

2.7.9 Concentration and Temperature Dependence of E_D, $\Delta\bar{H}_A$ and $\Delta\bar{S}_A$.

In systems where D increases with increasing c as a result of plasticisation, the activation energy for diffusion E_D generally decreases with increasing c as the progressive loosening of the polymer structure enables more segments to play a part in a unit diffusion step, thus facilitating the process.

On the other hand when clustering of water occurs with only monomer diffusing then since $D = D_o \exp(-E_D/RT)$, the temperature dependence of equation (2-93) can be written

as

$$-\frac{E_D}{R} = \frac{-E_{D(c=0)}}{R} + \left[\frac{\partial \ln \left(\frac{\partial c_1}{\partial c}\right)}{\partial (1/T)}\right] \qquad \ldots.(2\text{-}120)$$

When D decreases with c it can be argued qualitatively[59] that for a given concentration $\partial c_1 / \partial c$ will increase with increasing temperature because of the increasing ease of hydrogen bond rupture. Hence E_D will exceed $E_{D(c=0)}$ for all finite values of c. Since the proportion of hydrogen bonds available for breaking becomes greater for higher c, it can be predicted that E_D will increase continuously with c for a given temperature range.

For the random polycondensation model the concentration dependence of E_D has not previously been formulated quantitatively, but may be derived as follows.

The temperature dependence of equation (2-94) can be written

$$E_D = E_{D(c=0)} - 3R\left(\frac{\partial \ln (k-K)}{\partial (1/T)}\right) - R\left(\frac{\partial \ln \left[\frac{8K}{k} - \frac{3(k-K)}{c}\right]}{\partial (1/T)}\right) \qquad \ldots.(2\text{-}121)$$

Although E_D will be a function of both c and T the concentration dependence may be established for a mean value $\bar{E}_D$ over a given temperature range $(T\text{-}T_0)$ by the use of a reference temperature (T_0), where T_0 is most conveniently

identified with the lowest temperature of the range.

Since

$$\frac{\partial \ln K}{\partial (1/T)} = - \frac{\Delta H}{R} \qquad \ldots.(2\text{-}122a)$$

where ΔH is the energy required to break a hydrogen bond in an inert continuum[57] then on integration

$$\ln (K/K_0) = - \frac{\Delta H}{R} \left(\frac{1}{T} - \frac{1}{T_0} \right) \qquad \ldots.(2\text{-}122b)$$

where K_0 is the value of K at temperature T_0. It is also convenient to define a reduced concentration C as

$$C = \frac{4c}{3K_0} \qquad \ldots.(2\text{-}123)$$

so that C cannot exceed unity if the whole temperature range is to be included. k is now given by

$$k = K \left(1 + \frac{3 K_0 C}{K}\right)^{\frac{1}{2}} \qquad \ldots.(2\text{-}124)$$

From equations (2-121) to (2-124) it can be deduced (appendix 9.3) that

$$\bar{E}_D = E_{D(c=0)} + \Delta H \cdot \frac{(X-1)}{X} \left[2 + \frac{(X+1)}{X(2-X)} \right] \qquad \ldots.(2\text{-}125)$$

where $$X = \left(1 + 3C \exp \left[+ \frac{\Delta H}{R} \left(\frac{1}{T} - \frac{1}{T_0} \right) \right] \right)^{\frac{1}{2}} \qquad \ldots.(2\text{-}126)$$

so that $X \rightarrow 1$ as $C \rightarrow 0$.

Hence values for $\bar{E}_D$ can be calculated if ΔH

is known. Literature values[11] for ΔH span the range 3.4-6.6 kcal.mole^{-1}. Calculated values of $\bar{E}_D$ for various values of C over different temperature ranges using the maximum and minimum values for ΔH are given in Table 2-1. The value chosen for ΔH appears to be of less significance than the temperature range considered. It can be seen that $\bar{E}_D$ increases continuously with C as expected.

A similar procedure can be carried out to calculate the concentration dependence of the heat of dilution. A combination of equations (2-51) and (2-92) yields

$$\Delta\bar{H}_A = 4R \left(\frac{\partial \ln(k-K)}{\partial (1/T)} \right) - R \left(\frac{\partial \ln K}{\partial (1/T)} \right) \qquad \ldots.(2\text{-}127)$$

It follows (see appendix 9.3) that

$$\overline{\Delta \bar{H}_A} = \Delta H \left(\frac{2-X}{X} \right) \qquad \ldots.(2\text{-}128)$$

where $\overline{\Delta \bar{H}_A}$ is an average value of $\Delta\bar{H}_A$ over a given temperature range and X is defined by equation (2-126). As $C \rightarrow 0$, $X \rightarrow 1$ and $\overline{\Delta\bar{H}_A} \rightarrow \Delta H$ so that $\overline{\Delta\bar{H}_A}$ is very dependent on the value taken for ΔH. Computed values of $\overline{\Delta\bar{H}_A}$ are given for two different temperature ranges in Table 2-1. They are more dependent on the value of ΔH than on the temperature range, and decrease continuously with increasing C.

TABLE 2-1

Random Polycondensation of Water : Theoretical Values for $\Delta\bar{E}_D$ ($= \bar{E}_D - E_{D(c=0)}$), $\overline{\Delta\bar{H}_A}$ and $\overline{\Delta\bar{S}_A}$.

Temp. Range	C	$\Delta\bar{E}_D$ kcal.mole^{-1}		$\overline{\Delta\bar{H}_A}$ kcal.mole^{-1}		$\overline{\Delta\bar{S}_A}$ cal.deg^{-1} mole^{-1}	
		ΔH=3.4	ΔH=6.6	ΔH=3.4	ΔH=6.6	ΔH=3.4	ΔH= 6.6
	0	0	0	3.40	6.60	∞	∞
	0.1	0.93	0.97	2.94	6.12	11.9	22.6
	0.2	1.74	1.86	2.57	5.69	9.6	20.0
	0.3	2.46	2.69	2.25	5.30	8.1	18.2
	0.4	3.14	3.47	1.98	4.94	6.9	16.7
20-60°C	0.5	3.79	4.21	1.75	4.62	6.0	15.4
	0.6	4.43	4.92	1.54	4.32	5.2	14.2
	0.7	5.08	5.60	1.36	4.04	4.5	13.2
	0.8	5.77	6.27	1.19	3.78	3.9	12.3
	0.9	6.50	6.92	1.04	3.54	3.4	11.4
	1.0	7.31	7.57	0.91	3.32	2.9	10.7
	0	0	0	3.40	6.60	∞	∞
	0.1	1.28	1.85	2.78	5.70	11.0	20.6
	0.2	2.35	3.44	2.30	4.96	8.5	17.2
	0.3	3.31	4.88	1.92	4.33	6.8	14.7
	0.4	4.23	6.21	1.60	3.80	5.6	12.7
30-50°C	0.5	5.15	7.50	1.34	3.34	4.6	11.1
	0.6	6.14	8.77	1.11	2.94	3.7	9.6
	0.7	7.26	10.1	0.92	2.58	3.0	8.4
	0.8	8.60	11.4	0.74	2.26	2.4	7.3
	0.9	10.3	12.9	0.59	1.97	1.9	6.3
	1.0	12.8	14.6	0.45	1.71	1.4	5.5

The entropy of dilution $\Delta\bar{S}_A$ is given by equation (2-52). It is shown in appendix 9.3 that

$$\overline{\Delta\bar{S}_A} = \frac{-3\Delta H}{T_o} + \frac{2\Delta H}{T} \cdot \frac{(X+1)}{X} - 4R \ln (X-1) + 3R \ln (C)$$

where $\overline{\Delta\bar{S}_A}$ is an average value of $\Delta\bar{S}_A$ over a given temperature range. As $C \rightarrow 0$ it can be shown by the use of L'Hôpital's rule that $\overline{\Delta\bar{S}_A} \rightarrow \infty$. Values of $\overline{\Delta\bar{S}_A}$ are included in Table 2-1 and decrease with increasing C. $\overline{\Delta\bar{S}_A}$ is also much more dependent on the value of ΔH than on the temperature range.

2.7.10 Rates of Immobilisation of Water Molecules

Parts 2.7.2 - 2.7.9 of this section have been concerned with situations where the rate of immobilisation of penetrant is very rapid in comparison with the rate of diffusion. It has not been established that this is always the case for the immobilisation of water molecules and so more general situations in which the rates of diffusion and immobilisation are comparable have to be considered.

Crank[94] investigated the case of diffusion with a concurrent, reversible chemical reaction which is first order in that the forward reaction goes at a rate proportional to the concentration of mobile penetrant and the backward reaction at a rate proportional to the concentration of immobile penetrant, i.e.

$$\frac{\partial c_b}{\partial t} = \lambda c_f - \mu c_b \qquad \ldots.(2\text{-}129)$$

where λ and μ are the forward and backward rate constants. Equation (2-79) then becomes

$$\frac{\partial c_f}{\partial t} = \frac{\partial}{\partial x}\left(D_f \cdot \frac{\partial c_f}{\partial x} \right) - \left(\lambda c_f - \mu c_b \right) \ldots.(2\text{-}130)$$

With D_f constant Crank[94] obtained a solution to equation (2-130) for sorption into or desorption from a plane sheet in the form of expressions for M_t/M_∞ which involve series solutions. A number of reduced sorption curves were computed for various values of the ratios (λ/μ) and $(\mu l^2/D_f)$ where l is the thickness of the sheet. The latter ratio is a measure of the relative rates of immobilisation and diffusion. It was found[94] that when $(\mu l^2/D_f)$ is small (0.01), plots of M_t/M_∞ vs. $t^{\frac{1}{2}}/l$ display "shoulders" the heights of which increase as (λ/μ) is decreased. For $(\mu l^2/D_f)$ about unity, sigmoid shaped curves are obtained, and when $(\mu l^2/D_f)$ exceeds $\sim$ 10, the curves differ very little from those expected for a purely diffusion-controlled system.

In the case of water clustering, as an oversimplification the equilibria

$$(H_2O)_f + \left[(H_2O)_b\right]_n \rightleftharpoons \left[(H_2O)_b\right]_{n+1}$$

$$2\,(H_2O)_f \rightleftharpoons \left[(H_2O)_b\right]_2$$

can be considered, where monomeric water only is mobile, so that

$$\frac{\partial c_b}{\partial t} = c_f (\lambda_f c_f + \lambda_b c_b) - \mu_b c_b$$

where λ_b and μ_b represent some sort of average rate constants for the clustered water.

Unfortunately, this type of equation in conjunction with equation (2-79) has not been solved either analytically or numerically, although it is presumed that the principal features of reduced sorption curves would not be too different from those for the case of the unimolecular reaction. For non-random hydrogen bonding the situation would be further complicated in that (λ/μ) would depend on c_f and c_b.

No solution for permeation with non-instantaneous immobilisation has been formulated as yet. It has been pointed out[51] that for very slow rates of immobilisation an apparent or quasi-steady state could be set up giving a measured time lag independent of c even though the true steady state D decreases with increasing c.

CHAPTER 3

SORPTION, DIFFUSION AND PERMEATION IN FILLED POLYMERS

Fillers are generally introduced into elastomers for the purpose of improving their tensile strength. This reinforcing effect of a filler is due largely to strong interactions between polymer chain segments and filler particles and most reinforcing fillers are therefore wetted to some degree by bulk polymer. The solubilities of gases and vapours in filled polymers are often significantly increased[4] in comparison with those in the corresponding unfilled polymers illustrating that the filler surface need not be completely wetted by the polymer. The nature of polymer-filler interactions is not always clear[104] and for a given system may include chemical bonding, van der Waals interactions or both. Bueche[105] deduced that relatively non-porous fillers are more efficient than the porous type in their reinforcing action.

A uniform dispersion of filler in a polymer is difficult to achieve and aggregation of filler particles is often encountered. As the number of polymer-filler interactions depends on the interfacial area presented, the degree of aggregation can be an important factor in determining

the sorptive capacity of a filled polymer for a penetrant.

For fine silica fillers incorporated into silicone rubber, with which this present work is partly concerned, surface hydroxyl groups on the filler appear to play an important role[106]. The effect of milling the filler prior to incorporation in the gum is to reduce the interaction between filler and polymer. It was suggested[106] that some aggregated structure of silica particles is created during this process which is not destroyed on subsequent milling with the rubber.

3.1 Effect of Fillers on the Sorption of Permanent Gases

Different types of filler can affect the sorption process in a number of ways[4,22]. If sorption on or in the filler is negligible then the overall solubility σ of a gas is proportional to the fraction of bulk polymer, i.e.

$$\sigma = \sigma_B \phi_B \qquad \ldots.(3\text{-}1)$$

where ϕ is volume fraction and subscript B refers to bulk polymer. When sorption by the filler is important

$$\sigma = \sigma_B \phi_B + \sigma_F \phi_F \qquad \ldots.(3\text{-}2)$$

where subscript F refers to filler. If air gaps are also present the overall solubility is increased, and

$$\sigma = \sigma_B \phi_B + \sigma_F \phi_F + \sigma_G \phi_G \qquad \ldots.(3\text{-}3)$$

where subscript G refers to air gaps.

Partial agreement with equations (3-1) and (3-2) has been obtained in some filled polymer-gas systems[23,107].

3.2 Effect of Fillers on the Diffusion and Permeation of Gases

In the strictest sense, Fick's laws cannot be applied to diffusion in heterogeneous media which include dispersed phases. However a procedure which has often been adopted is to modify the equations of flow for corresponding homogeneous media (unfilled polymers) by means of structure factors[23,107, 108]. Thus the flux per unit cross-sectional area of filled polymer is

$$J = -D_B \phi_B \cdot \mathcal{K} \cdot \frac{\partial c_B}{\partial x} \qquad \ldots.(3\text{-}4)$$

provided that no transport through the filler or along interfaces occurs. $\mathcal{K}$ is termed the structure factor for the system and allows for, amongst other factors, the increase in the average diffusion path length due to the presence of the filler. From equation (3-4)

$$D \frac{\partial c}{\partial x} = D_B \phi_B \mathcal{K} \cdot \frac{\partial c_B}{\partial x} \qquad \ldots.(3\text{-}5)$$

where D is the experimentally observed diffusion coefficient cf gas in the filled polymer. When sorption on or in the

filler occurs then equation (3-2) may be applied so that

$$D = \mathcal{K} D_B \frac{\phi_B}{(\phi_B + \phi_F \cdot \sigma_F/\sigma_B)} \quad \ldots.(3\text{-}6)$$

For zero sorption on filler, $\sigma_F = 0$ and

$$D = \mathcal{K} D_B \quad \ldots.(3\text{-}7)$$

The permeation flux per unit area of unfilled polymer is given by $J_B = -D_B \cdot \partial c_B/\partial x$, so that

$$J = \mathcal{K} \phi_B J_B$$

or

$$P = \mathcal{K} \phi_B P_B \quad \ldots.(3\text{-}8)$$

where P and P_B are the permeability coefficients of gas in filled and unfilled polymer respectively. Equation (3-8) applies whether or not sorption by the filler occurs provided that any sorbed gas is immobile.

3.2.1 The Structure Factor

Expressions relating $\mathcal{K}$ to ϕ_B and the dimensions of filler particles have been derived from the electrical analogue of heterogeneous conductors, i.e. dispersions of particles with a conductivity different from that of the bulk phase. Maxwell[109] deduced that for a random array of non-conducting spheres sufficiently dilute so as to neglect

interference effects between spheres,

$$K = \frac{2}{3 - \phi_B} \qquad \ldots.(3\text{-}9)$$

More sophisticated treatments by Rayleigh[110], Fricke[111], Runge[112] and Meredith and Tobias[113] amongst others allowed for interference effects and also for various shapes of the dispersed particles. For example, Rayleigh obtained for non-conducting spheres[110]

$$K = \frac{1}{\phi_B} \left(\frac{2 - 2\phi_F - 0.394\ \phi_F^{10/3}}{2 + \phi_F - 0.394\ \phi_F^{10/3}} \right) \qquad \ldots.(3\text{-}10)$$

Nielsen[114] considered K simply as a tortuosity factor, defined as

$$K = \frac{\text{film thickness}}{\text{average distance travelled to get through the film}}$$

For simple non-interacting square plates of side L and thickness W uniformly oriented perpendicular to the direction of flow, then

$$K = \frac{1}{1 + (L/2W)\ \phi_F} \qquad \ldots.(3\text{-}11)$$

For oriented lamellar fillers, $L \gg W$ and K is relatively small. In the case of cubes, L=W and equation (3-11) reduces to equation (3-9), the same expression as for spheres[109].

3.3 Sorption and Diffusion of Water in Filled Polymers

3.3.1 Sorption and Diffusion in the Filler

The affinity of many inorganic fillers for water is often much greater than that of the polymer itself. When incorporated in the polymer the resulting sorptive capacity of the medium will be greatly influenced by the degree of wetting of the filler surface by the polymer. This degree of wetting could depend on the overall filler content of a sample due to, amongst other factors, changes in the degree of aggregation of the filler particles. Equation (3-2) might be rewritten as

$$\sigma = \sigma_B \phi_B + \sigma_F' (1 - f_F) \phi_F \qquad ,...(3\text{-}12)$$

where σ_F' refers to the solubility in pure, bulk filler and f_F is a factor representing the degree of wetting of the filler surface inside the polymer. Since σ_B and σ_F' are generally functions of the water concentration c, and f_F can depend both on c and on ϕ_F, the sorption of water by filled polymers is generally expected to be a complex process.

Although diffusion through or around the filler per se is often neglected, the possibility of this arises when continuous interfacial channels are formed through a film, when filler particles form porous aggregates containing amounts of free volume, or when the individual filler particles

are porous. For any of these situations, quantitative treatments for the diffusion and permeation of vapours and liquids through filled polymers would be extremely difficult to apply. The application of some simple models for vapour and liquid permeability through filled polymers in such cases has been examined in some detail by Nielsen[114] who illustrated that a great variety of P - ϕ_F relationships can be obtained depending on the precise properties and distribution of the filler in the polymer.

3.3.2 Water-Soluble Fillers

If a filler is water-soluble and the external water activity is higher than that corresponding to a saturated, aqueous solution of the filler, then sorption of water by the filled polymer can be very large and is usually controlled by an osmotic mechanism[45, 101, 115, 116] whereby water enters the polymer to dilute the pockets of internal solution. Eventually, equilibrium would be attained when the vapour pressure developed by the internal solution becomes equal to the external vapour pressure, although the restraining action of the polymer matrix may be significant[116], especially if crosslinks are present. Overall sorptive capacities for water are therefore governed largely by the solute concentration and by the degree of crosslinking of a sample.

CHAPTER 4

THE MEASUREMENT OF SOLUBILITY, PERMEABILITY AND DIFFUSION COEFFICIENTS FOR WATER VAPOUR

Particular difficulties are often experienced when attempting to measure σ, P or D for water vapour because of the possibility of the vapour being sorbed or condensing on the walls of the apparatus. In this chapter some of the procedures used to overcome these difficulties are discussed.

4.1 Measurement of P

4.1.1 The "Cup" or "Dish" Method

In this the polymer membrane is sealed across the mouth of the thermostatted vessel containing either liquid water or a strong dessicant and placed accordingly in a dry environment or one of known relative humidity. When the rate of change of the weight of the vessel and contents becomes steady, this is measured and P for water through the membrane calculated. The method is not especially accurate but is useful for some types of routine permeability measurements.

Problems associated with this technique have been discussed by Newns[117]. A more accurate modification of the same procedure was used by Wendisch and Plumer[118].

4.1.2 The Partition Cell Method

A partition cell apparatus has often been used[12,97] for accurate measurements of permeation rates and time lags. Essentially it consists of some kind of diffusion cell in which a sheet of polymer is clamped so as to separate an "upstream" compartment in which the pressure of penetrant is constant from a "downstream" one in which the pressure is initially zero. The downstream pressure is kept sufficiently small so as to be negligible in comparison with the upstream or ingoing pressure at all times. In the case of water vapour the upstream compartment of the apparatus is connected to a thermostatted liquid water reservoir[50]. When the reservoir is above room temperature heating tape is wound round the apparatus connecting the reservoir and the diffusion cell to prevent condensation of water vapour.

For permanent gases a McLeod gauge is often used to follow the pressure increase on the downstream side of the membrane, but for water vapour this is ruled out because of condensation problems and sorption on the glass walls of the apparatus. Yasuda and Stannett[42] have used a modified McLeod gauge system for water permeability and time lag measurements. The compression capillary was jacketed with

water at ~ 90°C to prevent vapour from condensing. Further, the glass surfaces of their receiving apparatus were pretreated with water vapour prior to the start of a run by the introduction of an initial vapour pressure of ~ 0.02 mm.Hg. to the downstream section. During a run, vapour was kept away from the membrane face by the use of a mercury diffusion pump in the downstream compartment.

It is questionable whether further sorption of water on the glass walls after pretreatment could be considered negligible in this procedure[119], and this point is discussed more fully when the time lag is considered. For very accurate measurements of water permeation rates it is generally preferable to use a system similar to that of Barrer and Barrie[50] in which effluent water vapour is rapidly sorbed on a suitably powerful dessicant thus maintaining the downstream pressure close to zero. In this way the amount of water in the vapour phase remains negligible in comparison with the total amount which has permeated the membrane. The latter is measured from the rate of the increase in weight of the dessicant.

4.2 Measurement of the Time Lag L.

4.2.1 Modified McLeod Gauge Procedure.

The procedure adopted by Yasuda and Stannett and

described in section 4.1 appears to be the only one used to date to measure time lags for water vapour. In a "typical" permeation run which lasted about three times the time lag, the downstream pressure increased from 0.02 to ~0.40 mm.Hg[42]. Studies by Frank[120] and by Barrett and Gauger[121] of water vapour sorption on pyrex glass surfaces at low pressures indicate that this pressure rise would lead to further relatively rapid and significant sorption on the glass walls of the apparatus. Some effects of this on measured permeation curves have been analysed[119] (see appendix 9.4) on the basis of the data of Frank and of Barrett and Gauger. This analysis indicates that in general P would be affected only slightly, but that L could, in certain circumstances, be increased very significantly. Also, the sorption effect would, for constant D, lead in most cases to a time lag which decreased with increasing c. Thus it would tend to mask to some extent the concentration dependence of L when D is a decreasing function of c. At best this analysis was only semi-quantitative, nevertheless it would seem to question the reliability of the modified McLeod gauge procedure which cannot therefore be considered to be very satisfactory, at least from the point of view of analysing the L-c dependence of a system. This is particularly

the case for systems where D decreases with increasing c since L, given by equation (2-28), is very dependent on the term $\int_0^{c_0} D\,(c)\,dc$. The relative variation of this term from Dc_0 (the same term for constant D) is often small when D decreases with c. This is discussed in detail, with a number of examples, in the published note[122] submitted with this thesis. If only a small relative variation in L is expected then any effect which tends to cancel it out could, in principle at least, be very serious.

4.2.2 Dessicant Method

The method of Barrer and Barrie[50] described in section 4.1 is very suitable for the determination of P, but its use for measuring water vapour time lags is questionable. This is because only small water uptakes by the dessicant would generally be expected during the relatively short period of a time lag run, thus increasing the ratio of water in the vapour phase to that sorbed in the dessicant. The effect of this would be to increase the importance of water sorption on the glass walls of the apparatus.

4.2.3 Other Methods

A better solution to the problem of measuring water vapour time lags would seem to lie in the use of an

all-metal receiving section incorporating a very sensitive diaphragm-type transducer, when sorption on the walls would be minimised. However such measuring instruments are expensive and a possible arrangement using a modified McLeod gauge or dessicant with more conventional glass apparatus might be to have the receiving volume in several sections such that its geometrical surface area A could be varied appreciably while keeping its overall volume constant. A series of time lags, for the same ingoing pressure of water, measured for various values of A could then in principle be extrapolated to zero A to obtain the "true" time lag each time. This would be tedious and time-consuming practically and for this reason no time lag measurements are made in the present work.

4.3 Differential Permeation

Although the expected relative variation of L with c is generally small in systems where D decreases with c[122], it could be increased if only a small pressure differential across the polymer membrane were used. The term $\int_{c'}^{c_0} D\,(c)\,dc$ would then become $D_{c=c_0}$ to a good approximation, where c_0 and c' are the water concentrations in the ingoing and outgoing faces respectively of the membrane.

Kishimoto and Kitahara[123] successfully applied this technique to the permeation of water through polyacrylamide membranes, but as yet it has not been applied to a system in which D decreases with increasing c.

4.4 Equilibrium and Kinetic Sorption Measurements

For permanent gases, for which the sorptive capacity of a polymer is generally very small, volumetric procedures have been used extensively for sorption studies[124]. One of two procedures is usually adopted:

a) A known amount of gas is introduced into the space, of known volume, which surrounds the polymer sample. The amount of gas still in the gas phase is obtained each time from pressure and volume measurements and hence the remainder, which has been taken up by the polymer, can be calculated.

b) Equilibrium is established between gas sorbed by the polymer and the gas phase at a known pressure. The gas phase is then displaced by mercury after which the sorbed gas is allowed to desorb into a known, large volume, the pressure in which is measured on a suitable gauge.

When measuring small uptakes of water, it is generally advantageous to use a gravimetric procedure, the main reasons being :-

i) With a sufficiently sensitive balance direct, gravimetric measurements are more accurate and convenient than indirect pressure and volume determinations. In connection with the terms "direct" and "indirect", it is emphasised that the unit of cc.s.t.p., in which quantities of sorbed water are usually expressed in this thesis, is a hypothetical unit obtained by conversion of a weight of water on the assumption that water vapour behaves as an ideal gas. Pressure and volume determinations would involve tedious calculations if rates of sorption were to be studied, and would normally require the use of a mercury-filled gas burette.

ii) Sorption and desorption can be recorded instantly and the attainment of equilibrium easily recognised by the condition of constant weight.

iii) No correction of pressure for temperature differences in different parts of the apparatus is required.

iv) There are no complications resulting from water sorption on the glass walls of the apparatus, so long as the vapour pressure is known accurately and can be kept constant.

This last point can be very important. The effect of water sorption on glass walls on a volumetric determination of sorption can be illustrated by a rough calculation. McHaffie and Lenher[125] found that at 25°C and ~ 0.96 relative humidity the water uptake by soft duroglass is ~6 x 10^{16} molecules cm^{-2}. For a small, exposed surface area of glass of 100 cm^2, the total amount sorbed would therefore be ~0.2 cc.s.t.p. For a sample of a hydrophobic polymer weighing only a fraction of a gram, the total uptake of water might only be of the same order as this. For example, Barrie and Platt[43] found polydimethylsiloxane to sorb ~0.9 cc.s.t.p. of water per gram at 35°C and ~ 0.96 relative humidity.

Hence the use of some type of vacuum microbalance is clearly desirable. The theory and some applications of vacuum microbalances have recently been reviewed[126]. Two of the most commonly used types are:-

a) The quartz spiral[127] which attains high sensitivity only at the expense of reduced capacity since its extension is proportional to the load. Its main disadvantage is its fragility.

b) Beam types of balance[128] which can be converted to null point instruments by the use of electromagnetic equipment. Since these are symmetrical, buoyancy corrections can be minimised, in theory, by the choice of an inert counterweight of a suitable density. However, for water vapour, it is probably safest to use an inert metal as a counterweight.

That the microbalance should be as sensitive as possible is particularly important when sorption kinetics are to be measured for a system in which D is a decreasing function of c. For such systems it is shown in appendix 9.5 that much smaller relative variations of the slopes of reduced sorption curves with c are to be expected in comparison with systems where D is an increasing function of c. This is analogous to the situation for concentration-

dependent time lags already discussed[122], since both I_s and L are dependent on "integral" diffusion coefficients and hence on terms similar to $\int_0^{c_0} D(c)\,dc$.

CHAPTER 5

EXPERIMENT

5.1 Materials

5.1.1 Methacrylate and Acrylate Polymers

Sheets of polymethylmethacrylate (PMMA), polyethylmethacrylate (PEMA), poly-n-propylmethacrylate (PPMA) and poly-n-butylmethacrylate (PBMA) were obtained from Imperial Chemical Industries Ltd. (Plastics Division) and were prepared by radical bulk polymerisation of the respective monomers. Evaporation of chloroform solutions of the polymers on clean mercury surfaces yielded thin films which were then outgassed under high vacuum at the highest temperature of the proposed study for at least two days (two weeks at 95°C in the case of PMMA) and used in permeation and sorption experiments.

Poly-n-propylacrylate (PPA) was obtained from Rohm and Haas Co., U.S.A. as a 40% solution in toluene and was prepared by refluxing solutions of the monomer for 16 hours in the presence of 0.3% benzoyl peroxide and 0.1% di-t-butyl peroxide. Thin films were made by allowing the toluene to evaporate "in situ" (see sections 5.2.2, 5.3.2 and 5.3.3) followed by outgassing at ~50°C under high vacuum for two days.

Some physical properties of the methacrylate polymers and PPA are given in table 5-1.

TABLE 5-1

Density (ρ), Number Average Molecular Weight ($\bar{M}_N$) and Glass Transition Temperature (T_g) for Methacrylate and Acrylate Polymers

Polymer	ρ ($g.cm^{-3}$)	$\bar{M}_N$	T_g (^oC)
PMMA	1.17	319,000	92
PEMA	1.17	-	70
PPMA	1.16	-	41
PBMA	1.19	435,000	24
PPA	1.2	-	-58

Densities were measured by the water displacement method except that of PPA which was estimated from mass and volume measurements. Values of $\bar{M}_N$ and T_g given in tables 5-1 and 5-2 were determined by Mr. H. McLean of the Polymer Characterisation Laboratory in this Department using a Mechrolab osmometer and a du Pont scanning differential thermal analyser respectively.

5.1.2 Polysiloxanes

Three separate samples of unfilled polydimethylsiloxane (DMS) were used.

Sample I - was obtained in sheet form from Midland

Silicones Ltd. and was press-cured with 2,4 dichlorobenzoyl peroxide for 5 minutes at 115°C followed by a post cure at 200°C for 2-3 days in an air-circulating furnace. The sample was then refluxed with acetone in a Soxhlet apparatus for 24 hours to extract last traces of low molecular weight impurities and outgassed under high vacuum for a day.

Sample II - was obtained in sheet form from I.C.I. Ltd. and was prepared by crosslinking a gumstock with 1% of 2,4-dichlorobenzoyl peroxide followed by a post cure at high temperature. The sheets were refluxed with acetone and outgassed.

Sample III - was supplied by Midland Silicones Ltd. as an uncrosslinked gum. It was purified by passing a benzene solution through a millipore filter followed by evaporation of the benzene. The purified gum was moulded into sheet form between glass plates. One plate was removed and the gum outgassed for 2 days under high vacuum. Membranes 2-4mm thick were crosslinked by exposure to γ-radiation from a Co^{60} source for about 30 hours followed by extraction with acetone and outgassing.

Two different types of filled DMS were studied.

i) Sodium chloride filled.

Analar grade sodium chloride was finely ground and dried in an oven at ~130°C for 3 days. The salt was

then mixed with the purified gum sample III in a fine rubber mill for about 15 minutes. The filled gum was moulded, outgassed, crosslinked, extracted with acetone and outgassed again. Three samples A, B and C were prepared in this way and contained 0.44, 1.32 and 4.19% by weight respectively of sodium chloride.

ii) Silica filled

Filled sheets obtained from Midland Silicones Ltd. were press-cured and came from the same polymer gumstock as the unfilled sample I. The silica filler was Aerosil 200B, an extremely fine powder. The sheets were given postcures, extracted and outgassed in the same manner as sample I. Samples D, E and F contained 20, 30 and 40% by weight respectively of silica. In addition, sample F contained about 1% by weight of ground quartz, and was opaque and rather brittle.

Other siloxane polymers studied were:-

A copolymer of dimethylsiloxane and methylphenyl siloxane (PMS), containing 7.5 mole % of methylphenyl groups, which was obtained from Midland Silicones Ltd. in sheet form, and was prepared in a similar manner to that of the DMS sample I. Sheets were postcured, extracted and outgassed as DMS sample I.

Poly 3,3,3-trifluoropropylmethyl siloxane (FMS)

which was obtained in sheet form from Dow-Corning Corporation, U.S.A. and was crosslinked with 2,5-bis (t-butylperoxy) 2,5-dimethylhexane and postcured for 1 hour at 150°C. The sheets were extracted with benzene and then methanol, each for 24 hours, and outgassed under high vacuum.

Some physical properties of the siloxane polymers used are given in table 5-2.

TABLE 5-2

Density (ρ), Number Average Molecular Weight ($\bar{M}_N$) and Glass Transition Temperature (T_g) for Polysiloxanes, Filled and Unfilled

Polymer	ρ ($g.cm^{-3}$)	$\bar{M}_N$	T_g(°C)
DMS (I)	0.97	-	-127
DMS (II)	0.97	-	-127
DMS (III)	0.97	250,000	-123
DMS (A)	0.97	250,000	-127
DMS (B)	0.98	250,000	-125
DMS (C)	0.99	250,000	-125
DMS (D)	1.13	-	-125
DMS (E)	1.20	-	-127
DMS (F)	1.26	-	-125
PMS	1.02	-	-114
FMS	1.33	-	- 70

5.1.3 Penetrant Vapours

i) Water Vapour

Distilled water was introduced into a small, pear-shaped vessel and connected to vacuum momentarily to remove the surrounding atmosphere. The sample was then frozen by surrounding the vessel with liquid nitrogen, connected to high vacuum and pumped on for several hours to remove most of the trapped air, and finally allowed to thaw, being connected to vacuum occasionally to remove air bubbles. This procedure was repeated several times and was considered sufficient to remove all dissolved air. The liquid water sample was then ready for supplying vapour to the experimental system under consideration.

ii) Methanol Vapour

Liquid methanol was also outgassed by the "freeze-pump-thaw" procedure, in a manner identical to that for water, and subsequently used as a source of vapour.

5.2 Apparatus

5.2.1 The Pumping Systems

Two separate but similar pumping systems were used. One was used with both the permeability apparatus and the sorption apparatus concerned with the larger uptakes of penetrant (system 1) and the other with the sorption apparatus concerned with relatively small uptakes of penetrant (system 2).

The essential features of both systems are shown in figure 5-1.

A one-stage mercury diffusion pump (B) backed by an Edwards two-stage rotary oil pump (A) produced an ultimate vacuum of about 10^{-6} mm.Hg. A large buffer volume (C) was attached to the low pressure side of the diffusion pump. The latter could be by-passed so as to introduce air into the vacuum lines without stopping the mercury pump. The pump (A) had a non-return valve to prevent oil from being sucked back into the pumping system in the event of a power failure.

A liquid nitrogen trap (D) condensed out any vapours present in the hyvac (E) section of the system, in which the pressure was measured using an Edwards Pirani gauge head (F). The Pirani gauge in system 1 was also included in the permeability section during a run. Also in system 1 were a mercury manometer (G) for the purpose of calibrating pressure transducers and a vessel (H) for outgassing polymer samples. System 2 had no mercury manometer in order to keep the amount of mercury vapour in the system to a minimum. In addition, a small piece of gold foil (I) was included in the hyvac line of system 2 to prevent traces of mercury vapour from entering the microbalance.

The apparatus for both systems was constructed of pyrex glass and, apart from the Pirani gauge heads which

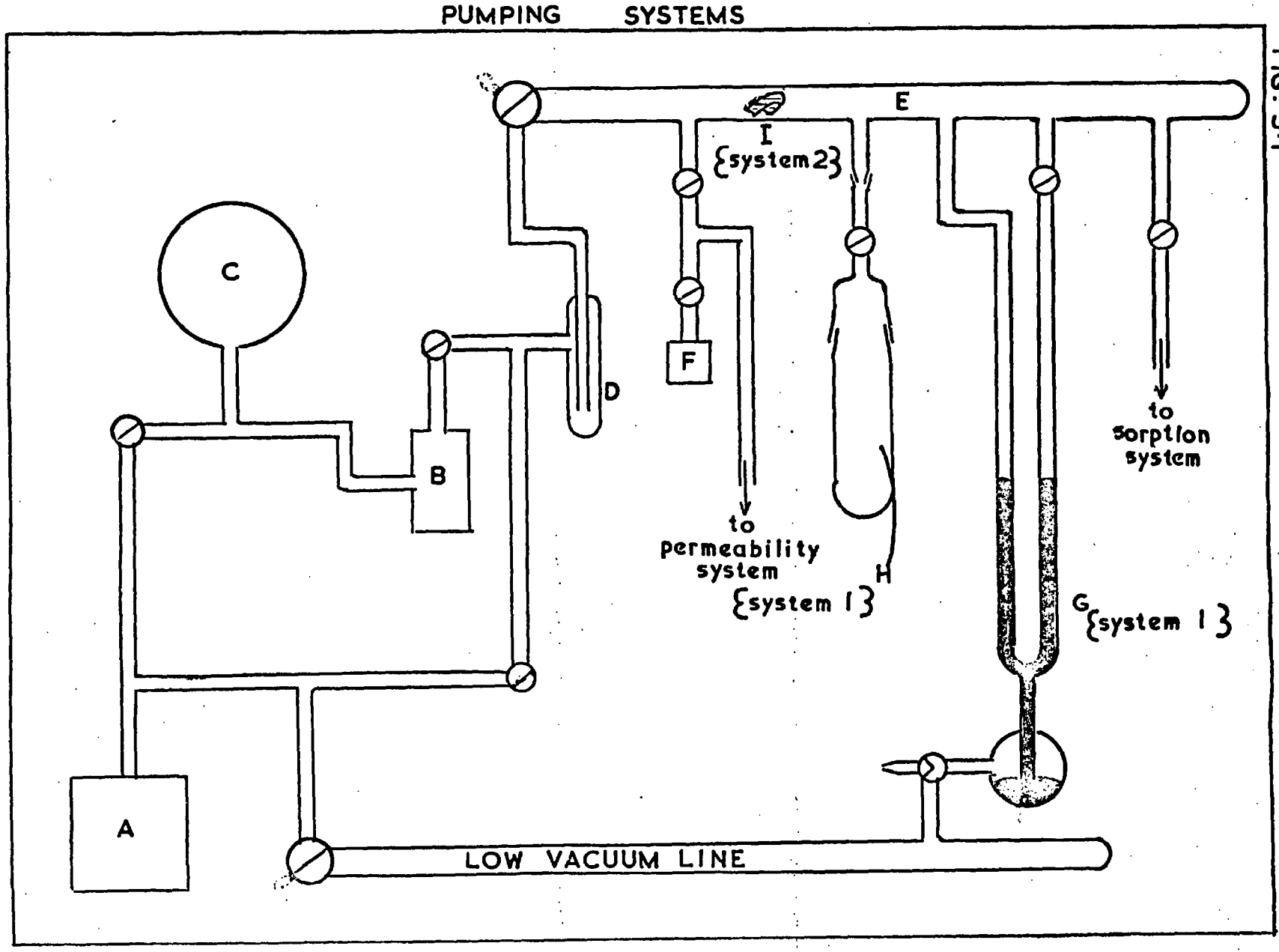
PUMPING SYSTEMS
A
B
C
D
E
F
G
H
I
{system 2}
to permeability system
{system 1}
to sorption system
{system 1}
LOW VACUUM LINE

FIG. 5·1

were connected in using Piecen wax seals, all taps and joints were lubricated with Apiezon N high vacuum grease. Underwater taps in the systems to be described in sections 5.2.2 and 5.2.3 were lubricated either with Apiezon T or a Silicone high vacuum grease.

5.2.2. The Permeability System

The system is illustrated in Figure 5-2.

i) The High Pressure (Ingoing) Section

Vapour at a known pressure was supplied from a liquid reservoir, accurately thermostatted by means of a water bath containing a mercury contact thermometer and a Sunvic electronic relay. The water bath was heated by two 300 W "red-rod" heaters and cooled, when necessary, by circulating tap water through a metal tubular coil immersed in the bath. The temperature of the reservoir could be controlled to within about $\pm$ 0.05°C. Also in the water bath and connected to the reservoir was a 500 cc. buffer volume which served to minimise any pressure fluctuations. An underwater three-way tap (T_1) enabled the reservoir to be connected either to the polymer membrane (M) or to the hyvac line via (T_2). When the membrane and reservoir were above room temperature the connecting glass tubing was heated with heating tape (H) to prevent condensation of the vapour.

Vapour pressures were taken from tables [129,130]

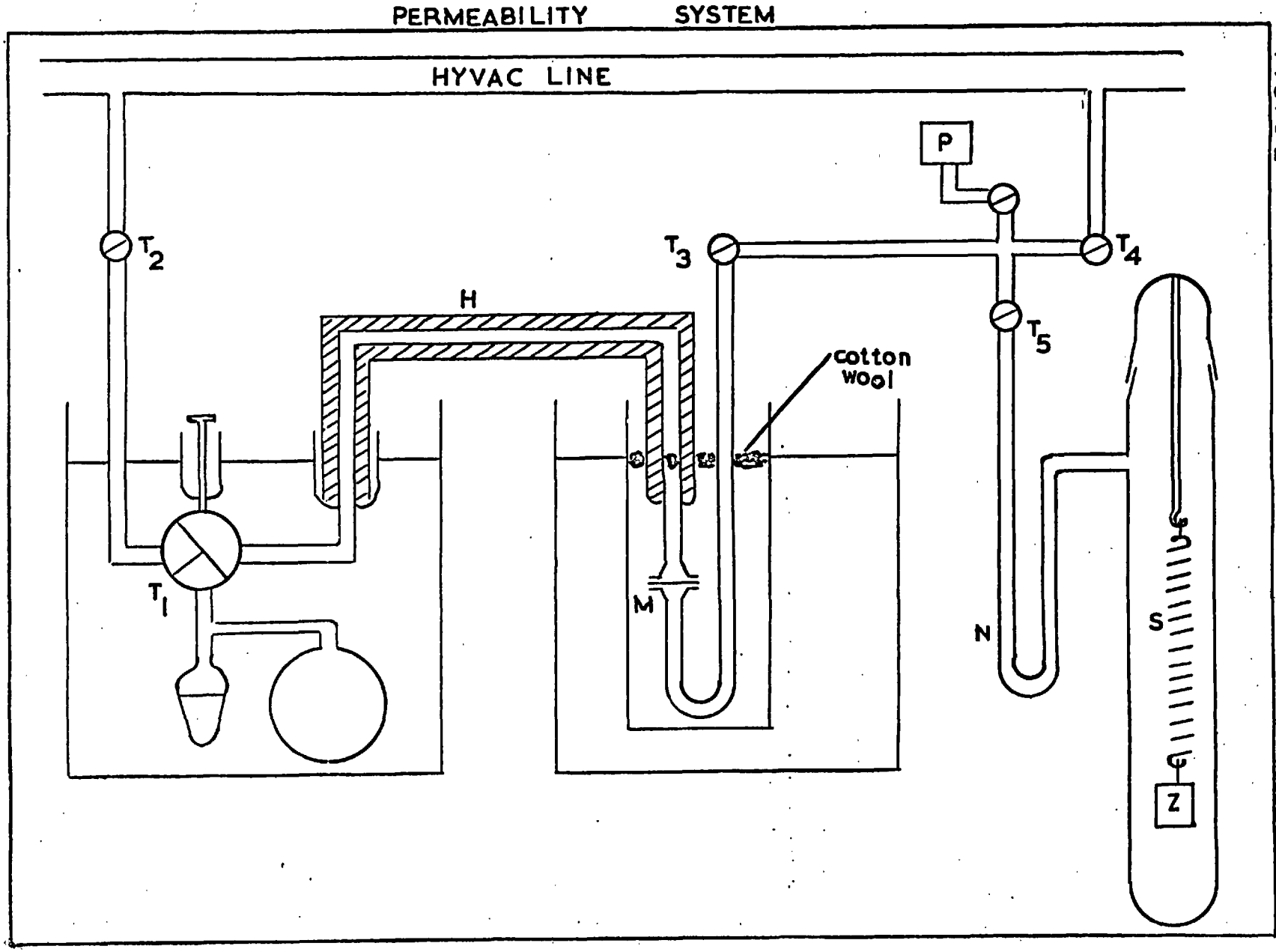
PERMEABILITY SYSTEM
HYVAC LINE
P
T2
T3
T4
T5
H
cotton wool
T1
M
N
S
Z

FIG. 5.2

but were checked periodically by means of the pressure transducer described in section 5.2.3.

ii) The Low Pressure (Downstream) Section

During a run, vapour which passed through the membrane (M) was sorbed in the zeolite (Z) (sodium faujasite, 13X) contained in a glass bucket suspended from a quartz spiral (S). The sorption of water by 13X is extremely rapid and, up to about 0.2 parts by weight of water to 1 part of zeolite, the equilibrium pressure in the vapour phase is extremely small at 30°C[131] so that the effect of water sorption on the glass walls of the apparatus, as mentioned in section 4.1.2, was minimised. Sorption isotherms for methanol in 13X have been found to be somewhat irreproducible[131] but the amounts sorbed at very low pressures are comparable with those for water.

The sensitivity under vacuum of the spiral (S), which was obtained from the Thermal Syndicate Ltd., was determined at various temperatures between 20 and 50°C as described in section 5.2.3. This enabled the amount of penetrant passing through (M) in a given time to be determined by observing the extension of (S) to $\pm$ 0.001 cm with a cathetometer and applying a correction for any variation in room temperature.

Effluent vapour could also be condensed in the liquid nitrogen trap (N) or pumped away through the hyvac line by

means of taps (T_3), (T_4) and (T_5). The "downstream" pressure could be measured by means of the Pirani gauge (P). When necessary, the zeolite was outgassed by connecting it to high vacuum and surrounding it by a furnace at $\sim 300^{o}C$ for about 6 hours.

iii) The Membrane Holder and Diffusion Cell

The membrane holder is illustrated in Figure 5-3(a).

The membrane (M) was gripped between two circular steel plates (P) each with a central circular hole of the same, well-defined diameter. One of the plates had a slight rim for improved clamping. The plates were screwed together by the six screws (S_1). When (M) was a hard plastic (polyalkylmethacrylates) the plates were screwed together hard. When (M) was rubbery, however, the plates were only screwed together moderately tightly to prevent bulging of (M) and six spacing screws (S_2) introduced to minimise any distortion of (M) when under pressure in the diffusion cell. The membrane was supported on its "downstream" side by a thin wire gauze (G) resting on a metal ring (H) screwed into the hole of one of the plates (P).

The membrane holder was held in the diffusion cell shown in Figure 5-3(b).. Thin rubber gaskets (R), with circular holes cut to the same diameter as the holes in the plates (P), separated the plates from the flanges of the

MEMBRANE HOLDER AND DIFFUSION CELLS

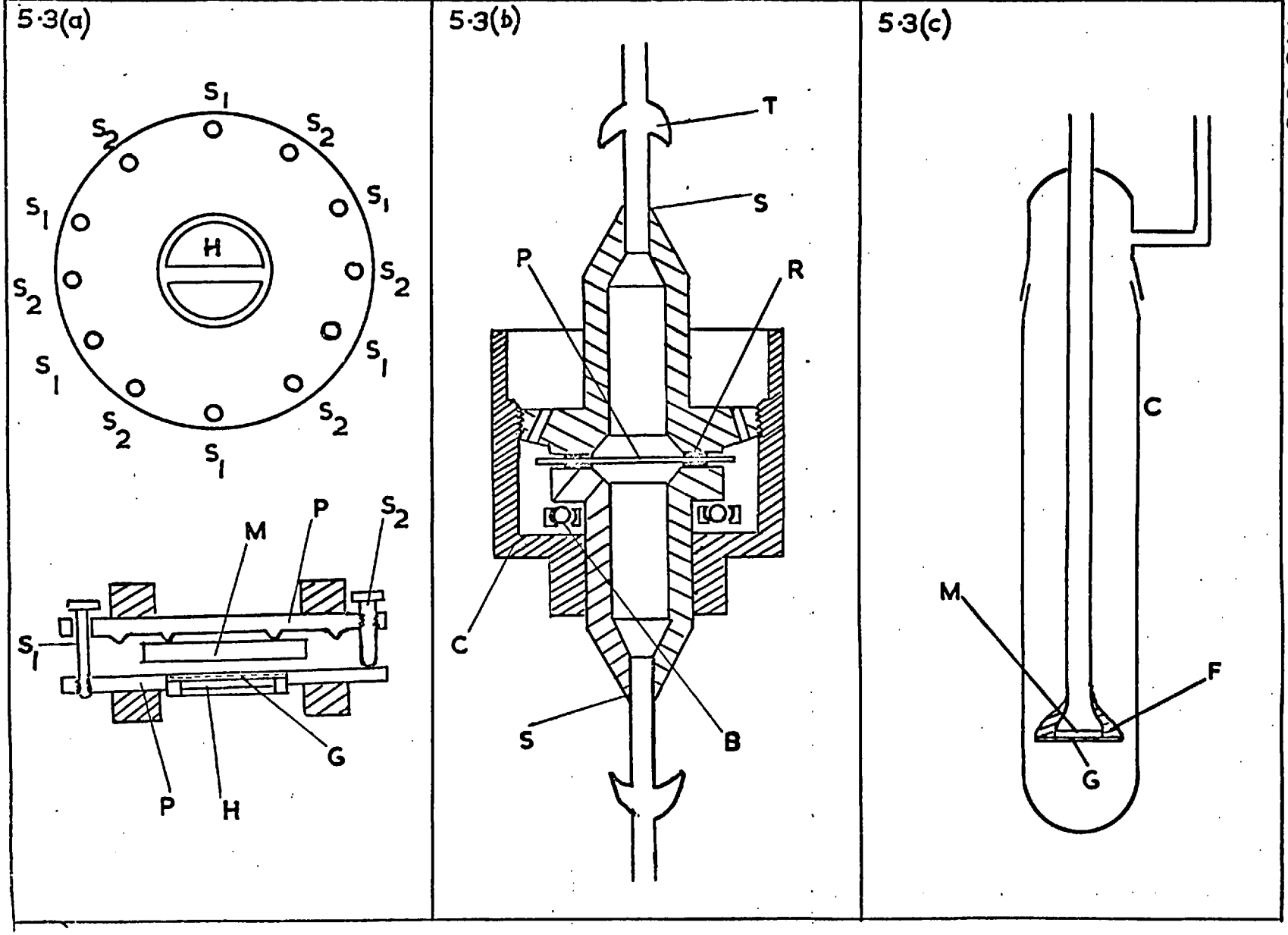

FIG. 5.3

steel tubes (S). The two flanges were screwed together by means of screw threads on the upper flange and the cup (C). A ball race (B) between the lower flange and the bottom of (C) prevented distortion of (M). The upper flange contained a number of small holes through which mercury was poured to ensure a gas-tight seal for the cell. The tubes (S) were connected to the glass apparatus by copper-glass seals (T) and the whole cell supported vertically in a copper cylinder which was immersed in a water bath thermostatted to within $\pm$ 0.05°C in a similar manner to that described in i) of this section.

This type of cell has been used and modified extensively in this Department by Barrer and co-workers [132].

iv) The Diffusion Cell for PPA

This polymer was studied in the form of a viscous gum and the simple, if rather crude, cell used is illustrated in Figure 5-3(c). A circle of strengthened filter paper (G) (Whatman grade 540) was attached by means of Araldite adhesive to a flange (F) on a vertical piece of glass tubing. PPA was introduced on top of the filter paper as a 40% toluene solution and the toluene pumped off. More solution was then added, pumping off the toluene each time until the resultant PPA gum had a level surface and formed the membrane (M). The glass tubing was contained in a vertical glass cylinder (C)

immersed in a water bath thermostatted to ± 0.05°C. The paper (G) was on the "downstream" side of (M) partly for support and partly to avoid any spurious penetrant concentrations at the ingoing interface.

Although of a somewhat crude design this apparatus was useful for measuring relative permeation rates at various ingoing pressures.

5.2.3 The Sorption Systems

i) The System for relatively large uptakes of Penetrant

When the uptake of penetrant was greater than about 0.2% of the dry weight of the polymer, a quartz spiral balance of the McBain and Bakr[127] type was used. The apparatus is illustrated in Figure 5-4. A thin sheet of polymer (P) was suspended, by a small piece of platinum wire, from the quartz spiral (S) obtained from the Thermal Syndicate Ltd. The spiral was suspended inside a vertical, cylindrical glass envelope (C) immersed in a water tank (W) which was thermostatted to ± 0.05°C in a manner similar to that described in section 5.2.2. The tank had two plate glass sides so that the spring extension could be measured with a cathetometer. The spring was calibrated under vacuum and also under atmospheric pressure, at several temperatures, by hanging on known glass weights. To obtain penetrant uptakes

SORPTION SYSTEM FOR RELATIVELY LARGE UPTAKES

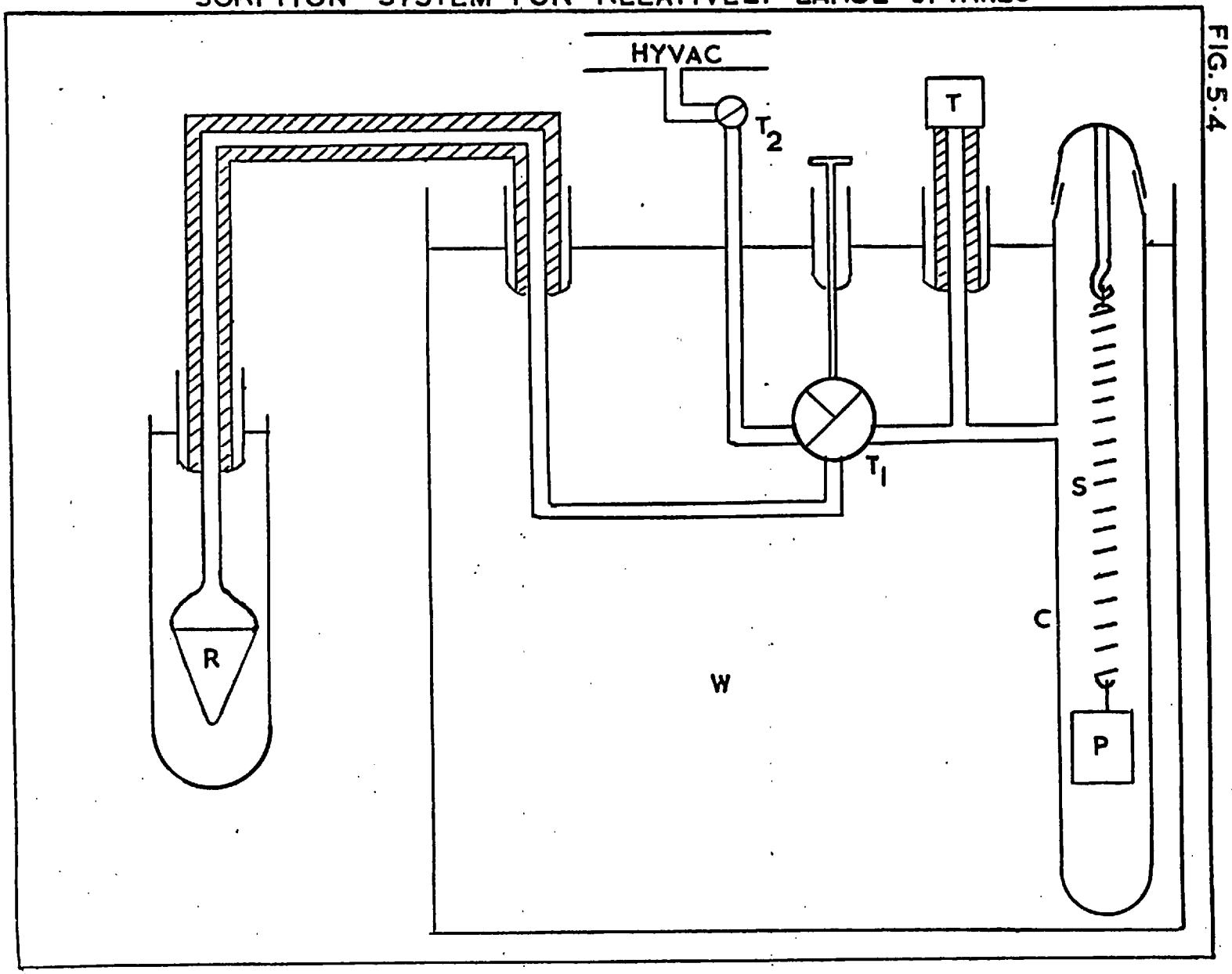

FIG. 5.4

from the corresponding spring extensions, small buoyancy corrections were necessary.

The vapour pressure in the system was measured with a strain-gauge pressure transducer (T) (0-15 p.s.i. absolute, obtained from Bell and Howell Ltd.) operated from a stable 10 volts D.C. supply. The voltage signal from the transducer was measured by a sensitive potentiometer and was directly proportional to the applied pressure. The transducer was calibrated against a mercury manometer and the calibration checked about once a year. Pressures were measured to within about $\pm$ 0.02 cm.Hg.

An underwater three-way tap (T_1) connected the balance system either to the hyvac line via (T_2) or to a liquid reservoir (R). The glass tubing connecting (R) with (W) and (T) with (W) was jacketed with heating tape to prevent condensation of vapour.

ii) <u>The System for relatively small Uptakes of Penetrant</u>

For water uptakes less than $\sim$0.2% of the weight of dry polymer a Sartorius 4102 electronic vacuum microbalance was used. The uptake was usually measured to within 1 μg. The balance was of the beam type and is illustrated pictorially in Figure 5-5(a). The beam was suspended inside a case (H) constructed from a massive block of stainless steel. On each end of the beam were diamond-tipped points

SARTORIUS MICROBALANCE: OVERALL AND BEAM ARRANGEMENTS

5·5(a)

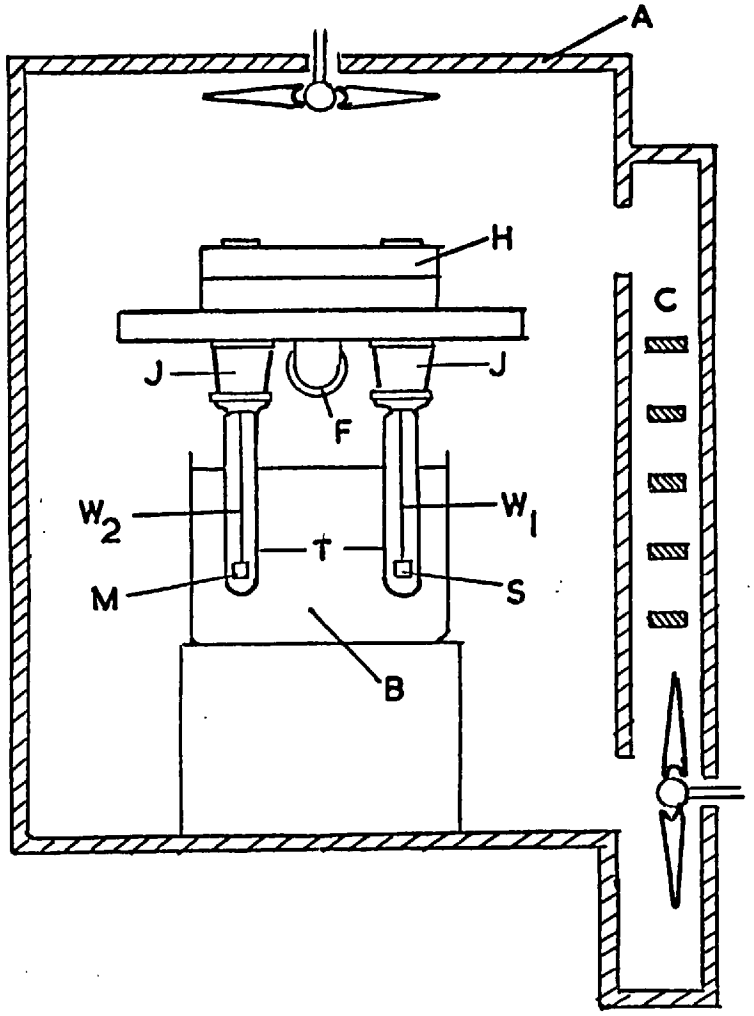

5·5(b)

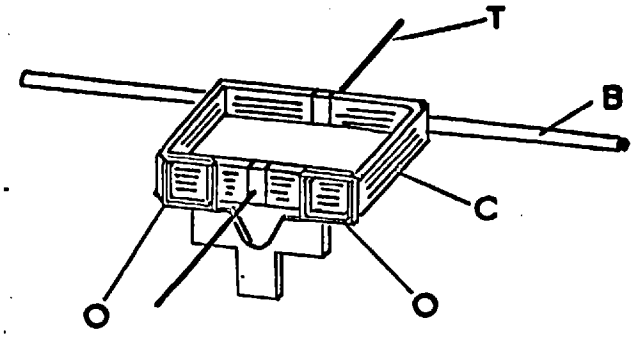

FIG. 5·5

on which aluminium stirrups were fitted by means of sapphire oups. Platinum wires (W_1, W_2) hung from the stirrups inside the glass tubes (T) which were connected to (H) by the cone-socket joints (J). The polymer sample (S) was hung from (W_1) and a metal counterweight (M) of known density from (W_2). The tubes (T) were covered with fine copper mesh, earthed to facilitate the removal of static electrical charges from the system. A metal flange (F) connected the balance to the remainder of the apparatus via a flexible, bellows-type metal coupling.

The weighing principle depended on automatic electrical compensation of a torque moment induced by the load. Figure 5-5(b) shows the beam (B), which was a quartz tube, attached to a moving coil (C) supported by a torsion wire suspension (T). A permanent magnet (not shown) inside (C) supported an oscillated coil (O) through which a high frequency A.C. was passed. At equilibrium (C) was exposed only to the constant field of the permanent magnet, but when the beam deviated from the horizontal position the high frequency field from the coil (O) induced a H.F. signal into the coil (C) which was rectified, phase-adjusted, amplified and returned to (C) in the form of a compensating current. The counter-torque thus induced was made almost identical to the applied force and returned the beam to its rest

position so that the balance was a continuous, null-point instrument. The counter-torque moment was proportional to the field intensity of the permanent magnet and the compensating direct current. Since the former was constant, the D.C. produced, which was measured either on a meter or a Honeywell strip chart recorder, was a direct measure of the weight applied.

The baseline of the balance output shifted slightly with changing air pressure ($\sim$10 μg. for 1 atmosphere change). With water vapour, significant shifts in the baseline were obtained during blank runs with similar weights of an inert material suspended from each end of the beam. Experiments in which the water vapour pressure, balance head temperature and temperature of the suspended weights were varied systematically showed that only the first two variables were significant. Also, since the shifts observed were not instantaneous but took about 10 minutes to reach equilibrium it seemed likely that they were due to sorption of water in or on some part of the weighing system inside the balance head. Accordingly, a "blank sorption isotherm" was measured and found to be almost independent of temperature when changes in weight were plotted against relative humidity. The single isotherm, which is illustrated in Figure 5-6, thus sufficed as a blank correction for all sorption

FIG. 5·6

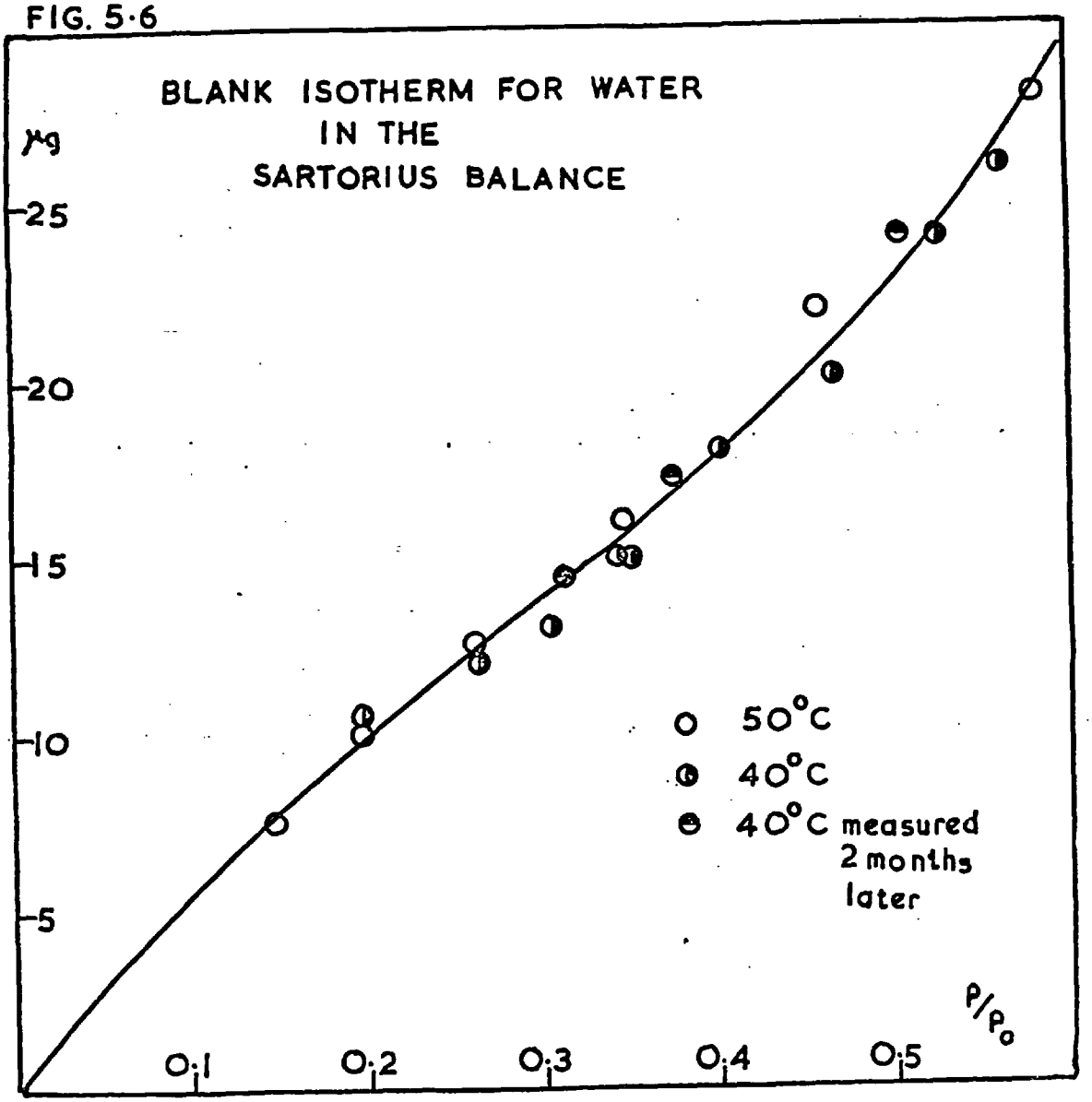
BLANK ISOTHERM FOR WATER
IN THE
SARTORIUS BALANCE
μg
25
20
15
10
5
0·1
0·2
0·3
0·4
0·5
P/P₀
50°C
40°C
40°C measured
2 months
later

measurements. The "blank sorption isotherm" was found to be reproducible after periods of several months. Water uptakes could thus be measured by applying buoyancy and blank corrections to the weight changes recorded by the balance.

The balance was supported on a wall bracket and enclosed in a large air thermostat, (A) in Figure 5-5(a), constructed of "Syndanio" board with a plate glass window for viewing. A circulating air channel (C) contained five 500W heaters some or all of which were controlled by a Sunvic relay with a contact thermometer in the main section of (A). Air circulation was provided by fans in (C) and the main section of (A). It was found that, above room temperature, a temperature gradient existed in (A), in the vertical direction only, and amounted to 8-10°C when the average temperature was ~60°C. This was not disadvantageous, however, since it ensured that the balance head was at a slightly higher temperature than other parts of the system and prevented condensation of water vapour on the beam. When in use the balance head was always kept above room temperature as a further precaution against the entry, by thermal diffusion, of corrosive mercury vapour.

The lower portions of the two tubes (T) in Figure 5-5(a) were immersed in a water bath (B) which was connected to an external thermocirculator (Churchill Instrument Co.) comprising

a 250W heater, pump, cooling coil and solid state sensing relay. The polymer sample was thus thermostatted over the range 20-50°C to within ± 0.1°C.

Vapour pressures were measured to ± 0.01 cm.Hg with a pressure transducer (0-10 p.s.i. absolute) similar to that described in i) of this section except that the output was recorded on a Honeywell strip chart recorder.

The remainder of the apparatus was similar to that in Figure 5-4 but the tap (T_1) and reservoir (R) were immersed in an external water bath, thermostatted to ± 0.05°C as described in section 5.2.2. A buffer volume of 1 litre was connected to (R). When the water bath was above ambient temperature, heating tape wound round the glass tubing connecting the water bath with the balance thermostat was used to prevent condensation of water vapour.

5.3 Procedure

5.3.1. Determination of Steady State Permeabilities (Figure 5-2)

The diffusion cell containing a membrane, after assembly, was tested for vacuum-tightness and joined to the apparatus. The cell was brought slowly to the highest proposed temperature of study, when both sides of the membrane were evacuated to about 10^{-5} mm.Hg, and then brought slowly to the required temperature.

Vapour was admitted to the high pressure side of the membrane via tap (T_1), whilst the outgoing side was evacuated. When a steady pressure was recorded on the Pirani gauge tap (T_5) was opened and, after a few minutes, (T_4) closed, so isolating the system from the hyvac line. When the Pirani gauge reading became steady the initial length of the spiral (S) was measured with a cathetometer and the room temperature noted. After penetrant had been sorbed by the 13X sufficient to cause an extension of (S) of at least 0.2 cm, the final length and hence extension of (S) after a time t (sec.) were measured. The room temperature at the end of the run was also noted and the spiral extension corrected accordingly. The permeation rate was calculated from the temperature-corrected extension Δh (cm.) using

$$J = \frac{\Delta h \times 2.24 \times 10^4}{M \times k \times A \times t} \qquad \ldots\ldots (5\text{-}1)$$

where J = permeation rate in cc. s.t.p. cm^{-2} sec^{-1},

k = sensitivity of (S) in $cm.g.^{-1}$,

A = cross sectional area of membrane in cm^2

and M = molecular weight of penetrant.

The area A was calculated from the diameter of the holes in the membrane holder which had been measured with a cathetometer. The permeability coefficient was then calculated

from

$$P = \frac{J \times \ell}{p} \qquad \ldots\ldots (5\text{-}2)$$

where P = permeability coefficient in $\frac{\text{cc. s.t.p. x cm.}}{\text{cm}^2 \text{ x sec. x (cm.Hg)}}$,

ℓ = membrane thickness in cm.

and p = ingoing vapour pressure in cm.Hg

The pressure, p, was read from tables and the thickness, ℓ, measured using a micrometer with the membrane already clamped in the holder. For PPA, ℓ was measured using a vertical glass pointer as described in section 5.3.3.

Occasional checks that permeation rates were measured in the steady state were carried out by taking several readings of Δh at different times during a run. The ratio ($\Delta h/t$) was always found to be constant to within $\pm$ 1%.

An average run for a permeation rate determination lasted about 20 hours, for both types of polymer used. The Pirani gauge was used to check that the "downstream" pressure did not increase excessively (in general not above $\sim 2 \times 10^{-2}$ mm.Hg).

5.3.2 Determination of Equilibrium Sorption Uptakes

i) Quartz Spiral Balance (Figure 5-4)

After outgassing the sample (P) at the highest temperature, some vapour ($\sim$3-12 cm.Hg) was admitted to the

balance chamber to effect thermal contact of (P) with (W). The system was then brought to the required temperature and outgassed until the length of the spiral (S) was constant and a vacuum of $\sim 10^{-5}$ mm.Hg obtained. Next (T_2) was closed and (T_1) adjusted to isolate the section containing the sample and pressure transducer (T). When the output from (T) was steady the reservoir (R) was brought to its required temperature by surrounding it with water in a Dewar flask and then connected to (P) and (T) via tap (T_1). After a few minutes the section containing (P) and (T) was isolated again. When the output from (T) and the length of (S) were both steady, equilibrium had been attained and the amount of penetrant sorbed was calculated from

$$Q = \frac{\Delta h \times 2.24 \times 10^4}{k \times M} + B \qquad \ldots\ldots (5\text{-}3)$$

where Q = amount sorbed in cc. s.t.p. of penetrant vapour,

Δh = extension of (S) in cm.,

k = sensitivity of (S) at the appropriate temperature in $cm.g.^{-1}$,

M = molecular weight of penetrant

and B = buoyancy correction in cc. s.t.p. obtained from tables of vapour densities

The concentration c ($cc.s.t.p.\ cm^{-3}$) of sorbed penetrant was obtained from $c = Q/V$ .....(5-4)

where V = volume of polymer sample in cm^3, and the solubility coefficient σ (cc. s.t.p. cm^{-3}. $(cmHg)^{-1}$) from

$$\sigma = c/p \qquad \ldots\ldots (5\text{-}5)$$

where p = surrounding vapour pressure in cm.Hg.

The reservoir was then brought to the next required temperature and the process repeated until the complete sorption isotherm had been constructed.

ii) Sartorius Balance (Figure 5-5(a))

The sample (S) and counterweight (M) were outgassed at the highest temperature and brought slowly to the required temperature. The balance head (H) was maintained at a temperature 10-15°C higher than that of (S) and (M) to reduce the magnitude of the blank correction (section 5.2.4). Water vapour ($\sim$3 cm.Hg) was introduced to improve thermal equilibration and facilitate the removal of static electrical charges from the system. Next (S) and (M) were evacuated to $\sim 10^{-5}$ mm.Hg until the output from the balance was steady.

The thermostatted reservoir (R) was connected to the balance via (T_1). When steady outputs from the balance and pressure transducer indicated that equilibrium had been attained, the weight change Δw (μg.) and vapour pressure were noted. The balance was connected to vacuum via (T_1) in order to check that the final and initial outputs from the

balance were consistent. Sorption experiments were thus essentially of the "integral" type as opposed to the "interval" type when using the quartz spiral balance. The amount Q (cc. s.t.p.) of water sorbed was obtained from

$$Q = \frac{2.24 \times 10^{-2}}{18.02} \quad (\Delta w + B + B^{1}) \qquad \ldots.(5\text{-}6)$$

where B = buoyancy correction in μg., obtained from tables and B^{1} = blank correction in μg., obtained from Figure 5-6.

The sorbed concentration (c) and solubility coefficient (σ) of water in the polymer were calculated from equations (5-4) and (5-5).

During desorption the temperature of (R) was adjusted to the next required value and the process repeated to obtain the complete isotherm.

The counterweight (M) was a piece of metal alloy of density 8.1 $g.cm^{-3}$, which did not sorb water, and consequently the value of B could not be made negligible through symmetry. When PPA was being studied the polymer was suspended in a quartz bucket with the metal counterweight suspended in a similar bucket.

5.3.3. Measurement of Sorption and Desorption Kinetics

i) Using the Quartz Spiral Balance (Figure 5-4)

Only a few kinetic measurements, using methanol, were carried out and, since the reservoir had no large buffer

volume, these were confined to lower relative pressure regions of sorption isotherms to minimise the time required for the pressure to build up to its equilibrium value.

The sample was outgassed as for equilibrium sorption, connected to the thermostatted reservoir and the time noted. The sample was isolated by (T_1) again as quickly as possible. The length of the spiral was measured at various times until equilibrium was reached and the pressure transducer output checked frequently. Next the sample was connected to vacuum via (T_1) and (T_2) and the spring length measured at various times until equilibrium was again reached. Spiral extensions E_t (cm.) at times t(sec.) were calculated and E_t/E_∞) plotted versus ($t^{\frac{1}{2}}/\ell$) for both sorption and desorption, where ℓ (cm) was the sample thickness measured with a micrometer and E_∞ (cm) the equilibrium extension.

Mean diffusion coefficients $\bar{D}$ ($cm^2 . sec^{-1}$) were obtained from $\bar{D} = \pi I^2/16$,

where I = initial slope ($cm.sec^{-\frac{1}{2}}$) of (E_t/E_∞) vs ($t^{\frac{1}{2}}/\ell$). Buoyancy corrections were generally negligible. $\bar{D}$ was analysed for concentration-dependence as described in section 2.4.

ii) Using the Sartorius Balance (Figure 5-5(a))

The system was brought to equilibrium as described in section 5.3.2 and the reservoir connected to the balance

via (T_1). From the recorder trace of weight increase vs. time obtained the curve of (M_t/M_∞) vs. ($t^{\frac{1}{2}}/\ell$) was constructed, where M_t, M_∞ (μg.) were the weight increases at time t (sec.) and equilibrium, ℓ being the membrane thickness. M_t and M_∞ also included equilibrium buoyancy and blank corrections. The reduced desorption curve was obtained from the trace of weight decrease versus time in a similar manner.

In the case of PPA the quartz bucket and sample were levelled carefully to obtain a uniform thickness of polymer. The thickness was measured using a vertical glass pointer on which a reference mark was made. The point was adjusted to touch the top and bottom of the sample in turn and the descent of the reference mark measured with a cathetometer. The thickness obtained was doubled to obtain ℓ since water entered the sample from one side only.

$\bar{D}$ was obtained as in part 1) of this section.

The output from the pressure transducer served as a check on the consistency of the boundary conditions during each run.

5.4 Accuracy of Measurements

5.4.1. Permeability Measurements

The permeability coefficient P is given, from a combination of equations (5-1) and (5-2), by

$$P = \frac{\Delta h \times \ell \times 2.24 \times 10^4}{M \times k \times A \times t \times p}$$

with symbols as in section 5.3.1. The accuracy of measurement of the individual quantities in the expression for P are discussed below.

Δh:- The cathetometer was read to 0.001 cm. so that each extension (Δh) was measured to within $\pm$ 0.002 cm. As most extensions were at least 0.2 cm. the maximum error involved was $\pm$ 1%. A further source of error, due to changes in room temperature, was allowed for to some extent by applying correction factors, but the temperature of the spiral itself may have differed slightly from room temperature. However, this would not have introduced an error greater than $\sim \pm$ 0.5% so that the maximum error in Δh was $\sim \pm$ 1.5%.

k:- A good straight line of spiral extension vs. load was obtained. The error in the slope (k) was estimated to be not greater than $\pm$ 1%.

A:- Since the membrane diameter was measured with a cathetometer, the error involved in A was probably less than $\sim$0.5%. However, the presence of the supporting gauze may have diminished the effective area.

ℓ :- Thicknesses (ℓ) of polymethacrylates and press-cured polysiloxanes were consistent to within $\pm$ 2% and of radiation-crosslinked DMS to within $\pm$ 4% as measured in several places with a micrometer. The maximum error in ℓ for PPA was estimated at $\sim \pm$ 10%.

p:- Values of pressure (p) read from tables were occasionally checked against a pressure transducer or mercury manometer when agreement to within $\sim \pm$ 1.5% was obtained.

Others: When the thickness of a membrane becomes appreciable compared with its diameter some distortion of diffusive flow lines occurs[133]. This effect was negligible for polymethacrylate membranes. From curves relating percentage correction to the thickness/diameter ratio[133] it was deduced that errors less than $\sim$ 4% were introduced for polysiloxane membranes.

The maximum absolute error involved in a determination of P was estimated to be about $\pm$ 7-10% (15% for PPA) and the maximum error in relative measurements on the same membrane $\sim \pm$ 3%. However, it was unlikely that all the individual errors augmented each other and, in fact, permeability coefficients were generally found to be reproducible to within $\pm$ 1-2%.

5.4.2. Equilibrium Sorption Measurements

i) Quartz Spiral Balance

The solubility coefficient σ is given, from a combination of equations (5-3), (5-4) and (5-5), by

$$\sigma = \frac{\Delta h \times 2.24 \times 10^4}{k \times M \times p \times V} + \frac{B}{p \times V}$$

with symbols as in section 5.3.2. Accuracies of individual quantities in this expression are discussed below.

Δh:- The cathetometer was read to 0.001 cm. so that Δh was measured to $\pm$ 0.002 cm. For polymethacrylates maximum values of Δh were of the order 0.1 (cm.) for water sorption so that errors ranged from $\sim\pm$ 2% to $\pm$ 30% at the upper and lower ends of sorption isotherms, but were only about a fifth of these values for methanol sorption.

k:- As for the permeability spiral, k was estimated to within $\pm$ 1%.

B:- The volumes of sample, spiral and platinum wire were accurately known and so, since B itself was only a small correction, errors in buoyancy were considered negligible.

V:- Negligible error was incurred in weighing the sample. The density was measured to within $\pm$ 1% which was thus the error involved in V.

p:- The transducer output was measured to within ± 1% and its sensitivity, as obtained from a calibration graph, was known to within ± 1%. The maximum error in any value of p was thus less than ± 2%.

Others:- Errors involved through temperature fluctuations of the sample were estimated as less than ± 0.5% except at vapour pressures close to saturation where small fluctuations in (p/p_o) gave rise to larger fluctuations in uptake.

From the above discussion, the maximum possible error in each value of σ obtained from one isotherm point was large, especially at low pressures. However, a minimum mean squares deviation technique was used to fit non-linear isotherms and the maximum scatter generally observed to be ~ ± 5%. Isotherms were generally reproducible to within ± 3% over their whole ranges.

ii) Sartorius Balance

In this case

$$\sigma = \frac{2.24 \times 10^{-2}}{18.02 \times p \times V} (\Delta w + B + B^1)$$

with symbols as in section 5.3.2. Individual errors were :-

Δw:- Minimum values of Δw were ~20 μg. and were measured to within ± 1 μg. The error was thus less than ± 5%.

B:- Considered negligible, as for the quartz spiral.

B^1:- Blank corrections were estimated to $\pm$ 1μg. thus introducing errors of less than $\pm$ 5%.

p:- Errors totalled $\sim \pm$ 2% as for the quartz spiral.

V:- Errors totalled $\sim \pm$ 1% as for the quartz spiral.

Others:- Errors in (p/p_o) involved through temperature fluctuations of the sample were estimated as less than $\pm$ 1%.

The maximum total error in any isotherm point was thus less than $\pm$ 15%. This was considerably reduced on drawing an isotherm through several points, and isotherms were generally found to be reproducible to within $\pm$ 2% over most of their ranges.

5.4.3. Rates of Sorption Measurements

i) Quartz Spiral Balance (PEMA-MeOH)

Errors in individual quantities were as follows (symbols as section 5.3.3.).

t:- Significant errors were involved at early times since the balance and reservoir were connected for periods of $\sim$20 sec. to allow the pressure to build up in the system.

ℓ:- The thickness (ℓ) was measured to within $\pm$ 2%

E_t, E_∞ :- Extensions were difficult to measure accurately and quickly leading to further appreciable errors at short times.

Pressure:- As the transducer output was not continuously recorded, the accuracy of the assumed boundary conditions, at short times, was not known with certainty.

Heats of Sorption:- As quite large amounts of methanol were sorbed by PEMA the sample temperature may have increased for a short time, decreasing (p/p_o) and hence the rate of sorption.

It was difficult to estimate quantitatively the above errors, but the total absolute errors involved in calculating the initial slope (I) of a reduced sorption curve was estimated as less than $\pm$ 20%. Relative errors in a series of runs were much less than this and the observed reproducibility to within $\pm$ 2% was sufficient to justify a comparison of steady and transient state data.

ii) Sartorius Balance (PPA and PEMA-H_2O)

Errors in individual quantities were as follows (symbols as in section 5.3.3.).

t:- The early time error in t was negligible since the balance response was rapid in comparison with rates of sorption.

M_t, M_∞ :- Uptakes were continuously recorded and had maximum estimated errors of $\pm$ 2% during the early stages of a run. Blank corrections were negligible except, perhaps, for very early times.

ℓ :- Errors were as for permeability measurements.

Pressure:- Pressure increases were very rapid in comparison with sorption rates so that, in general, boundary conditions were consistent throughout a run.

Heats of Sorption:- Small errors may have been introduced at very early times but these probably died away relatively rapidly and were considered negligible.

Others:- For PPA, runs lasted $\sim$ 24h. during which time baseline shifts caused uncertainties of $\sim$ 1-2% in M_∞.

The absolute errors involved in calculating the slope of a reduced sorption curve were estimated as $\pm$ 5% and $\pm$ 15% for PBMA and PPA. Relative errors between runs were estimated as $\pm$ 1% so that concentration dependences could be accurately established.

iii) Sartorius Balance (Polysiloxanes - H_2O)

As before, individual errors are considered separately.

t:- Significant early time errors were introduced since the balance response time was comparable with the smaller values of t.

M_t, M_∞ :- Values of M_∞ were generally in the range 20-200 μg. and maximum errors in M_t at early times in the range $\pm$ 5-50%. Rates of water sorption on the balance itself were similar to rates of uptake by the polysiloxane samples. The assumption was made that each value of M_t was affected by the same relative amount and therefore that the reduced sorption curve did not change. This may have introduced appreciable errors.

ℓ :- Thicknesses were measured to within $\pm$ 4%.

Pressure:- Times taken for vapour pressures to increase to their equilibrium values were comparable with the smaller values of t so that appreciable errors were introduced by the assumption of constant boundary conditions.

Heats of Sorption:- Heats of sorption were very small, but may have introduced significant errors since sorption rates were so rapid.

Others:- Typical sample dimensions were 2 x 1 x 0.3 (cm) so that the plane sheet assumption probably introduced further appreciable errors.

Overall errors were obviously large and values of D obtained were only suitable for use as rough checks on the accuracy of values obtained from steady state measurements.

CHAPTER 6

RESULTS AND DISCUSSION

POLYMETHACRYLATES AND PPA

6.1 Equilibrium Sorption Results

Equilibrium sorption isotherms for water in PMMA, PEMA, PPMA, PBMA and PPA are shown in Figures 6-1 to 6-5 respectively. Data leading to their construction are presented in appendix 9.6 and a sample calculation is also given in 9.9. No appreciable hysteresis was observed in any of the isotherms.

6.1.1 Sorptive Capacities of the Polymers

There is no linear region to the sorption isotherms and the solubility coefficients were determined from the limiting, initial slopes. Values of $\sigma_{c=0} = \lim_{c \to 0} (c/p)$ are given in Table 6-1 and for PMMA and PEMA at $\sim 50^{\circ}C$ agree to within 20 and 3% respectively of previous results[43,42]. For a given temperature $\sigma_{c=0}$ decreases in the order

$$\text{PMMA} > \text{PEMA} > \text{PPMA} > \text{PBMA}$$

with the value for PPA close to that for PEMA at $\sim 49^{\circ}C$. This order is consistent with the water molecule having the strongest affinity for the ester grouping in the polymer.

FIG. 6·1

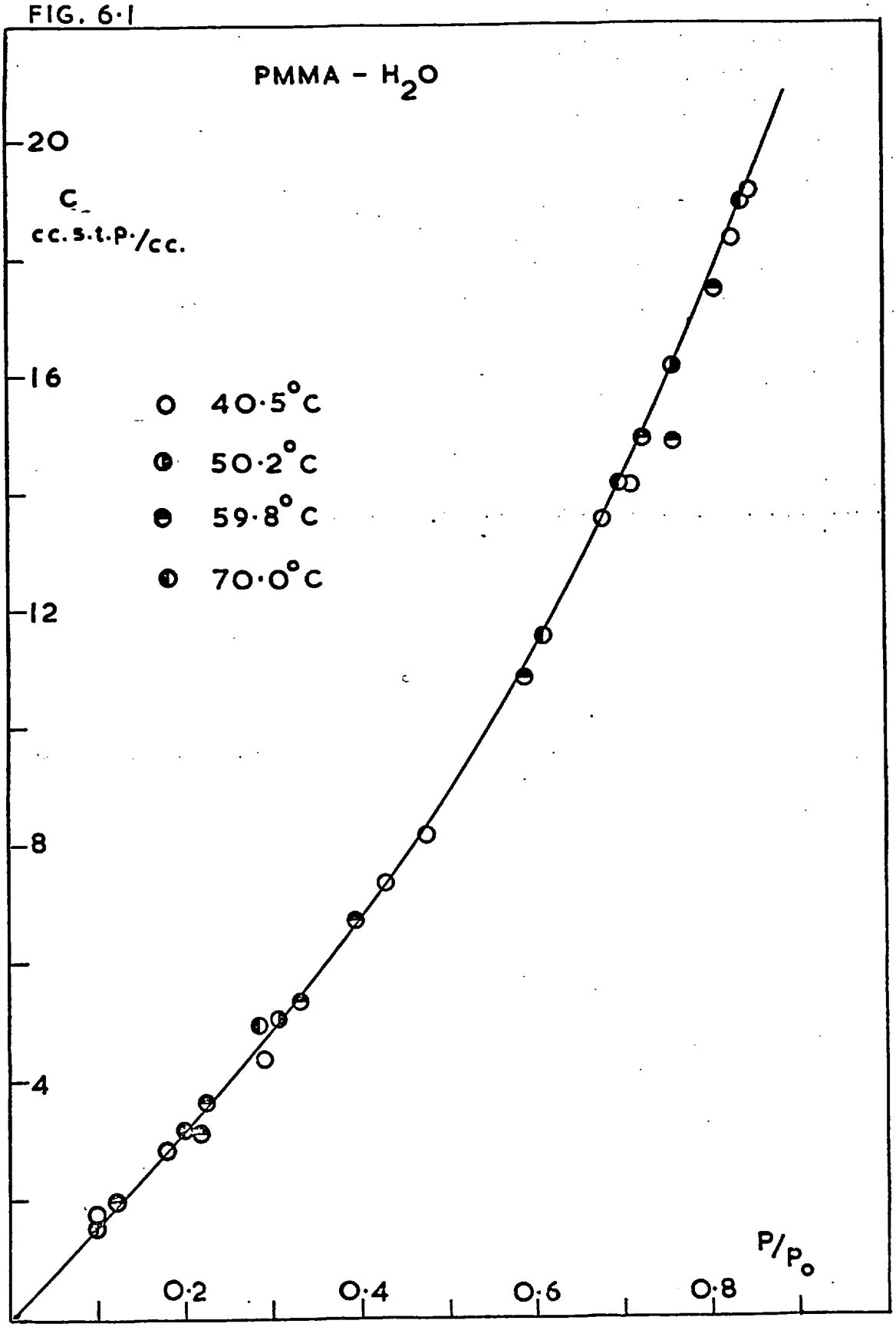
PMMA - H_2O
20
C
cc.s.t.p./cc.
16
12
8
4
40·5°C
50·2°C
59·8°C
70·0°C
0·2
0·4
0·6
0·8
P/P₀

FIG. 6·2

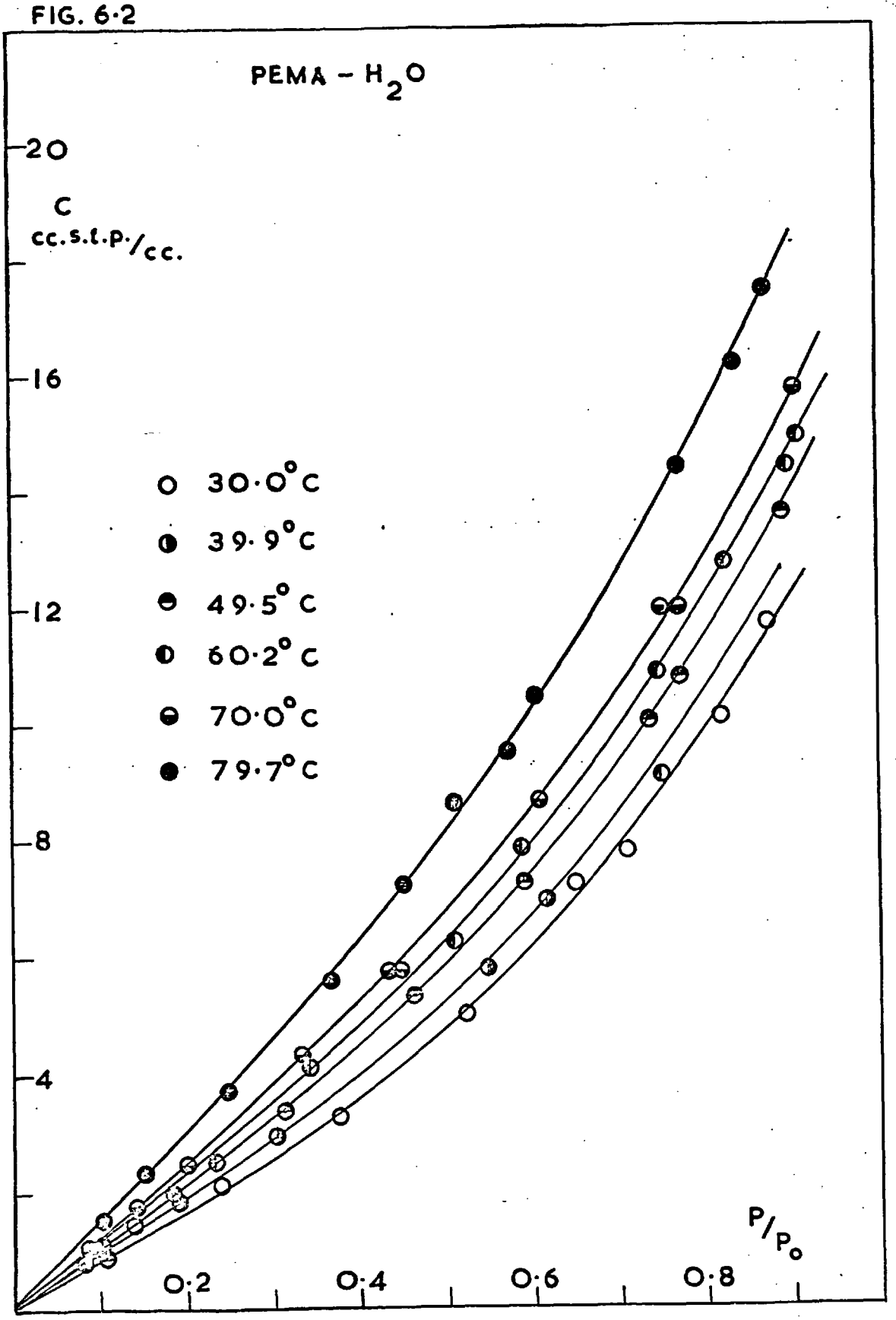
PEMA – H_2O
20
C
cc.s.t.p./cc.
16
12
8
4
30·0°C
39·9°C
49·5°C
60·2°C
70·0°C
79·7°C
0·2
0·4
0·6
0·8
P/Po

FIG. 6·3

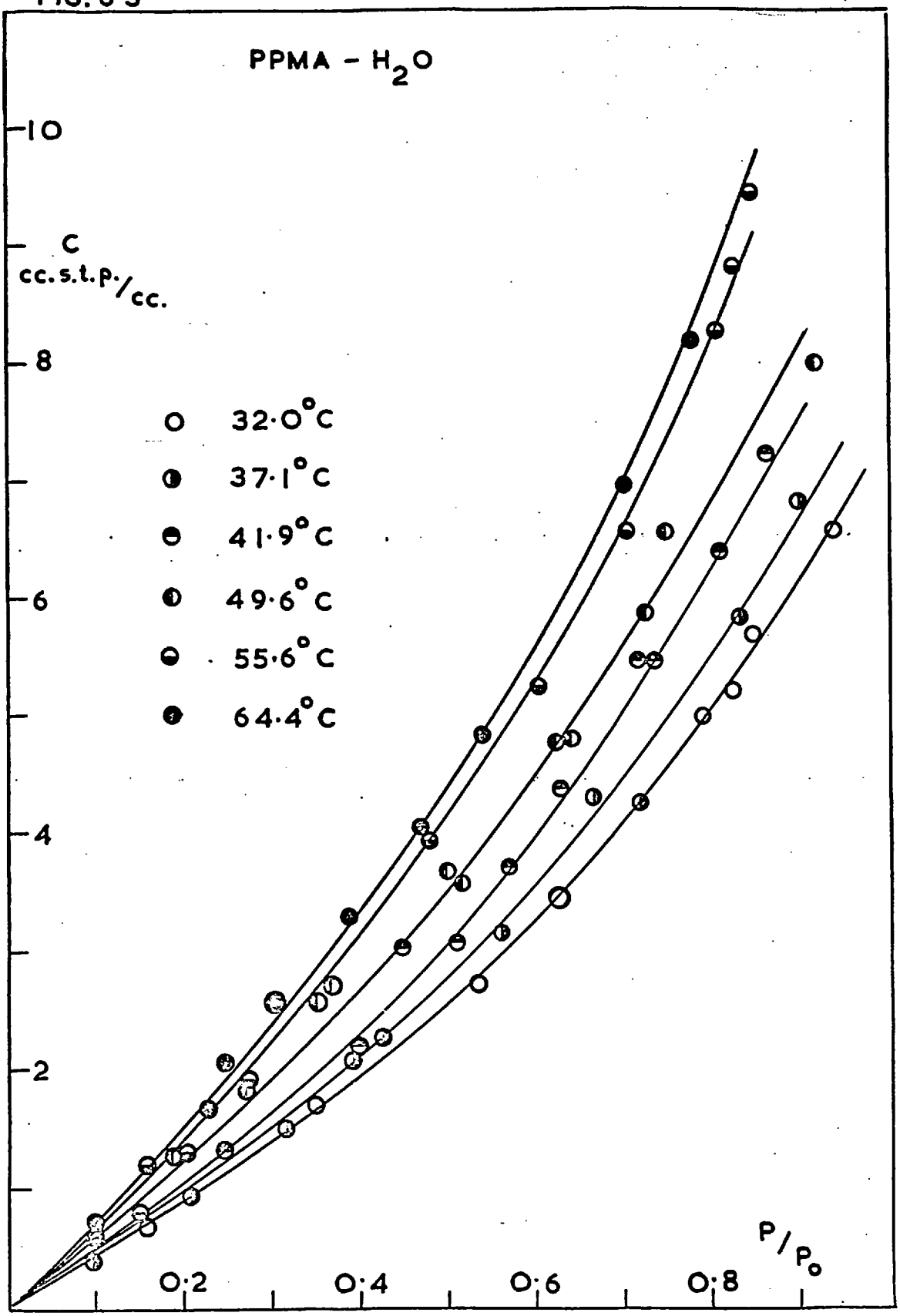
PPMA – H_2O
10
8
6
4
2
C
cc. s.t.p./cc.
32·0°C
37·1°C
41·9°C
49·6°C
55·6°C
64·4°C
0·2
0·4
0·6
0·8
P/P₀

FIG. 6·4

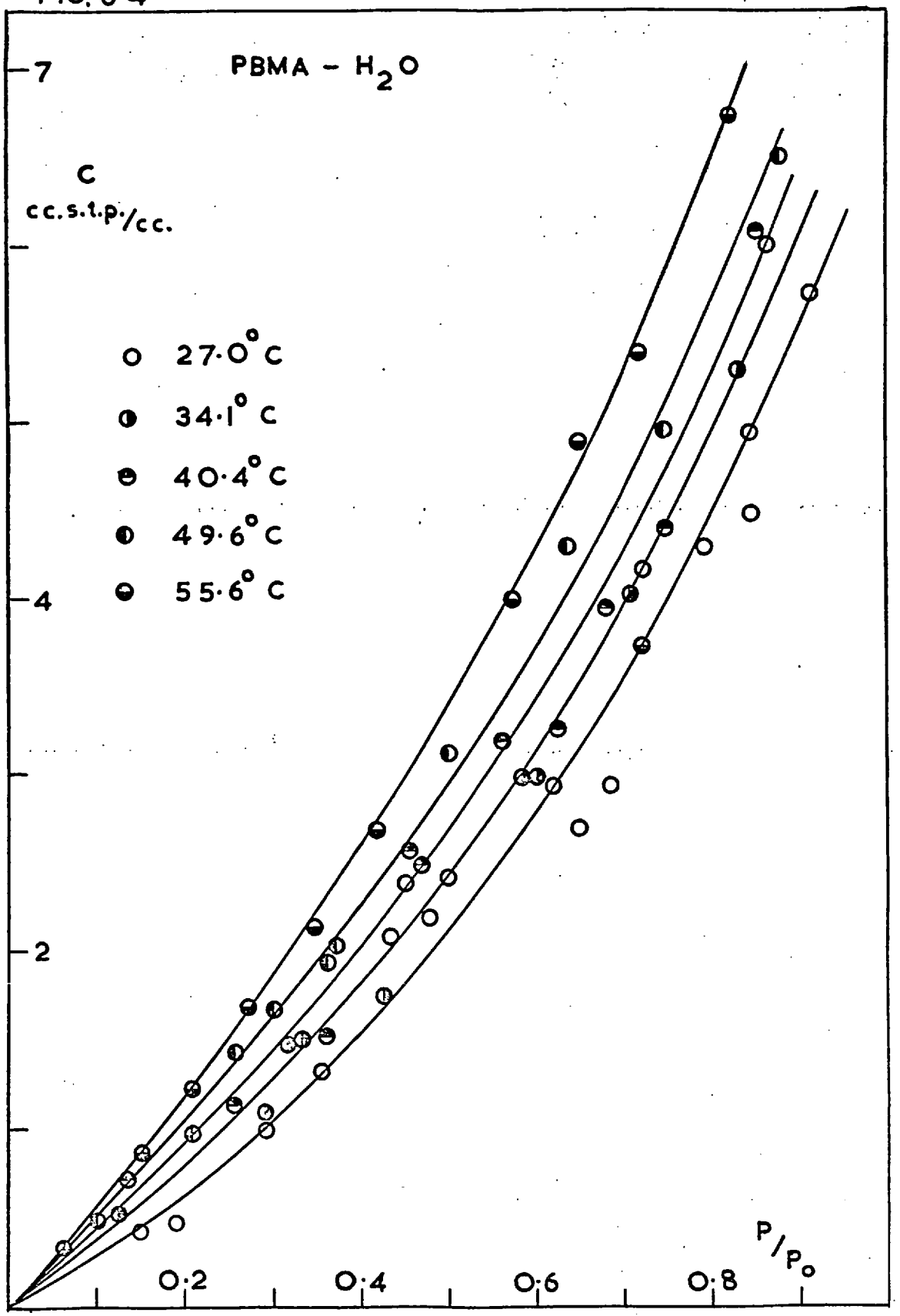

FIG. 6·5

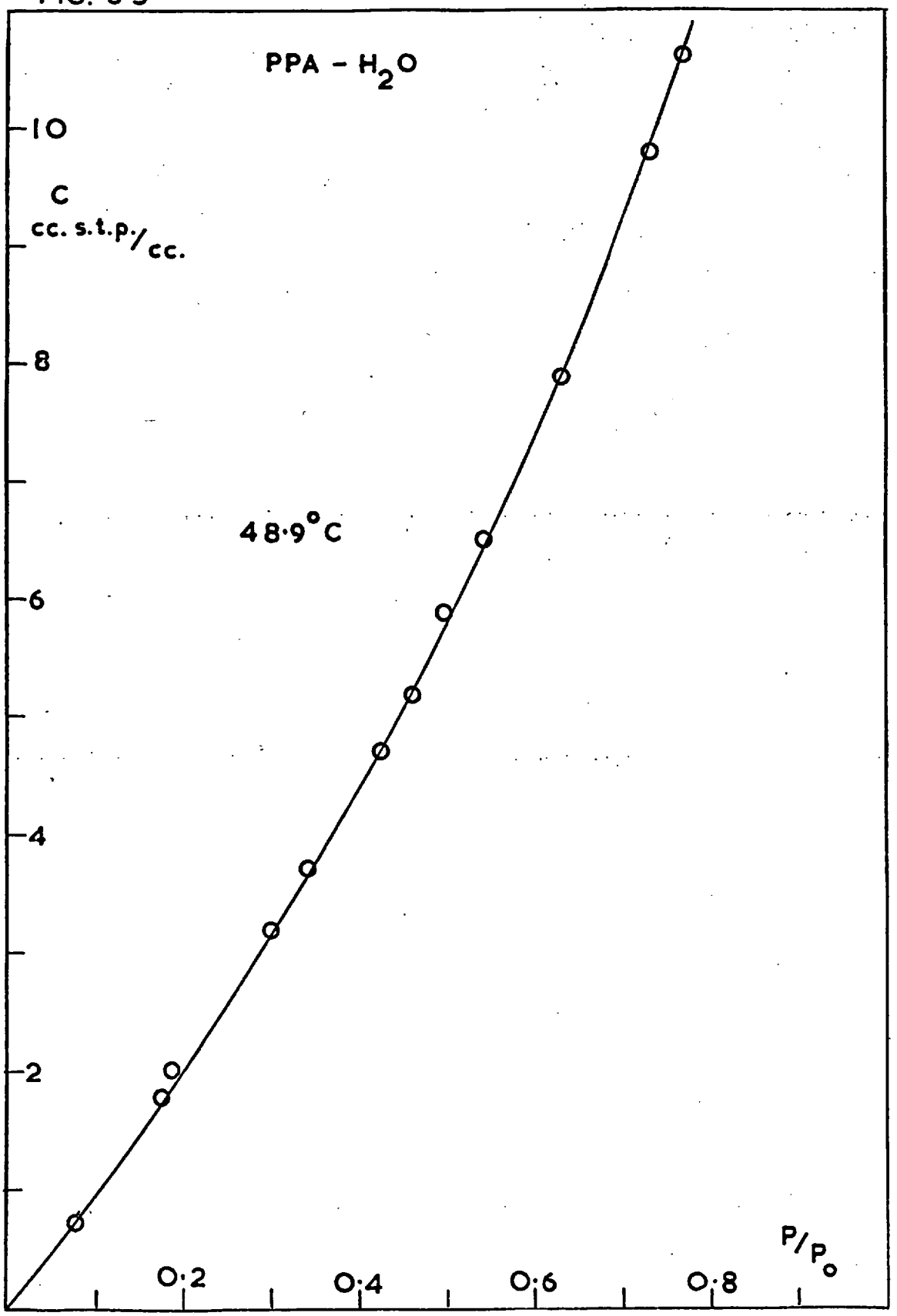

TABLE 6-1

Limiting Henry's Law Solubility Coefficients $\sigma_{c=0}$ for Water

Polymer	Temperature °C	$\sigma_{c=0}$ cc.s.t.p. · $cm^{-3}(cmHg)^{-1}$
PMMA	40.5	2.82
"	50.2	1.71
"	59.8	1.08
"	70.0	0.68
PEMA	30.0	2.59
"	39.9	1.73
"	49.5	1.12
"	60.2	0.74
"	70.0	0.54
"	79.7	0.43
PPMA	32.0	1.12
"	37.1	0.87
"	41.9	0.79
"	49.6	0.67
"	55.6	0.53
"	64.4	0.43
PBMA	27.0	1.06
"	34.1	0.87
"	40.4	0.75
"	49.6	0.56
"	55.6	0.47
PPA	48.9	1.18

The structure of a polyalkylmethacrylate (-acrylate) repeat unit is

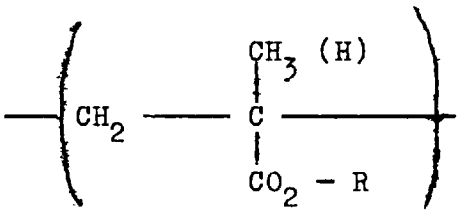

....(6-1)

where R is the appropriate alkyl group. Apart from the ester ($- CO_2 -$) link, the unit is completely hydrophobic. The sorptive capacity for water therefore decreases with the ratio Z, defined as $\frac{\text{no. of ester links}}{\text{no. of hydrophobic groups}}$, in each repeat unit, where each methyl or methylene group is termed hydrophobic. The addition to or removal from R of a methylene group has less effect on water sorption as R becomes larger. Figure 6-6 shown an approximate log-log relationship to hold between $\sigma_{c=0}$ and Z at $\sim 50^{\circ}C$. It is also of interest that the values of $\sigma_{c=0}$ for PEMA and PPA are so close since these polymers have the same Z value. However such comparisons have to be treated with caution since values of σ can vary slightly between different samples of the same polymer, particularly so if the polymer is below T_g as was PEMA in this instance.

Newns[16] found $\sigma_{c=0}$ for benzene in a series of polyalkylmethacrylates to decrease with increasing Z. In this case the penetrant had a stronger affinity for the more

FIG. 6·6

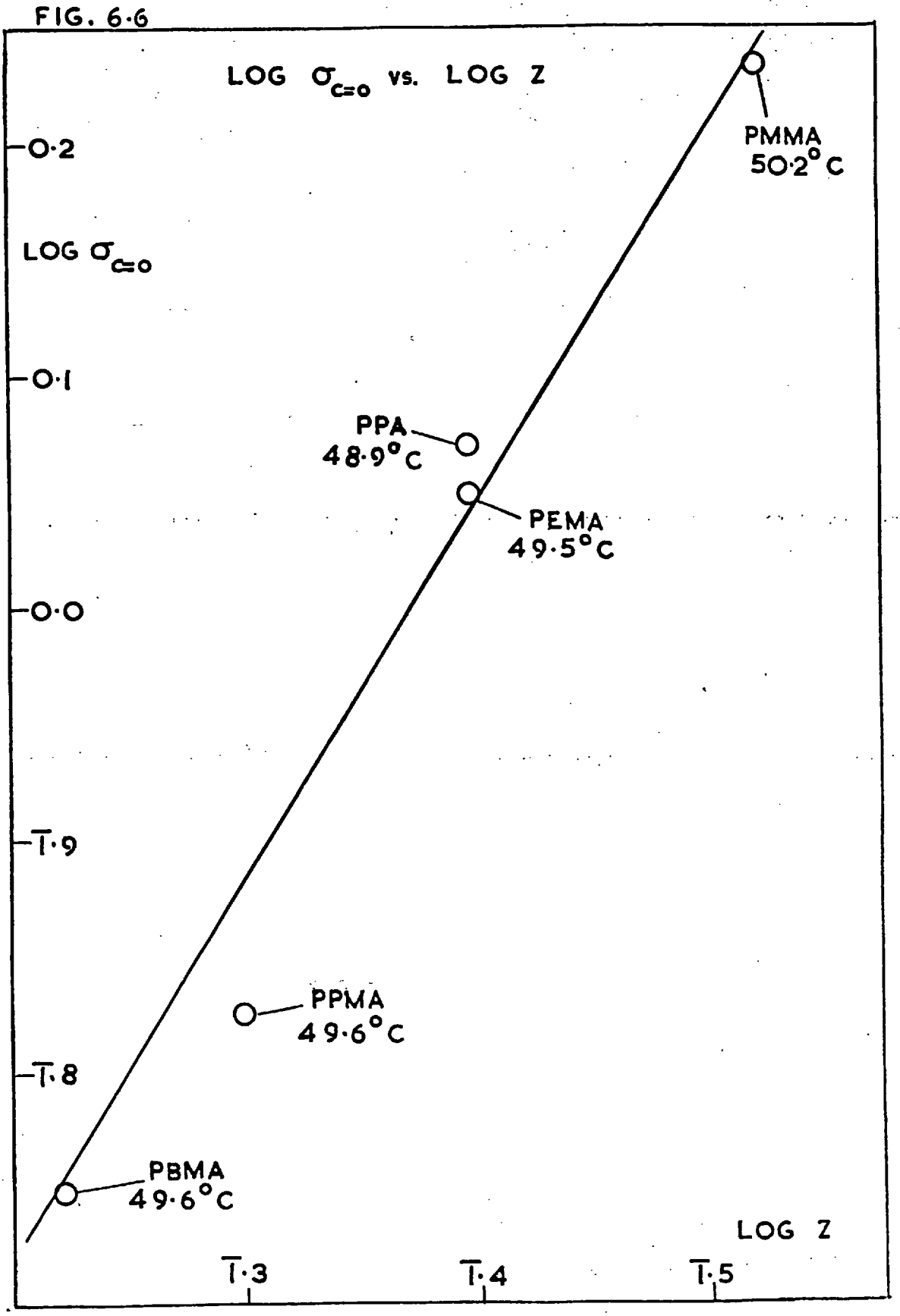
LOG $\sigma_{c=o}$ vs. LOG Z
LOG $\sigma_{c=o}$
0·2
0·1
0·0
$\bar{1}$·9
$\bar{1}$·8
PMMA
50·2°C
PPA
48·9°C
PEMA
49·5°C
PPMA
49·6°C
PBMA
49·6°C
LOG Z
$\bar{1}$·3
$\bar{1}$·4
$\bar{1}$·5

hydrophobic groups in the polymer.

Sorption isotherms for methanol in PEMA, measured at two temperatures only, are shown in Figure 6-7. The values of $G_{c=0}$ are 2.08 and 1.45 at 29.8°C and 40.6°C respectively. These are rather less than the corresponding values for water and indicate therefore that the larger sorptive capacity of PEMA for methanol at a given relative vapour pressure is principally a consequence of the lower boiling point of methanol compared with that of water.

6.1.2 Isotherm Shapes

i) Clustering Functions

All the isotherms are convex to the pressure axis. Clustering tendencies (G_{AA}/v_A) and mean cluster sizes ($1 + \phi_A G_{AA}/v_A$) were calculated from equations (2- 69) and (2- 70) and are presented in Table 6-2 together with a few values for other systems taken from the literature. Typical plots of a_A/ϕ_A vs. a_A and of log (ϕ_A) vs. log (a_A) are shown in Figure 6-8. Since both clustering functions were determined from the slopes of such curves their accuracy is somewhat limited.

Table 6-2 indicates that mean cluster sizes for water for a given temperature are approximately equal in

FIG. 6·7

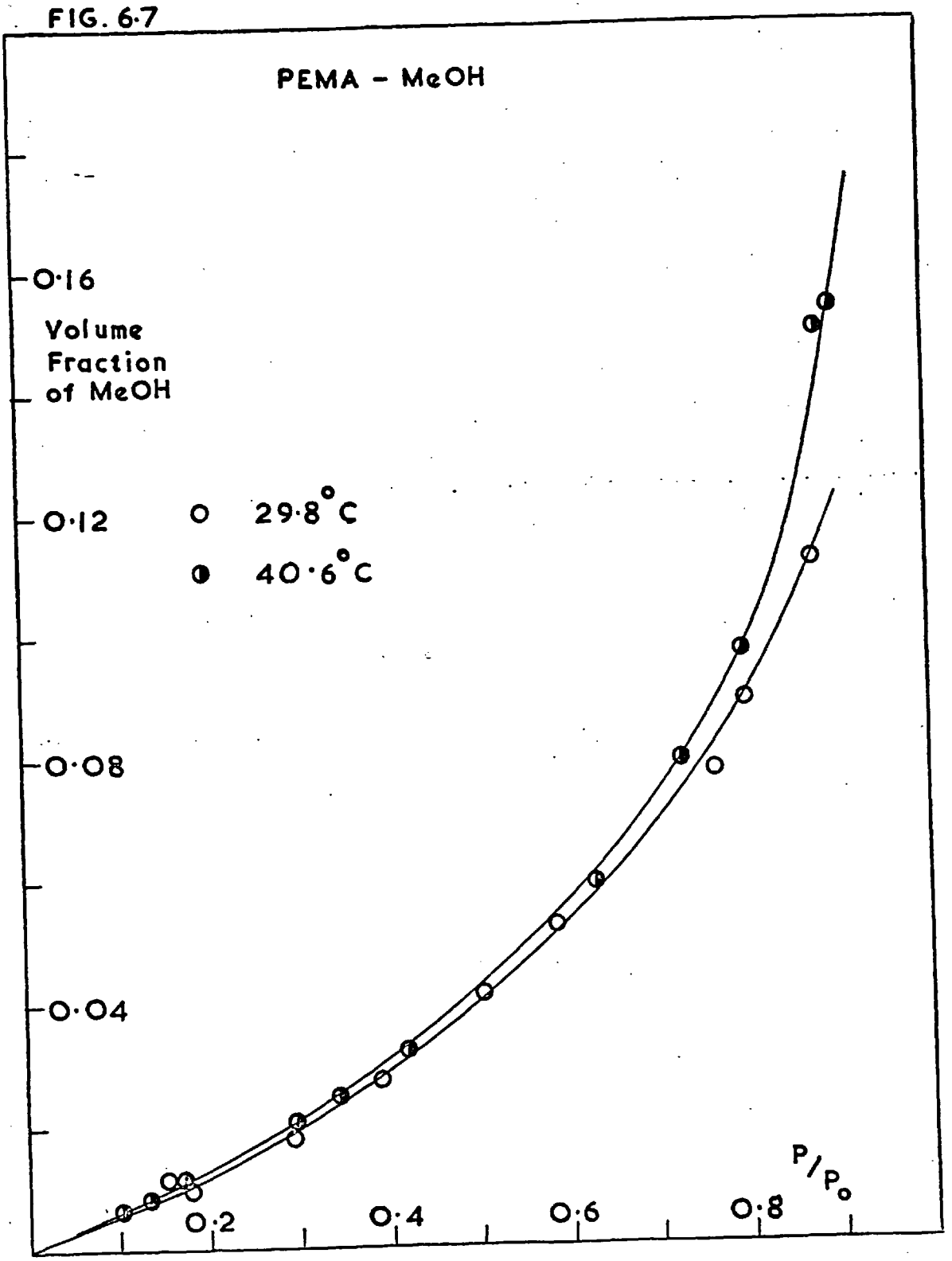
PEMA – MeOH
0·16
Volume Fraction of MeOH
0·12
0·08
0·04
o 29·8°C
● 40·6°C
0·2
0·4
0·6
0·8
P/Po

FIG. 6·8

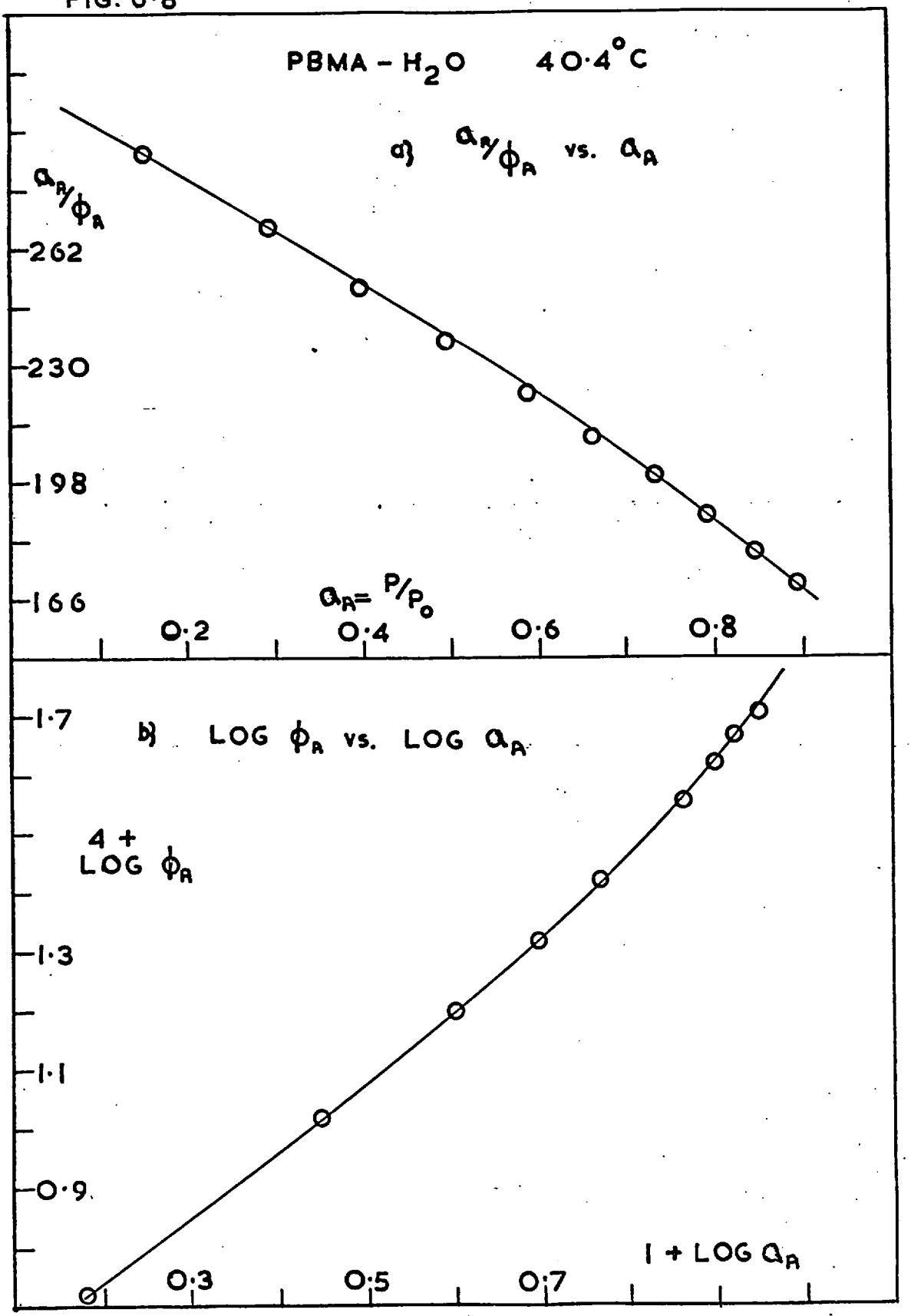
PBMA – H_2O 40·4°C
a) a_R/ϕ_R vs. a_R
a_R/ϕ_R
262
230
198
166
$a_R = P/P_o$
0·2
0·4
0·6
0·8
b) LOG ϕ_R vs. LOG a_R
4 + LOG ϕ_R
1·7
1·3
1·1
0·9
0·3
0·5
0·7
1 + LOG a_R

TABLE 6-2

Clustering Functions

System	T°C	$a_A = 0.3$		$a_A = 0.5$		$a_A = 0.7$	
		$\frac{G_{AA}}{\nu_A}$	$1+\frac{\phi_A G_{AA}}{\nu_A}$	$\frac{G_{AA}}{\nu_A}$	$1+\frac{\phi_A G_{AA}}{\nu_A}$	$\frac{G_{AA}}{\nu_A}$	$1+\frac{\phi_A G_{AA}}{\nu_A}$
PMMA	40.5	24	1.09	34	1.22	42	1.43
- H_2O	50.2	24	1.09	34	1.22	42	1.43
"	59.8	24	1.09	34	1.22	42	1.43
"	70.0	24	1.09	34	1.22	42	1.43
PEMA	30.0	55	1.12	80	1.32	102	1.66
-H_2O	39.9	36	1.11	43	1.20	53	1.34
"	49.5	45	1.01	51	1.24	59	1.52
"	60.2	31	1.08	50	1.25	65	1.54
"	70.0	19	1.07	36	1.21	54	1.46
"	79.7	14	1.05	25	1.17	35	1.38
PPMA	32.0	145	1.10	166	1.33	183	1.62
-H_2O	37.1	197	1.23	181	1.34	142	1.51
"	41.9	145	1.19	158	1.37	146	1.59
"	49.6	87	1.13	89	1.24	73	1.34
"	55.6	110	1.18	105	1.30	108	1.53
"	64.4	53	1.10	63	1.24	78	1.44
PBMA	27.0	287	1.27	287	1.50	238	1.73
-H_2O	34.1	211	1.21	269	1.48	276	1.87
"	40.4	147	1.18	149	1.32	162	1.56
"	49.6	113	1.14	106	1.26	103	1.39
"	55.6	70	1.12	80	1.21	102	1.43
PPA-H_2O	48.9	41	1.10	57	1.22	85	1.53
PEMA	29.8	14	1.30	13	1.53	-	-
-MeOH	40.6	4	1.08	8	1.34	14	2.06
RHC* -H_2O(42)	25	69	1.18	98	1.50	197	2.92
EC≠ -H_2O(42)	25	-	1.12	-	1.32	-	1.94
PVAc** -H_2O(61)	40	-	1.7	-	1.25	-	1.5

* Rubber hydrochloride ≠ Ethyl cellulose ** Polyvinylacetate

each polymer, and therefore that the clustering tendency increases with the size of R (equation (6-1)) since ϕ_A correspondingly decreases. Mean cluster sizes for methanol in PEMA are slightly larger than those for water but values of G_{AA}/v_A are considerably less as methanol is sorbed to a much greater extent. This is possibly indicative of the fact that hydrogen bond formation occurs more readily for water than for methanol.

At lower relative vapour pressures the mean cluster sizes for water in ethylcellulose[42], rubber hydrochloride[42] and the polymers studied here are similar, but at 0.7 relative humidity larger values of $(1 + \phi_A G_{AA}/v_A)$ occur for rubber hydrochloride. Mean cluster sizes invariably increase with sorbed water concentration in the polymers investigated here and no evidence for any minimum value, as found for water in polyvinylacetate[61], can be detected.

ii) Comparison with Theoretical Isotherms

Reliable estimates of sorbed water concentrations at saturation could not be made so a reduced concentration is defined as $C' = c/c^*$ rather than c/c_s, where c^* is the value of c at 0.9 relative humidity. Reduced isotherms for PEMA-H_2O at 30.0 and 79.7°C are shown in Figure 6-9

FIG. 6·9

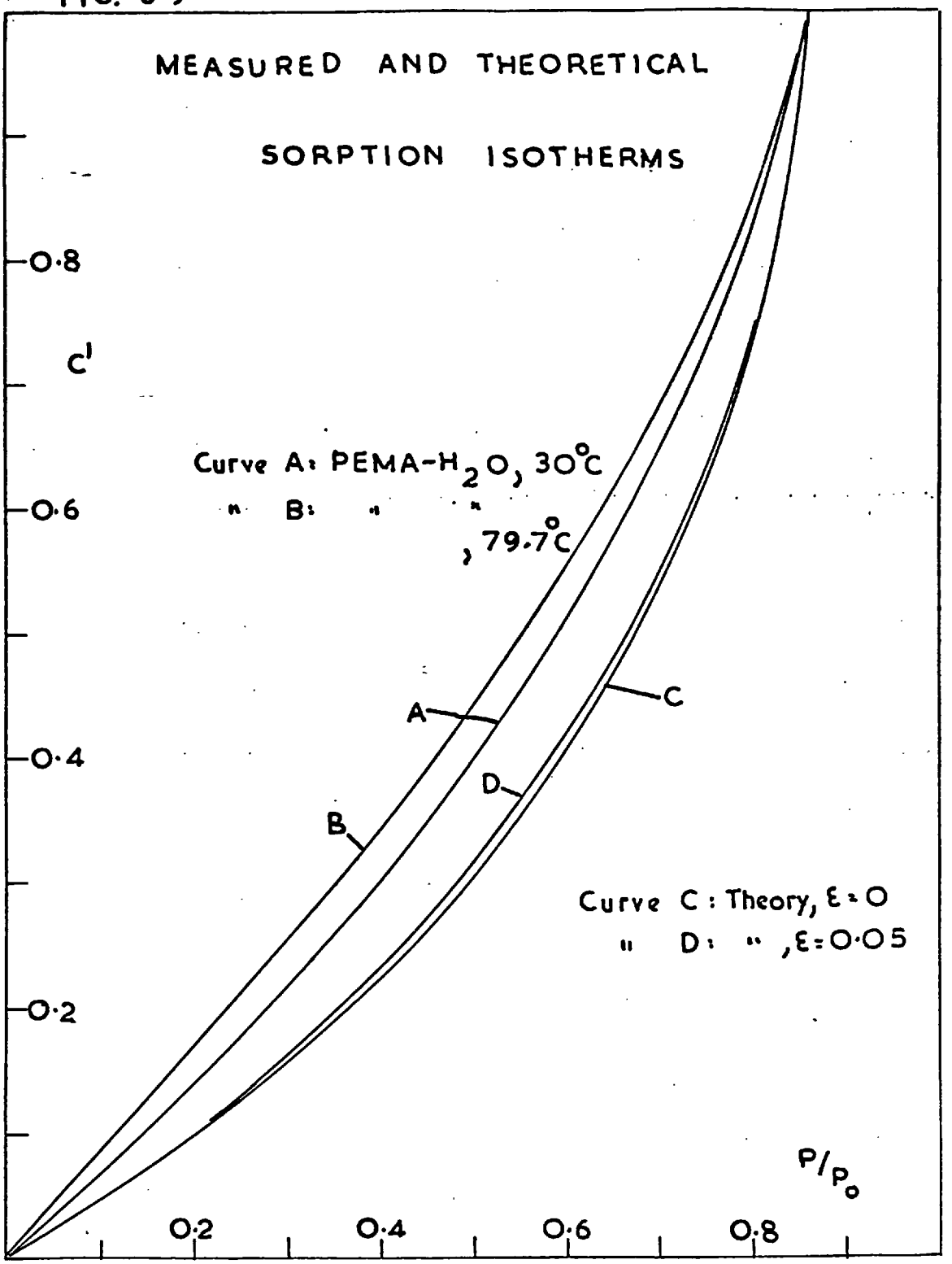
MEASURED AND THEORETICAL
SORPTION ISOTHERMS
0·8
C'
0·6
0·4
0·2
Curve A: PEMA-H2O, 30°C
" B: " " , 79·7°C
A
B
C
D
Curve C: Theory, ε=0
" D: " , ε=0·05
P/Po
0·2
0·4
0·6
0·8

together with the corresponding theoretical reduced isotherms for random polycondensation and for non-random polycondensation with ϵ = 0.05 (section 2.7.5). The agreement between theory and experiment is rather poor and suggests that these simple clustering models are not adequate descriptions of this system. As suggested previously[43], these polymers are not representative of inert media to water, and this point is illustrated further in part 6.1.1 of this section by the effect of the ester grouping on sorptive capacities. The introduction of a co-operative effect into hydrogen bonding improves the agreement marginally but as the perturbation treatment holds only for small ϵ the effect of a stronger co-operative effect cannot be tested quantitatively here.

The applicability of Flory's lattice theory[87] to the system PEMA-MeOH was tested for the sorption isotherm at 40.6°C. At lower relative vapour pressures calculations indicated that the interaction parameter χ varies appreciably with concentration. However, when p/p_o is above ~0.5 a plot of $\ln (a_A/\phi_A) - \phi_B$ vs. ϕ_B^2 is approximately linear, the slope χ being ~3.6 (equation (2-62)). Since the criterion of a good solvent[91] is χ close to 0.5, this can be taken as an indication of the poor solvent power of methanol for PEMA.

6.1.3 Temperature Dependence of Isotherms

i) Heats of Sorption and Heats and Entropies of Dilution

Heats of sorption $\Delta\bar{H}_s$ as $c \rightarrow 0$ were determined from $\sigma_{c=0} = \sigma_0 \exp(-\Delta\bar{H}_s/RT)$. Graphs of $\log \sigma_{c=0}$ vs. $1/T$ are presented in Figure 6-10 and values of $\Delta\bar{H}_s$ are given in Table 6-3.

TABLE 6-3

Heats of Sorption $\Delta\bar{H}_s$ as $c \rightarrow 0$ ($kcal.mole^{-1}$)

System	$\Delta\bar{H}_s$	System	$\Delta\bar{H}_s$
PMMA - H_2O	- 10.4	PBMA-H_2O	- 5.5
PEMA - H_2O	- 8.4	PEMA-MeOH	$\sim$ - 1
PPMA-H_2O	- 6.0		

$\Delta\bar{H}_s$ becomes less exothermic as the size of R in equation (6-1) is increased and the polymer becomes more hydrophobic. However $\Delta\bar{H}_s$ can be treated as a composite quantity, i.e. as the sum of the heats of condensation and dilution. For water the heat of condensation is $\sim$ - 10.4 $kcal.\ mole^{-1}$. Heats $\Delta\bar{H}_A$ and entropies $\Delta\bar{S}_A$ of dilution were calculated for various sorbed water concentrations using equations (2-51) and (2-52). Typical plots of $\log (p/p_o)$ vs. $1/T$ are shown in Figure 6-11. The corresponding

FIG. 6·10

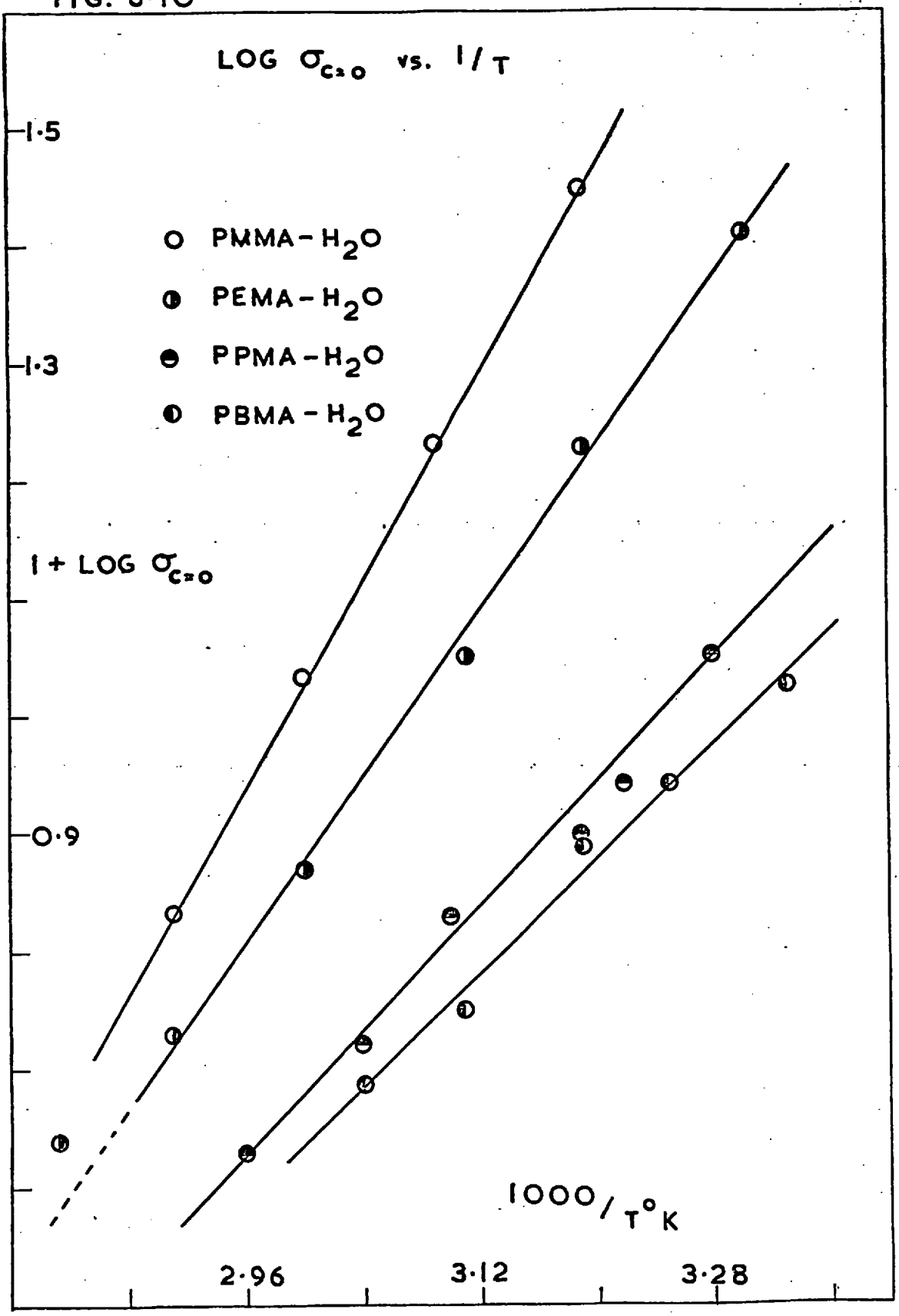
LOG $\sigma_{c=0}$ vs. 1/T
1·5
1·3
0·9
O PMMA-H_2O
PEMA-H_2O
PPMA-H_2O
PBMA-H_2O
1 + LOG $\sigma_{c=0}$
1000/T°K
2·96
3·12
3·28

FIG. 6·11

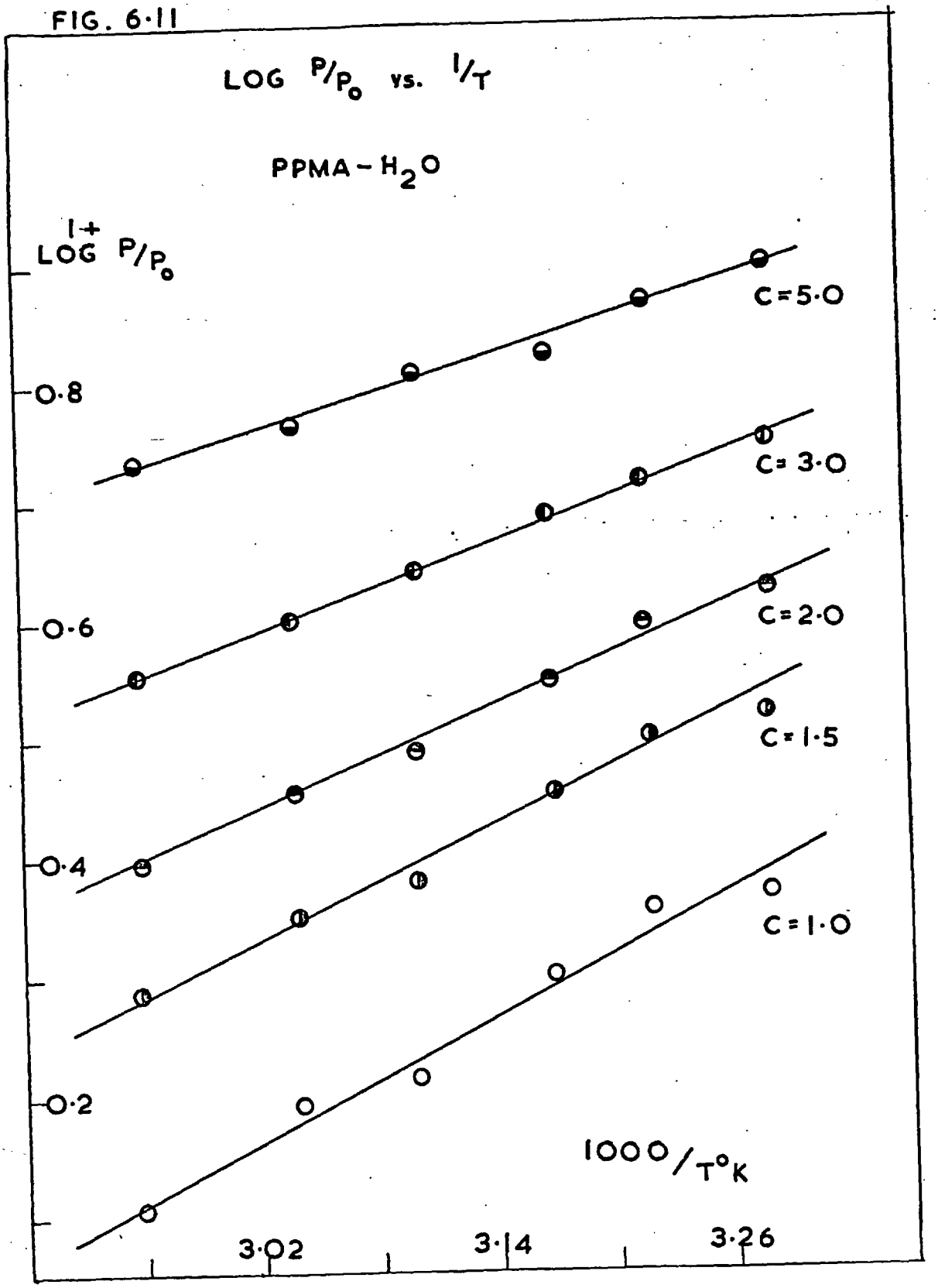
LOG P/P₀ vs. 1/T
PPMA – H₂O
1+ LOG P/P₀
0·8
0·6
0·4
0·2
C = 5·0
C = 3·0
C = 2·0
C = 1·5
C = 1·0
1000/T°K
3·02
3·14
3·26

plots of log (p/p_o) vs. - log (T), used to determine $\Delta\bar{S}_A$, are similar. Mean values $\overline{\Delta\bar{H}_A}$ and $\overline{\Delta\bar{S}_A}$ over the temperature ranges investigated are given in Table 6-4.

TABLE 6-4

Mean Heats $\overline{\Delta\bar{H}_A}$ and Entropies $\overline{\Delta\bar{S}_A}$ of Dilution

System	c cc.s.t.p.cm^{-3}	$\overline{\Delta\bar{H}_A}$ kcal.mole^{-1}	$\overline{\Delta\bar{S}_A}$ cal.mole^{-1}deg.$^{-1}$
PEMA - H_2O 30-80°C	0	+ 2.0	∞
	2	2.0	10.3
	4	1.6	7.2
	6	1.4	5.8
	8	1.2	4.5
	10	0.9	3.6
PPMA - H_2O 30-65°C	0	+ 4.4 (4.4)	∞
	1	4.1 (4.0)	+ 16.1 (15.1)
	1.5	3.8 (3.8)	14.5 (14.4)
	2	3.5 (3.7)	13.1 (13.4)
	3	2.9 (3.4)	10.5 (11.9)
	5	2.3 (2.8)	8.1 (9.6)
PBMA - H_2O 25-60°C	0	+ 4.9 (4.9)	∞
	1	3.7 (4.5)	+ 15.5 (22.4)
	1.5	3.3 (4.3)	13.5 (21.1)
	2	2.9 (4.1)	10.5 (20.0)
	3	2.3 (3.8)	8.7 (18.4)
	4	1.7 (3.5)	6.6 (17.1)

$\Delta\bar{H}_A$ is zero for PMMA since the sorption isotherms plotted as c vs. p/p_o for water in this polymer are superposable. As the alkyl group R is made larger $\overline{\Delta\bar{H}_A}$

becomes increasingly endothermic. There are at least two effects to consider here. Firstly, the decreasing affinity of the polymer for water as the size of R is increased progressively inhibits the overall degree of mixing. Secondly, the larger R the more rubbery is the polymer and so the smaller is the proportion of voids or cavities present. PMMA was well below T_g over the whole range and its structure presumably included "frozen-in" voids. If most of the sorbed water were present in voids then relatively little disturbance of the polymer matrix would occur[50] and it would be expected that the change

$$H_2O \text{ (bulk liquid)} \longrightarrow H_2O \text{ (liquid in cavities)}$$

would contribute little to $\Delta\bar{H}_A$ or $\Delta\bar{S}_A$. Similar behaviour was observed previously for small gas molecules in polyethyleneterephthalate[129] and for water in PEMA[49] when the polymers were below T_g.

Values of $\overline{\Delta\bar{H}}_A$ (with the exception of PMMA) and of $\overline{\Delta\bar{S}}_A$ all decrease with increasing c. This is in qualitative accord with the behaviour expected of systems in which penetrant-penetrant interactions assume increasing importance as c is increased. Theoretical values of $\overline{\Delta\bar{H}}_A$ and $\overline{\Delta\bar{S}}_A$ from the random polycondensation model are included, in parentheses, in Table 6-4 in the cases of PPMA and PBMA.

Values of ΔH for hydrogen bond rupture were taken as $\lim_{c \to 0} \Delta \bar{H}_A$ in each case. Even after allowing for experimental uncertainties the values do not compare well with experiment, except those for PPMA at lower values of c, and indicate that such a simple model is inadequate to describe the temperature dependence of sorption for these systems.

ii) Temperature Dependence of Clustering Functions

For a given water activity, although some scatter due to experimental uncertainties was observed, both clustering functions (Table 6-2) generally decrease with increasing temperature. Some decrease is to be expected since additional thermal energy must break some fraction of the hydrogen bonds present in a system.

The case of PMMA is less clear since the clustering functions are independent of temperature. If water sorbed in this polymer exists mainly in pre-existing cavities, then to explain the results obtained it would have to be postulated that for a given water activity the water content of the cavities depends only on the volume fraction and mean size of cavities and not on the temperature. Perhaps the effect of the surrounding polymer structure is to

stabilise the occluded water and to minimise any tendency for associated water in voids to dissociate with increases in the thermal energy of the system.

6.2 Steady State Permeability Results

Data leading to permeability results and a sample calculation are presented in the appendix (9.7 and 9.9 respectively). Graphs of permeation rate vs. relative vapour pressure for water and methanol in PEMA are illustrated in Figure 6-12.

6.2.1 Concentration Dependence of P

For water, graphs of the permeation rate $J\ell$ vs. p/p_o are linear at temperatures up to $\sim 60^oC$ so that P is constant in each case. This feature was also observed previously for other polymers[59] (section 2.7.8). If it is assumed that monomeric water has a constant diffusion coefficient and is sorbed according to Henry's law then the results indicate that the associated water does not contribute appreciably to the flux. Above $\sim 60^oC$ (PMMA and PEMA only studied in this region) P increases slightly with c at the higher concentrations, possibly because of slight plasticisation of the polymer so that in this region the term B_f of equation (2-78) increases slightly with c.

FIG. 6·12

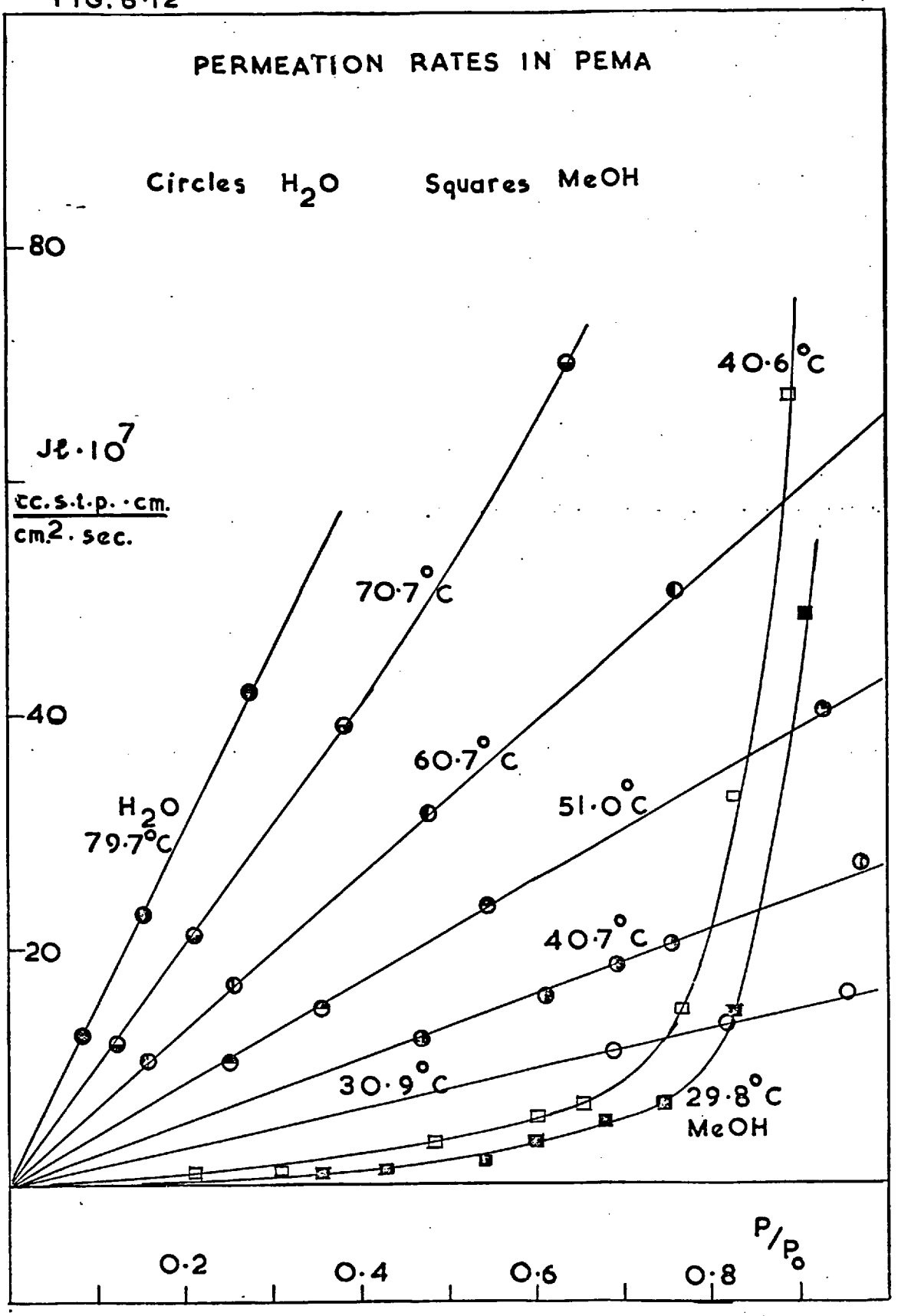
PERMEATION RATES IN PEMA
Circles H_2O Squares MeOH
80
40
20
$Jl \cdot 10^7$
cc.s.t.p.·cm.
cm.2·sec.
70·7°C
40·6°C
60·7°C
H_2O
79·7°C
51·0°C
40·7°C
30·9°C
29·8°C
MeOH
0·2
0·4
0·6
0·8
P/Po

Barrie and Platt[43] actually observed a slight decrease in P with increasing c for the system PMMA-H_2O, although this may have been an experimental effect caused by the supporting gauze decreasing the effective surface area of the membrane at the higher ingoing pressures.

P increases markedly with c for methanol in PEMA (Figure 6-12). As methanol is sorbed to a much greater extent than water, considerable plasticisation of the polymer most likely takes place.

6.2.2 Absolute Magnitudes of P

Values of P are given in Table 6-5. Where P varies with c, values in the limit ($c \rightarrow 0$) were taken. The permeabilities for water in PMMA and PEMA of this investigation are within 5 and 25% respectively of results of previous workers[135, 49] although the value for PMMA agrees only to within 50% with that of Barrie and Platt[43]. Differences of this order are perhaps to be expected between different samples of a glassy polymer. PPMA films of two different thicknesses give almost identical values for P. Sample (A) (Table 6-5) was 1.76×10^{-2} cm and sample (B) 9.6×10^{-3} cm in thickness. Wendisch and Plumer[118] found P for water in PBMA to increase slightly with increasing

TABLE 6-5

Permeability Coefficients P (cc. s.t.p. cm. cm.$^{-2}$ sec.$^{-1}$ (cmHg)$^{-1}$)

System	T°C	P x 10^7	System	T°C	P x 10^7
PMMA - H_2O	39.8	1.39	PMMA - H_2O	41.9	5.35 (A)
"	50.0	1.44	"	42.2	5.35 (B)
"	59.8	1.50	"	49.6	5.24 (A)
"	70.7	1.59	"	49.8	5.22 (B)
PEMA - H_2O	30.9	5.11	PBMA - H_2O	26.4	4.40
"	40.7	4.73	"	33.6	4.54
"	51.0	4.44	"	40.5	4.76
"	60.7	4.30	"	47.5	4.99
"	70.7	4.20	"	55.5	5.21
"	80.6	4.09			
			PPA - H_2O	48.9	29.6
PPMA - H_2O	26.9	5.75 (A)			
"	31.8	5.55 (A)	PEMA-MeOH	29.8	0.05
"	31.9	5.44 (B)	"	40.6	0.12
"	37.1	5.50 (A)			
"	37.4	5.48 (B)			

membrane thickness. However their membranes were two orders of magnitude thinner than the ones used in this investigation and accurate measurements were correspondingly more difficult to make. Their value for P at 50°C is within 40% of the corresponding value obtained here.

At ~50°C, P for water increases in the order

PMMA < PEMA < PPMA ~ PBMA < PPA

i.e. with increasing rubbery character of the polymer.

Since P depends on both D and σ, a more detailed discussion of this observation is postponed until the diffusion coefficient results are discussed. For the same reason a discussion of the lower P values for methanol in the limit ($c \rightarrow 0$) is left for a later section (6.3.1).

6.2.3 Temperature Dependence of P

Values for the temperature coefficient of the permeability E_P were calculated from $P = P_o \exp(-E_P/RT)$ and are presented in Table 6-6. Graphs of log P vs. 1/T are shown in Figure 6-13.

TABLE 6-6

Temperature Coefficients of the Permeabilities E_P(kcal.mole^{-1})

System	E_P	System	E_P
PMMA - H_2O	+ 0.9	PBMA - H_2O	+ 1.2
PEMA - H_2O	- 0.9	PEMA-MeOH	$\sim$+14 ($c \rightarrow o$)
PPMA - H_2O	- 0.6		

The values of E_P for water are small in comparison with those for most other polymers[11]. They are close to zero indicating that $\Delta\bar{H}_s$ is (numerically) similar to E_D, with $\Delta\bar{H}_s$ slightly exceeding E_D for PEMA and PPMA. This

FIG. 6·13

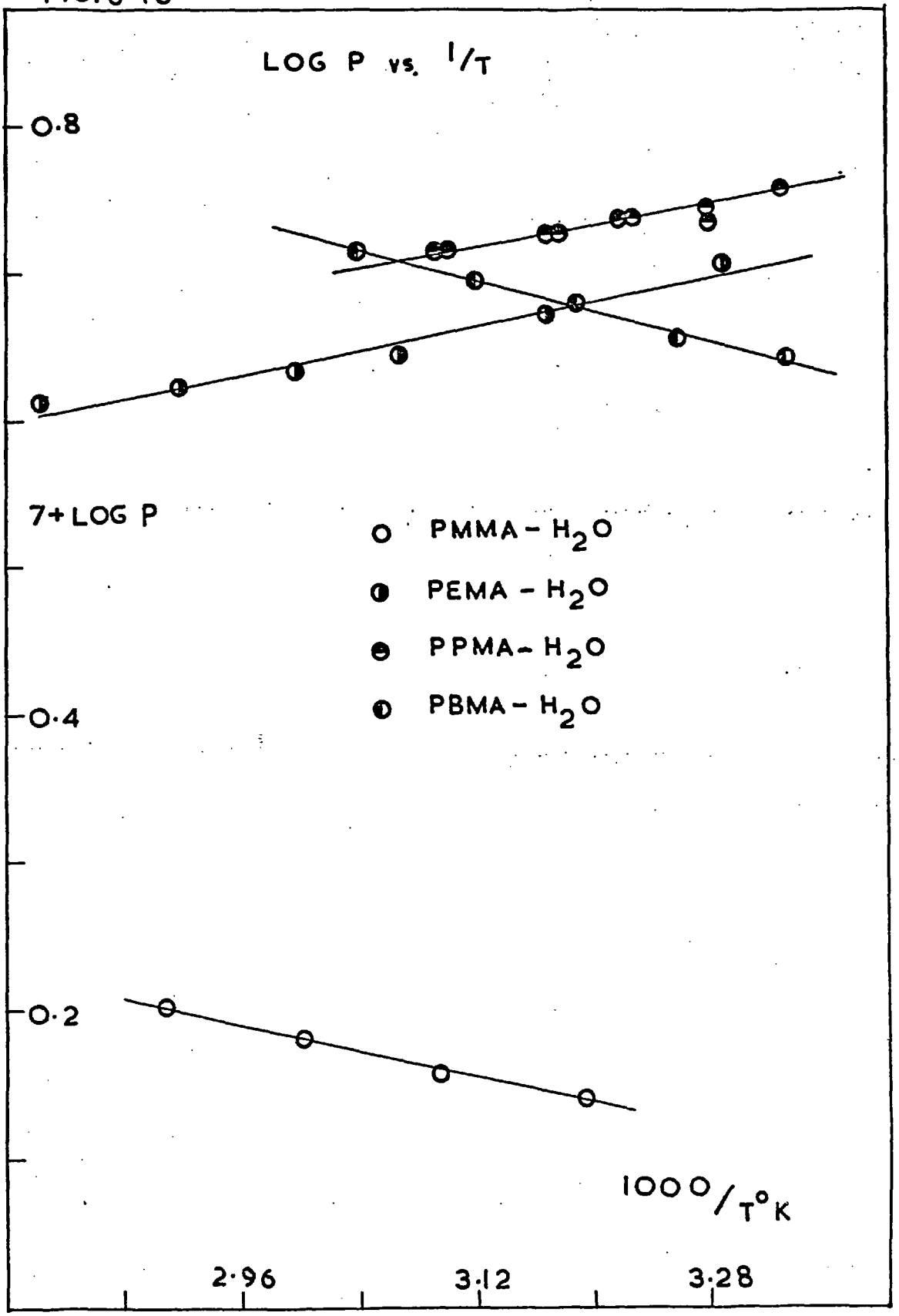
LOG P vs. 1/T
0·8
7+LOG P
O PMMA - H2O
PEMA - H2O
PPMA - H2O
PBMA - H2O
0·4
0·2
1000/T°K
2·96
3·12
3·28

contrasts slightly with results of Stannett and Williams[49] who found virtually zero E_p for PEMA - H_2O.

The temperature ranges used were too small to enable accurate values for P_o to be determined.

6.3 Diffusion Coefficients

6.3.1 Steady State Diffusion

Diffusion coefficients for water were calculated from a combination of steady state permeability and equilibrium sorption results as described in section 2.4.1. A curve-fitting procedure was used to describe the sorption isotherms by expressing the relative vapour pressure as three and four term polynomials in c, i.e. as

$$(p/p_o) = \alpha c + \beta c^2 + \gamma c^3 + \delta c^4 = \alpha' c + \beta' c^2 + \gamma' c^3 \quad \ldots.(6\text{-}2)$$

In general $J\ell$ is a linear function of p/p_o. Denoting the slope of the straight line by g, then

$$J\ell = g(\alpha c + \beta c^2 + \gamma c^3 + \delta c^4)$$
$$= g(\alpha' c + \beta' c^2 + \gamma' c^3)$$

Analytical differentiation gives D(c) in the form

$$D(c) = \alpha g + 2\beta gc + 3\gamma gc^2 + 4\delta gc^3 = \alpha' g + 2\beta' gc + 3\gamma' gc^2$$

or

$$D(c) = D_{c=0}(1 + Ac + Bc^2 + Cc^3) = D'_{c=0}(1 + A'c + B'c^2) \quad ...(6-3)$$

where $A = 2\beta/\alpha$, $B = 3\gamma/\alpha$ etc. The polynomial coefficients α, α' etc. were computed using a minimum mean squares deviation technique. From Figure 6-14 it is clear that both the three and four term polynomials provide good fits to an experimental isotherm. Values of the computed polynomial coefficients are given in Table 6-7. In practice limiting values of D at zero water concentration were obtained by averaging $D_{c=0}$ and $D'_{c=0}$ of equation (6-3) and will now be referred to for convenience as $D_{c=0}$.

Graphs of ϕ_A vs p/p_o and $J\ell$ vs. p/p_o for methanol in PEMA were combined to give $J\ell$ as a function of ϕ_A, where ϕ_A is the volume fraction of methanol. Slopes of the $J\ell - \phi_A$ curves were measured graphically at various points to obtain the mutual diffusion coefficient $D^V(\phi_A) = d(J\ell)/d\phi_A$, the unit of material quantity in J being cc. of liquid methanol.

i) Values of $D_{c=0}$

Values of $D_{c=0}$ are given in Table 6-8. The values for PEMA-H_2O are within 20% of previous results[49].

FIG. 6·14

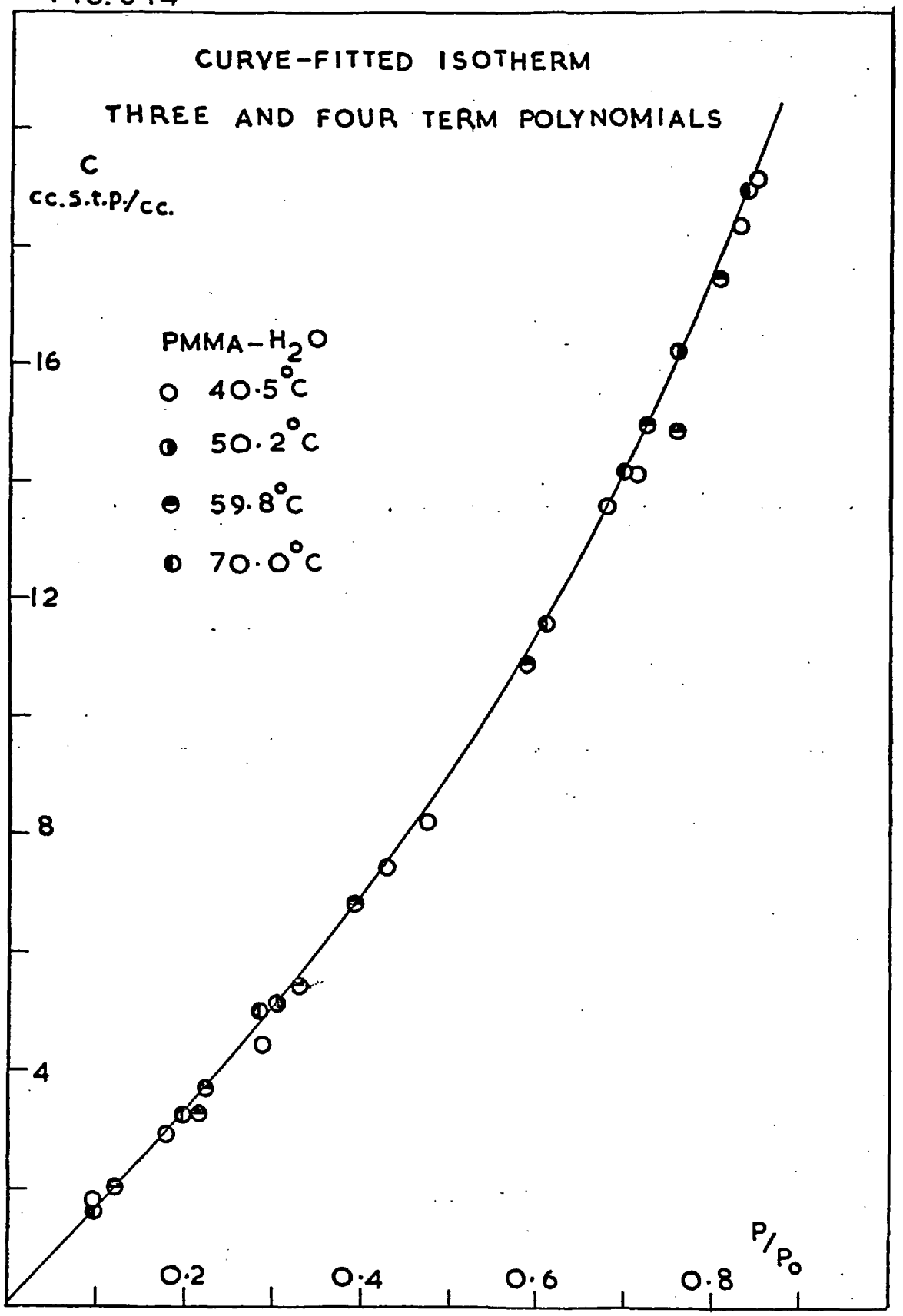
CURVE-FITTED ISOTHERM
THREE AND FOUR TERM POLYNOMIALS
C
cc.S.t.p./cc.
PMMA-H2O
40·5°C
50·2°C
59·8°C
70·0°C
16
12
8
4
0·2
0·4
0·6
0·8
P/Po

TABLE 6-7

Values of Polynomial Coefficients in equation (6-2)

System	T°C	α x10	βx10^2	γx10^3	δx10^4	α' x10	β'x10^2	γ'x10^3
PPMA-H_2O	40.5to 70.0	0.645	-0.067	-0.053	0.017	0.665	-0.133	0.0082
PEMA-H_2O	30.0	1.28	-0.460	-0.101	0.086	1.31	-0.595	0.095
"	39.9	1.09	-0.260	-0.048	0.033	1.10	-0.321	0.033
"	49.5	1.04	-0.346	+0.038	0.0068	1.04	-0.360	0.056
"	60.2	0.933	-0.089	-0.258	0.117	0.992	-0.343	0.056
"	70.0	0.806	+0.029	-0.253	0.089	0.873	-0.224	0.021
"	79.7	0.667	-0.012	-0.092	0.025	0.689	-0.090	-0.011
PPMA-H_2O	32.0	2.60	-2.76	1.54	-0.122	2.60	-2.70	1.39
"	37.1	2.60	-3.95	4.60	-2.23	2.48	-2.88	1.78
"	41.9	2.21	-2.35	1.49	-0.229	2.20	-2.23	1.18
"	49.6	1.76	-1.24	0.622	-0.039	1.76	-1.21	0.563
"	55.6	1.68	-1.55	1.28	-0.548	1.62	-1.10	0.376
"	64.4	1.33	-0.42	-0.170	+0.147	1.35	-0.53	0.061
PBMA-H_2O	27.0	3.56	-7.52	11.2	-7.26	3.35	-5.16	3.68
"	34.1	3.10	-4.32	1.82	1.60	3.15	-4.84	3.49
"	40.4	2.49	-2.77	2.15	-0.819	2.46	-2.40	1.15
"	49.6	2.13	-1.95	1.54	-0.592	2.10	-1.67	0.799
"	55.6	1.78	-0.943	0.262	-0.131	1.77	-0.878	0.093
PPA-H_2O	48.9	0.999	-0.190	-0.116	0.045	1.01	-0.243	-0.027

A comparison of the values for water at $\sim 50^\circ C$ reveals that

PMMA $<$ PEMA $<$ PPMA $<$ PBMA $<$ PPA

i.e. virtually the same order as for the permeability coefficients indicating that the trend in the latter is

TABLE 6-8

$D_{c=O}$ in cm^2 $sec.^{-1}$ (Mean Values from 3 and 4 term polynomials)

System	T^oC	$D_{c=O} \times 10^7$	System	T^oC	$D_{c=O} \times 10^7$
PMMA - H_2O	40.5	0.52	PPMA - H_2O	49.6	8.3
"	50.2	0.89	"	55.6	10.3
"	59.8	1.5	"	64.4	12.2
"	70.0	2.4			
			PBMA - H_2O	27.0	4.0
PEMA - H_2O	30.0	2.1	"	34.1	5.8
"	39.9	2.9	"	40.4	6.7
"	49.5	4.2	"	49.6	9.7
"	60.2	6.3	"	55.6	11.2
"	70.0	8.2			
"	79.7	9.8	PPA - H_2O	48.9	26
PPMA - H_2O	32.0	5.1	PEMA-MeOH	29.8	0.039
"	37.1	6.5	"	40.6	0.093
"	41.9	7.2			

mainly determined by the values of the diffusion coefficients. The order in this series can be readily explained in terms of the relative segmental mobilities of the polymers[136] and is in the order of decreasing T_g. Returning again to the monomeric repeat unit

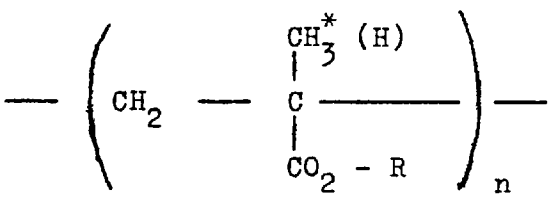

if the hydrogen atom in parentheses is replaced by the

starred methyl group then the latter introduces both mass and rigidity and so decreases the chain mobility. Polyacrylates therefore have lower T_g's than the corresponding polymethacrylates and this is reflected in the relatively high value of $D_{c=0}$ for PPA. On the other hand the introduction of a methylene group into R, where R remains a n-alkyl group, increases not only the mass of the side chain but also its flexibility and hence increases the value of $D_{c=0}$ for water. Similar observations were made by Newns[16] with benzene as penetrant.

The lower values of $D_{c=0}$ (and of P) for methanol compared with those for water in PEMA are simply a consequence of the larger size of the methanol molecule, since complicating effects of polymer plasticisation and of penetrant-penetrant interactions are minimised as $c \rightarrow 0$.

ii) Concentration Dependence of D

For water, D decreases with increasing c in each polymer. Values at a relative humidity of 0.8 - 0.9 are between 1/2 and 1/6 of those at zero water concentration. In general the relative decrease from $D_{c=0}$ is greater the lower the temperature. On the other hand D^V for methanol in PEMA increases with c or ϕ_A until, at a relative vapour

pressure of ~ 0.7, it is about three times its value at c=0. The concentration dependence of the relative diffusion coefficient D', defined as $D' = D/D_{c=0}$, for water in each polymer is illustrated in Figures 6-15 to 6-19.

The D'-c curves for water in PMMA and PBMA at ~50°C are compared in Figures 6-15 and 6-18 with theoretical curves calculated on the basis of the polycondensation models assuming that only monomeric water diffuses. As expected from the corresponding sorption isotherm analysis (section 6.1.2 part ii)) the agreement is poor although slightly better for $\xi = 0.05$ than for random polycondensation with $\xi = 0$. If the polycondensation theory were to hold for water in a truly inert medium then it would seem that PBMA does not constitute any better an approximation to such an idealised medium than does PMMA, despite the larger value of Z (section 6.1.1) and increased glassy nature of the latter. As D' decreases with increasing c, some form of water association is still the dominant factor in determining the observed D'- c dependences. It was pointed out by Barrie and Platt[43] that in the case of PMMA some degree of specific interaction between water and polymer and of polymer plasticisation may occur concurrently with water association.

FIG. 6·15

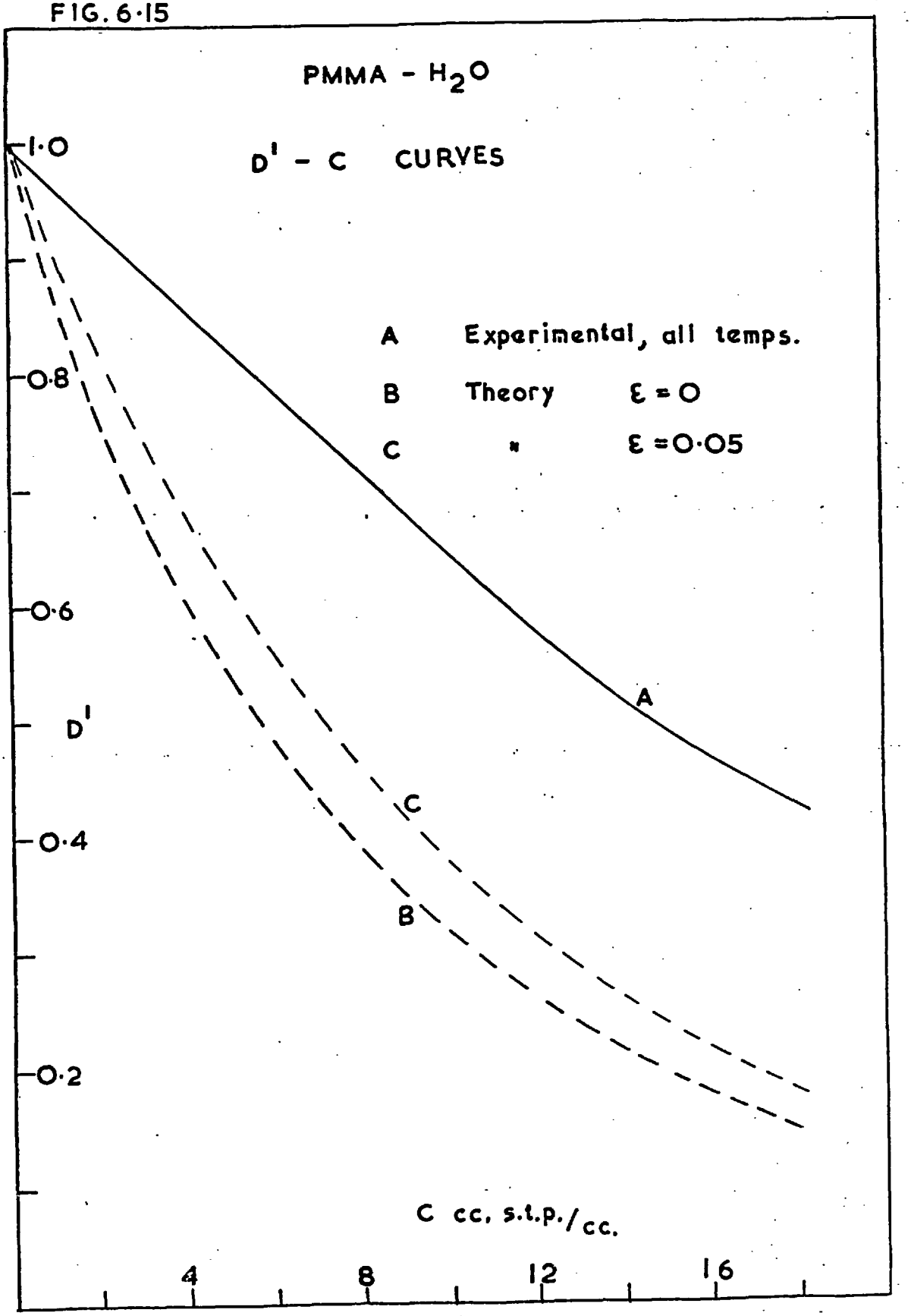
PMMA - H_2O
D' - C CURVES
A Experimental, all temps.
B Theory ε = 0
C " ε = 0·05
1·0
0·8
0·6
0·4
0·2
D'
A
C
B
C cc. s.t.p./cc.
4
8
12
16

FIG. 6·16

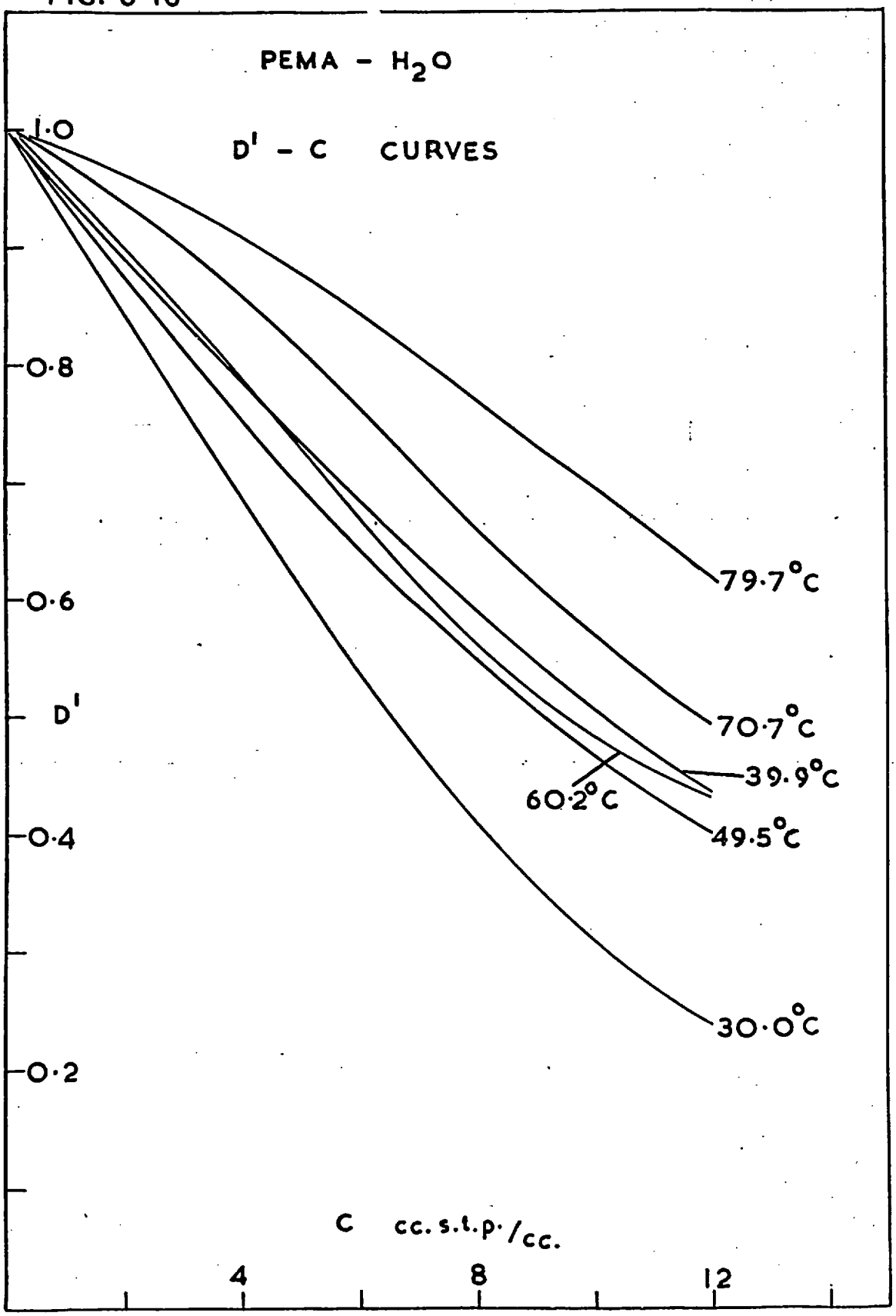
PEMA - H_2O
D' - C CURVES
1·0
0·8
0·6
0·4
0·2
D'
79·7°C
70·7°C
39·9°C
60·2°C
49·5°C
30·0°C
C cc. s.t.p./cc.
4
8
12

FIG. 6·17

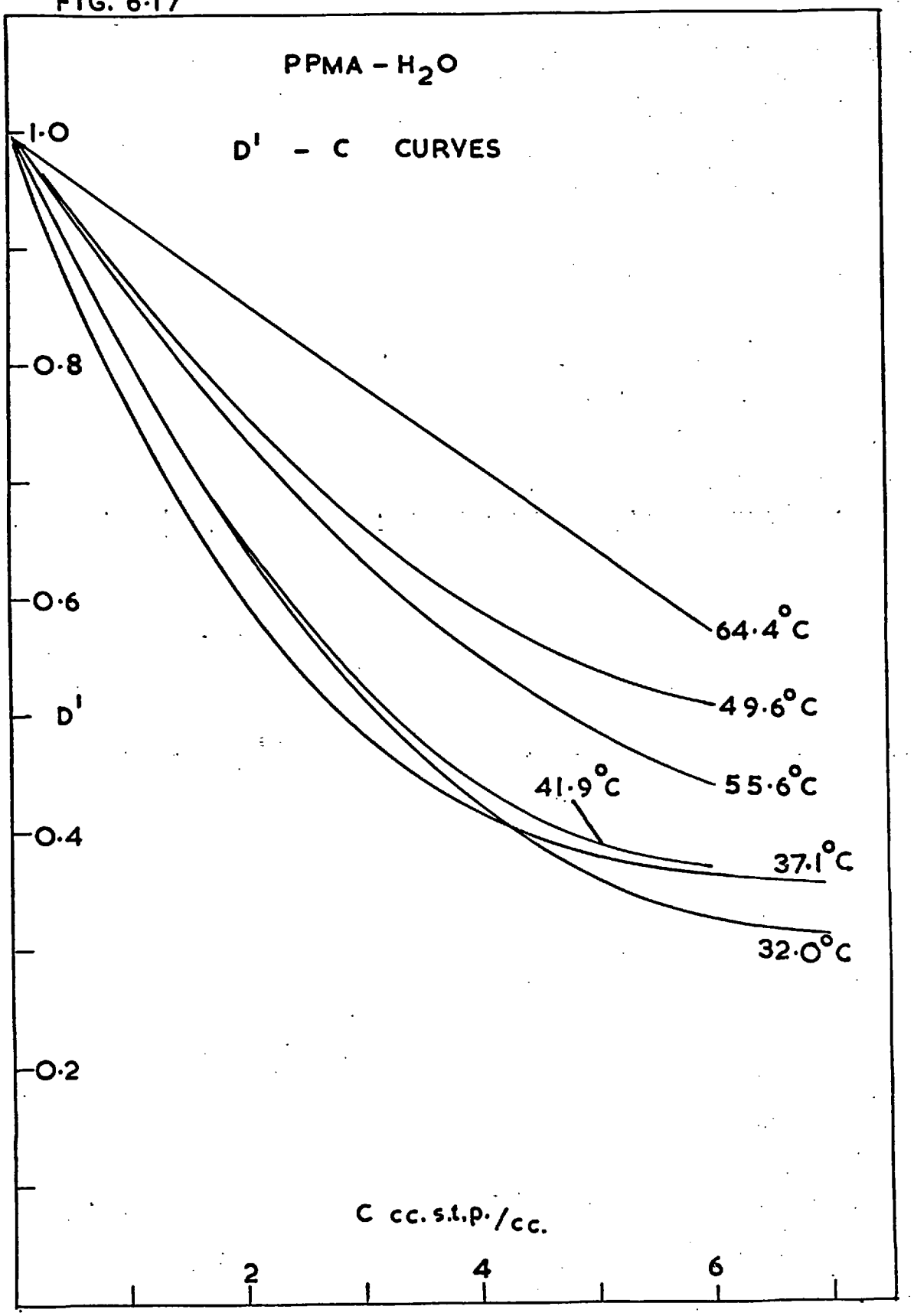
PPMA – H_2O
D' – C CURVES
1·0
0·8
0·6
0·4
0·2
D'
64·4°C
49·6°C
55·6°C
41·9°C
37·1°C
32·0°C
C cc. s.t.p./cc.
2
4
6

FIG. 6·18

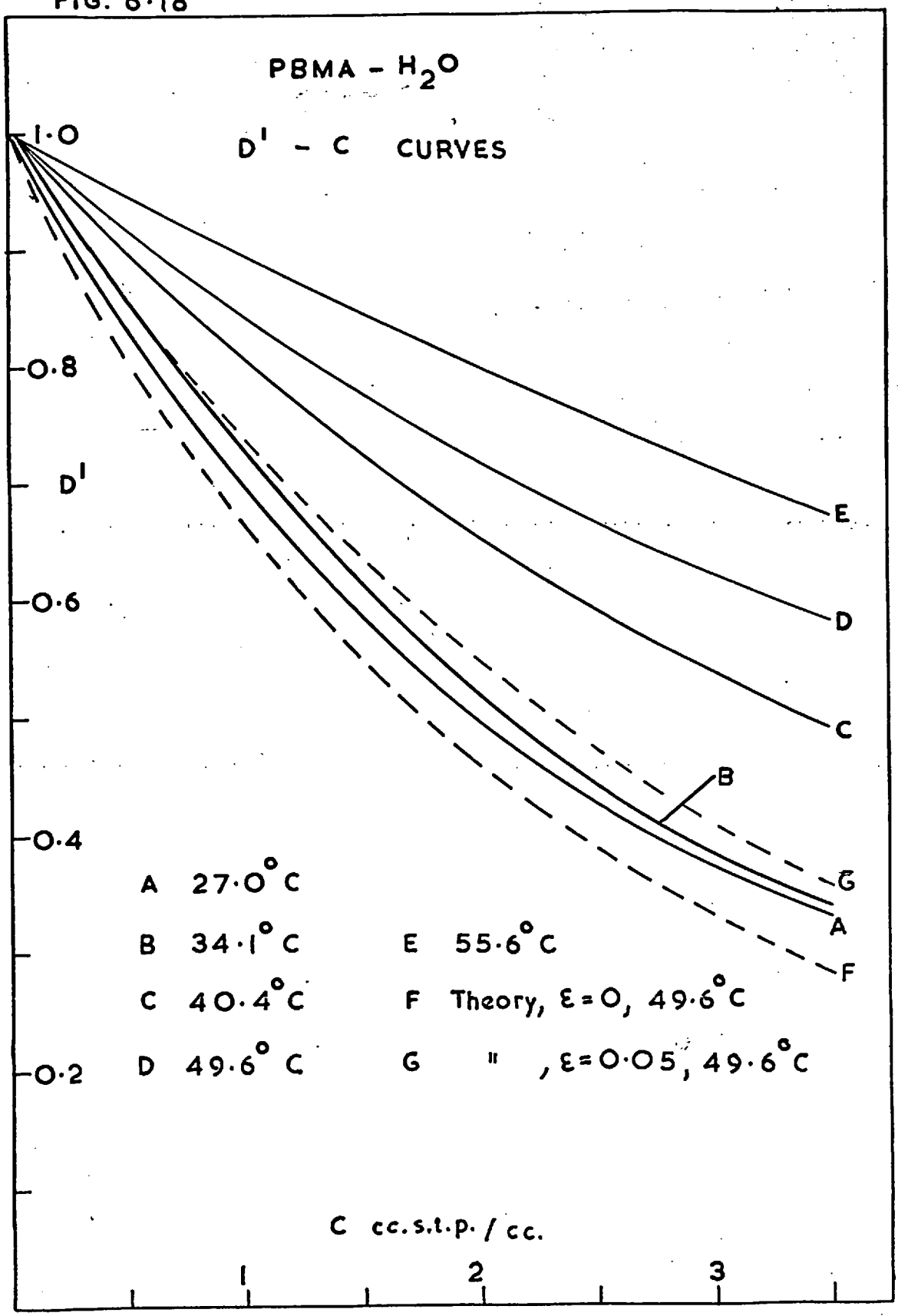
PBMA - H_2O
D' - C CURVES
1·0
0·8
D'
0·6
0·4
0·2
E
D
C
B
G
A
F
A 27·0° C
B 34·1° C
C 40·4° C
D 49·6° C
E 55·6° C
F Theory, ε = 0, 49·6° C
G " , ε = 0·05, 49·6° C
C cc.s.t.p. / cc.
1
2
3

FIG. 6·19

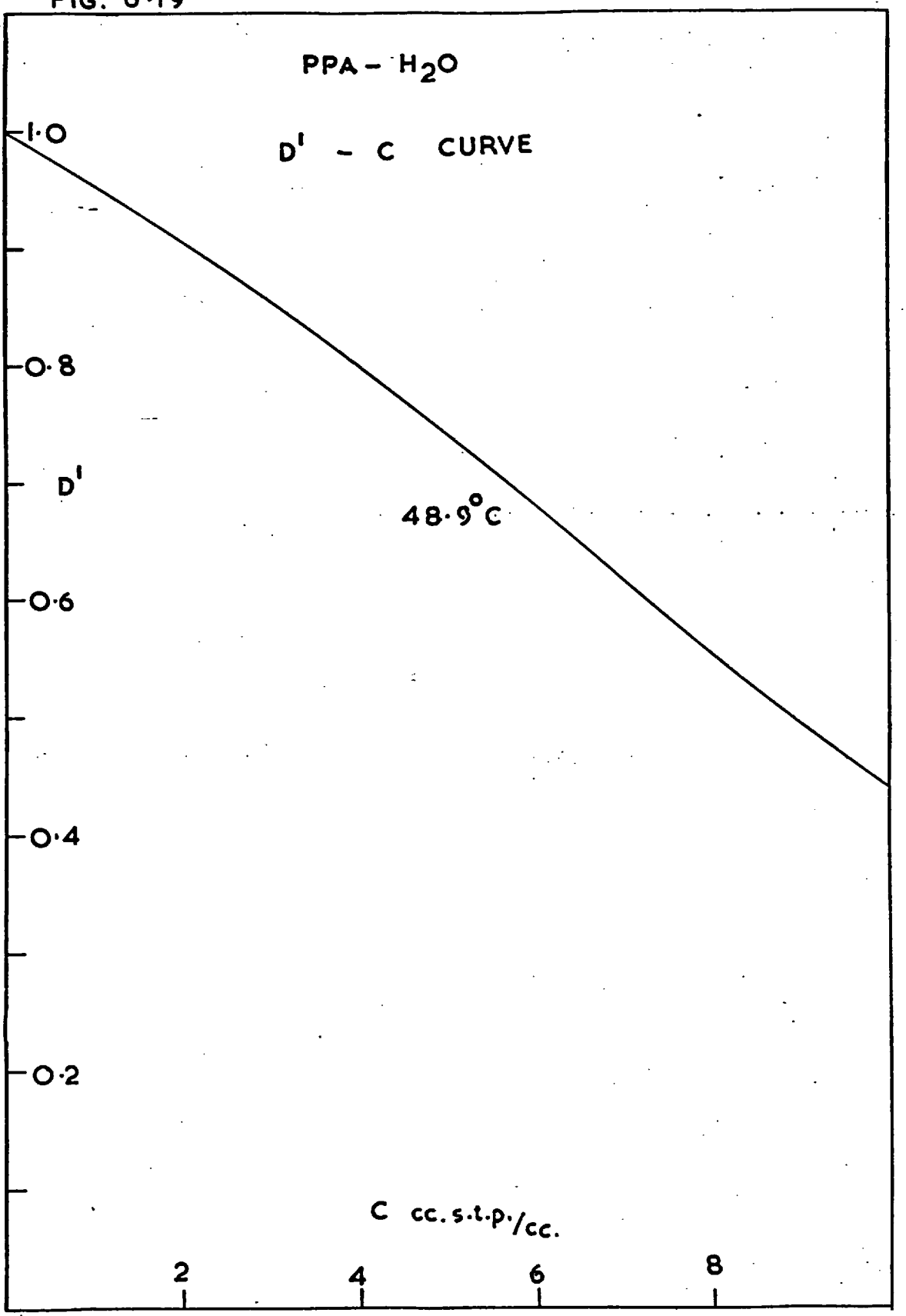

Methanol is sorbed to a much greater extent than water in PEMA and clustering, as evidenced from the sorption isotherm analysis, is significant. Even so, plasticisation of polymer is much more marked than in the case of water and sufficiently so as to cause D' to increase with c or ϕ_A. In fact the sorption of methanol is large enough to lead to appreciable differences between the various types of diffusion coefficient as discussed in section 2.2.5. Thus,

$$\mathcal{D}_A = D^V/\phi_B = D_A^B/\phi_B^3$$

Since the $J\ell - \phi_A$ and not the $J\ell - c$ curve was differentiated,

$$\frac{d(J\ell)}{d\phi_A} = \frac{d(J\ell)}{dc} \cdot \frac{dc}{d\phi_A} = \mathcal{D}_A \phi_B^3 \cdot \frac{dc}{d\phi_A}$$

where c is expressed in cc. of liquid methanol per cc. of dry polymer so that $dc/d\phi_A = 1/\phi_B^2$. Hence

$$\frac{d(J\ell)}{d\phi_A} = \mathcal{D}_A \phi_B = D^V$$

In Figure 6-20 $\mathcal{D}_A$ and D^V are plotted vs. ϕ_A at 29.8°C.

6.3.2 Transient State Diffusion

Of the several systems investigated three only were subjected to a transient state analysis, viz. PPA-H_2O

FIG. 6·20

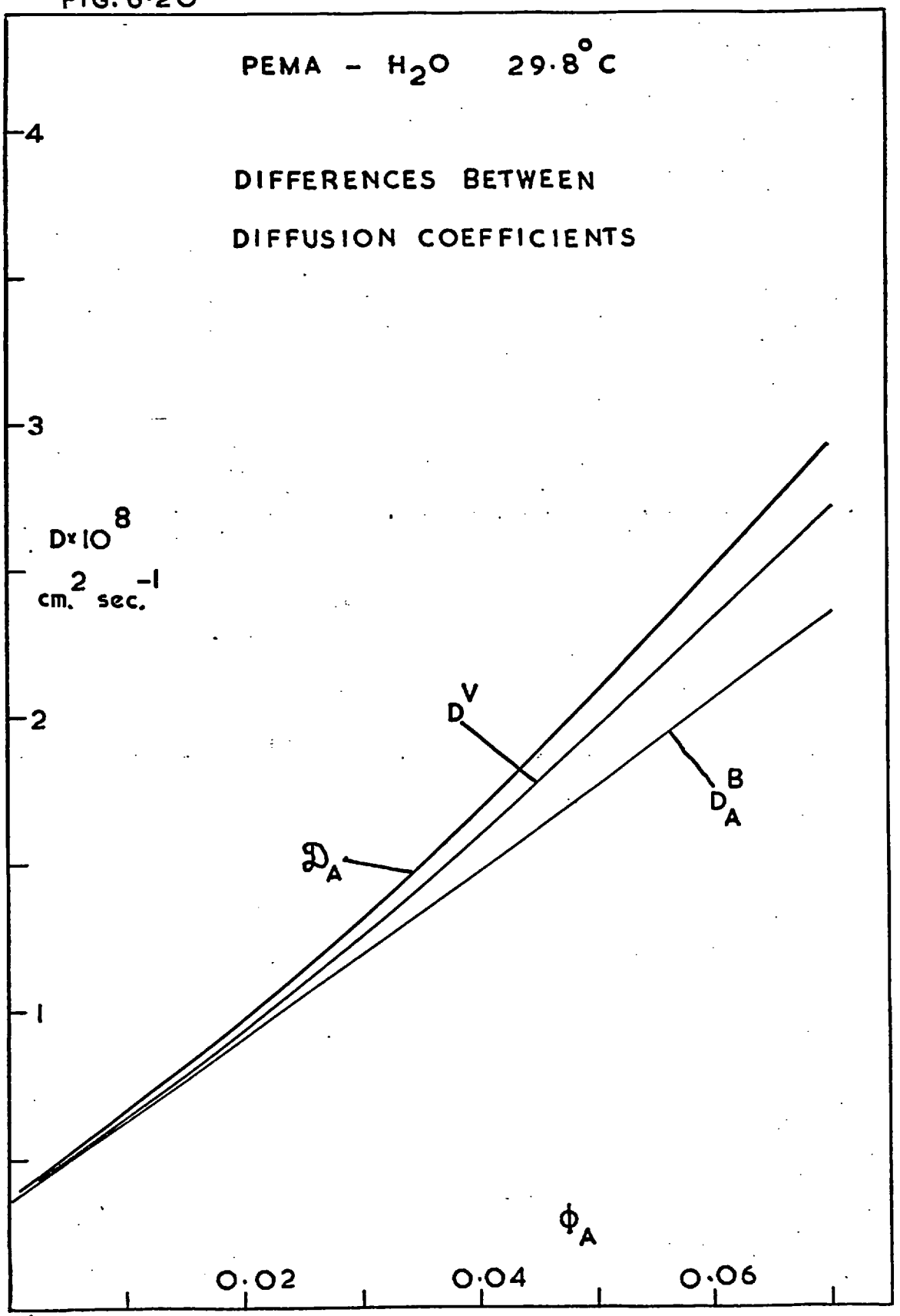
PEMA - H_2O 29·8°C
DIFFERENCES BETWEEN
DIFFUSION COEFFICIENTS
4
3
2
1
$D \times 10^8$
$cm.^2\ sec.^{-1}$
D^V
D_A^B
$\mathcal{D}_A$
ϕ_A
0·02
0·04
0·06

at 48.9°C, PBMA-H_2O at 39.8°C and PEMA-MeOH at 40.6°C. The object was to compare $D_{c=0}$ values and D'-c relationships with those obtained from the steady state.

i) Reduced Sorption and Desorption Curves

Reduced curves for each system are linear initially, becoming concave to the $t^{\frac{1}{2}}/\ell$ axis at longer times. The linear portions of all the curves for water pass on extrapolation through the origin whereas those of the desorption curves corresponding to the higher volume fractions of methanol sorbed at equilibrium cut the zero time axis at positive values of M_t/M_∞. In addition these desorption curves cross beneath the conjugate sorption curves at longer times suggesting that sorption is faster than desorption. The latter is also indicated at lower volume fractions of sorbed methanol when I_s slightly exceeds I_d. The reason for the desorption behaviour at higher ϕ_A is not clear. The latter may have been an experimental effect (see section 5.4.3) rather than a true effect of the system. Only the sorption curves were analysed quantitatively for PEMA-MeOH.

Typical conjugate curves for each system are shown in Figure 6-21. Data used for plotting all reduced curves are presented in appendix 9.8.

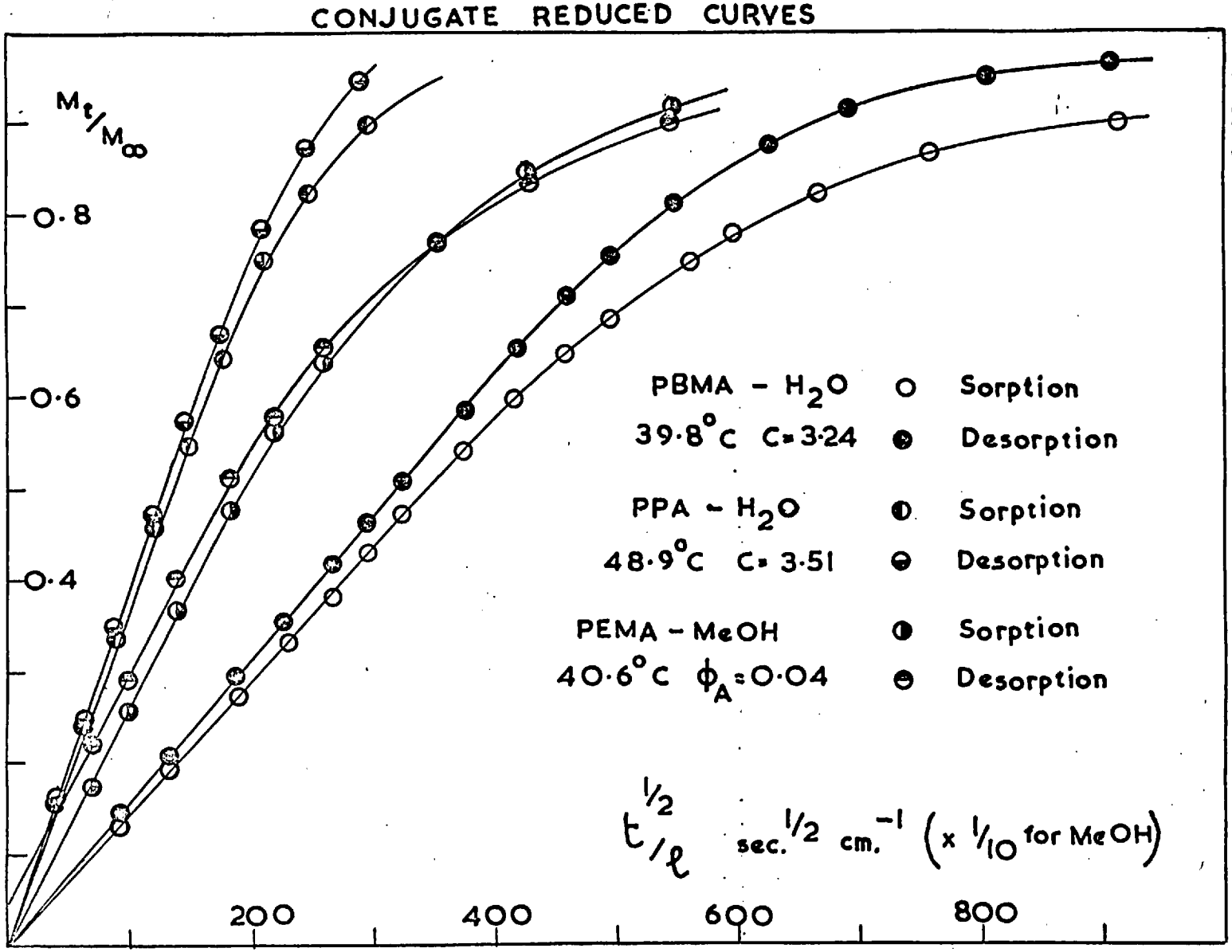
CONJUGATE REDUCED CURVES
M_t/M_∞
0·8
0·6
0·4
200
400
600
800
PBMA – H_2O
39·8°C C = 3·24
PPA – H_2O
48·9°C C = 3·51
PEMA – MeOH
40·6°C ϕ_A = 0·04
Sorption
Desorption
Sorption
Desorption
Sorption
Desorption
$t^{1/2}/\ell$ sec.$^{1/2}$ cm.$^{-1}$ (x 1/10 for MeOH)

FIG. 6·21

ii) Determination of Diffusion Coefficients

Mean diffusion coefficients $\bar{D}_s$ and $\bar{D}_d$ were calculated from $\bar{D}_s = \pi I_s^2/16$ and $\bar{D}_d = \pi I_d^2/16$, where I_s and I_d are the corresponding initial slopes of reduced sorption and desorption curves respectively. Values of I_s, I_d, $\bar{D}_s$ and $\bar{D}_d$ are given in Table 6-9. Differential diffusion coefficients D were calculated from $\bar{D}$ for each system by four (three for PEMA-MeOH) separate procedures which were considered in section 2.4.3.

a) Graphical differentiation of $\bar{D}_{AV} = 1/2(\bar{D}_s + \bar{D}_d)$ vs. c gave D using

$$D(c) = \frac{d(c\bar{D}_{AV})}{dc} = \bar{D}_{AV} + c.\frac{d\,\bar{D}_{AV}}{dc}$$

b) Graphs of $\bar{D}_s$ vs. c were plotted and D obtained from equation (2-36) using p = 1.67 for PEMA-MeOH and p = 1.85 for PPA and PBMA-H_2O. As before, differentiation was performed graphically.

c) I_s was plotted vs. c and smooth curves drawn through the points. From these curves numerous points were read off and fed into the simultaneous equations (2-39) which were solved using a minimum mean squares deviation technique to obtain D(c) (see also appendix 9.2).

TABLE 6-9 (a)

Initial Slopes I_s, I_d ($cm.sec^{-\frac{1}{2}}$) of Reduced Sorption Curves and Mean Diffusion Coefficients $\bar{D}_s$, $\bar{D}_d$ (cm^2 $sec.^{-1}$)

System	c $cc.s.t.p.cm^{-3}$	$I_s x10^3$	$I_d x10^3$	$\bar{D}_s x10^7$	$\bar{D}_d x10^7$
PPA-H_2O	0.73	3.9_6	4.0_1	31	31.5
"	1.89	3.8_4	3.9_5	29	31
"	3.51	3.7_4	3.9_2	27.5	30
"	6.43	3.6_1	3.7_8	26	28
"	9.58	3.3_1	3.6_3	21.5	26
PBMA-H_2O	0.76	1.70	1.73	5.7	5.9
"	3.24	1.47	1.58	4.2	4.9
"	4.68	1.31	-	3.4	-
"	5.51	1.27	-	3.1	-
"	4.74	1.34	-	3.5	-
"	0.95	1.68	1.72	5.6	5.8
"	1.90	1.59	1.65	4.9	5.4
"	2.53	1.53	1.62	4.6	5.2
"	2.33	1.54	1.62	4.7	5.2
"	1.23	1.64	1.69	5.3	5.6
"	1.49	1.62	1.69	5.1	5.6
"	2.11	1.56	1.64	4.8	5.3
"	3.47	1.44	1.58	4.1	4.9
"	3.28	1.45	1.57	4.1	4.9

TABLE 6-9 (b)

I_s and $\bar{D}_s$ for PEMA - MeOH 40.6°C

c cc.s.t.p. cm^{-3}	ϕ_A	$I_s \times 10^4$ $cm.sec.^{-\frac{1}{2}}$	$\bar{D}_s \times 10^8$ $cm^2.sec.^{-1}$
0.40	0.0072	2.2	0.95
0.50	0.0090	2.2	0.97
0.65	0.0117	2.2	0.98
1.18	0.0212	2.2	0.99
1.40	0.0250	2.3	1.05
1.80	0.0319	2.5	1.2
2.31	0.0405	2.7	1.4

d) A procedure involving a step function approximation to D vs. c was carried out only to act as a rough check on the other methods. The details of the calculations are not given here but followed exactly those in the original paper by Prager[80]. Five equal concentration steps were used for each system. The diffusion coefficient D_i for the i-th step was calculated and a smoothing out process was

performed using

$$\bar{D}(c) = \frac{1}{c_K} \int_0^{c_k} D(c)dc = \frac{1}{k} \cdot \sum_{i=1}^{k} D_i \quad ....(6-4)$$

where c_k is the concentration corresponding to the k-th step. D(c) was obtained from $\bar{D}$ in a manner analogous to that from $\bar{D}_{AV}$ in a) above. Values of D_i, $\bar{D}$ and D for each system are given in Table 6-10.

iii) Comparison of $D_{c=0}$ with Steady State Values

Values of $D_{c=0}$ obtained from each transient state analysis and from the steady state analysis are given in Table 6-11.

Agreement between these values is good, with respect to both the various transient state analyses and the transient/steady state comparison, and is within the experimental error. Thus the larger relative difference between steady and transient state $D_{c=0}$ for water in PPA can be ascribed to the relatively crude measurements of membrane thickness that were made in this case.

TABLE 6-10

Values of D_i, $\bar{D}$ and D ($cm^2 . sec.^{-1}$) from Prager's Step Function Procedure[80]. Equation (6-4)

System	Concentration Step cc.s.t.p.cm^{-3}	i	$D_i x10^7$	$\bar{D}$ $x10^7$	D $x10^7$
PPA-H_2O	0-2	1	29	29	28
"	2-4	2	26.5	28	25
"	4-6	3	23	26	22
"	6-8	4	20	25	17.5
"	8-10	5	16.5	23	14
PBMA-H_2O	0-1	1	5.5	5.5	5.0
"	1-2	2	4.6	5.1	4.1
"	2-3	3	3.7	4.6	3.2
"	3-4	4	2.7	4.1	2.3
"	4-5	5	2.0	3.7	1.6
PEMA-MeOH	0 -0.0075*	1	0.095	0.095	0.096
"	0.0075-0.015	2	0.097	0.096	0.10
"	0.015 -0.0225	3	0.11	0.10	0.12
"	0.0225-0.03	4	0.13	0.11	0.13
"	0.03 -0.0375	5	0.13	0.11	-

* Volume Fractions

TABLE 6-11

Comparison of $D_{c=0}$ ($cm^2 . sec^{-1}$): Steady and Transient States

		$D_{c=0}$ x 10^7				
System	T^oC	From $\bar{D}_{AV}$	From Weighted Mean $\bar{D}_s$	From Lin Hwang's Procedure (9.2)	From Prager's Step Function Procedure	From the Steady State
PPA-H_2O	48.9	3.1	31	31.5	30.5	26
PBMA-H_2O	39.8	6.3	6.3	6.3	6.1	6.5
PEMA-MeOH	40.6	-	0.095	0.094	0.094	0.093

iv) Concentration Dependence of D : Comparison with Steady State.

a) Water

Relative diffusion coefficients D' (= $D/D_{c=0}$) for water in PPA and PBMA, calculated from both steady and transient states, are plotted vs. c in Figures 6-22 and 6-23. The figures illustrate that the agreement between the D'-c curves calculated from the steady state and from the various transient state procedures is good. This indicates that diffusion in these systems is "Fickian" and not complicated by any time-dependent features. Similar agreement was previously obtained[51] for the ethyl cellulose - H_2O system.

It is of interest at this stage to consider the time lag results of Stannett et al.[42,49,51] and the nature of the sorption-kinetic analysis. Stannett found the time lag for water to be constant for a number of polymers in which the steady state D decreased with increasing c, and suggested that water does not cluster under permeation conditions[51]. On this basis, no clustering of water would be expected to occur in the first stages of sorption when the water concentration at the centre of the sheet is negligible. However, diffusion

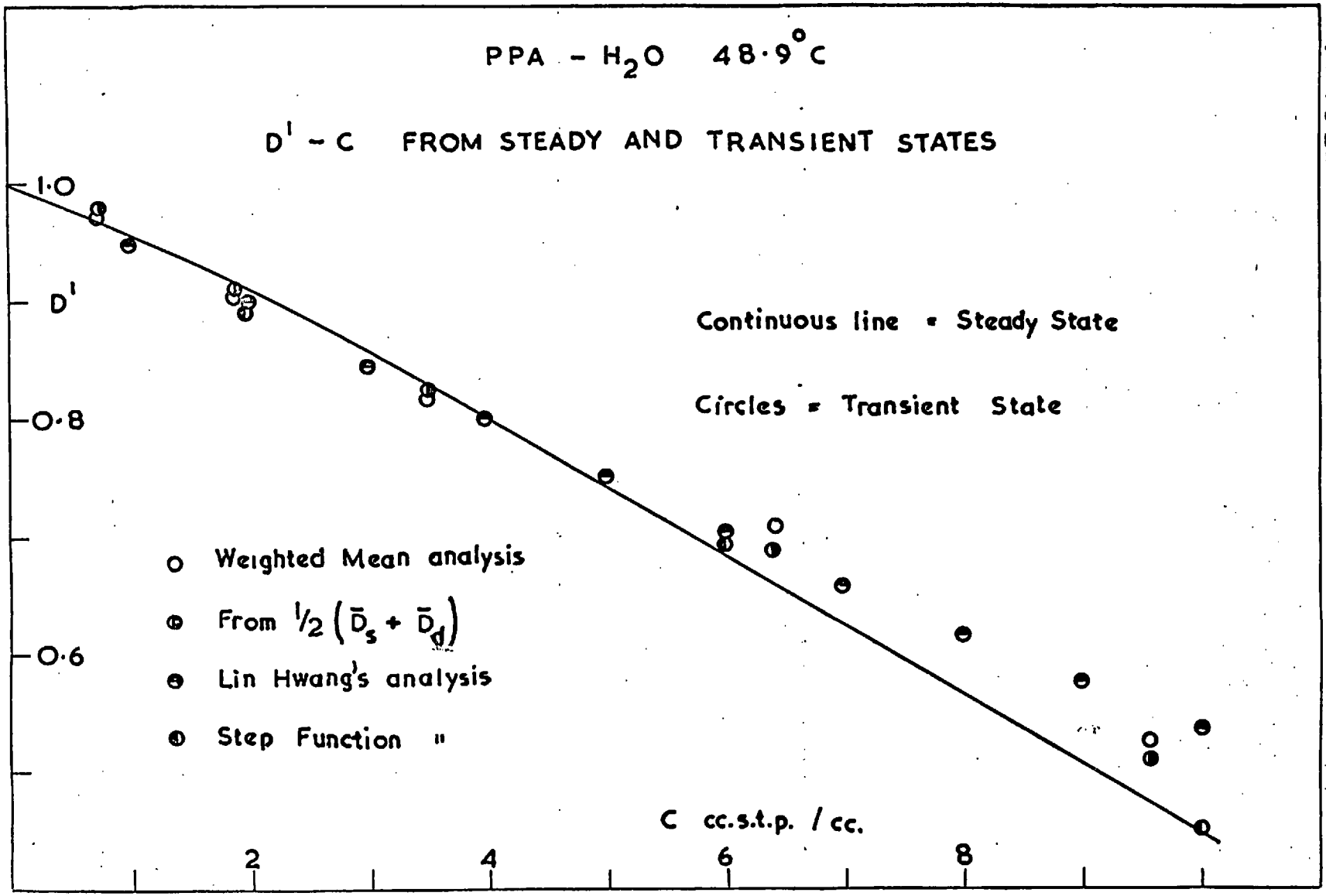
PPA - H_2O 48·9°C
D' - C FROM STEADY AND TRANSIENT STATES
1·0
D'
0·8
0·6
Continuous line = Steady State
Circles = Transient State
Weighted Mean analysis
From ½ ($\bar{D}_s$ + $\bar{D}_d$)
Lin Hwang's analysis
Step Function "
C cc.s.t.p. / cc.
2
4
6
8

FIG. 6·22

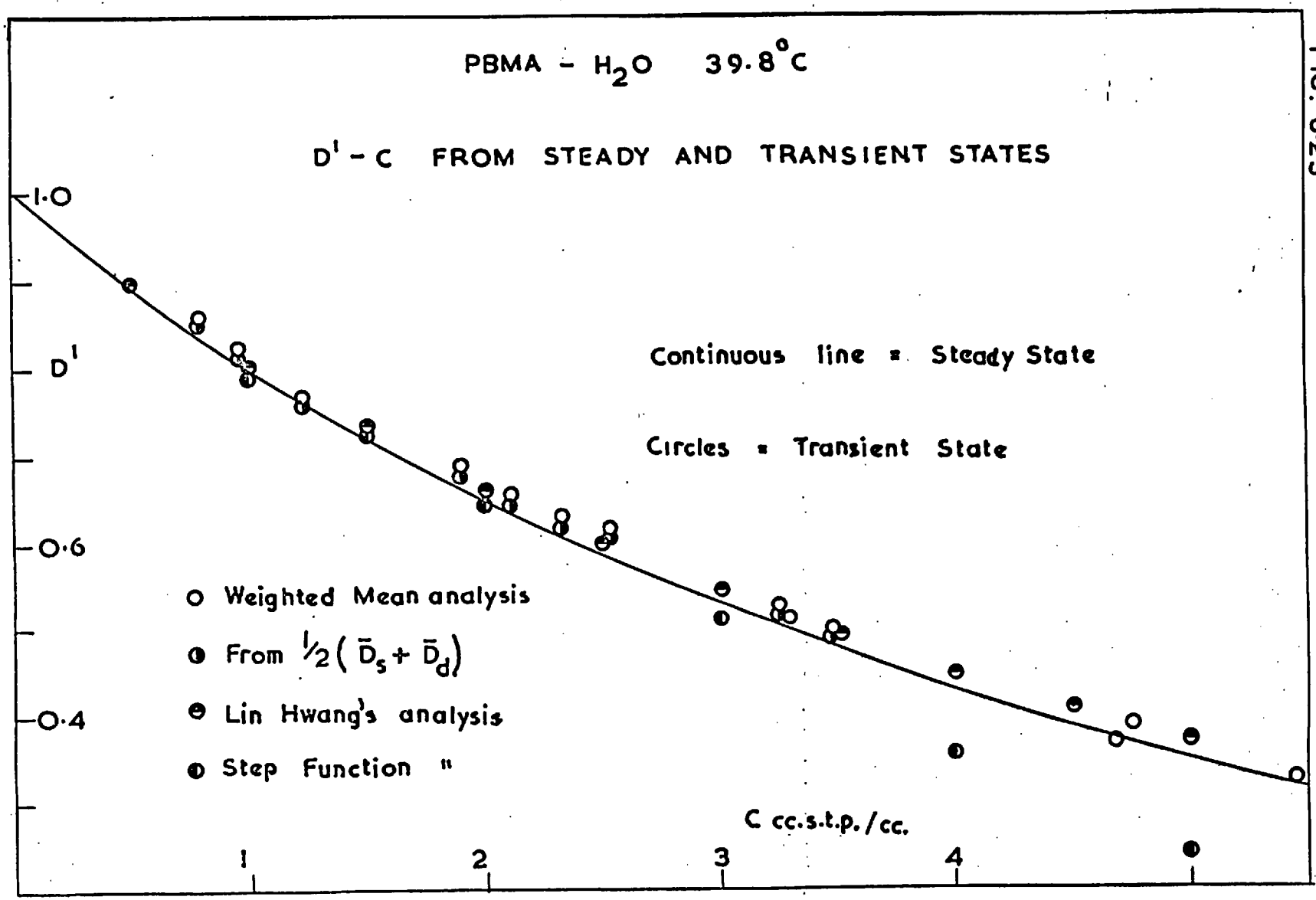
PBMA - H_2O 39.8°C
D' - C FROM STEADY AND TRANSIENT STATES
1·0
D'
0·6
0·4
Continuous line = Steady State
Circles = Transient State
O Weighted Mean analysis
◑ From ½ ($\bar{D}_s + \bar{D}_d$)
⊖ Lin Hwang's analysis
◐ Step Function "
C cc.s.t.p./cc.
1
2
3
4

FIG. 6.23

coefficients calculated from initial sorption rates depend on the ratio M_t/M_∞ and even if M_t did not include any contribution from clustering nevertheless M_∞ would be affected as the latter is an equilibrium parameter. For a system in which penetrant association becomes more pronounced at higher c and in which D decreases with increasing c, it follows that if there is an induction period to the clustering process such that in the early stages of sorption associated species do not contribute to M_t, then as c is increased M_t would become an increasingly smaller fraction of the corresponding value of M_t which would have been obtained had the clustering process been instantaneous. Hence the concentration dependence of D as measured from initial sorption rates would be exaggerated in comparison with that obtained from steady state measurements. On the other hand rates of desorption would remain unaffected but these vary relatively little with c in any case[137] (appendix 9.5).

To examine more quantitatively the expected differences between the steady and transient states when clusters are not formed in the initial stages of sorption, it can be assumed that the <u>absolute</u> initial sorption rates are governed by $D_f = D_{c=0}$ where subscript f refers to

"free" water. The following procedure is carried out to obtain an expression, involving quantities which can all be measured experimentally, for the transient state I_s-c relationship in terms of the steady state D-c relationship.

Considering first the case of a system with constant $D = D_f$, then

$$M_\infty = k \cdot (c_f)_\infty \qquad \text{where k is a constant}$$

and $$\frac{d(M_t \cdot \ell / t^{\frac{1}{2}})}{d(c_f)_\infty} = \frac{d(I_s k (c_f)_\infty)}{d(c_f)_\infty} = k \left(I_s + (c_f)_\infty \frac{dI_s}{d(c_f)_\infty} \right)$$

$$= k \cdot I_s \qquad \ldots\ldots(6\text{-}5)$$

since $dI_s/d(c_f)_\infty = 0$ for a system with constant D.

For concentration-dependent D, $M_\infty = kc_\infty$. As $p/p_o \rightarrow 0$, $c_\infty \rightarrow (c_f)_\infty \rightarrow 0$ and the value of I_s referred to above in the case of constant D can be identified with $I_{s(c_\infty = 0)}$. Hence when D decreases with c, equation (6-5) becomes

$$\frac{d(M_t \ell / t^{\frac{1}{2}})}{d (c_f)_\infty} = \frac{d (k c_\infty I_s)}{d (c_f)_\infty} = k I_{s(c_\infty = 0)}$$

or $$\frac{d (k c_\infty I_s)}{dc_\infty} = k I_{s(c=0)} \cdot \frac{\partial (c_f)_\infty}{\partial c_\infty} \qquad \ldots\ldots(6\text{-}6)$$

If only "free" water diffuses, then the steady state D is given (equation (2- 82)) by

$$D(c) = D_{c=0} \cdot \frac{\partial c_f}{\partial c} \quad \text{or} \quad D' = \frac{\partial c_f}{\partial c} .$$

Using square brackets to denote steady state quantities, equation (6-6) then becomes

$$I_s + c_\infty \cdot \frac{dI_s}{dc_\infty} = I_{s(c_\infty = 0)} \cdot \left[D'\right]_{c=c_\infty} \quad \ldots.(6\text{-}7)$$

All the terms involved in equation (6-7) can be determined experimentally, and for PPA-H_2O and PBMA-H_2O these are listed in Table 6-12. The R.H.S. of equation (6-7) decreases much more markedly with increasing c than does the L.H.S., the difference between the two relative decreases being of the order of 50% at the highest values of c_∞. This discrepancy is well outside the experimental error involved in determining I_s - c or $\left[D'\right]$- c relationships. Hence it can be inferred that even if the clustering process is not instantaneous in these systems, it must contribute appreciably to M_t in the early stages of sorption and therefore must be comparatively rapid. The effect of a slow immobilisation process on the measured D-c relationship is discussed further in Chapter 7.

TABLE 6-12

Quantities involved in Equation (6-7)

System	$c_{c\infty}$ cc.stp cm^{-3}	$I_{s(c_\infty=0)}$ x 10^3 $cm.sec.^{-\frac{1}{2}}$	$\frac{dI_s}{dc_\infty}$ x 10^3	I_s x 10^3 $cm.sec^{-\frac{1}{2}}$	$\left[D\right]_{c=c_\infty}$	Equation (6-7) (L.H.S.) x 10^3	Equation (6-7) (R.H.S.) x 10^3
PPA-H_2O	1	9.8	-0.17	9.6	0.96	9.4	9.4
"	2	"	"	9.4	0.91	9.1	8.9
"	3	"	"	9.3	0.86	8.8	8.4
"	4	"	"	9.1	0.80	8.4	7.8
"	5	"	"	8.9	0.74	8.1	7.3
"	6	"	"	8.8	0.68	7.7	6.7
"	7	"	"	8.6	0.62	7.4	6.1
"	8	"	"	8.4	0.565	7.1	5.5
"	9	"	"	8.25	0.505	6.7	4.9
"	10	"	"	8.1	0.44	6.4	4.3
PBMA-H_2O	0.5	1.8	-0.12	1.73	0.89	1.7	1.6
"	1.0	"	-0.11	1.68	0.80	1.6	1.4
"	1.5	"	-0.10	1.62	0.72	1.5	1.3
"	2.0	"	-0.10	1.57	0.65	1.4	1.2
"	2.5	"	-0.10	1.52	0.58	1.3	1.0
"	3.0	"	-0.09	1.48	0.53	1.2	0.9
"	3.5	"	-0.09	1.44	0.48	1.1	0.9
"	4.0	"	-0.08	1.40	0.43	1.1	0.8
"	4.5	"	-0.08	1.35	0.38	1.0	0.7
"	5.0	"	-0.08	1.31	0.35	0.9	0.6

b) Methanol

The plot of $D'(= D^V/D_{\phi_A = 0})$ vs. ϕ_A for methanol in PEMA is shown in Figure 6-24. The dependence of D' on ϕ_A is much more pronounced in the steady state than in the transient state although the various transient state analyses give results in reasonable agreement with each other. This type of discrepancy was observed in other polymer-organic penetrant systems in which the polymer was below or close to T_g [5,10] and was attributed to time-dependent effects arising from slow relaxation processes occurring in the polymer. In this case the PEMA sample was $\sim 30^{\circ}C$ below its measured T_g (Chapter 5) and so slow relaxation processes might well have been expected to interfere with the transient state diffusion measurements. The steady state results are therefore considered to be the more reliable for the PEMA-MeOH system.

6.3.3 Temperature Dependence of D.

Graphs of log D vs. 1/T, shown in Figures 6-25 to 6-28, were plotted to obtain E_D from $D(c) = D_o \exp(-E_D/RT)$. Mean values of E_D for the temperature ranges of the investigation are given in Table 6-13, and are accurate to $\sim \pm 0.5$ kcal.mole^{-1}. The temperature ranges used were too small to enable accurate values for D_o to be determined.

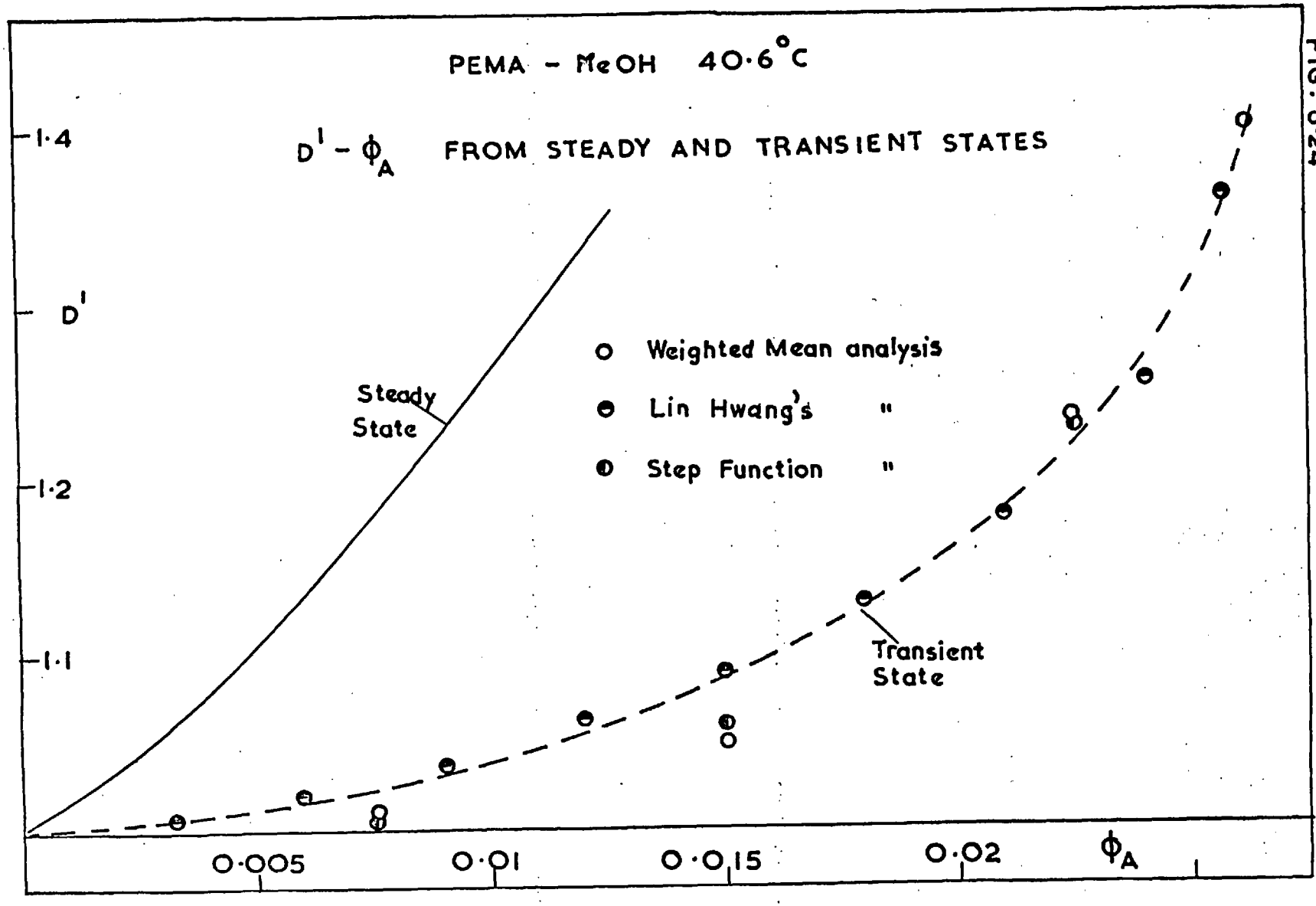
PEMA - MeOH 40·6°C
D' - φA FROM STEADY AND TRANSIENT STATES
1·4
D'
1·2
1·1
Steady State
Weighted Mean analysis
Lin Hwang's "
Step Function "
Transient State
0·005
0·01
0·015
0·02
φA

FIG. 6·24

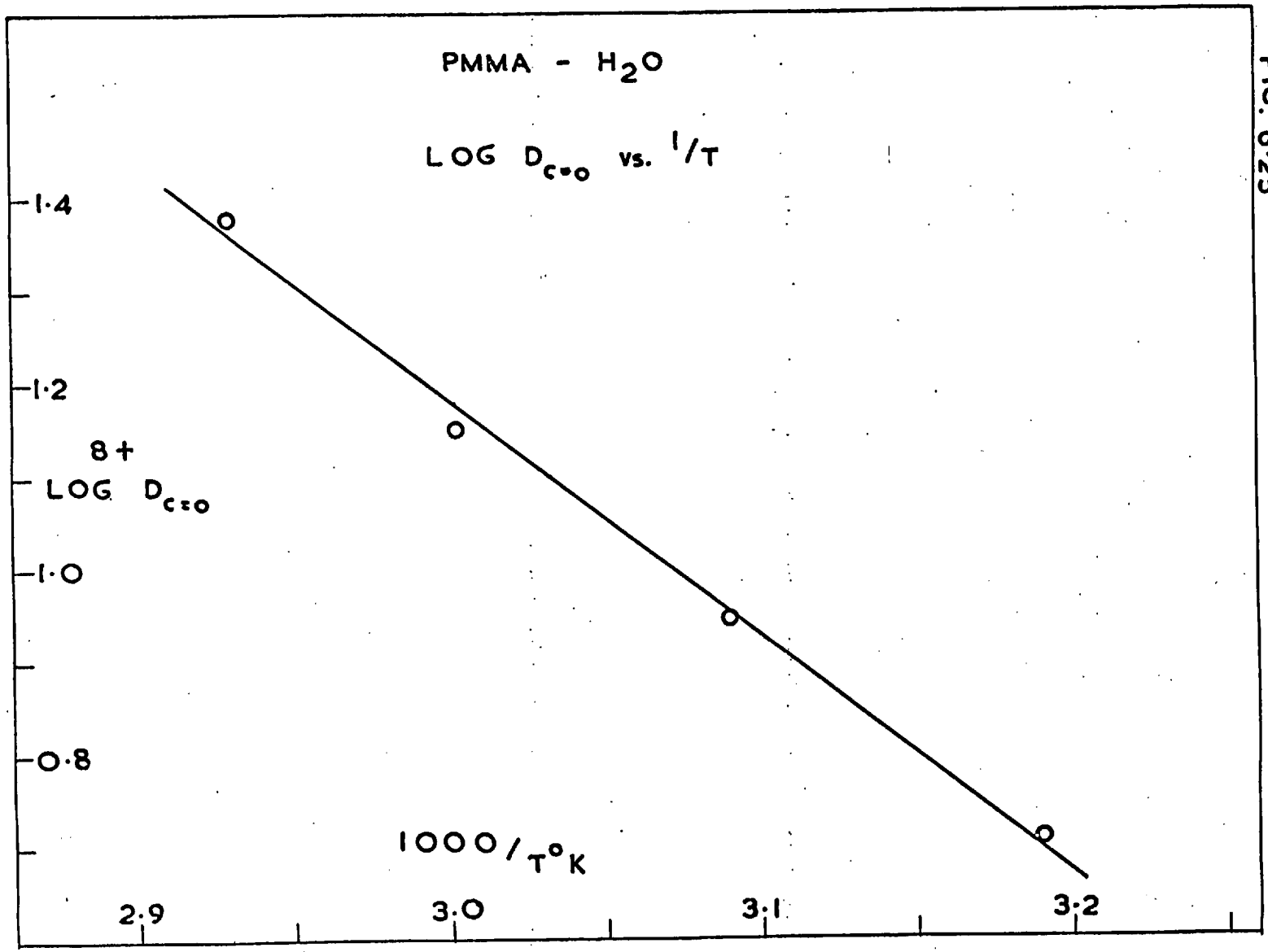

FIG. 6·25

FIG. 6·26

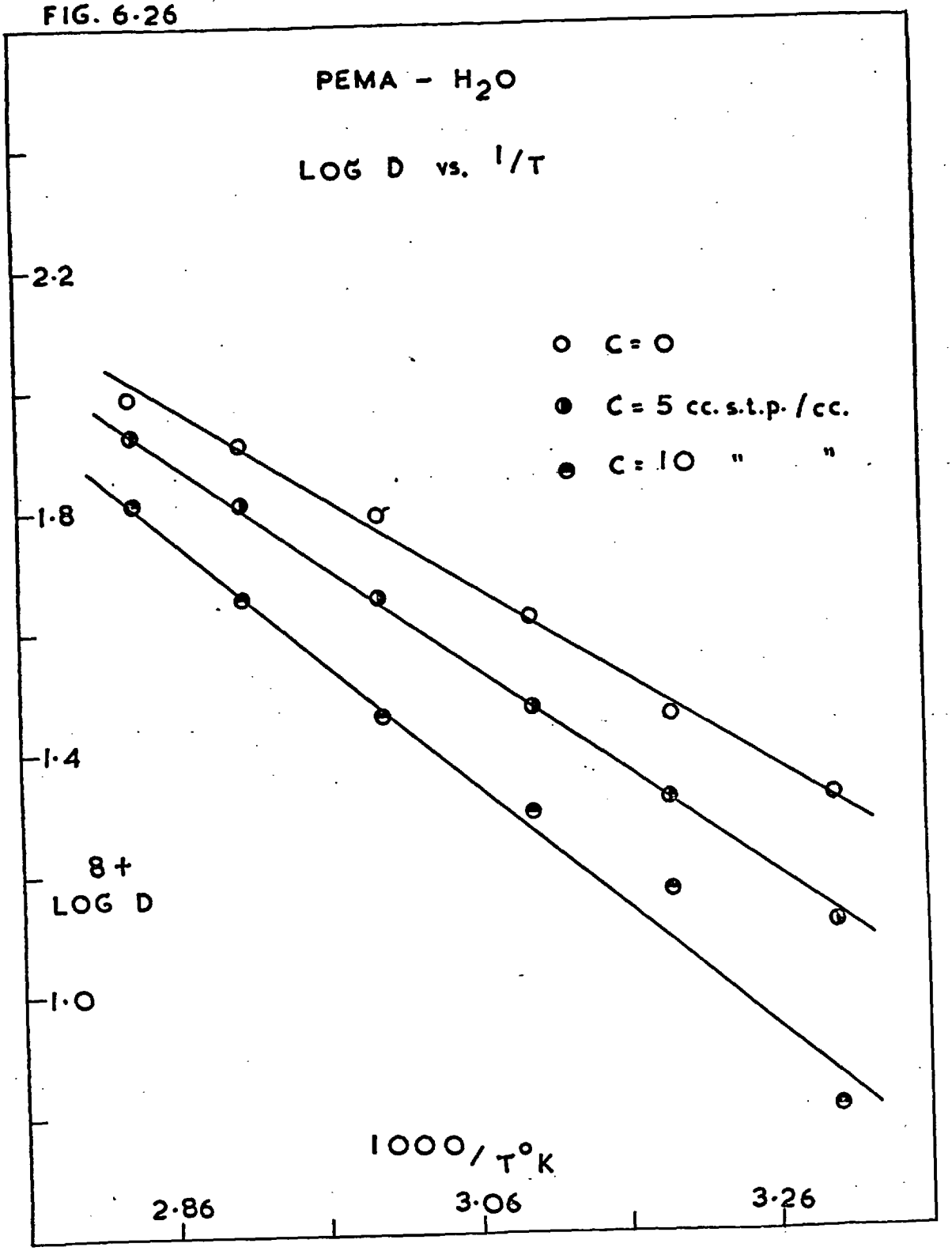
PEMA - H_2O
LOG D vs. 1/T
C = 0
C = 5 cc. s.t.p. / cc.
C = 10 " "
2·2
1·8
1·4
1·0
8 + LOG D
1000 / T°K
2·86
3·06
3·26

FIG. 6·27

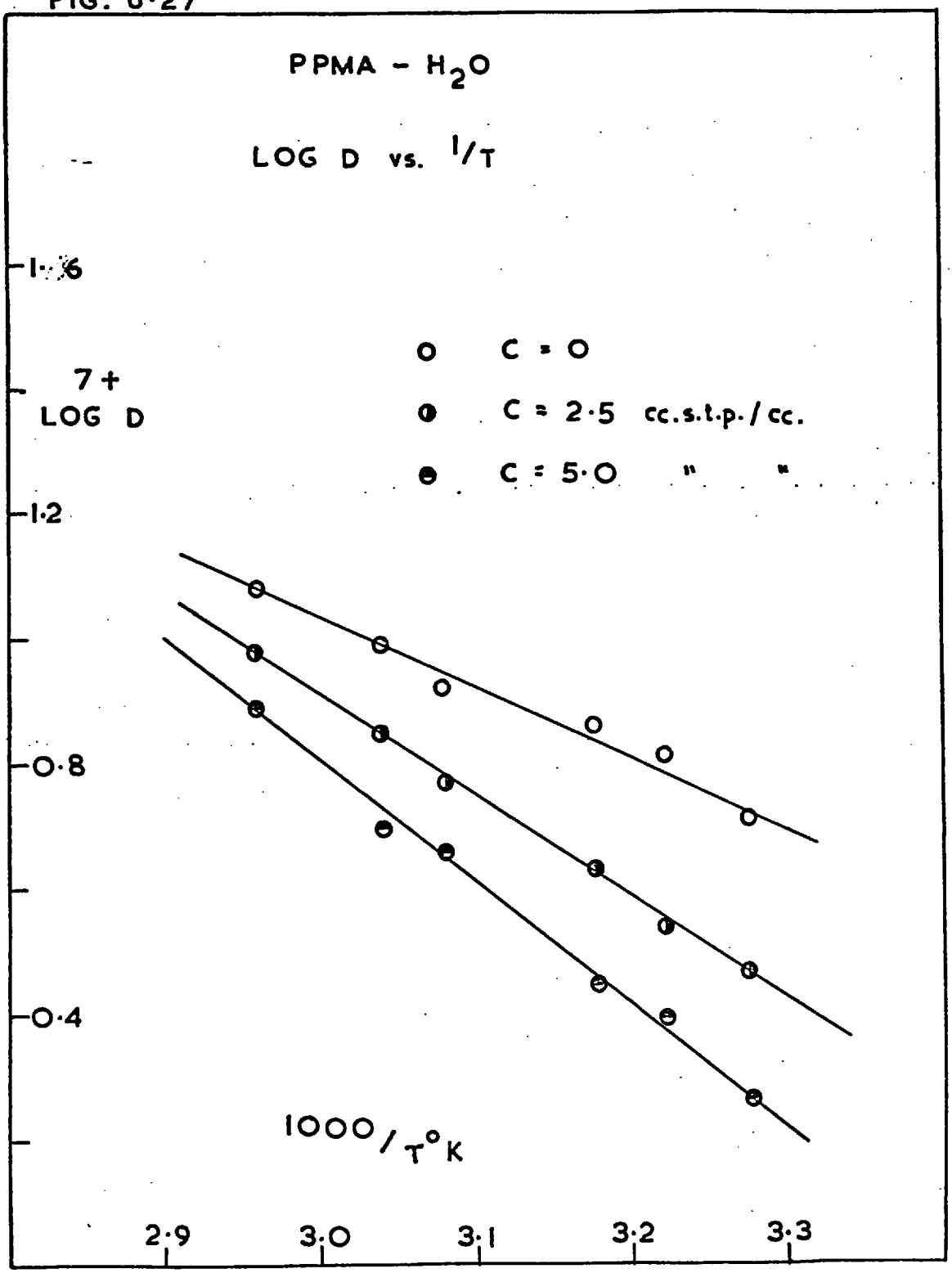
PPMA – H_2O
LOG D vs. $1/T$
C = 0
C = 2·5 cc.s.t.p./cc.
C = 5·0 " "
7 + LOG D
1·6
1·2
0·8
0·4
1000/T°K
2·9
3·0
3·1
3·2
3·3

FIG. 6·28

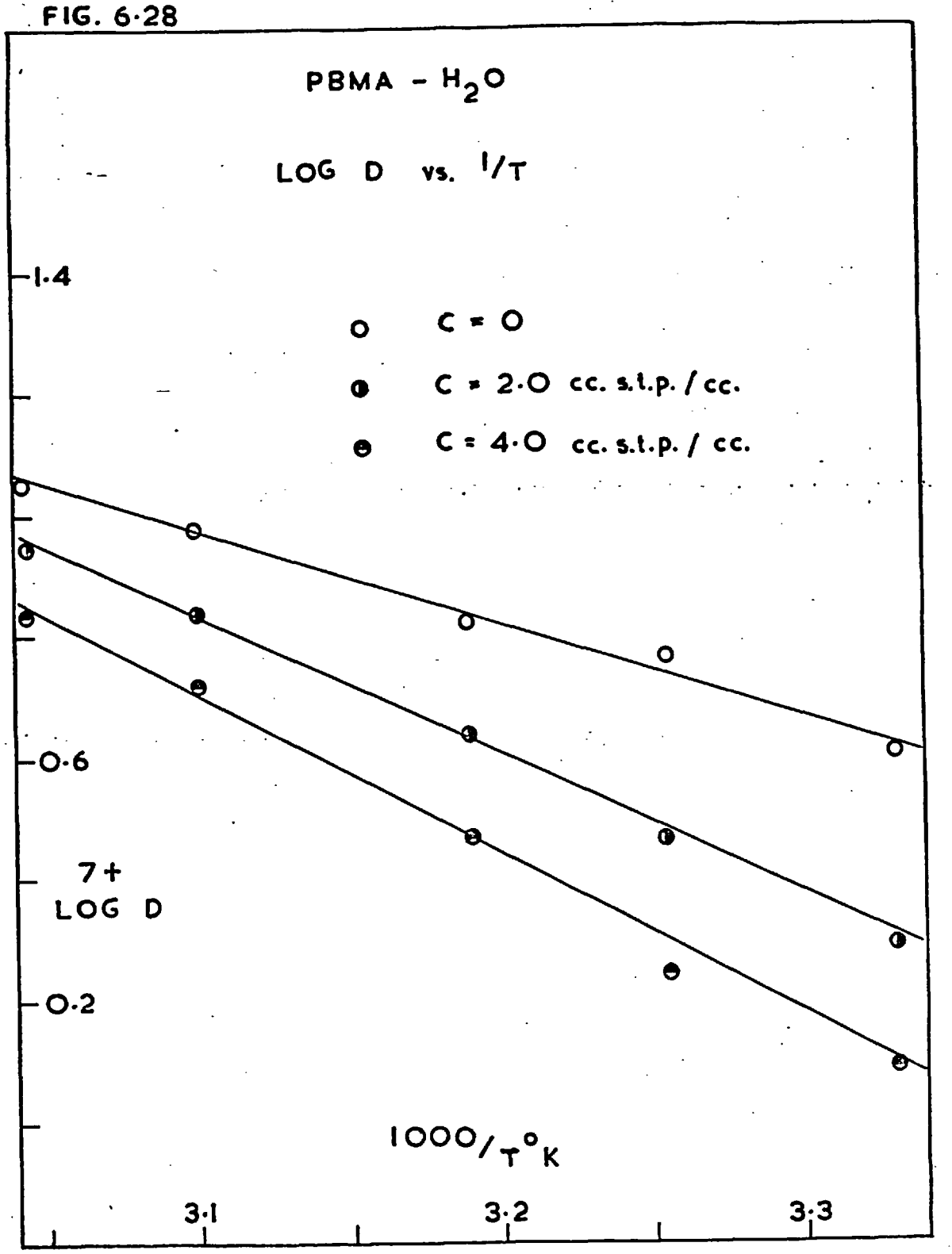
PBMA - H_2O
LOG D vs. 1/T
1·4
C = O
C = 2·O cc. s.t.p. / cc.
C = 4·O cc. s.t.p. / cc.
0·6
7+
LOG D
0·2
1000/T°K
3·1
3·2
3·3

TABLE 6-13

Mean Values of E_D (kcal.mole^{-1})

System	Temperature Range in °C	c cc.stp. cm^{-3}	E_D (measured)	E_D (theory)	
				$\Delta H = 6.6$ (kcal.mole^{-1})	$\Delta H = 3.4$ (kcal.mole^{-1})
PMMA-H_2O	40-70	0-20	11.9	11.9-17.1	11.9-15.8
PEMA-H_2O	30-80	0	7.0	7.0	7.0
"	"	5.0	8.6	8.3	8.4
"	"	10.0	10.1	9.5	9.5
PPMA-H_2O	32-64	0	5.3	5.3	5.3
"	"	2.5	7.6	7.5	7.0
"	"	5.0	9.0	9.3	8.5
PBMA-H_2O	27-56	0	6.6	6.6	6.6
"	"	2.0	10.5	8.6	8.4
"	"	4.0	11.9	10.3	9.4
PEMA-MeOH	29-40	0	15	-	-

i) Values of E_D at c=0.

At c=0, E_D decreases as the n-alkyl group in the side chain is lengthened, except for PPMA and PBMA where the order is reversed. The decrease is a reflection of the increasing segmental mobility as the side chain becomes more flexible, as discussed in part 6.3.1 of this section.

Although the experimental points (Figure 6-27) for the PPMA-H_2O system exhibit a rather larger degree of scatter than do those for the other systems, the low value of E_D for this system is apparently outside the experimental uncertainty and is somewhat puzzling. It was suspected, although unfortunately insufficient sample was available for investigation, that the molecular weight of the PPMA sample may have been especially low. Thus on dissolving the original material in chloroform a large proportion of insoluble gel was observed which was removed to leave a soluble fraction from which the membranes were cast.

In interpreting E_D measured close to T_g some care must be exercised since the polymer is essentially heterogeneous and consists of a mixture of glassy and rubbery material[138]. For water in PEMA, Stannett and Williams[49] observed a discontinuity at T_g in a plot of log D vs. 1/T. No changes of this nature were observed for the systems of this investigation. It may be that the temperature ranges used did not extend far enough away from T_g to establish the effect with any degree of certainty.

The value of E_D for water in PEMA lies between

the values for neon and oxygen in this polymer[49] although water has a larger molecular diameter than either. A similar comparison by Stannett and Williams[49] was carried out not at c=0 but at ~ 0.2 relative humidity. The corresponding value of E_D obtained here (~ 7.8 kcal. $mole^{-1}$) is reasonably close to that (8.7) of Stannett and Williams[49]. Kumins and Roteman[139] observed a similar anomaly for water diffusion in a vinyl chloride-vinyl acetate copolymer, although these measurements also did not refer to c=0. Both sets of investigators interpreted their results in terms of plasticisation of the polymer by water. In the limit ($c \rightarrow 0$) water molecules cannot have any bulk plasticising effect on the polymer. However, to explain the relatively low values of E_D at c=0, it must be assumed that individual water molecules exhibit some kind of interaction with the chemical structure of the polymer (presumably ester links) in their immediate vicinity and that this interaction tends in some way to facilitate the diffusion process.

The approximate value of 15 kcal. $mole^{-1}$ for E_D for the PEMA-MeOH system is in reasonable agreement with that (14.7 kcal. $mole^{-1}$) obtained by Zhurkoff and Ryskin[74].

ii) Concentration Dependence of E_D.

With the exception of PMMA, E_D for water increases with increasing c in accord with the clustering concept (section 2.7.9). Values of E_D are compared in Table 6-13 with theoretical values calculated from the random polycondensation model, assuming that only monomeric water diffuses. The agreement is reasonable for PEMA and PPMA although the experimental uncertainties involved detract to some extent from the value of any interpretation put on this agreement. The discrepancy for PBMA is outside the experimental error.

The constant E_D for PMMA remains to be explained. If, for a given water activity, most of the clustered water were present in voids and relatively stable over the whole temperature range as suggested in an earlier section (6.1.3), then the term $\partial c_1/\partial c$, where subscript 1 refers to monomeric water, would not vary appreciably with temperature and the principal factor determining the increase in D with temperature would simply be the activation energy for the diffusion of monomeric water in the bulk polymer. Hence, following equation (2-120), E_D would not be expected to increase appreciably with c.

CHAPTER 7

RESULTS AND DISCUSSION

POLYSILOXANES

A UNFILLED POLYMERS

7.1 Equilibrium Sorption Results

Equilibrium sorption isotherms for water in DMS (samples I and II), PMS and FMS are shown in Figures 7-1 to 7-4 respectively. Data incorporating the blank corrections for water sorbed on the Sartorius balance and leading to the construction of the isotherms are presented in appendix 9.6. No hysteresis was observed in the sorption isotherms for water in these rubbery polymers.

7.1.1 Sorptive Capacities of the Polymers

As the sorption isotherms for water are initially linear, values of $\sigma_{c=0}$ in each polymer were determined accurately and are given in Table 7-1. Accurate comparisons of $\sigma_{c=0}$ with earlier work could not be made, but the magnitudes of the uptake of water by DMS at high relative humidities agree to within 5% with results obtained by Barrie and Platt[43].

FIG. 7·1

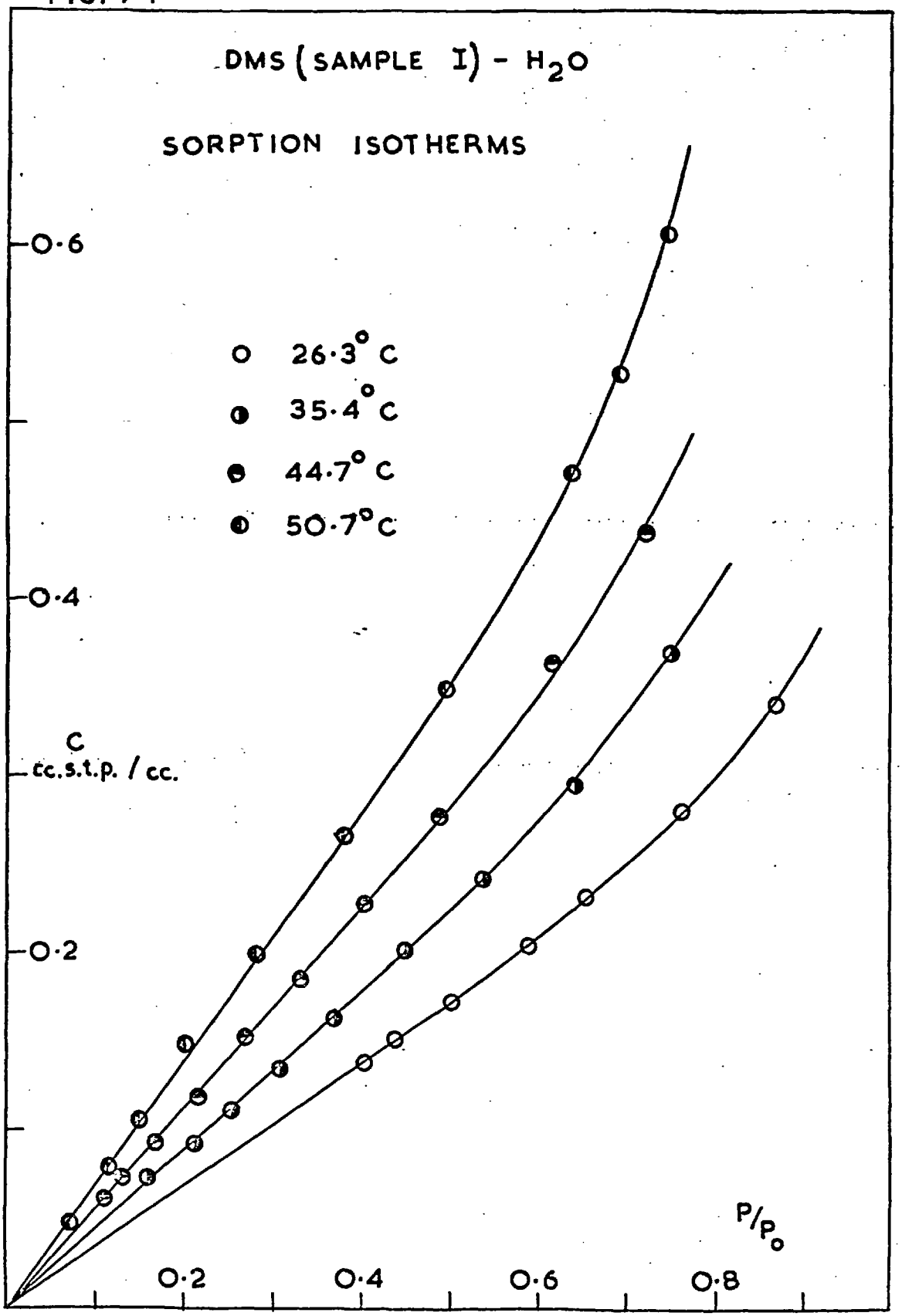
DMS (SAMPLE I) - H_2O
SORPTION ISOTHERMS
26·3° C
35·4° C
44·7° C
50·7° C
C
cc.s.t.p. / cc.
0·6
0·4
0·2
0·2
0·4
0·6
0·8
P/P₀

FIG. 7·2

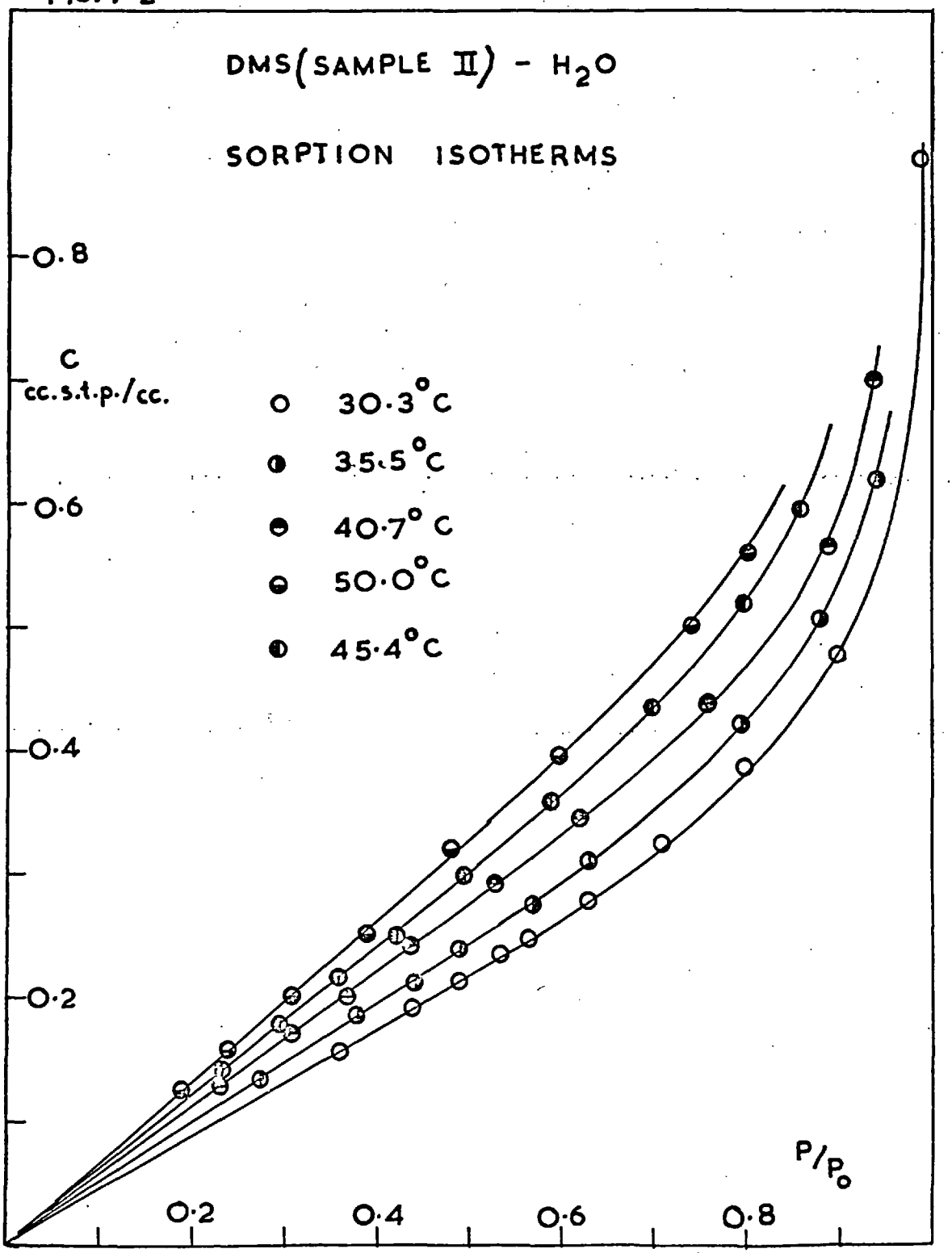
DMS (SAMPLE II) - H_2O
SORPTION ISOTHERMS
C
cc.s.t.p./cc.
0·8
0·6
0·4
0·2
30·3°C
35·5°C
40·7°C
50·0°C
45·4°C
P/P₀
0·2
0·4
0·6
0·8

FIG. 7·3

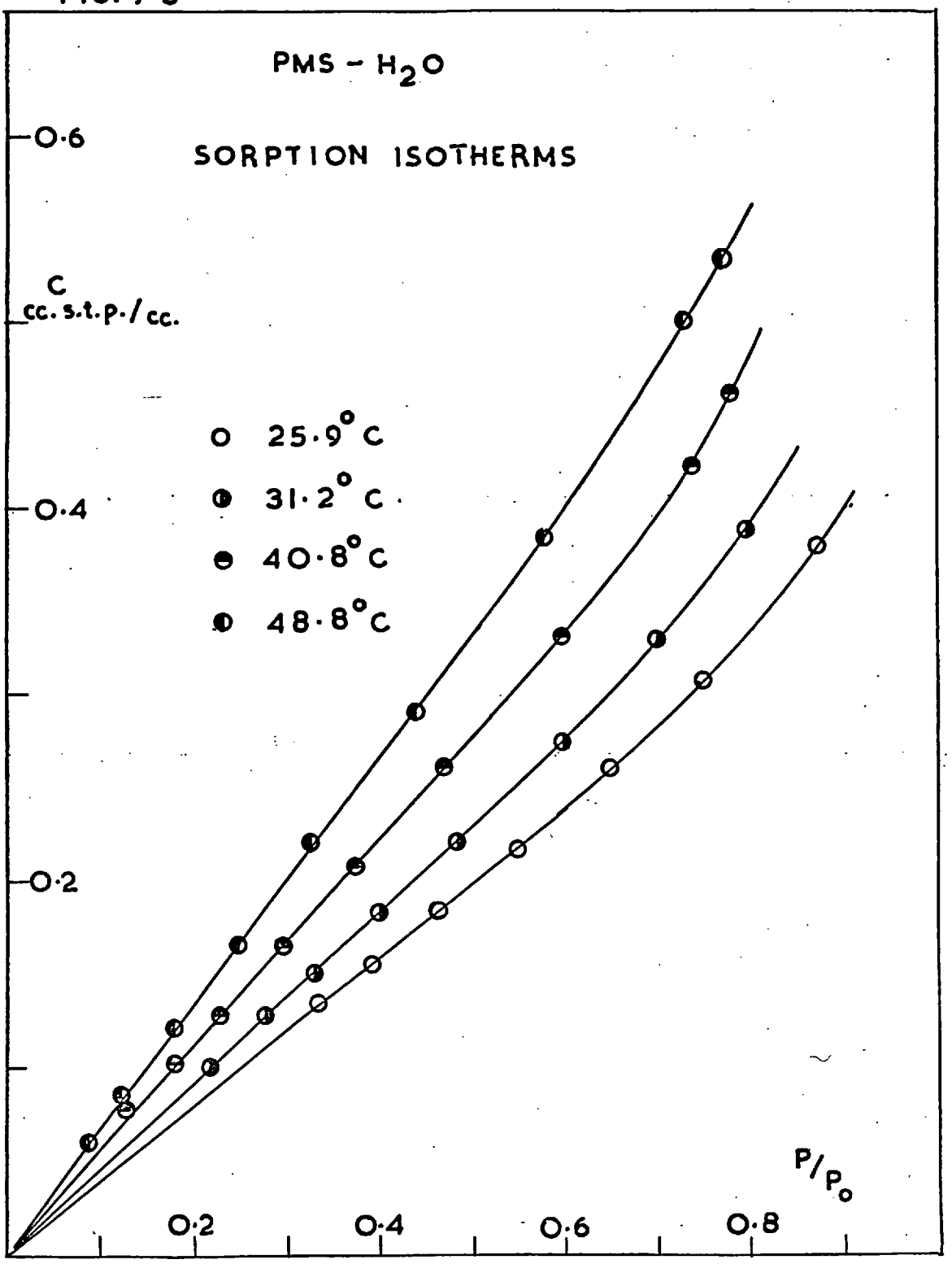
PMS – H_2O
SORPTION ISOTHERMS
0·6
0·4
0·2
C
cc. s.t.p./cc.
25·9° C
31·2° C
40·8° C
48·8° C
0·2
0·4
0·6
0·8
P/P₀

FIG. 7·4

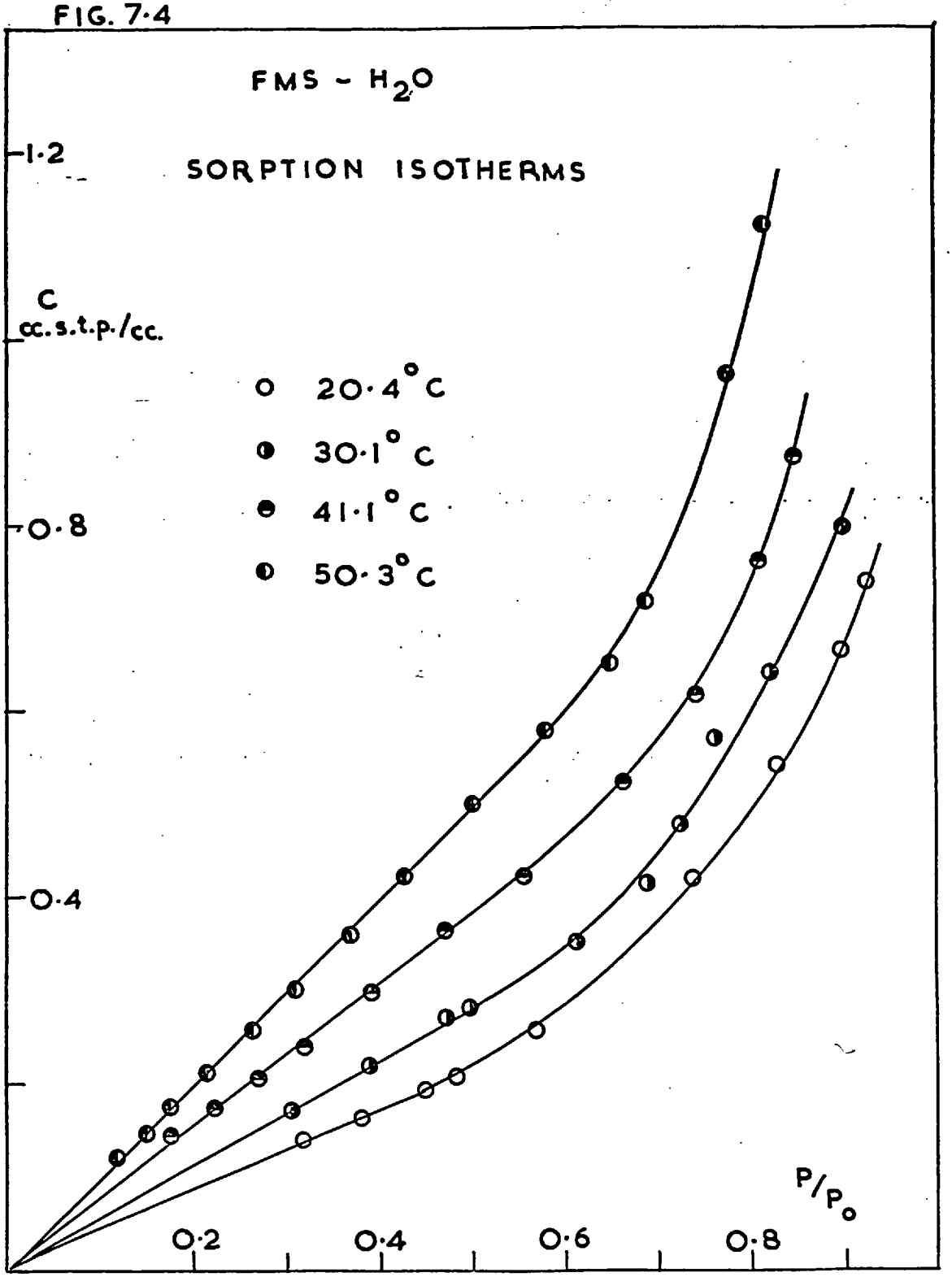
FMS - H_2O
SORPTION ISOTHERMS
C
cc.s.t.p./cc.
1·2
0·8
0·4
20·4°C
30·1°C
41·1°C
50·3°C
0·2
0·4
0·6
0·8
P/P₀

TABLE 7-1

Limiting Henry's Law Solubility Coefficients $\sigma_{c=0}$ (cc. s.t.p. $cm.^{-3}$ $(cmHg)^{-1}$) for water

Polymer	$T^{\circ}C$	$\sigma_{c=0} \times 10$	Polymer	$T^{\circ}C$	$\sigma_{c=0} \times 10$
DMS (I)	26.3	1.34	DMS (III)	30.3	1.36
"	30.7	1.20	"	50.0	0.70
"	35.4	1.04			
"	44.3	0.89	PMS	25.9	1.58
"	44.7	0.81	"	31.2	1.33
"	50.7	0.73	"	40.8	1.00
			"	48.8	0.77
DMS (II)	30.3	1.34			
"	35.5	1.13	FMS	20.4	2.33
"	40.7	0.94	"	30.1	1.75
"	45.4	0.81	"	41.1	1.29
"	50.0	0.69	"	50.3	1.04

For a given temperature, values of $\sigma_{c=0}$ for the different samples of DMS and for PMS are all very close whereas the corresponding value for FMS is 30-50% higher. This is consistent with the principle that the affinity of a polymer for water is governed by the proportion and type of polar groups present in the polymer. Thus PMS differs from DMS only in that a relatively small proportion of the methyl groups are replaced by phenyl groups. Both these types of group are essentially hydrophobic. On the other hand FMS contains the relatively polar trifluoropropyl group

in its repeat unit, the structure of which is

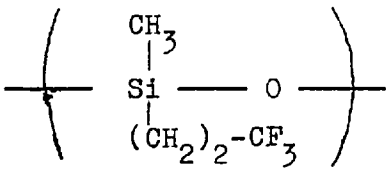

The presence of the fluorine atoms in the trifluoropropyl group must confer on it sufficient affinity for water to account for the increased values of $\sigma_{c=0}$ for FMS compared with those for DMS. These values of $\sigma_{c=0}$ for the silicones are about an order of magnitude lower than the corresponding values for the polymethacrylates (Table 6-1), illustrating the influence of the ester linkage on water sorption in the latter group of polymers. On the other hand at high relative humidities DMS has a sorptive capacity for water of the order of three times larger than that of polyethylene or polypropylene[11] when allowance is made for the crystalline regions in the two polyolefins. This might possibly be a consequence of water clustering in this region being initiated by the Si-O bond or by trace amounts of polar impurities, which could not be removed by refluxing (see part 7.1.2 of this section). The partial ionic character (51%) of the Si-O bond acts so as to protect the methyl groups in DMS from oxidative degradation or other forms of chemical attack[140] and so water sorption by impurities introduced through oxidation is perhaps unlikely.

The Si-O bonds are shielded to some extent by the methyl groups and so presumably only present a relatively small number of sites for water sorption at low relative humidities. $\sigma_{c=0}$ is similar for water in DMS and in the amorphous fractions of polyethylene and polypropylene[11].

Equilibrium sorption isotherms for methanol in FMS are illustrated in Figure 7-5. Values of $\sigma_{c=0}$ were calculated as 0.33 and 0.23 cc. s.t.p. cm^{-3}. $(cmHg)^{-1}$ at 30.0 and 40.0°C respectively and are approximately twice as large as the corresponding values for water. In contrast to PEMA therefore (section 6.1.1), FMS has a stronger inherent affinity for methanol than for water in addition to the increased sorptive capacity resulting from the lower boiling point of methanol compared with that of water. Uptakes of methanol by FMS at high relative vapour pressures at 30°C are almost identical with those found in the case of DMS[59], illustrating that the introduction of polar groups has less effect on methanol sorption than on water sorption.

7.1.2 Isotherm Shapes

The major difference between the isotherm shapes for water and methanol in the polymethacrylates and in the silicone rubbers is that the latter are virtually linear in the region of lower relative vapour pressures.

FIG. 7·5

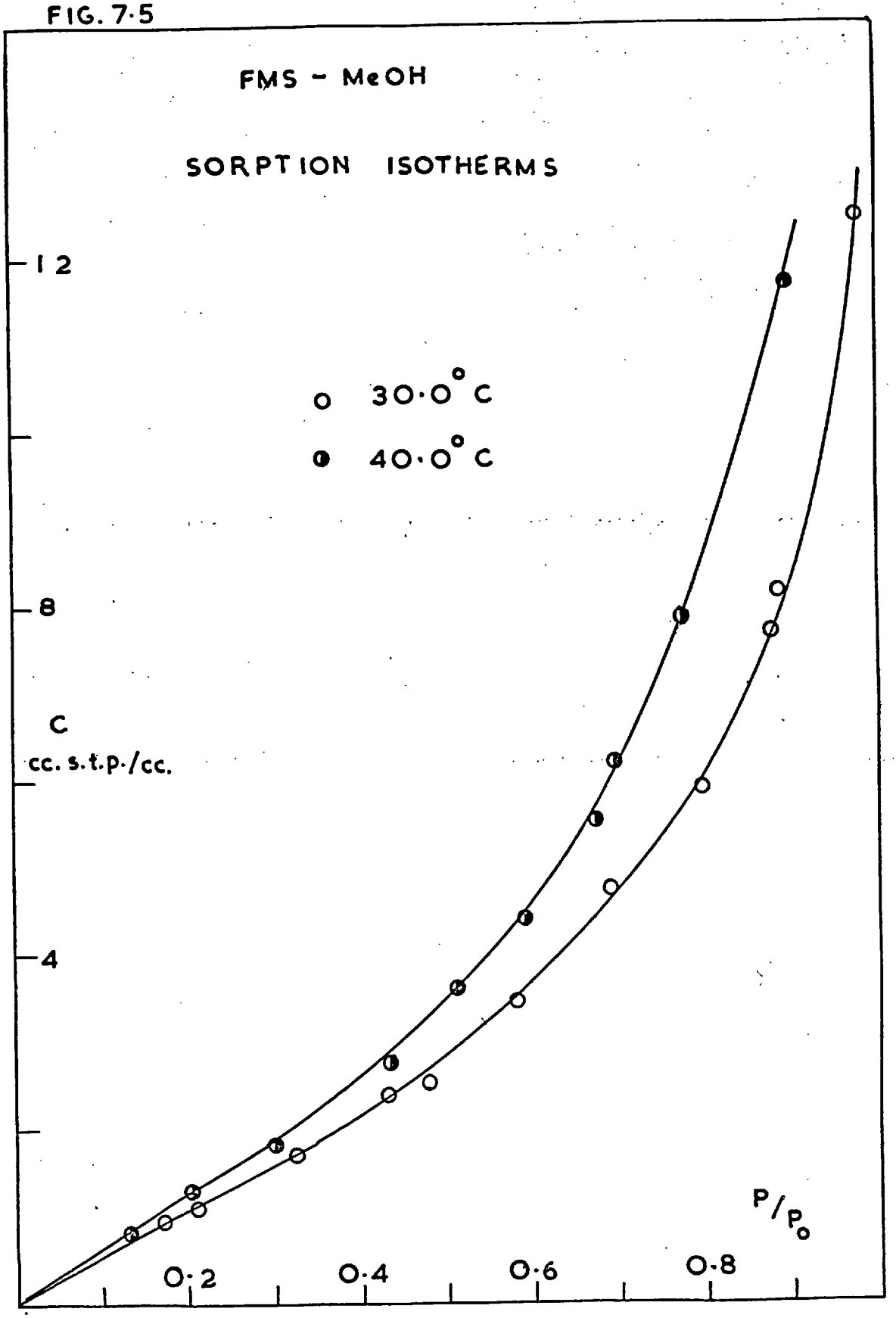
FMS - MeOH
SORPTION ISOTHERMS
12
8
4
C
cc. s.t.p./cc.
o 30·0° C
● 40·0° C
0·2
0·4
0·6
0·8
P/Po

i) Clustering Functions

Although isotherms are linear at lower pressures, curvature becomes more and more pronounced the higher the relative pressure such that the isotherms are convex to the pressure axis. The clustering functions G_{AA}/v_A and $(1 + \phi_A G_{AA}/v_A)$, which will now be referred to for convenience as Y and Z respectively, were calculated for various activities of penetrant. Plots of a_A/ϕ_A vs. a_A and of log (ϕ_A) vs. log (a_A) are similar to those for the polymethacrylates (e.g. Figure 6-8) except that for small a_A, corresponding to the linear regions of the isotherms, a_A/ϕ_A is constant and log (ϕ_A) is linear with log (a_A). Typical plots are shown in Figure 7-6. Values of the clustering functions Y and Z are given in Table 7-2 together with some values[59] for the DMS-MeOH system. The values of -1 and +1 respectively for Y and Z correspond to the linear regions of the isotherms.

A comparison of the clustering functions for water in a variety of polymers is complicated because at least two effects have to be considered. Firstly, the intrinsic tendency for water molecules to cluster inside any medium will depend on the activity of the water so that a true comparison should be carried out at the same

FIG. 7·6

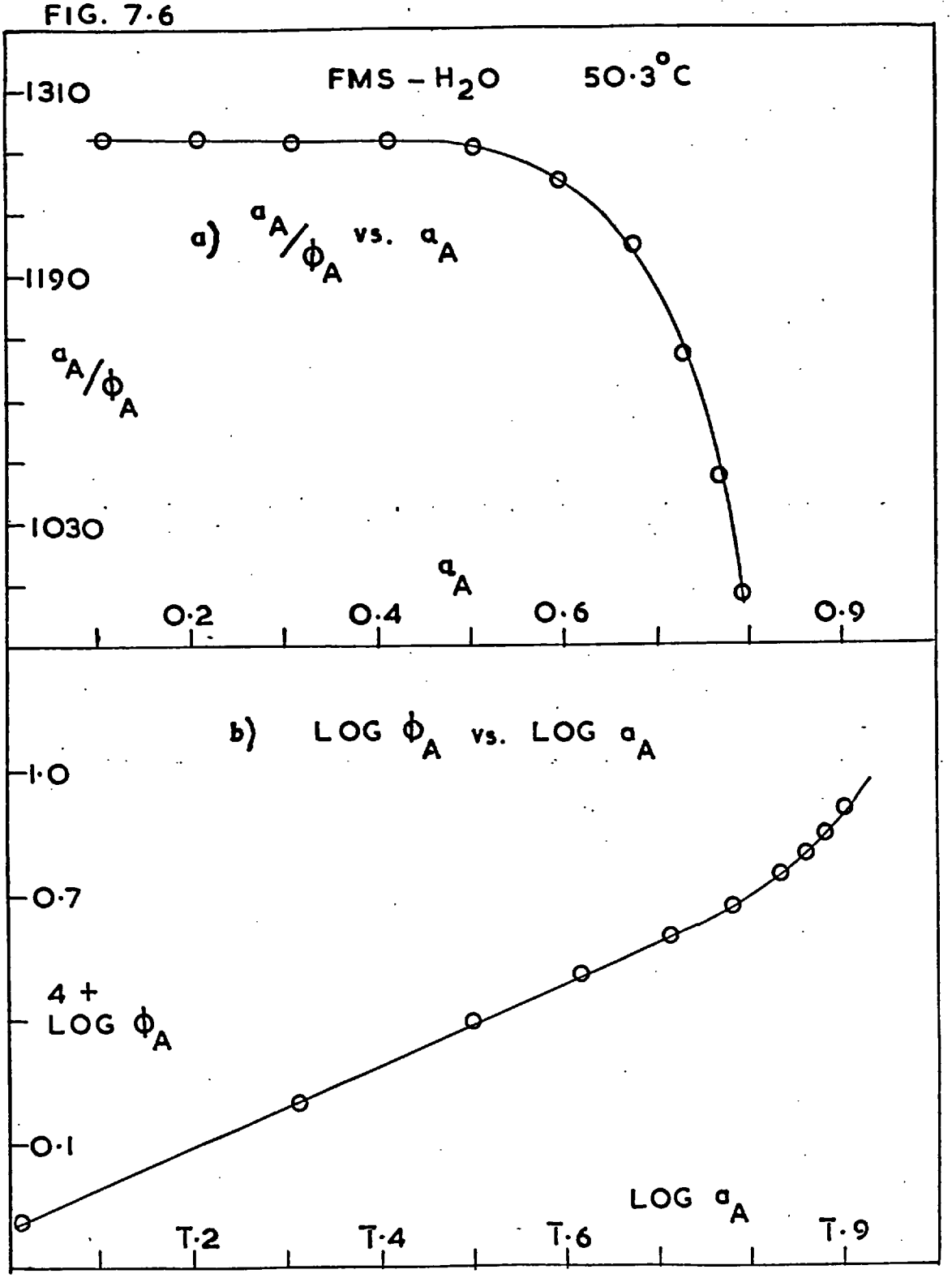
FMS – H_2O 50·3°C
a) a_A/ϕ_A vs. a_A
1310
1190
1030
a_A/ϕ_A
a_A
0·2
0·4
0·6
0·9
b) LOG ϕ_A vs. LOG a_A
1·0
0·7
0·1
4 + LOG ϕ_A
LOG a_A
T·2
T·4
T·6
T·9

TABLE 7-2

Clustering Functions. $Y = G_{AA}/v_A$, $Z = (1 + \phi_A G_{AA}/v_A)$

System	T°C	a_A = 0.3		a_A = 0.5		a_A = 0.7	
		Y	Z	Y	Z	Y	Z
DMS(I)-	35.4	-1	1	-1	1	1500	1.5
H_2O	44.7	-1	1	-1	1	1300	1.5
DMS(II)	30.3	-1	1	-1	1	960	1.3
-H_2O	35.5	-1	1	-1	1	740	1.2
"	40.7	-1	1	-1	1	660	1.2
"	45.4	-1	1	-1	1	930	1.3
"	50.0	-1	1	200	1.05	370	1.2
PMS-	25.9	-1	1	-1	1	780	1.2
H_2O	31.2	-1	1	-1	1	700	1.2
"	40.8	-1	1	-1	1	840	1.3
"	48.8	-1	1	-1	1	440	1.1
FMS-	20.4	-1	1.0	510	1.1	3400	2.0
H_2O	30.1	-1	1	-1	1	2800	1.9
"	41.1	-1	1	-1	1	760	1.4
"	50.3	-1	1	-1	1	1300	1.8
FMS-	30.0	3.0	1.0	51	1.3	93	1.7
MeOH	40.0	14	1.1	65	1.4	110	2.2
DMS	10.0	100	1.15	140	1.4	-	-
-MeOH[59]	30.0	54	1.1	62	1.3	120	1.9

water activity in each polymer. On the other hand the effect of the polymer matrix on water clustering will be dependent on the sorbed concentration rather than the activity of the water. Practically it is more convenient to make comparisons at constant activity, especially when comparing polymers which have widely differing sorptive capacities for water, and this is done in the present case.

At relative humidity 0.7 both the clustering functions for water are similar for DMS and for PMS but significantly larger for FMS. In this region therefore, FMS appears to promote more water clustering in addition to exhibiting a higher overall sorptive capacity for water. Comparisons carried out at a given water concentration yield relatively small differences between Y for water in DMS and in FMS. For example, for water in FMS at $\sim 30^{\circ}C$ and $p/p_o = 0.7$, $c = \sim 0.43$ cc.s.t.p. cm^{-3} which corresponds to $p/p_o = \sim 0.83$ in the case of the DMS-H_2O system. It was calculated that

$$Y \ (DMS\text{-}H_2O, \quad a_A = 0.83, \quad T = 30.3^{\circ}C) = 2800$$

and $$Y \ (FMS\text{-}H_2O, \quad a_A = 0.7, \quad T = 30.1^{\circ}C) = 2800.$$

The trend, at constant water activity, of an increase in Y with the relative polar group content of the

polymer is opposite to that observed for the polymethacrylate series (Table 6-2). However, comparisons of water clustering within the series of the methacrylate polymers, and of that series with the silicone rubbers, are further complicated by differences in the physical states of the polymers and in the overall sorptive capacities for water. Thus it is expected that a rubbery polymer matrix can accommodate clusters, especially large ones, more readily than can a rigid matrix in which the degree of clustering may depend primarily on the proportion of microvoids frozen into the structure. In addition, the higher the sorptive capacity of a polymer for water the greater is the overall restriction imposed by the matrix on further cluster formation, for a given proportion of clustered molecules present.

Consider then the polymethacrylate series from PMMA → PBMA in which the flexibility or rubbery character of the polymer increases while the sorptive capacity for water decreases by a factor of 3-4. The first effect would be expected to increase Z while the second would be expected to increase Y, quite apart from any specific effect of the polar ester group on clustering. An increase in Y is, in fact, observed (Table 6-2) while Z remains approximately

constant. This behaviour indicates that, for this series, the rigidity of the matrix exhibits relatively little effect on water clustering. In addition, little evidence is offered for increased clustering resulting from an increase in the ratio of ester linkages to hydrophobic units present (section 6.1.1). The effect of the sorptive capacity for water of the polymer on Y is more marked when the polymethacrylates and the silicone rubbers are compared at 0.7 relative humidity. Y is about an order of magnitude higher for the silicone rubbers, which sorb correspondingly less water, whereas in general Z is marginally higher for the polymethacrylates.

In connection with the effect of polymer rigidity, it is of interest that the sorption of water by polyethyleneterephthalate[42] follows Henry's law although the sorptive capacity of this polymer for water is roughly equivalent to that of PEMA. Polyethyleneterephthalate is an exceptionally rigid polymer at room temperature and is partly crystalline so that cluster formation would be discouraged if it were to require significant perturbation of the matrix.

At higher relative vapour pressures, both Y and Z for methanol in FMS are similar in magnitude to the

corresponding values in DMS[59]. The differences observed between the two systems at $p/p_o = 0.3$ arise from the different curve-fitting procedures adopted in the two cases. For the DMS-MeOH system, the experimental isotherm points in the region of low pressures exhibited a degree of scatter and Barrie[59] drew a smooth curve through the points although they could equally well have been represented by a linear isotherm. The isotherm measured for FMS-MeOH in the present investigation is apparently linear (Figure 7-5) in the low pressure region, although the experimental uncertainty was such that curvature could not be ruled out.

ii) Comparison with Theoretical Isotherms: Water

There is a major difference between the DMS-H_2O isotherms of this investigation and those of Barrie and Platt[43]. The agreement at higher relative humidities is reasonable but Barrie and Platt were not able to determine their isotherms with the same degree of precision. This was particularly the case at the lower relative humidities where the errors were large. These investigators, in the absence of more accurate measurements, represented the isotherms by smoothed curves over the whole range of relative pressure. The more sensitive weighing procedure of this investigation reveals an initial linearity in the

isotherms which cannot be explained on the basis of the simple polycondensation models for water association. The discrepancy with theory is illustrated in Figure 7-7 in which an experimental sorption isotherm for DMS-H_2O is compared with theoretical isotherms constructed for $\varepsilon = 0$ and $\varepsilon = 0.05$ (section 2.7.5). Again, a reduced concentration $C' = c/c^*$ was employed where c^* is the value of c corresponding to $p/p_o = 0.9$.

Interpretation of the isotherm shapes is, in fact, somewhat difficult. Some possible explanations are discussed below but as yet these remain somewhat speculative.

a) The simplest explanation for the linear region of the isotherms is in terms of an ideal solution of monomeric water in the rubber, since the sorption of monomeric water is generally assumed to follow Henry's law. This explanation would require the existence of a critical concentration for the formation of clusters corresponding to the point where the isotherm starts to deviate from linearity. However, if clustering is regarded as a purely statistical process, an example of which is the random polycondensation model, then clustering should occur at all finite concentrations.

FIG. 7·7

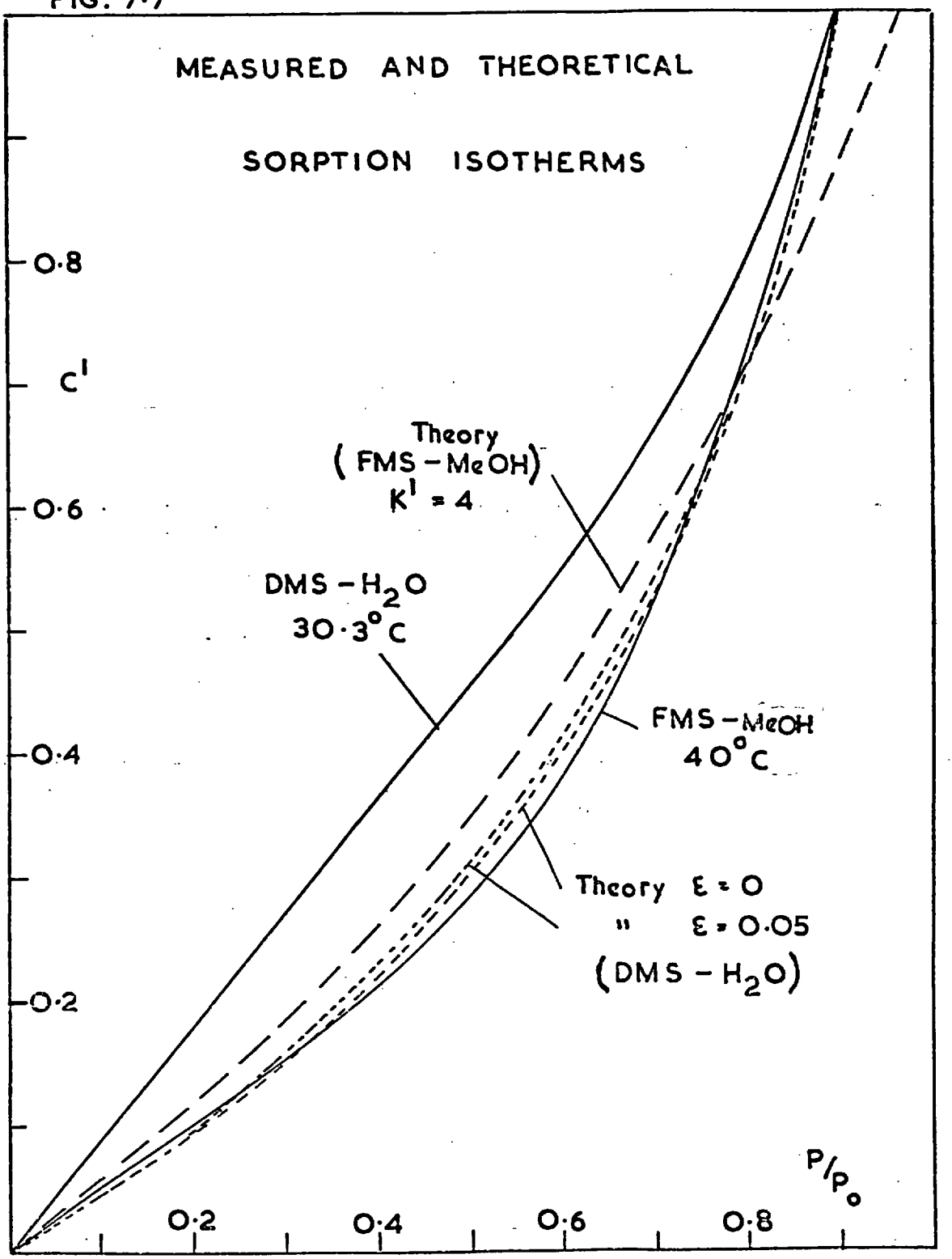
MEASURED AND THEORETICAL
SORPTION ISOTHERMS
0·8
C¹
0·6
0·4
0·2
Theory
(FMS – MeOH)
K¹ = 4
DMS – H2O
30·3°C
FMS – MeOH
40°C
Theory ε = 0
" ε = 0·05
(DMS – H2O)
P/Po
0·2
0·4
0·6
0·8

b) In principle, an initial linear region to the isotherms would obtain if both clustering of water molecules and immobilisation of water molecules by sorption on specific sites in the polymer were to occur simultaneously. At first sight this would require what would appear to be an extremely fortuitous combination of a Langmuir type and a clustering type of isotherm, particularly as the isotherms for water in DMS and in FMS exhibit linearity for all the temperatures of the investigation. However, in the region of low relative pressures the curvature resulting from clustering need not be very marked (e.g. see Figure 2-1) and only a weak Langmuir-type of sorption would be required to yield a resultant linear isotherm.

A relatively small number of specific sites in the polymer may be provided by trace catalyst. If, in addition, these sites were to act so as to provide centres for the initiation or nucleation of a stronger clustering process, then when the sites were occupied clustering would become more marked. This behaviour would then

lead to an apparent "critical" concentration for cluster formation, as is observed experimentally for these systems.

For water sorption in a polyurethane elastomer the initial regions of the isotherms are almost linear, with small, but definite "knees"[141]. This polymer contains polar groups and it may well be that both specific site sorption and clustering of water determine the isotherm shape in this system.

c) The existence of an appreciable fraction of $(H_2O)_2$ dimers in the gas phase does not appear very likely on the available evidence[36]. If dimerization were to occur to a small extent, and if the associated water in the rubber were present mainly in the form of dimers up to $p/p_o = \sim 0.5$ (the observed range of linearity), then assuming Henry's law is obeyed for each species

$$c_1 = \sigma_1 p_1 \quad \text{and} \quad c_2 = \sigma_2 p_2$$

where subscripts 1 and 2 refer to monomeric and dimeric water respectively. Hence

$$c = c_1 + c_2 = \sigma_1 p_1 + \sigma_2 p_2$$

$$\text{or } c = p(\sigma_1 x_1 + \sigma_2 x_2) = p(\sigma_1 + x_2(\sigma_2 - \sigma_1)) \quad \ldots.(7\text{-}1)$$

where x is mole fraction and p is the total gas phase pressure. Equation (7-1) indicates that a linear isotherm would be obtained if $\sigma_1 \approx \sigma_2$.

For the random clustering model, the concentrations of dimer and of trimer at $p/p_o = 0.5$ are about 30% and 10% respectively of the monomeric water concentration. There is no evidence for association of water to this extent in the vapour phase.

d) If small amounts of water-soluble impurities, particularly salts, were present in the rubber, then specific site sorption of water on these would be so low as to have little effect on the isotherm shape. In effect an ideal solution of monomeric water in the rubber would exist until the relative humidity exceeded that of a saturated aqueous solution of the impurities, when "clusters" or pockets of solution would form.

For the specific case of sodium chloride as an impurity it was calculated from Figure 7-23 (to be discussed in part B of this chapter) that only 0.002-0.005% by weight of salt would need to be present in the rubber to explain the observed deviation of the DMS-H_2O isotherms from linearity at $p/p_o = 0.8$.

3) The simple perturbation treatment of section 2.7.5 does not lead to appreciable changes in the initial curvature of the sorption isotherm (Figure 2-1) from that of the random polycondensation model. Nevertheless, it is conceivable that with a stronger co-operative effect, not necessarily confined to the first shell substitution effect of section 2.7.5, the initial region of the theoretical isotherm would approach more closely to linearity. This possibility in particular can only be considered as speculative at present.

iii) Comparison with Theoretical Isotherms : Methanol

The sorption isotherm for methanol in FMS at 40.0°C is compared in Figure 7-7 with a theoretical isotherm

calculated from the random polycondensation model for methanol. $\sigma_{c=0}$ was equated with the experimental value and a suitable value was chosen for the parameter K in equation (2-109). For convenience, reduced variables $C' = c/c^*$ and $K' = K/c^*$ are used, where c^* is the value of c corresponding to $p/p_o = 0.9$. The closest fit to the experimental isotherm is obtained with $K' \cong 4$ and the comparison between theory and experiment is closer for methanol than for water. Barrie[59] obtained a reasonable fit to the DMS-MeOH sorption isotherm at 30°C with $K = 2.5 \times 10^{-2}$ g. cm^{-3}, which corresponds to $K' = 2$.

This procedure, in which K is regarded as a purely arbitrary adjustable parameter, can be qualified a little. Thus equations (2-109) and (2-110) are

$$K = \frac{c(1-2\alpha)(1-\alpha)}{\alpha} \quad \text{and} \quad c_1 = c(1-\alpha)^2(1-2\alpha).$$

If these equations are combined they yield

$$K = \frac{c_1}{(1-\alpha)\,.\,\alpha} \qquad \ldots.(7\text{-}2)$$

A first approximation to K would be to assume that the gel point of the polycondensation could be identified with the saturation point of the system, as for the case of water, when α_s would be 1/2[96]. Hence from equation (7-2),

$$K = 4 (c_1)_s \qquad \ldots.(7\text{-}3)$$

where $(c_1)_s$ is the concentration of monomeric methanol at saturation. The gel point cannot strictly be identified with the saturation point (section 2.7.7), and so α_s becomes the adjustable parameter. However, equation (7-2) shows that $4(c_1)_s$ is, in fact, a minimum value for K. Hence a lower limit is placed on the value chosen for K. Moreover, the value of K is relatively insensitive tc the value chosen for α_s. For example, if $\alpha_s = 1/8$ then $K = \sim 9(c_1)_s$. Hence if the minimum value of α_s were estimated as 1/8, a practical range, from which K should be chosen, would be defined, i.e.

$$4(c_1)_s < K < 9 (c_1)_s$$

The value of $(c_1)_s$ can be estimated from the experimental isotherm, so that K can be guessed to within a factor of about two. For the FMS-MeOH isotherm at 40°C, $(c_1)_s = \sim 1/2\ c^*$ so that the range from which the corresponding value of K' should be chosen is $2 < K' < 4.5$. Hence the actual value (4) for K' which gives the closest fit to the experimental isotherm is at least of the correct order of magnitude, and the agreement is perhaps as close as can be expected for such a simple model.

7.1.3 Temperature Dependence of Isotherms

i) Heats of Sorption and Heats and Entropies of Dilution

Heats of sorption $\Delta\bar{H}_s$ in the limit ($c \rightarrow 0$) were calculated and are given in Table 7-3. Plots of log $\sigma_{c=0}$ vs. 1/T for water in each polymer are shown in Figure 7-8.

TABLE 7-3

Heats of Sorption $\Delta\bar{H}_s$ in the limit ($c \rightarrow 0$) (kcal.mole^{-1})

System	$\Delta\bar{H}_s$
DMS (I) - H_2O	- 5.0
DMS (II) - H_2O	- 6.5
PMS - H_2O	- 5.9
FMS - H_2O	- 5.1
FMS - MeOH	$\sim$ - 7

The values of $\Delta\bar{H}_s$ exhibit quite a large scatter about $\sim$ - 5.5 kcal.mole^{-1}. A more exothermic value for FMS might have been expected as this polymer contains polar groups and sorbs more water. However, the scatter in the values of $\Delta\bar{H}_s$ for the DMS and the PMS samples is probably sufficiently great to attribute the relatively low value for FMS to experimental error. As expected, the values of $\Delta\bar{H}_s$ are lower than the corresponding values for PMMA and PEMA

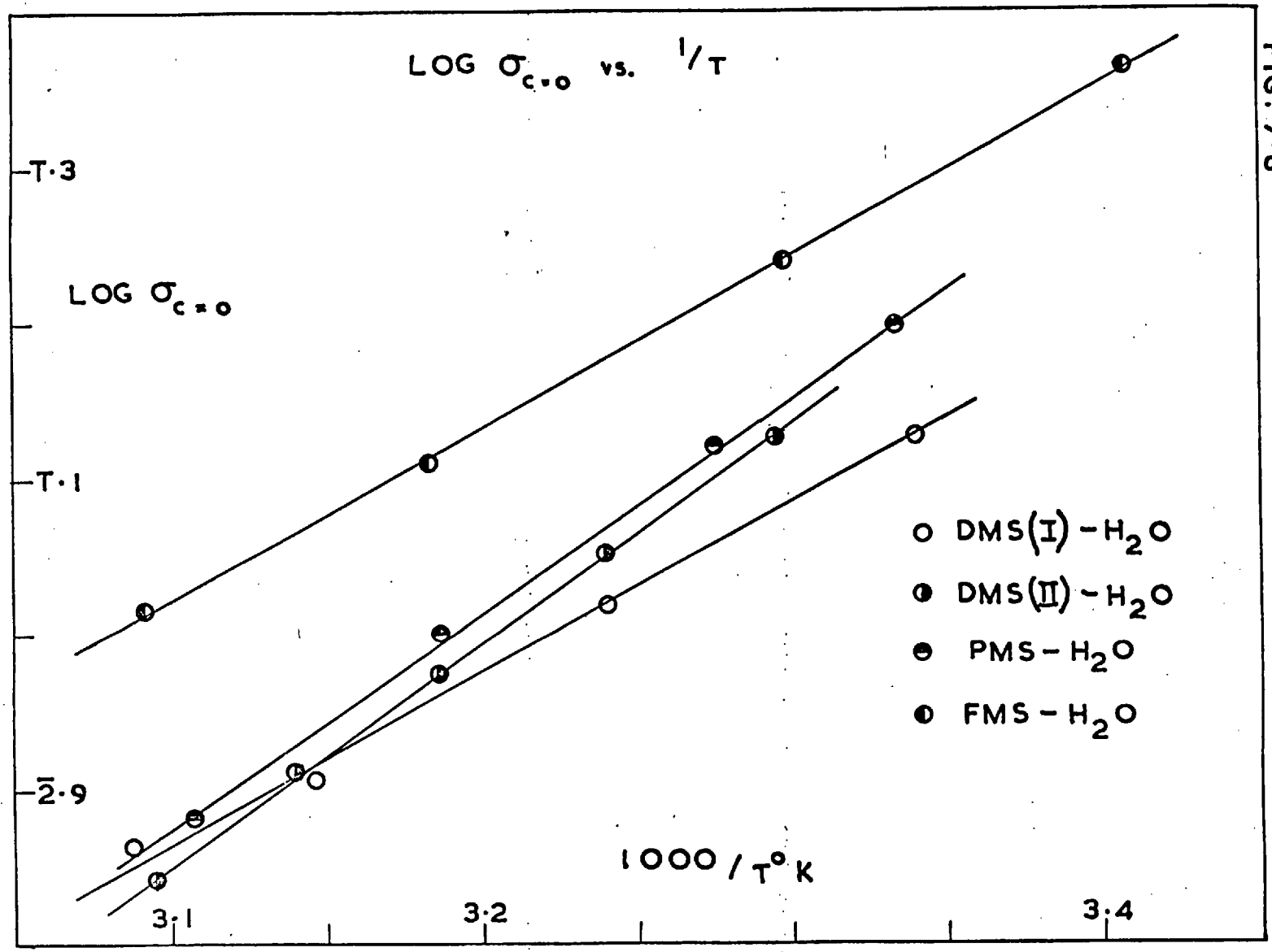
LOG $\sigma_{c=0}$ vs. $^1/_T$
T·3
LOG $\sigma_{c=0}$
T·1
$\bar{2}$·9
1000 / T° K
3·1
3·2
3·4
DMS(I) – H_2O
DMS(II) – H_2O
PMS – H_2O
FMS – H_2O

FIG. 7·8

(Table 6-3). They approach closely to those for PPMA and PBMA where the effect of the polar ester group on water sorption is relatively diminished.

Heats and entropies of dilution were calculated for various values of c using equations (2-51) and (2-52). Mean values $\overline{\Delta\bar{H}_A}$ and $\overline{\Delta\bar{S}_A}$ over the temperature ranges of study are given in Table 7-4. For FMS-H_2O, $\Delta\bar{H}_A$ and $\Delta\bar{S}_A$ vary appreciably with temperature. Plots of log (p/p_o) vs. 1/T for this system are illustrated in Figure 7-9. For FMS, the curvature in the isotherms at higher relative pressures is more marked than that for DMS. The marked curvature observed in the plots of log (p/p_o) vs. 1/T for c = 0.30 - 0.75 cc.s.t.p.cm^{-3} arises because this concentration range corresponds to the regions of the isotherms where departure from linearity is first observed (Figure 7-4). The plot of log (p/p_o) vs. 1/T for c = 0.15 cc.s.t.p.cm^{-3} is linear because this concentration corresponds to the linear regions of the isotherms over the whole temperature range.

As for water in the polymethacrylates, $\overline{\Delta\bar{H}_A}$ and $\overline{\Delta\bar{S}_A}$ decrease with increasing c, which again is qualitatively consistent with clustering of water becoming more pronounced at higher c. The concentration dependences of $\overline{\Delta\bar{H}_A}$ and $\overline{\Delta\bar{S}_A}$

FIG. 7·9

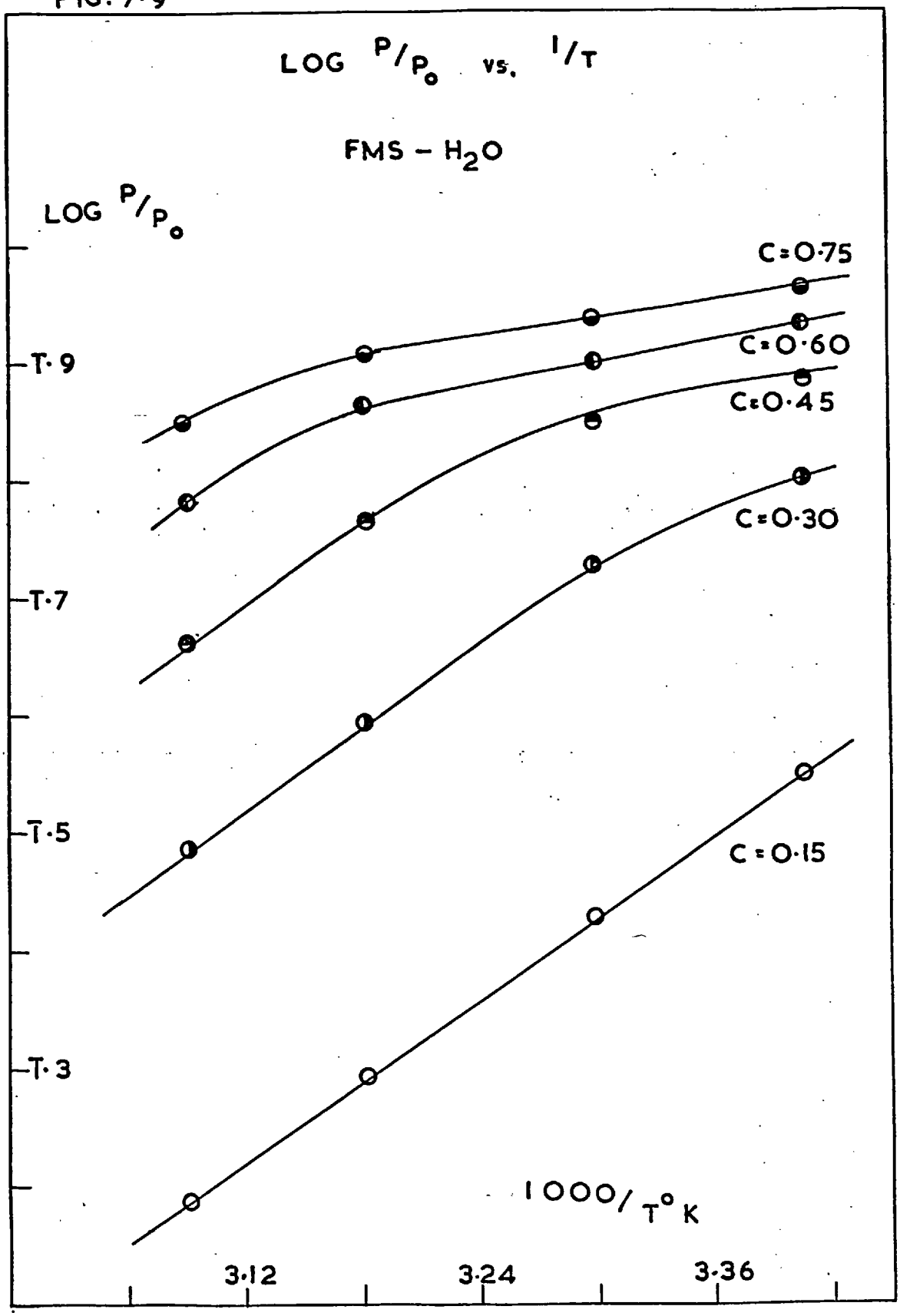
LOG P/P₀ vs. 1/T
FMS – H₂O
LOG P/P₀
C=0·75
C=0·60
C=0·45
C=0·30
C=0·15
T·9
T·7
T·5
T·3
1000/T°K
3·12
3·24
3·36

TABLE 7-4

Mean Heats ($\overline{\Delta\bar{H}}_A$) and Entropies ($\overline{\Delta\bar{S}}_A$) of Dilution

System and Temperature Range	Concentration of sorbed water cc.s.t.p. cm^{-3}	$\overline{\Delta\bar{H}}_A$ kcal.$mole^{-1}$	$\overline{\Delta\bar{S}}_A$ cal.$deg.^{-1}$ $mole^{-1}$
	0	3.9 (3.9)	∞
	0.12	3.9 (3.1)	15 (11.8)
DMS(II)-H_2O	0.24	3.8 (2.5)	14 (8.9)
30-50°C	0.36	3.4 (2.0)	12 (7.0)
	0.48	2.2 (1.6)	8 (5.6)
	0.60	1.3 (1.3)	4 (4.4)
	0	4.5 (4.5)	∞
	0.08	4.3 (3.9)	17 (14.8)
PMS-H_2O	0.16	4.3 (3.3)	16 (12.1)
25-50°C	0.24	4.3 (2.9)	15 (10.2)
	0.32	3.8 (2.5)	13 (8.7)
	0.40	3.0 (2.2)	10 (7.5)
	0	5.3 (5.3)	∞
	0.15	5.3 (4.6)	20 (17.5)
FMS-H_2O	0.30	3.8 (4.1)	14 (14.7)
20-50°C	0.45	3.4 (3.6)	12 (12.7)
	0.60	3.4 (3.2)	11 (11.0)
	0.75	2.3 (2.9)	10 (9.7)

are compared in Table 7-4 with those expected on the basis of the random polycondensation model for water (in parentheses).

ΔH for hydrogen bond rupture was taken as $\lim_{c \to 0} (\overline{\Delta H}_A)$ in each case. In general the agreement is poor, particularly at the lower values of c corresponding to the linear regions of the isotherms, and serves to illustrate the limitations of the simple model.

ii) Temperature Dependence of Clustering Functions.

Table 7-2 shows that, despite some scatter, both the clustering functions show a tendency to decrease with increasing temperature for a given water activity corresponding to the non-linear regions of the isotherms. The reverse tendency observed for the FMS-MeOH system is probably due to experimental error since this system was studied at two temperatures only.

7.2 Steady State Permeability Results

Data used for the calculation of permeability coefficients are presented in appendix 9.7. Permeation rates for water and methanol in FMS at various relative pressures are shown in Figure 7-10.

7.2.1 Concentration Dependence of P.

For water in each polymer, P is constant as plots of $J\ell$ vs. p/p_o are all linear over the whole of the range of p/p_o. The slight decrease in P with increasing c

FIG. 7·10

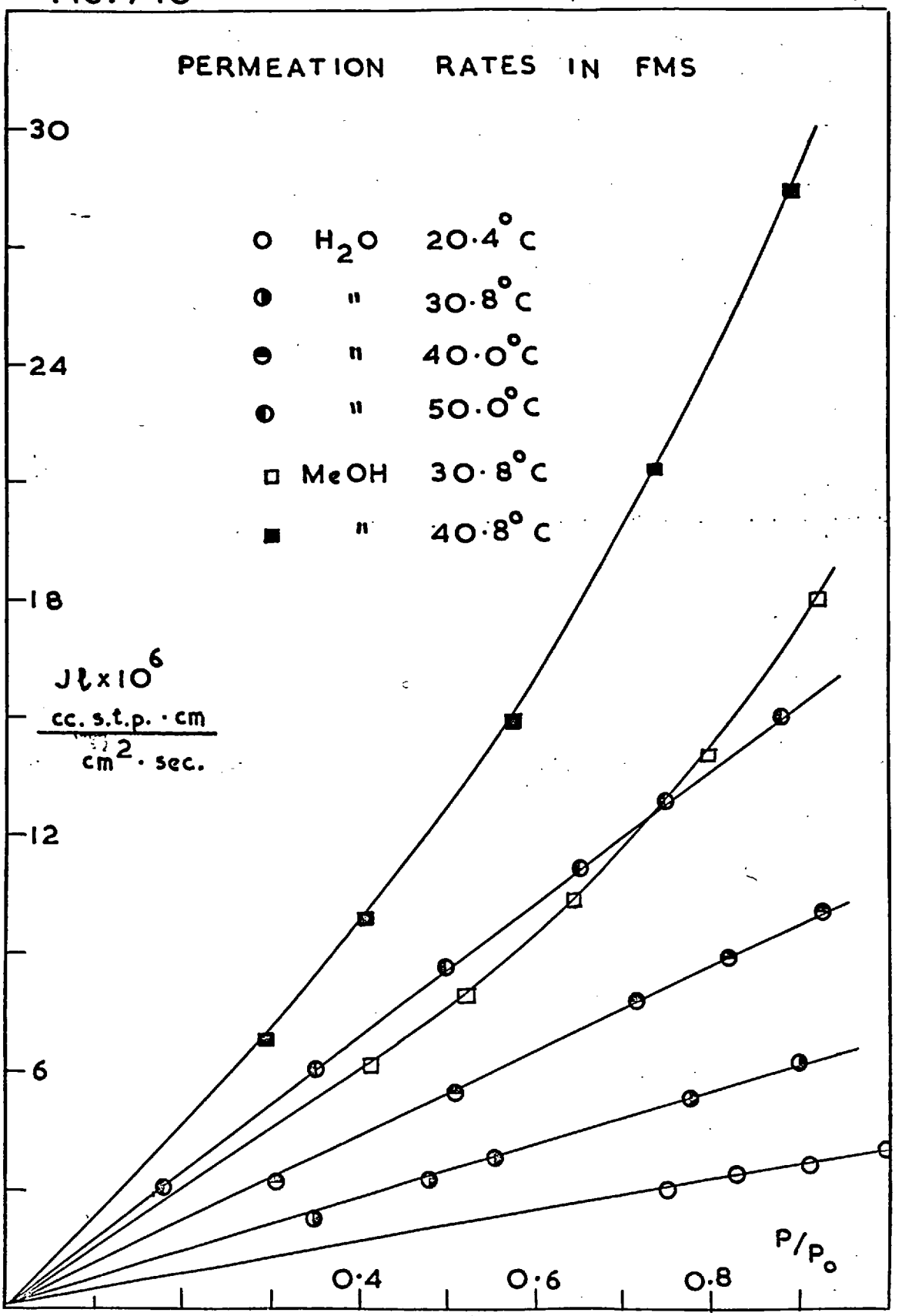
PERMEATION RATES IN FMS
30
24
18
12
6
$J\ell \times 10^6$
cc. s.t.p. · cm
cm² · sec.
O H_2O 20·4°C
◑ " 30·8°C
⊖ " 40·0°C
◐ " 50·0°C
□ MeOH 30·8°C
■ " 40·8°C
0·4
0·6
0·8
P/P₀

previously observed[43] for DMS-H_2O was possibly a consequence of a decrease in the effective area of the membrane at higher ingoing pressures due to the presence of a supporting gauze.

For methanol in FMS P increases slightly with increasing c, whereas for methanol in DMS P was found to be constant[59]. This is probably a reflection of the increased amenability to plasticisation of FMS which contains bulkier side groups than DMS. At room temperature DMS is so rubbery that very little plasticisation is to be expected.

7.2.2 Absolute Magnitudes of P

Values of P for each system ($\lim_{c \to 0}$ P for methanol in FMS) are given in Table 7-5. For water at $\sim 40^{\circ}C$, P increases in the order

FMS < PMS < DMS (I and III) < DMS (II).

This order is not consistent with that for the sorptive capacities for water (FMS > DMS) so that the principal effect is the decrease in D with the addition of bulky side groups. This point is discussed more fully in section 7.3. The higher values of P for sample II of DMS are rather surprising. Although samples I and II came from different

TABLE 7-5

Permeability Coefficients P (cc. s.t.p. cm.cm.$^{-2}$ sec.$^{-1}$ (cmHg)$^{-1}$)

System	Temperature °C	P x 10^6
DMS (I)-H_2O	26.0	4.77
"	35.7	4.34
"	43.0	4.05
"	50.2	3.79
DMS (II)-H_2O	30.7	6.57
"	40.0	5.66
"	50.1	4.84
DMS (III)-H_2O	35.8	4.59
"	49.8	4.12
PMS - H_2O	22.8	4.27
"	31.9	3.77
"	40.9	3.53
"	50.8	3.18
FMS - H_2O	20.4	2.19
"	30.8	2.07
"	40.0	1.95
"	50.0	1.84
FMS-MeOH	30.8	0.86
"	40.8	0.85

sources, they sorb similar quantities of water (Figures 7-1 and 7-2) and discrepancies of 30-50% in P are not normally to be expected between different samples of such a rubbery polymer. P for sample I of DMS agrees to within about 7% of previous results for DMS-H_2O[43].

Barrie[59] found P = 3.7 and 5.5 x 10^{-6} cc. s.t.p. cm. $cm.^{-2}.sec^{-1}$. $(cmHg)^{-1}$ at 30 and 10°C respectively for methanol in DMS. These values are a factor of 4-5 higher than those obtained here for FMS-MeOH (Table 7-5) and again the difference can be attributed to the effect of the more bulky trifluoropropyl group on the diffusion coefficient.

7.2.3 Temperature Dependence of P

Values for E_P calculated from $P = P_o \exp(-E_P/RT)$ are given in Table 7-6. The corresponding graphs of log P vs. 1/T for water are shown in Figure 7-11. Accurate values for P_o could not be determined on account of the relatively small temperature ranges used.

TABLE 7-6

Values of E_P (kcal.$mole^{-1}$)

System	E_P
DMS(I) - H_2O	- 1.8
DMS (II)-H_2O	- 3.1
PMS - H_2O	- 2.1
FMS - H_2O	- 1.1
FMS - MeOH	$\sim$ - 0.3

The negative values obtained for E_P show that $\Delta\bar{H}_s$ is numerically larger than E_D for these systems. This

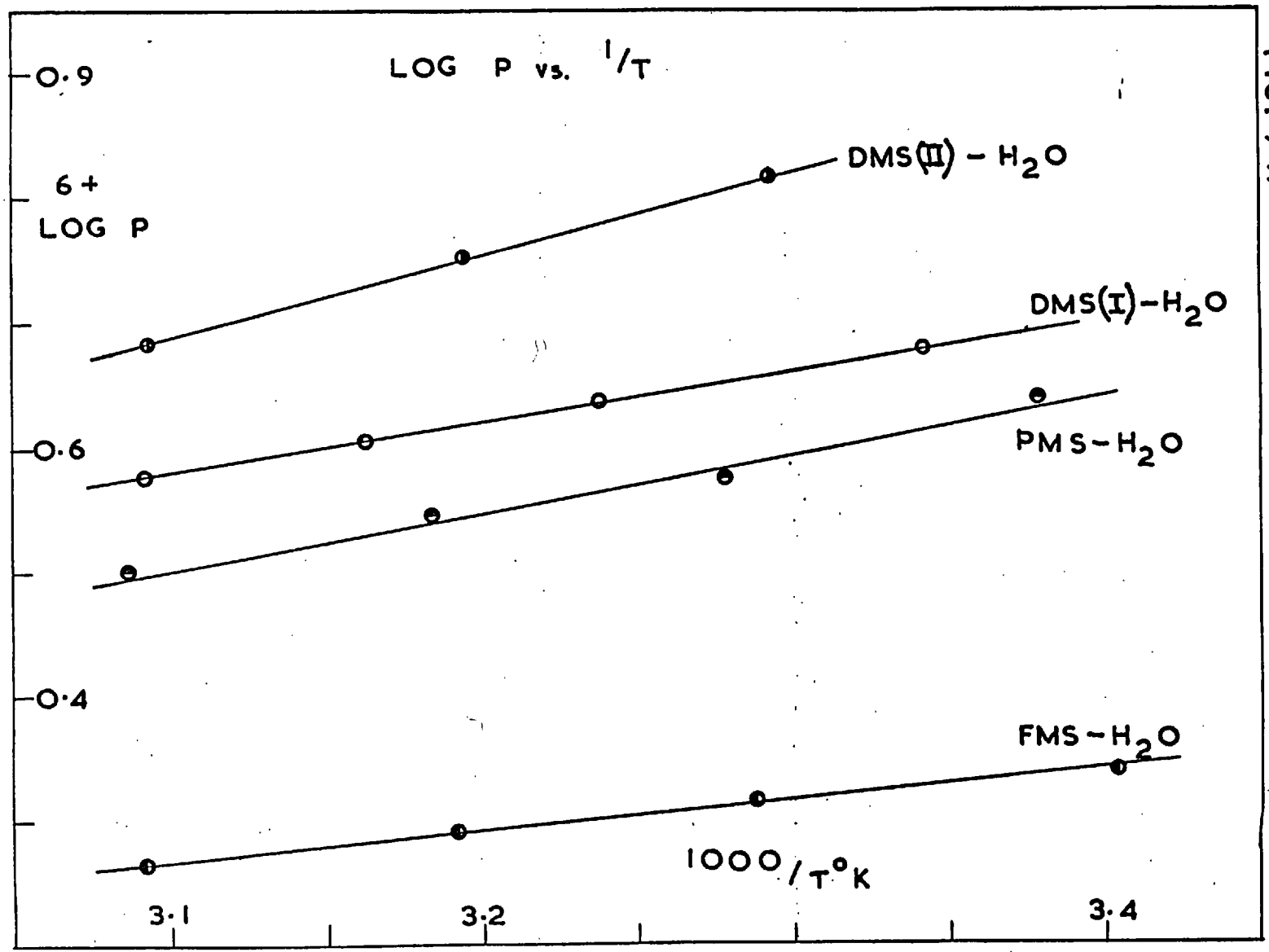
LOG P vs. 1/T
0·9
6 +
LOG P
0·6
0·4
DMS(II) – H2O
DMS(I)–H2O
PMS–H2O
FMS–H2O
1000/T°K
3·1
3·2
3·4

FIG. 7.11

behaviour was also found for other small penetrant molecules in polysiloxanes[13,108,142].

7.3 Diffusion Coefficients

7.3.1 Steady State Diffusion

Steady state diffusion coefficients were determined as described in section 2.4. Since the sorption isotherms include linear regions they could not be expressed in polynomial form (cf. section 6.3.1) over the whole range. Moreover, difficulty was experienced in curve-fitting the regions where the isotherms first deviate from linearity. For this reason, $J\ell$ vs. c curves were constructed and differentiated graphically to obtain the D-c relationships.

i) Values of $D_{c=0}$

Values of $D_{c=0}$ are given in Table 7-7. For DMS-H_2O they are lower than those given by Barrie and Platt[43], but may be considered as being the more accurate as the corresponding sorption isotherms were determined with greater precision. The high values of $D_{c=0}$ for water in sample II of DMS, compared with samples I and III, are shown up in Table 7-7 and are responsible for the higher values of P observed for this sample. No appreciable distortion of any of the membranes was apparent on their removal from the

TABLE 7-7

Values of $D_{c=0}$ (cm^2. $sec.^{-1}$)

System	T°C	$D_{c=0} \times 10^5$	System	T°C	$D_{c=0} \times 10^5$
DMS (I)-	26.3	3.5	PMS-	25.9	2.6
H_2O	35.4	4.1	H_2O	31.2	2.9
"	44.7	5.0	"	40.8	3.6
"	50.7	5.2	"	48.8	4.2
DMS (II)	30.3	4.9	FMS-	20.4	0.94
$-H_2O$	35.5	5.4	H_2O	30.1	1.2
"	40.7	5.9	"	41.1	1.5
"	45.4	6.4	"	50.3	1.8
"	50.0	6.9			
			FMS-	30.4	0.28
DMS(III)	30.3	4.4	MeOH	40.4	0.39
$-H_2O$	50.0	5.9			

diffusion cell and this discrepancy in the results is largely unaccounted for.

A comparison of $D_{c=0}$ for water at $\sim 30^{\circ}C$ reveals that

$$FMS \ll PMS < DMS$$

This order also determines that for P, and is a consequence of the introduction of a bulky side group, in going from DMS to PMS or FMS, which decreases the segmental mobility. This

is further illustrated by the T_g values which are in the reverse order (Table 5-2) to that for $D_{c=0}$. In fact, the phenyl group is more rigid than the trifluoropropyl group, but the proportion of phenyl groups present in the PMS copolymer is small ($\sim$ 5.4%) and so less overall restriction on segmental mobility is incurred in going from DMS to PMS than from DMS to FMS. Similar behaviour was observed for permanent gas diffusion in these three polymers[142,143].

The lower values of $D_{c=0}$ for methanol compared with those for water in FMS are a consequence of the larger size of methanol as a penetrant molecule.

The values of D observed here for water in DMS, PMS and FMS are all high on comparison with corresponding values in most other polymers. For example, they are two orders of magnitude higher than those for the polymethacrylates. High values of D were observed for several other penetrants in silicone rubbers and have been attributed[13] to the exceptionally high degree of freedom for rotation about the Si–O–Si chain linkage.

ii) Concentration Dependence of D

At higher relative vapour pressures D decreases with increasing c for each system. For relative vapour

pressures in the region 0.8 - 0.95, values of D are only 1/2 - 1/6 of the values at c = 0 and the relative decreases are greater the lower the temperature. The overall decreases for water are thus comparable with those for water in the polymethacrylates (section 6.3.1). However, a major difference in the case of the silicone rubbers is that D does not vary initially with c, as a consequence of the linear regions of the sorption isotherms. For methanol in FMS, D decreases to $\sim$1/3 of its value at c=0, for a relative pressure of $\sim$0.9 although again D is constant initially. This behaviour contrasts sharply with that of the PEMA-MeOH system. The concentration dependence of $D' = D/D_{c=0}$ for each system is illustrated in Figures 7-12 to 7-16.

The apparent existence of a "critical" concentration for penetrant clustering is shown up more clearly in the D'-c plots than in the sorption isotherms as D' starts to decrease at some finite value of c. The precise shape of the D'-c curve in the region where D' first starts to decrease is open to some doubt since the shape in this region is rather sensitive to small changes in the shape of the sorption isotherm.

FIG. 7·12

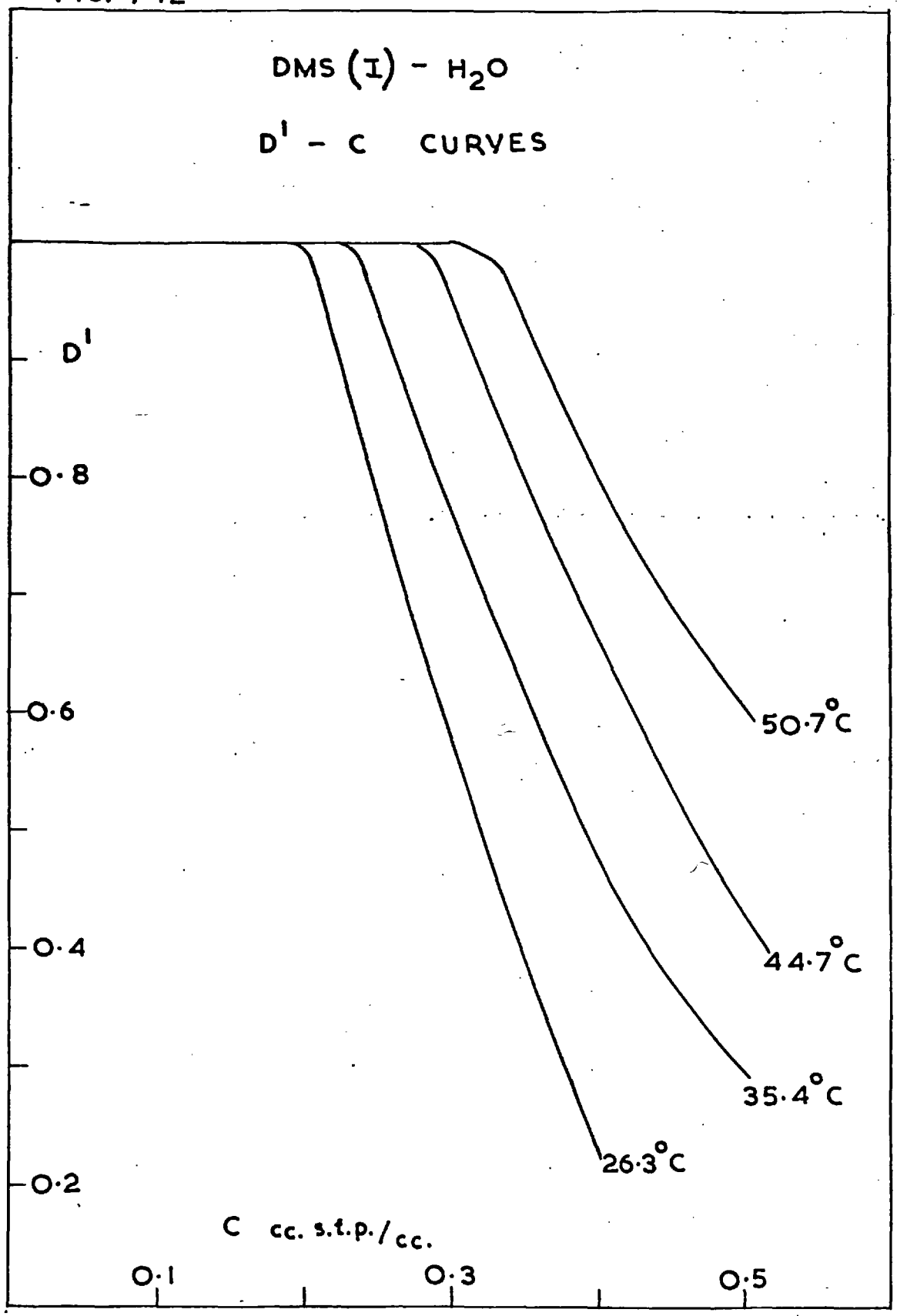
DMS (I) - H2O
D' - C CURVES
D'
0·8
0·6
0·4
0·2
50·7°C
44·7°C
35·4°C
26·3°C
C cc. s.t.p./cc.
0·1
0·3
0·5

FIG. 7·13

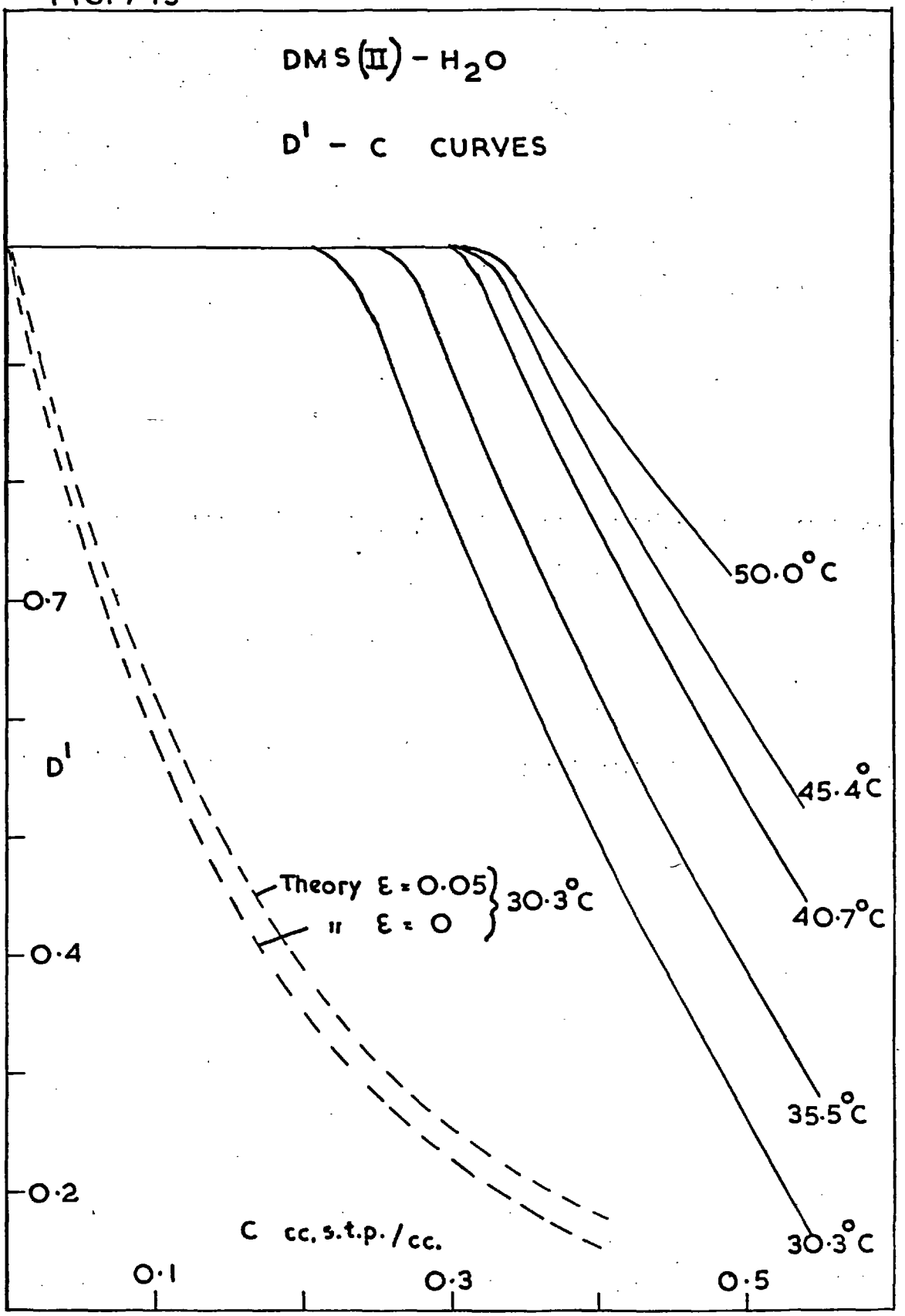
DMS (II) – H2O
D' – C CURVES
50·0°C
45·4°C
40·7°C
35·5°C
30·3°C
Theory ε = 0·05
" ε = 0
30·3°C
0·7
0·4
0·2
D'
C cc. s.t.p. / cc.
0·1
0·3
0·5

FIG. 7·14

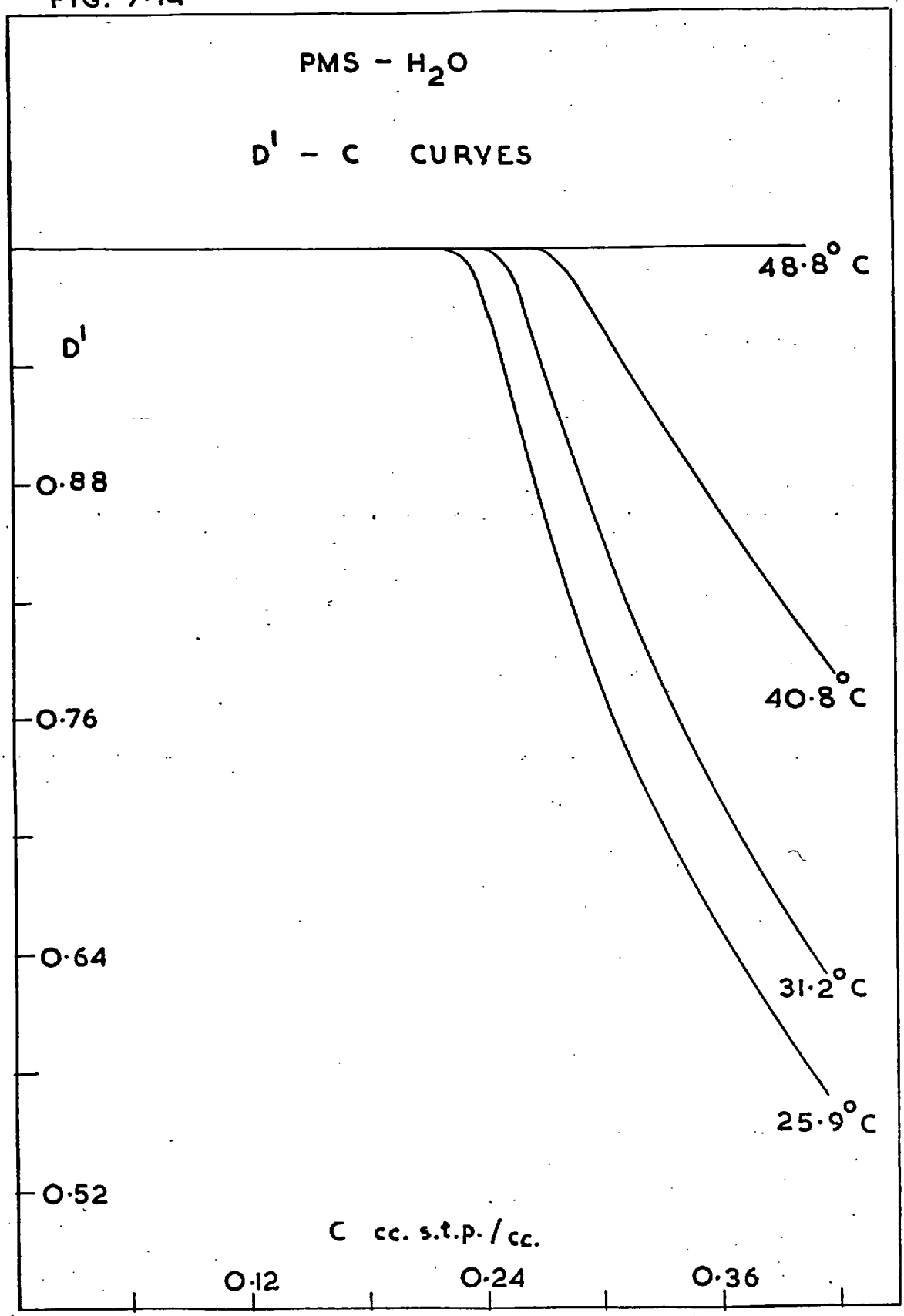
PMS – H_2O
D' – C CURVES
48·8° C
40·8° C
31·2° C
25·9° C
D'
0·88
0·76
0·64
0·52
C cc. s.t.p. / cc.
0·12
0·24
0·36

FIG. 7·15

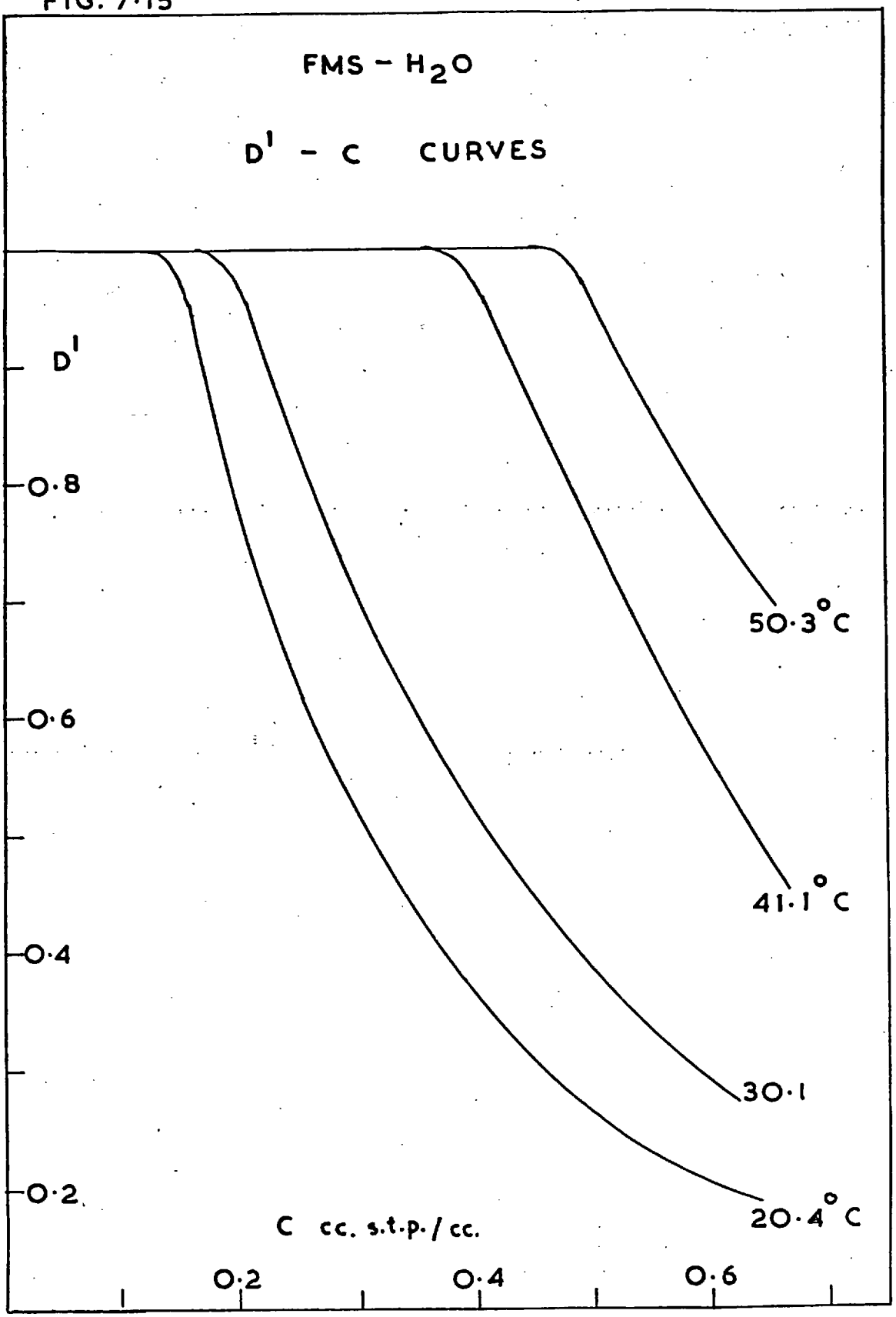
FMS – H_2O
D^1 – C CURVES
D^1
0·8
0·6
0·4
0·2
50·3°C
41·1°C
30·1
20·4°C
C cc. s.t.p./cc.
0·2
0·4
0·6

FIG. 7·16

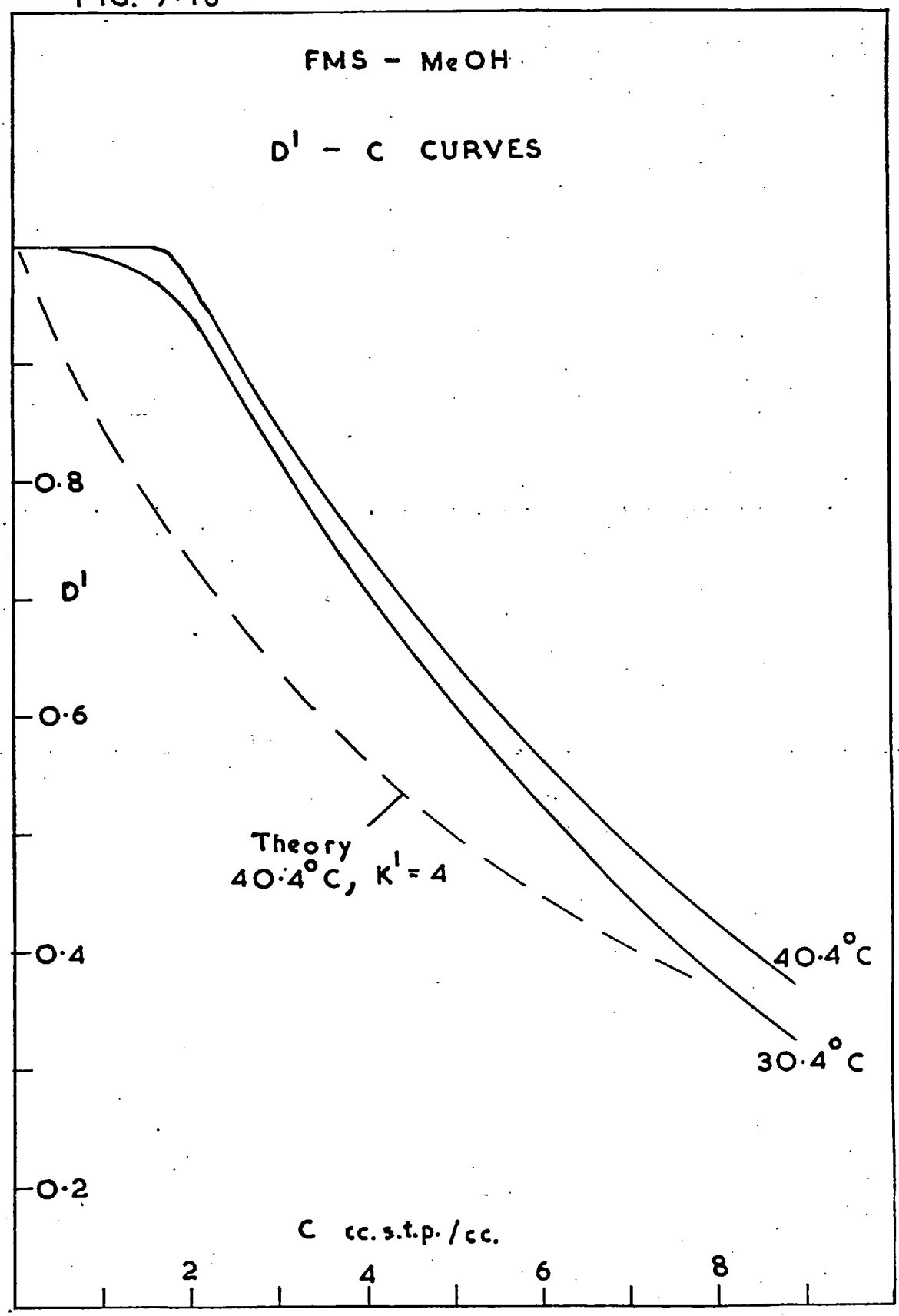
FMS – MeOH
D' – C CURVES
0·8
D'
0·6
0·4
0·2
Theory
40·4°C, K' = 4
40·4°C
30·4°C
C cc. s.t.p. / cc.
2
4
6
8

For corresponding ranges in water activity, decreases in D' are greater for FMS than for DMS as a consequence of the higher degrees of clustering in the former polymer (section 7.1.2). However, for corresponding ranges in c, D' decreases rather less in FMS than in DMS.

The D'-c curves obviously do not correspond well with the simple polycondensation models for water and methanol on account of the initial region of constant D. In Figure 7-13 the curve for the DMS (II) - H_2O system at 40.7°C is compared with the theory for $\varepsilon = 0$ and $\varepsilon = 0.05$ and assuming diffusion of monomeric water only. The discrepancy, as expected, is large except for the higher values of c. In Figure 7-16 the D'-c curve for methanol in FMS at 40°C is compared with that calculated from the random polycondensation model. Monomeric methanol diffusion only is assumed and K' is taken as 4, the same value as for the isotherm fit. The agreement between theory and experiment is better than in the case of water but not quite so good as obtained by Barrie[59] for methanol in DMS.

7.3.2 Transient State Diffusion

The take up of water by the silicone rubbers is considerably less than by the polymethacrylates and in addition occurs more rapidly. Consequently, the accuracy

of diffusion coefficients determined from rates of sorption and desorption is very much less in the case of the polysiloxanes, as indicated in section 5.4. Sorption kinetic measurements for water in the polysiloxanes were made principally for the purpose of providing rough comparisons with the corresponding steady state results.

i) Reduced Sorption and Desorption Curves

Typical pairs of conjugate reduced sorption/desorption curves for water in DMS, PMS and FMS are shown in Figure 7-17. The initial stages could not be followed with any degree of certainty and only small portions of what appeared to be the linear regions of the curves were available for analysis. Back extrapolations rarely went through the origin, which was not entirely unexpected in view of the errors involved and the difficulties encountered in establishing stable boundary conditions quickly. As expected[137], curves always become concave to the $t^{\frac{1}{2}}/\ell$ axis at longer times.

Data used for the construction of typical reduced curves are presented in appendix 9.8.

ii) Determination of Diffusion Coefficients

$\bar{D}_s$ and $\bar{D}_d$ were calculated from $\bar{D}_{s(d)} = \frac{\pi I^2_{s(d)}}{16}$,

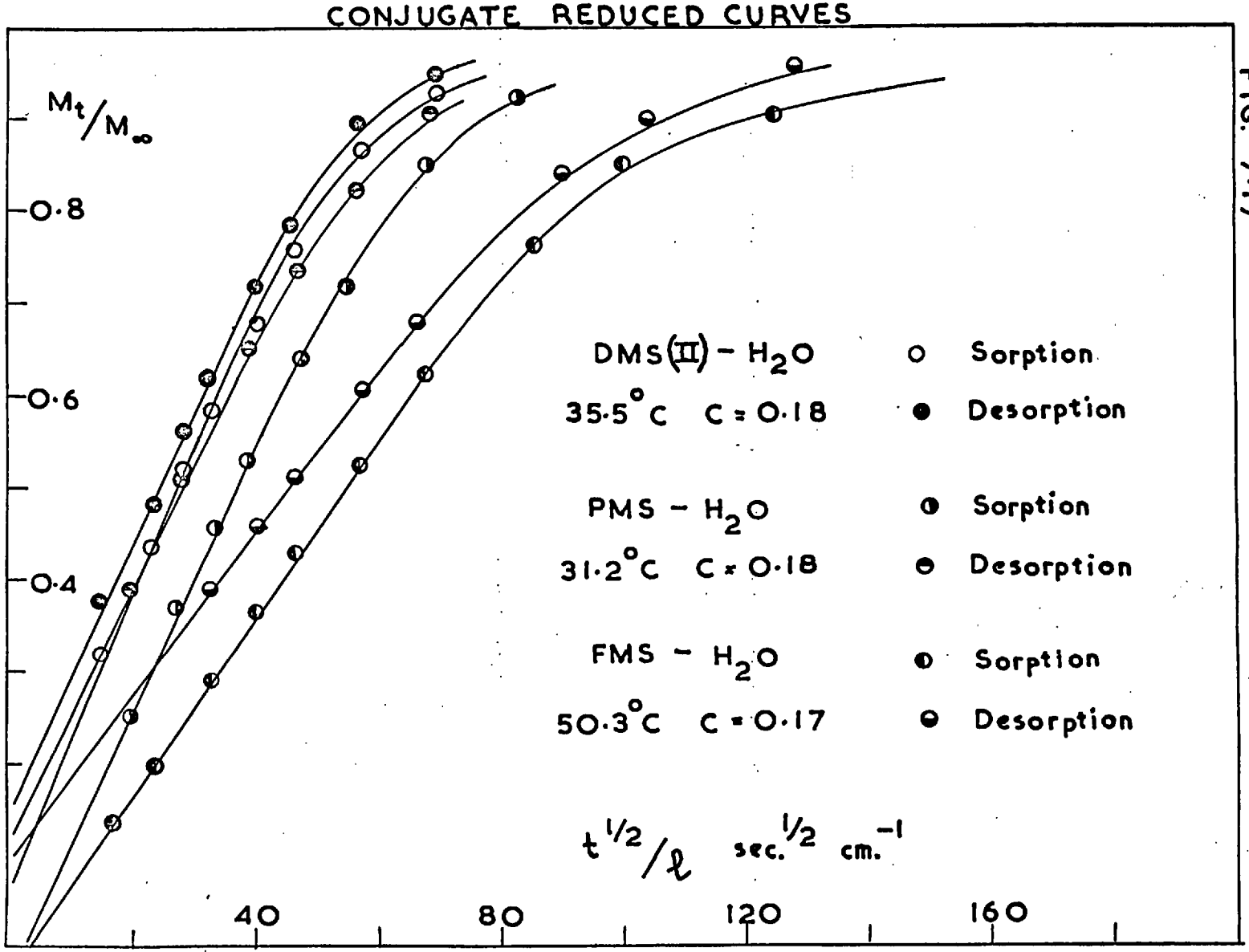
CONJUGATE REDUCED CURVES
M_t/M_∞
0·8
0·6
0·4
DMS(II) – H_2O
35·5°C C = 0·18
PMS – H_2O
31·2°C C = 0·18
FMS – H_2O
50·3°C C = 0·17
Sorption
Desorption
Sorption
Desorption
Sorption
Desorption
$t^{1/2}/l$ sec.$^{1/2}$ cm.$^{-1}$
40
80
120
160

FIG. 7.17

and values of $\bar{D}_s$, $\bar{D}_d$ and of the initial slopes I_s and I_d are given in Table 7-9.

For each system the scatter in $\bar{D}_s$ and $\bar{D}_d$ is large and apparently random for smaller values of c. Values of $\bar{D}_s$, $\bar{D}_d$ for concentrations corresponding to the linear regions of the sorption isotherms were averaged and are compared in Table 7-10 with the steady state $D_{c=0}$ values.

iii) Comparison of $\bar{D}_s$, $\bar{D}_d$ for small c with teady State $D_{c=0}$.

Considering the experimental errors involved, Table 7-10 shows that the transient state diffusion coefficients agree reasonably well with the corresponding steady state values. In general the agreement is better for FMS than for DMS and in turn is better for DMS than for PMS. This is probably due largely to the relative numbers of measurements made for each system and hence to the relative reliabilities of the averaged values for $\bar{D}_s$ and $\bar{D}_d$. The particularly close agreement observed in the case of FMS must be considered to some extent fortuitous in view of all the possible sources of error.

The higher values of D for water in sample II of DMS compared with sample I are also observed by this transient state analysis. There appears therefore to be a real difference between the two samples, the reason for which remains obscure.

TABLE 7-9

Mean Diffusion Coefficients $\bar{D}_s$, $\bar{D}_d$ ($cm^2 . sec.^{-1}$) and Initial Slopes I_s, I_d ($cm.sec^{-\frac{1}{2}}$) of Reduced Curves

System	T°C	c cc.stp cm^{-3}	I_s x 10^2	I_d x 10^2	$\bar{D}_s$ x 10^5	$\bar{D}_d$ x 10^5	$\frac{\bar{D}_s+\bar{D}_d}{2}$ x 10^5
DMS (I)	26.3	0.20	1.4	-	3.8	-	-
-H_2O	50.7	0.27	1.6	-	5.0	-	-
DMS (II)	30.3	0.21	1.5	1.55	4.5	4.7	4.6
- H_2O	"	0.25	1.45	-	4.1	-	-
"	"	0.23*	1.5	1.5	4.3	4.4	4.4
"	"	0.88*	0.8	-	1.3	-	-
"	30.7	0.16	1.5	1.5	4.5	4.5	4.5
"	"	0.14*	1.5	-	4.6	--	-
"	"	0.47*	1.35	-	3.6	-	-
"	"	0.40*	1.4	-	4.1	-	-
"	"	0.34*	1.4	1.5	4.0	4.4	4.2
"	"	0.30*	1.45	1.4	4.1	3.8	4.0
"	"	0.24	1.5	-	4.4	-	-
"	"	0.20	1.5	-	4.3	-	-
"	35.5	0.18	1.6	1.5	4.8	4.6	4.7
"	"	0.21	1.6	1.55	4.8	4.7	4.8
"	"	0.24	1.5	1.5	4.5	4.2	4.4
"	40.7	0.17	1.8	1.8	6.1	6.1	6.1
"	"	0.20	1.7	-	5.7	-	-
"	"	0.24	1.7	-	5.4	-	-
"	45.4	0.14	1.7	1.75	5.9	6.0	5.9
"	"	0.17	1.7	1.8	5.8	6.7	6.2
"	"	0.21	1.7	1.7	5.7	5.7	5.7
DMS (II)	50.0	0.13	1.85	1.9	6.7	7.0	6.9
- H_2O	"	0.16	1.8	-	6.5	-	-
"	"	0.20	1.75	-	6.0	-	-
"	"	0.25*	1.8	-	6.0	-	-
"	"	0.32*	1.6	-	5.3	-	-
"	"	0.39*	1.7	-	5.5	-	-
"	"	0.50*	1.6	-	5.0	-	-
"	"	0.56*	1.5	-	4.5	-	-

TABLE 7-9 (contd.)

System	T°C	c cc.stp cm^{-3}	I_s x 10^2	I_d x 10^2	$\bar{D}_s$ x 10^5	$\bar{D}_d$ x 10^5	$\frac{\bar{D}_s+\bar{D}_d}{2}$ x 10^5
PMS	25.9	0.16	1.3	1.2	3.2	2.7	3.0
-H_2O	"	0.21	1.3	1.25	3.5	3.1	3.3
"	31.2	0.18	1.4	1.3	3.7	3.4	3.6
"	"	0.27	1.4	1.3	3.9	3.3	3.6
"	40.8	0.16	1.5	1.45	4.4	4.1	4.3
"	"	0.26	1.4	-	4.0	-	-
"	48.8	0.22	1.5	1.5	4.5	4.6	4.5
"	"	0.29	1.5	1.5	4.3	4.3	4.3
FMS	20.4	0.25	0.64	0.67	0.81	0.88	0.85
-H_2O	"	0.28*	0.61	0.66	0.73	0.86	0.79
"	"	0.42*	0.47	0.53	0.44	0.55	0.49
"	"	0.16	0.70	0.62	0.97	0.75	0.86
"	"	0.19	0.70	0.60	0.96	0.70	0.83
"	"	0.20	0.70	0.61	0.96	0.73	0.84
"	"	0.13	0.73	0.58	1.0	0.67	0.86
"	30.1	0.17	0.77	0.75	1.2	1.1	1.1
"	"	0.22	0.77	0.75	1.2	1.1	1.1
"	"	0.26	0.76	0.77	1.1	1.1	1.1
	"	0.31	0.75	0.73	1.1	1.1	1.1
	"	0.35*	0.75	0.75	1.1	1.1	1.1
"	"	0.64*	0.47	0.66	0.44	0.86	0.65
"	"	0.64*	0.45	0.64	0.39	0.81	0.60
"	"	0.41*	0.79	0.79	1.2	1.2	1.2
"	"	0.56*	0.49	0.64	0.48	0.80	0.64
"	"	0.28	0.79	0.74	1.2	1.1	1.2
"	"	0.34	0.77	0.77	1.2	1.1	1.2
"	"	0.35	0.75	0.79	1.1	1.2	1.2
"	"	0.36*	0.76	0.79	1.1	1.2	1.2
"	"	0.80*	0.37	-	0.28	-	-
"	"	0.37*	0.78	0.79	1.2	1.2	1.2
"	41.1	0.14	0.92	0.84	1.6	1.4	1.5
"	"	0.17	0.89	0.84	1.6	1.4	1.5
"	"	0.21	0.87	0.86	1.5	1.4	1.5
"	"	0.24	0.90	0.85	1.6	1.4	1.5
"	"	0.30	0.86	0.84	1.4	1.4	1.4
"	"	0.36	0.86	0.86	1.5	1.4	1.5
"	"	0.42*	0.90	-	1.6	-	-
"	"	0.52*	0.85	-	1.4	-	-

TABLE 7-9 (contd.)

System	T°C	c cc.stp cm^{-3}	I_s x 10^2	I_d x 10^2	$\bar{D}_s$ x 10^5	$\bar{D}_d$ x 10^5	$\frac{\bar{D}_s+\bar{D}_d}{2}$ x 10^5
FMS -H_2O	50.3	0.14	0.94	0.90	1.7	1.6	1.7
"	"	0.17	0.96	0.93	1.8	1.7	1.7
"	"	0.21	0.98	0.90	1.9	1.6	1.7
"	"	0.26	0.94	0.92	1.7	1.7	1.7
"	"	0.30	0.95	0.91	1.8	1.6	1.7
"	"	0.36	0.94	-	1.7	-	-
"	"	0.42	0.93	0.88	1.7	1.5	1.6
"	"	0.50	0.94	0.90	1.7	1.6	1.7
"	"	0.57	0.96	-	1.8	-	-

* Denotes value in non-linear region of isotherm.

TABLE 7-10

Steady and Transient State Diffusion Coefficients ($cm.^2$ sec^{-1}).

System	Temperature °C	Averaged $\bar{D}_s$ x 10^5	Averaged $\frac{\bar{D}_s+\bar{D}_d}{2}$ x 10^5	Steady* State $D_{c=0}$ x 10^5
DMS (I)	26.3	3.8	-	3.5
-H_2O	50.7	5.0	-	5.2
DMS (II)	30.3	4.3	4.4	4.9
-H_2O	30.7	4.5	4.5	-
"	35.5	4.7	4.6	5.4
"	40.7	5.7	5.8	5.9
"	45.4	5.8	6.0	6.4
"	50.0	6.4	6.6	6.9
PMS-	25.9	3.4	3.1	2.6
H_2O	31.2	3.8	3.6	2.9
"	40.8	4.2	4.2	3.6
"	48.8	4.4	4.4	4.2
FMS-	20.4	0.91	0.84	0.94
H_2O	30.1	1.1	1.1	1.2
"	41.1	1.5	1.5	1.5
"	50.3	1.8	1.7	1.8

* Some values interpolated.

iv) Concentration Dependence of D : Comparison with the Steady State

Since such large errors were involved, D-c relationships could not be determined with sufficient quantitative accuracy. However, Tables 7-9 and 7-10 indicate that values of $\overline{D}_s$ and $\overline{D}_{AV}$ when c corresponds to the non-linear regions of the sorption isotherms (starred values in Table 7-9) are smaller in general than the corresponding averaged values of $\overline{D}_s$, $\overline{D}_{AV}$ (Table 7-10) calculated in the linear regions of the isotherms. This is in qualitative agreement with the steady state results.

For FMS-H_2O at 30.1°C, curves of $\overline{D}_s'$ and $\overline{D}_d'$ vs. c, where $\overline{D}_s' = \overline{D}_s/\overline{D}_{c=0}$ and $\overline{D}_d' = \overline{D}_d/\overline{D}_{c=0}$, are compared in Figure 7-18 with those expected from the steady state results on the basis of equations (2-34) and (2-35). The agreement is perhaps as good as can be expected considering the experimental errors.

Despite the initial scatter, no trend of $\overline{D}_s$ or $\overline{D}_d$ with c is apparent for any of the systems at lower values of c.

7.3.3 Temperature Dependence of D.

Plots of log D vs. 1/T at various values of c for each system are shown in Figures 7-19 to 7-22. Values of

FIG. 7·18

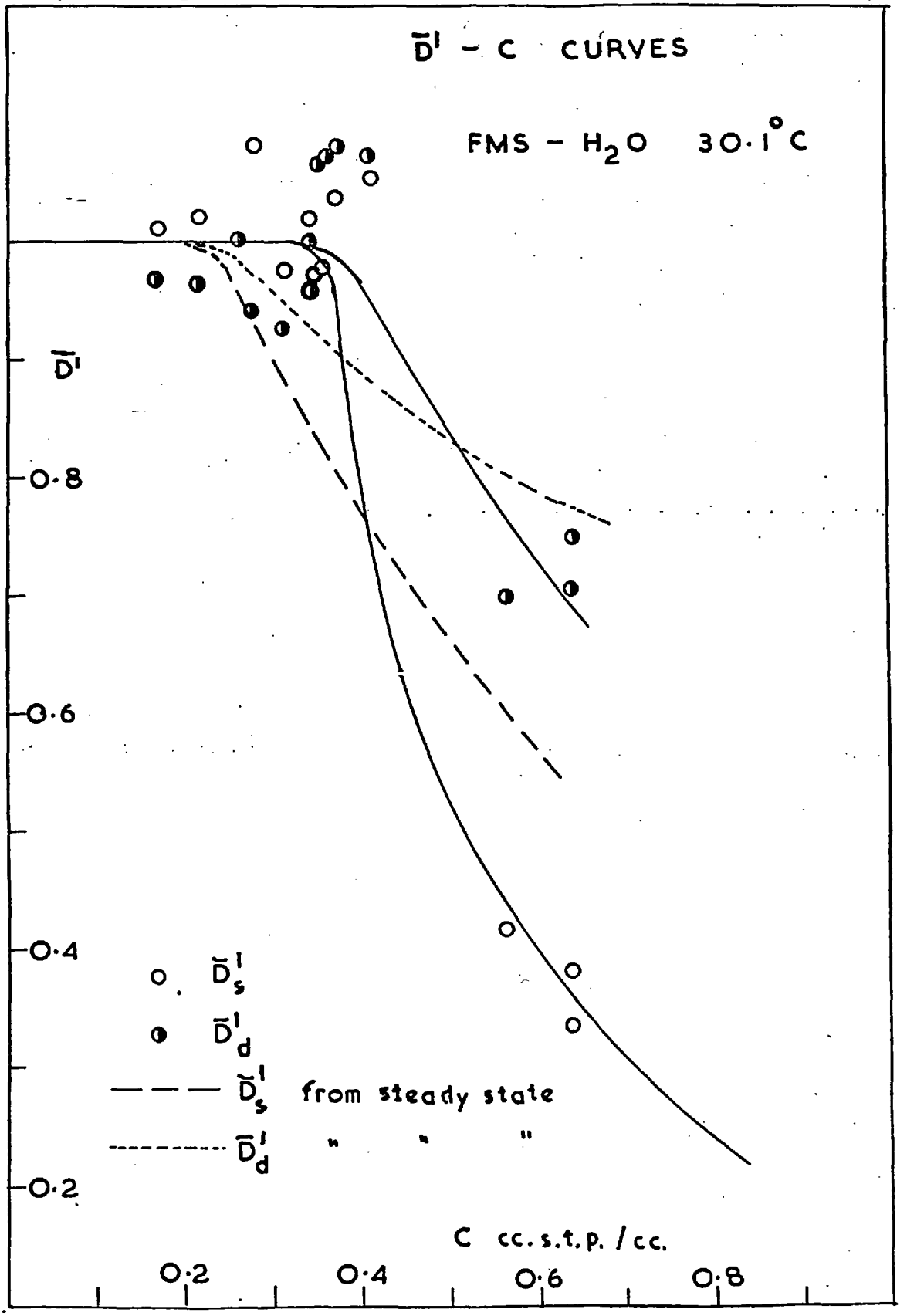
$\bar{D}^1$ – C CURVES
FMS – H_2O 30·1°C
$\bar{D}^1$
0·8
0·6
0·4
0·2
$\bar{D}^1_s$
$\bar{D}^1_d$
$\bar{D}^1_s$ from steady state
$\bar{D}^1_d$ " " "
C cc. s.t.p. / cc.
0·2
0·4
0·6
0·8

FIG. 7·19

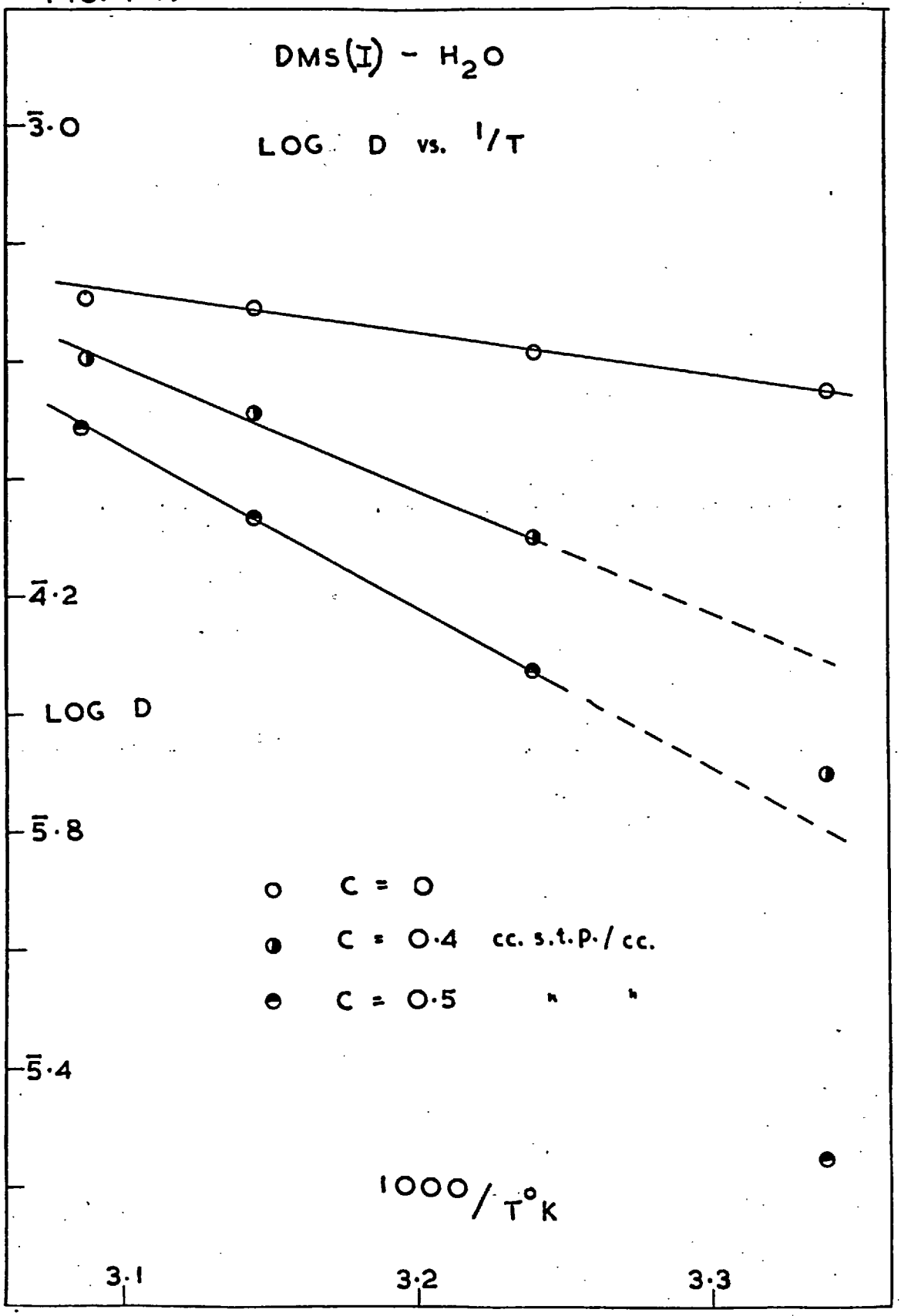
DMS(I) - H_2O
LOG D vs. 1/T
$\bar{3}\cdot0$
$\bar{4}\cdot2$
LOG D
$\bar{5}\cdot8$
$\bar{5}\cdot4$
C = 0
C = 0·4 cc. s.t.p./cc.
C = 0·5 " "
1000/T°K
3·1
3·2
3·3

FIG. 7·20

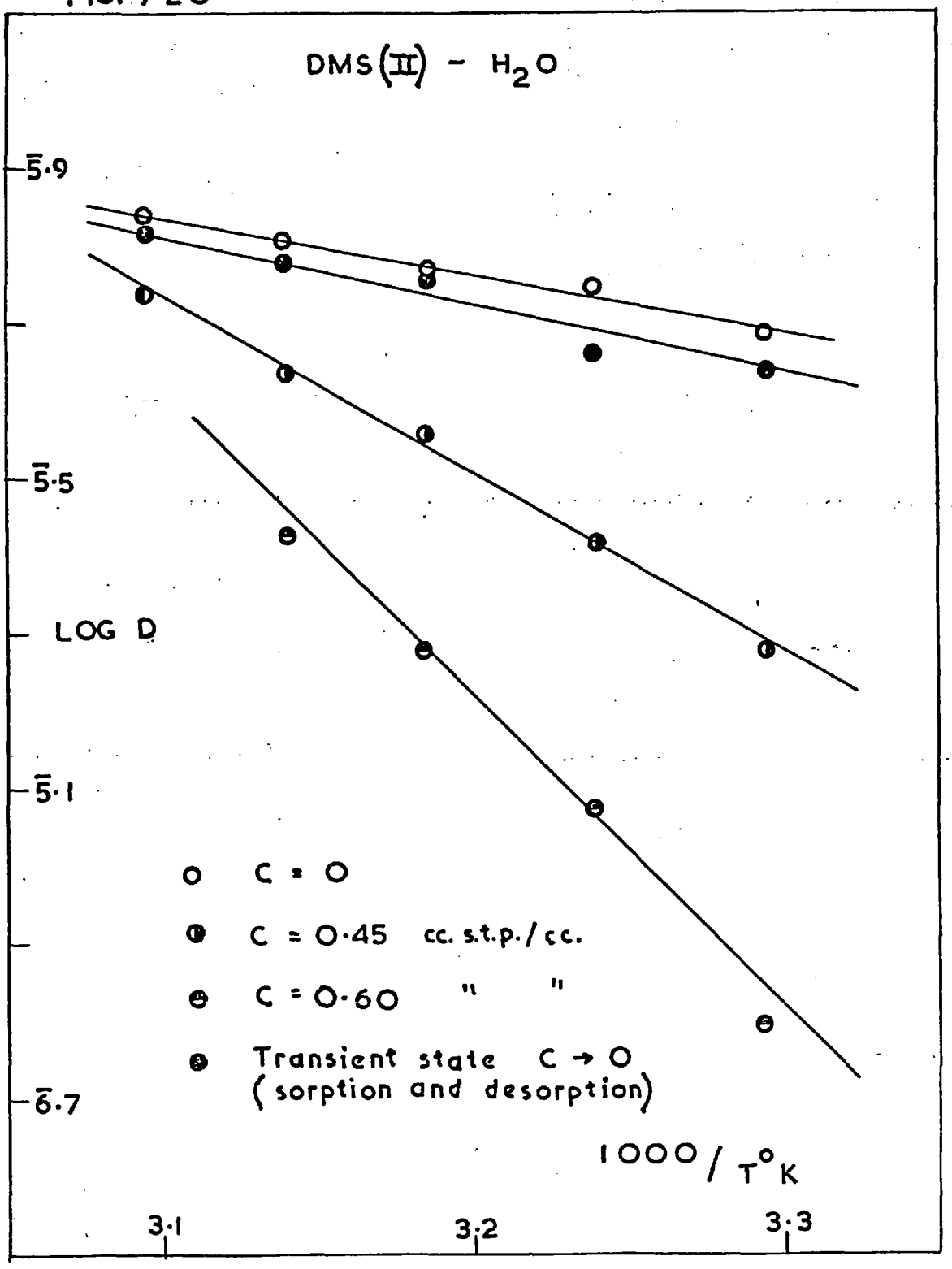
DMS (II) - H_2O
$\bar{5}\cdot9$
$\bar{5}\cdot5$
$\bar{5}\cdot1$
$\bar{6}\cdot7$
LOG D
C = O
C = 0·45 cc. s.t.p./cc.
C = 0·60 " "
Transient state C → O
(sorption and desorption)
1000 / T°K
3·1
3·2
3·3

FIG. 7·21

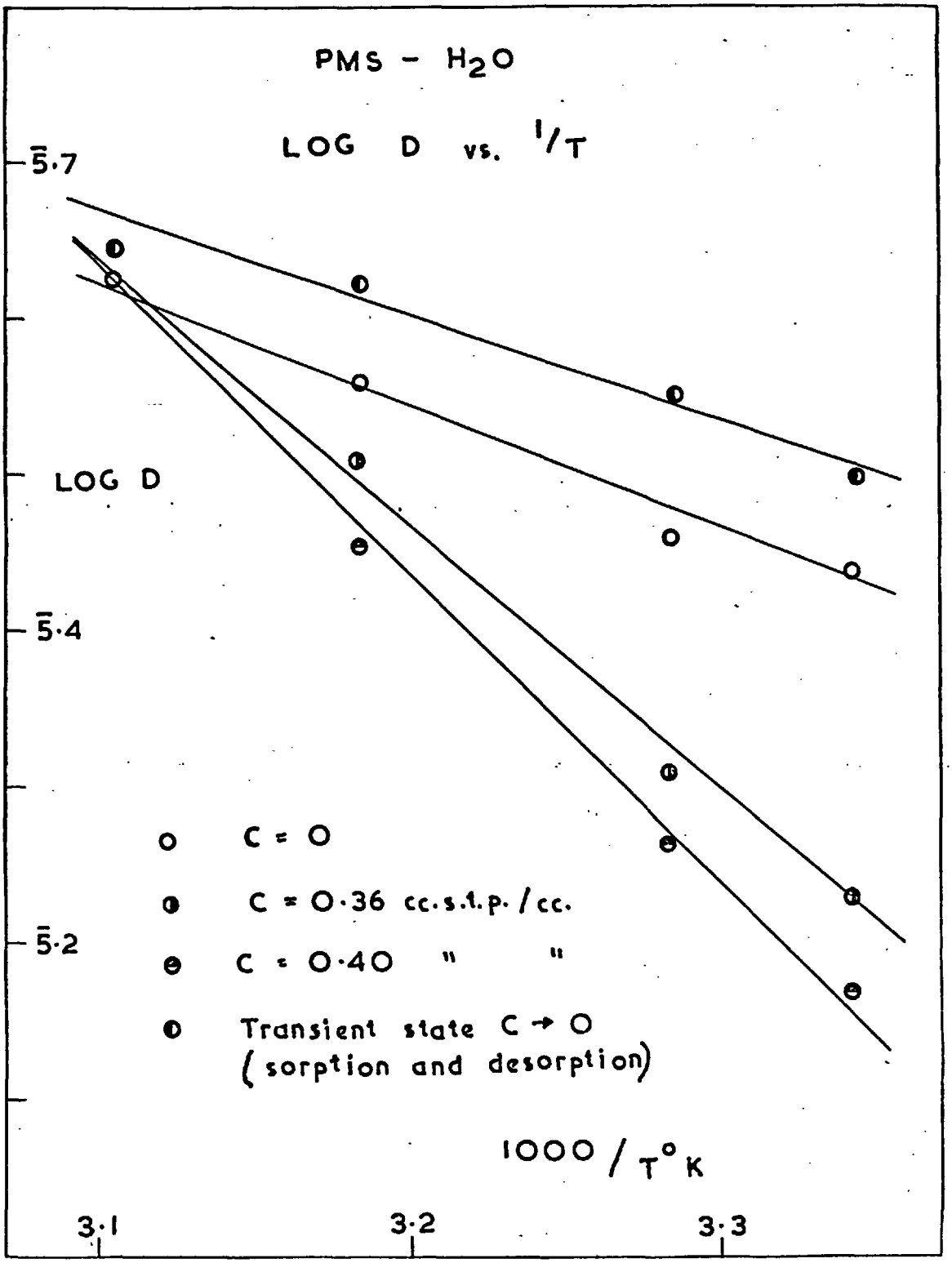
PMS - H_2O
LOG D vs. $^1/_T$
$\bar{5}\cdot7$
LOG D
$\bar{5}\cdot4$
$\bar{5}\cdot2$
C = O
C = O·36 cc.s.t.p./cc.
C = O·40 " "
Transient state C → O
(sorption and desorption)
1000 / T°K
3·1
3·2
3·3

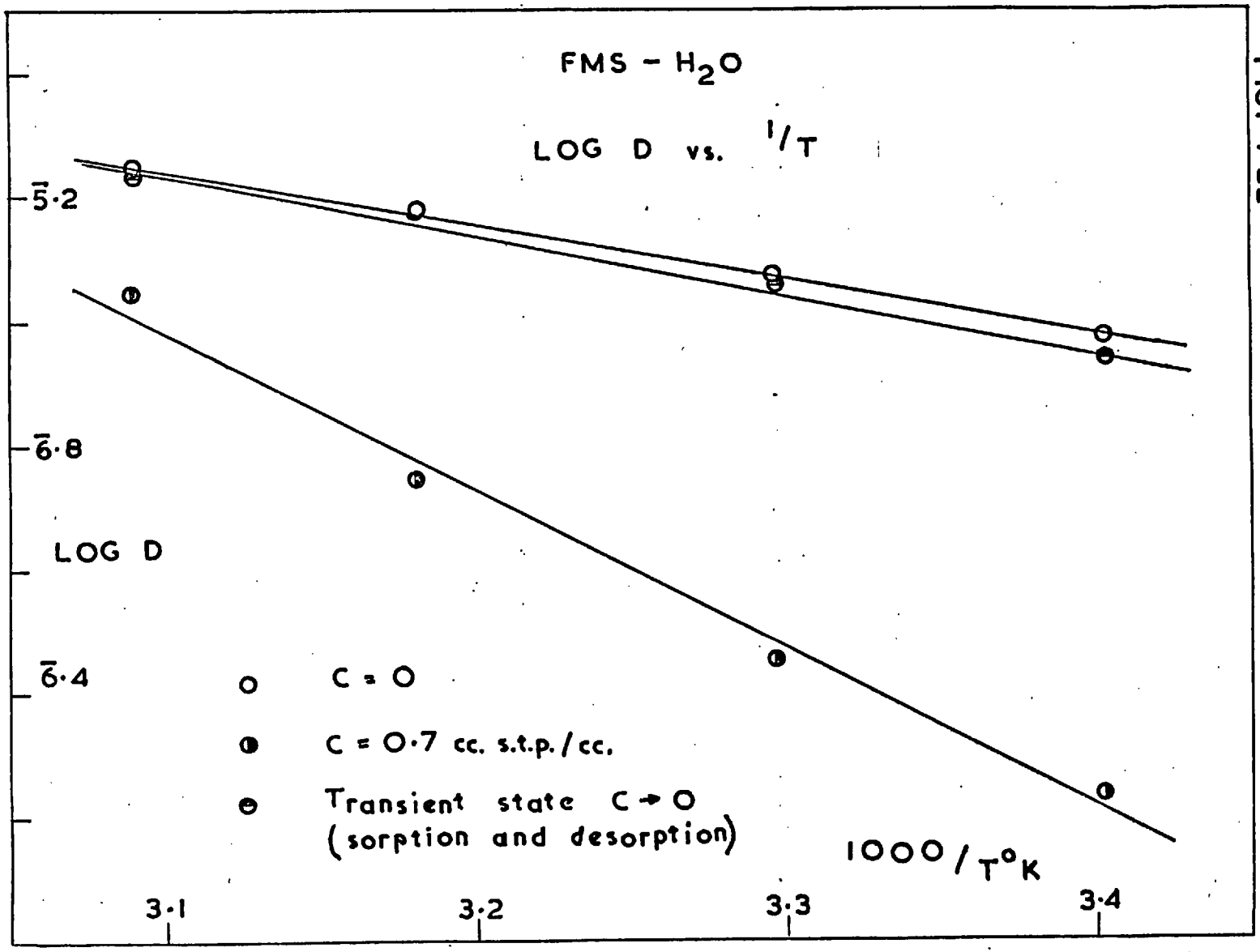
FMS - H_2O
LOG D vs. $^1/_T$
$\bar{5}\cdot2$
$\bar{6}\cdot8$
LOG D
$\bar{6}\cdot4$
C = O
C = O·7 cc. s.t.p./cc.
Transient state C → O
(sorption and desorption)
1000 / T°K
3·1
3·2
3·3
3·4

FIG. 7.22

E_D calculated from the steady state results are given in Table 7-11 and from the transient state results in Table 7-12. Results were not obtained over a sufficiently wide temperature range to calculate accurate values for D_o.

TABLE 7-11

Values of E_D (kcal.mole^{-1}) from the Steady State

System	Temperature Range	c cc.stp cm^{-3}	E_D	Theoretical E_D (polycondensation model)	
				$\Delta H = 6.6$	$\Delta H = 3.4$
DMS (I)		0	3.1	3.1	3.1
-H_2O	25 - 50°C	0.4	8.6	8.9	7.3
"		0.5	13	10.1	8.3
DMS (II)		0	3.4	3.4	3.4
-H_2O	30 - 50°C	0.45	11	8.2	8.2
"		0.6	18	12.3	9.6
PMS-		0	3.8	3.8	3.8
H_2O	25 - 50°C	0.36	7.8	9.6	8.0
"		0.4	9.4	10.1	8.5
FMS		0	4.0	4.0	4.0
-H_2O	20 - 50°C	0.7	12	9.4	8.3
FMS-		0	6	-	-
MeOH	30-- 40°C	4	7	-	-
"		8	9	-	-

TABLE 7-12

Values of E_D (kcal.mole^{-1}) from the Transient State (small c)

System	E_D
DMS (II)-H_2O	3.9
PMS-H_2O	3.0
FMS-H_2O	4.5

i) Values of E_D at c=0

For water at c=0, E_D increases in the order

$$DMS < PMS < FMS$$

which is consistent with the order of increasing hindrance to segmental motion due to bulky side groups in the polymer.

If water is compared with small permanent gas penetrants in DMS[9] then E_D is slightly higher than the value found for krypton, which is in accordance with the relative diameter of the water molecule. The higher E_D observed for methanol compared with water in FMS can be attributed to the larger molecular diameter of methanol.

Values for E_D calculated from the transient state are fairly consistent with the corresponding steady state values in view of the limited accuracy of the former. The scatter involved in plots of log $\bar{D}_{AV}$ vs. 1/T for small c is illustrated in Figures 7-20 to 7-22.

ii) Concentration Dependence of E_D

In the linear regions of the sorption isotherms E_D is constant, whereas at higher values of c E_D increases with increasing c in qualitative accord with clustering theories. The observed values of E_D for water are compared in Table 7-11 with theoretical values calculated from the

random polycondensation model. As expected, the agreement is poor. In general the observed values increase more markedly than do the theoretical values, illustrating the relatively strong tendency at higher relative humidities for water to cluster in these systems.

B SODIUM CHLORIDE - FILLED SAMPLES OF DMS.

In order to interpret more fully the sorption results for water in the samples of filled polymer, a few measurements were made of water sorption by pure NaCl.

7.4 Water Sorption by pure NaCl.

Measured concentrations of water sorbed by finely ground crystals of NaCl at relative humidities below 0.65 are given in Table 7-13. Their order of magnitude is such that they were just detectable with the Sartorius balance, i.e. $\sim$ 1-5 μg. for a 0.5 g. sample of NaCl. The negative value obtained reveals a small uncertainty ($\sim$1 μg.) in the magnitude of the blank correction (section 5.2.3). As the errors involved in measuring these small uptakes of water probably exceeded $\sim$ 100% of their absolute values, the shape of a sorption isotherm could not be established.

The quantity of water sorbed by NaCl presumably depends on the available surface area presented by the NaCl crystals and on the number of defects or cracks present in the crystal structure, since these would constitute the most likely "sites" at which sorption would take place. Although the crystals used were finely crushed with a pestle and mortar, the mixing of the salt with DMS involved the use

of a fine mill so that the state of subdivision of the salt was probably somewhat higher when incorporated into the rubber.

TABLE 7-13

Concentration c (cc.s.t.p. cm^{-3}) of Water sorbed by NaCl, Water Activity $\leq$ 0.65

Sample at 35.7°C		Sample at 44.4°C	
Relative Humidity (p/p_o)	c x 10^3	Relative Humidity (p/p_o)	c x 10^3
0.21	3	0.11	0
0.27	0	0.15	-0.5
0.34	4	0.20	1
0.44	7	0.25	3
0.55	5	0.33	6
0.62	5	0.42	10
		0.52	16
		0.58	11

At 30-50°C and for water activities above 0.73-0.75, NaCl dissolves in water. A "sorption isotherm", which is approximately independent of temperature in the range of interest here, was obtained from standard thermodynamic tables[144] for aqueous NaCl solutions and is shown in Figure 7-23.

At relative humidities between 0.65 and 0.75 a few sorption measurements were made with the quartz spiral balance.

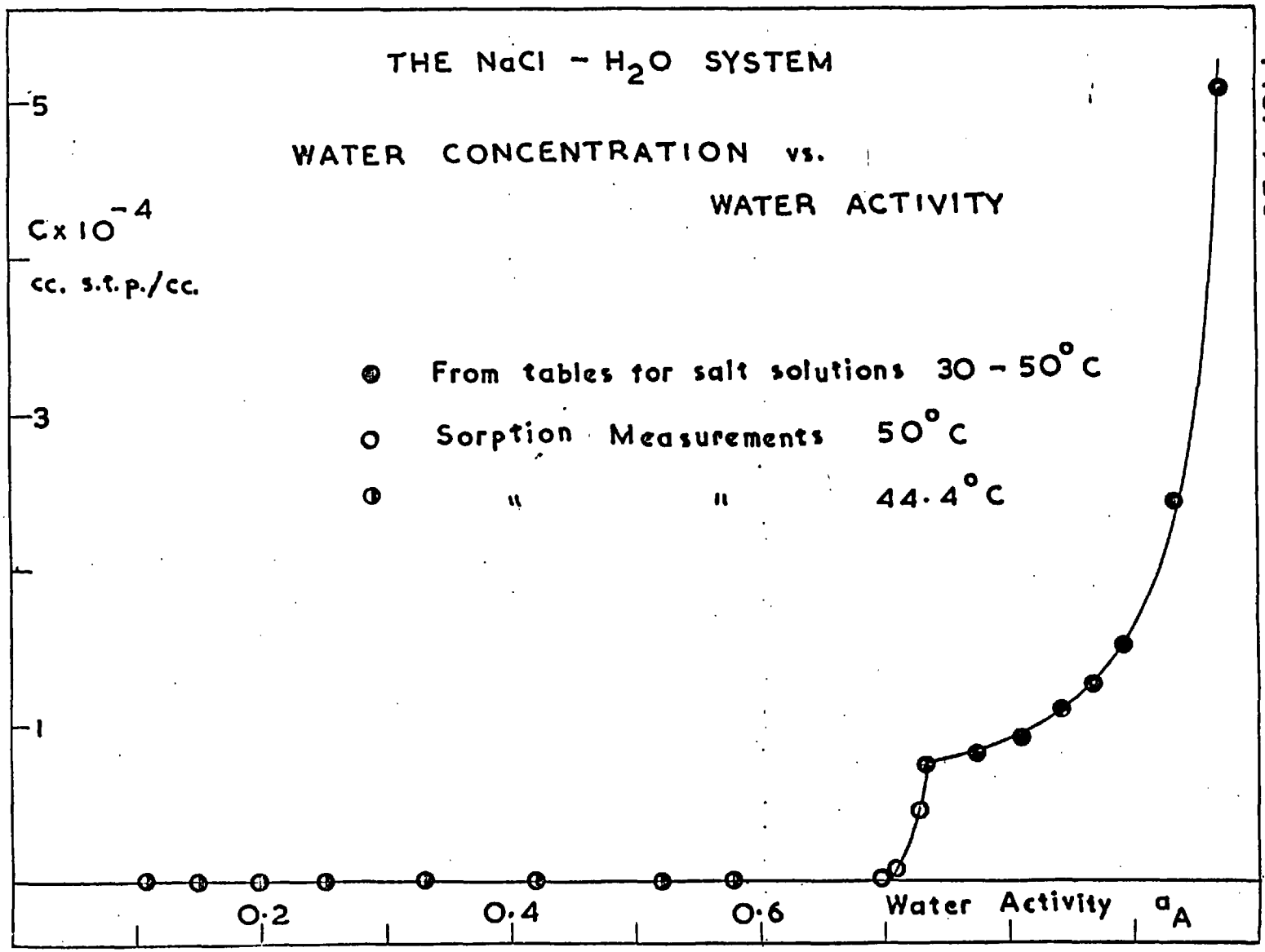
THE NaCl - H_2O SYSTEM
WATER CONCENTRATION vs.
WATER ACTIVITY
$C \times 10^{-4}$
cc. s.t.p./cc.
5
3
1
From tables for salt solutions 30 - 50° C
Sorption Measurements 50° C
" " 44.4° C
0·2
0·4
0·6
Water Activity a_A

FIG. 7.23

These are given in Table 7-14 and are intermediate between those given in Table 7-13 and the values taken from the tables for NaCl solutions. The NaCl-H_2O system over the whole range of water activity (0-1.0) is illustrated in Figure 7-23, which reveals the rapid increase in water concentration from virtually dry salt at a water activity of $\sim$ 0.70 to a saturated aqueous solution of salt at a water activity of $\sim$0.73.**

TABLE 7-14

Concentration c (cc.s.t.p.cm^{-3}.) of Water sorbed by NaCl at 49.9°C, 0.65 $<$ Water Activity $<$ 0.75.

Relative Humidity (p/p_o)	c
0.70	61
0.71	370
0.73	4500

7.5 Equilibrium Sorption Results

Samples A, B and C of DMS contain 0.44, 1.32 and 4.19% by weight respectively of NaCl.

7.5.1 Sorption in the range 0- $\sim$ 0.75 Relative Humidity

Equilibrium sorption isotherms for water in samples A, B and C of DMS and in the unfilled sample I are shown in

**Footnote This point was first brought to the author's notice during a discussion with Mr. A. G. Thomas and Mr. E. Southern of the Natural Rubber Producers Research Association.

Figure 7-24. The primary measurements from which these isotherms were constructed are presented in appendix 9.6.

Below $\sim$0.65 relative humidity very little difference is observed between the isotherms for the filled and unfilled samples of DMS. This is consistent with the fact that the salt filler sorbs such small quantities of water in this range. Between $\sim$0.65 and $\sim$0.75 relative humidity the filled samples sorb slightly more water than the unfilled so that the isotherms for the former exhibit more pronounced curvature in this range.

Values of $\sigma_{c=0}$ for water in samples A, B and C at $\sim 35^{\circ}C$ and $\sim 50^{\circ}C$ are compared in Table 7-15 with the corresponding values in the unfilled samples I and III.

TABLE 7-15

Values of $\sigma_{c=0}$ (cc.s.t.p. $cm.^{-3}$ $(cmHg)^{-1}$) for Water in Unfilled and Salt-Filled DMS

Sample of DMS	Temperature $^{\circ}C$	$\sigma_{c=0}$
I	35.4	1.04
I	50.7	0.73
III	30.3	1.36
III	50.0	0.70
A	35.2	1.12
A	50.0	0.71
B	35.7	1.06
B	50.8	0.70
C	35.6	1.13

FIG. 7·24

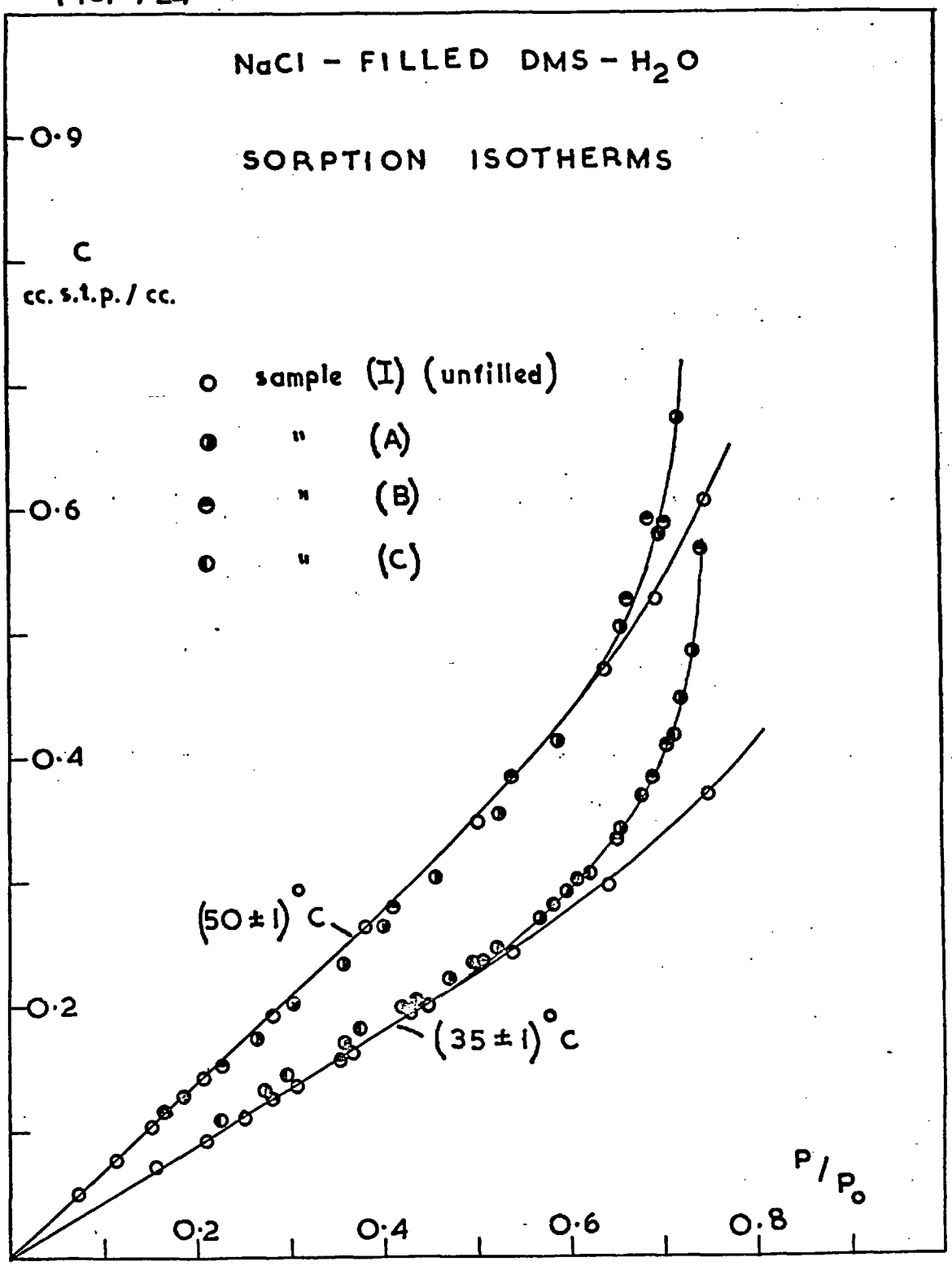
NaCl - FILLED DMS - H_2O
SORPTION ISOTHERMS
C
cc. s.t.p. / cc.
0·9
0·6
0·4
0·2
o sample (I) (unfilled)
● " (A)
● " (B)
● " (C)
(50 ± 1)° C
(35 ± 1)° C
0·2
0·4
0·6
0·8
P / Po

7.5.2 Sorption in the range ~0.75 - 1.0 Relative Humidity

In this region uptakes of water by samples, A, B and C are considerably greater than for any other system studied in this investigation. Although a few isotherm measurements were made using the vacuum microbalances, in general it was found to be more convenient to immerse weighed samples of filled polymer in aqueous NaCl solutions of known water activity[144]. After immersion for a week there was usually little further change in weight, even so samples were left for about a month to ensure that equilibrium was, in fact, attained. In addition, measurements were made on samples crosslinked to different extents by exposure for different lengths of time to the Co^{60} source. These samples were compared to examine the effect of changes in crosslink density on water sorption.

Results, expressed both as water concentrations and as percentage uptakes of water relative to the weight of the dry, filled polymer, are given in Table 7-16. The principal features are :

a) Results obtained using the vacuum balances are fairly consistent with those obtained from the immersion measurements.

TABLE 7-16

Uptakes of Water by Salt-Filled DMS above ~ 0.75 Relative Humidity

Sample	Time of Exposure to Co^{60} Source	Temperature °C	Water Activity (Relative Humidity) a_A	Concentration of sorbed water cc.stp.cm^{-3}	Weight % water uptake
A	30h.	20	0.75	3	0.2
"	"	"	0.845	22	1.7
"	"	"	0.95	58	4.6
"	"	"	1.0	740	57
"	90h.	"	0.75	15	1.2
"	"	"	0.845	22	1.7
"	"	"	0.95	55	4.3
"	"	"	1.0	160	12
B	30h.	20	0.75	4	0.3
"	"	"	0.845	62	4.9
"	"	"	0.95	150	12
"	"	"	1.0	1000	78
"	"	35	0.77	2.5*	0.2*
"	"	"	0.81	19*	1.5*
"	90h.	20	0.75	19	1.5
"	"	"	0.83	65	5.1
"	"	"	0.95	130	10
"	"	"	1.0	140	11
C	30h.	20	0.845	210	16
"	"	"	0.95	530	42
"	"	35	0.81	46*	3.6*
"	"	"	0.87	140	11*
"	"	50	(0.67)	(3.5**)	(0.3**)
"	"	"	(0.72)	(6.7**)	(0.5**)
"	"	"	0.75	11**	0.8**
"	60h.	35	0.82	83**	6.5**
"	"	"	0.85	190**	15**

* Denotes Sartorius balance measurement.
** Denotes quartz spiral measurement.

b) For the most lightly crosslinked (~30h. exposure to the Co^{60} source) samples, uptakes of water for activities of water below unity are approximately proportional to the salt content of the sample.

c) For the most heavily crosslinked (~90h. exposure to the Co^{60} source) samples, uptakes of water for activities of water below unity are similar to those in the more lightly crosslinked samples, with the exception of the largest uptake (sample B, a_A = 0.95) which is somewhat less for the former samples.

d) Uptakes of water at unit water activity are reduced by factors of 5-8 when the time of exposure of the sample to the Co^{60} source is increased from ~30h. to ~90h.

e) The ratio of sorbed water concentrations corresponding to water activities of 0.95 and 0.845 respectively is approximately constant at ~2.5 for each sample. This value is low compared with the ratio (~3.1) of the amounts of water present per unit amount of salt for aqueous NaCl solutions at the same two water activities[144].

The above features indicate that for water activities of less than unity, water uptakes at equilibrium depend chiefly on the salt content rather than on the crosslink density of the sample, until either reaches some critical value above which both variables become significant. At unit water activity, both the salt content and the crosslink density would seem to be important. However, the quantitative effect on water sorption of variations in the crosslink density of the sample is not readily ascertained because of uncertainties in the exact does of γ-radiation received by each sample. Moreover, the possibility that a proportion of the salt diffuses out of the polymer and lowers the external water activity cannot be ruled out with certainty.

The above results are consistent with a sorption mechanism in which water diffuses into the rubber to dilute internal "pockets" of salt solution. In a sense this is a similar situation to the clustering of sorbed water molecules observed for the unfilled rubbers in that relatively high local concentrations of water are created inside the rubber. Equilibrium is attained when the internal and external water activities are equal, or when the driving force for sorption is equalised by the retractive force exerted by the polymer network.

To test whether the polymer network does influence water sorption in the most lightly crosslinked samples below unit activity of water, the observed percentage uptakes of water are compared in Table 7-17 with those expected from the amounts of salt present[144], assuming no network effects.

TABLE 7-17

Theoretical and Observed Uptakes of Water by Salt-Filled DMS (~30h. exposure to Co^{60} source).

Water Activity	Percentage NaCl in sample.	Theoretical % Uptake of Water (no effect of network)	Observed % Uptake of water
0.845	0.44	1.8	1.7
0.95	"	5.5	4.6
0.845	1.32	5.4	4.9
0.95	"	17	12
0.845	4.19	17	16
0.95	"	53	42

Only for the smallest equilibrium uptake is good agreement obtained between theory and experiment. As the salt content or the water activity is increased, the observed uptakes fall increasingly short of the theoretical values indicating that the polymer network does exert a significant pressure on the internal pockets of salt solution. This observation is further supported by a comparison of the

increases in water activity and in the salt content of the polymer sample which yield the same theoretical increase in uptake from that of the lowest uptake (Table 7-17). The discrepancy between theory and experiment is greater for the increase in water activity than for the increase in salt content. This behaviour can be attributed to the fact that in the former case, where the number of internal "pockets" of salt solution is smaller, the polymer network immediately surrounding the pockets of solution would need to be disturbed to a greater extent than in the latter case to accommodate the same overall amount of sorbed water.

7.6 Steady State Permeability Results

Within the experimental error, permeation rates increase linearly with pressure over the whole range in relative humidity. Values of P are therefore constant and are compared in Table 7-18 with values of P for water in unfilled DMS. The observed linearity of J_ℓ with pressure is illustrated in Figure 7-25.

Values of P differ but little from the corresponding values in unfilled DMS. This is to be expected at low relative humidities since the incorporated salt particles sorb little water in this region and are not present in

FIG. 7·25

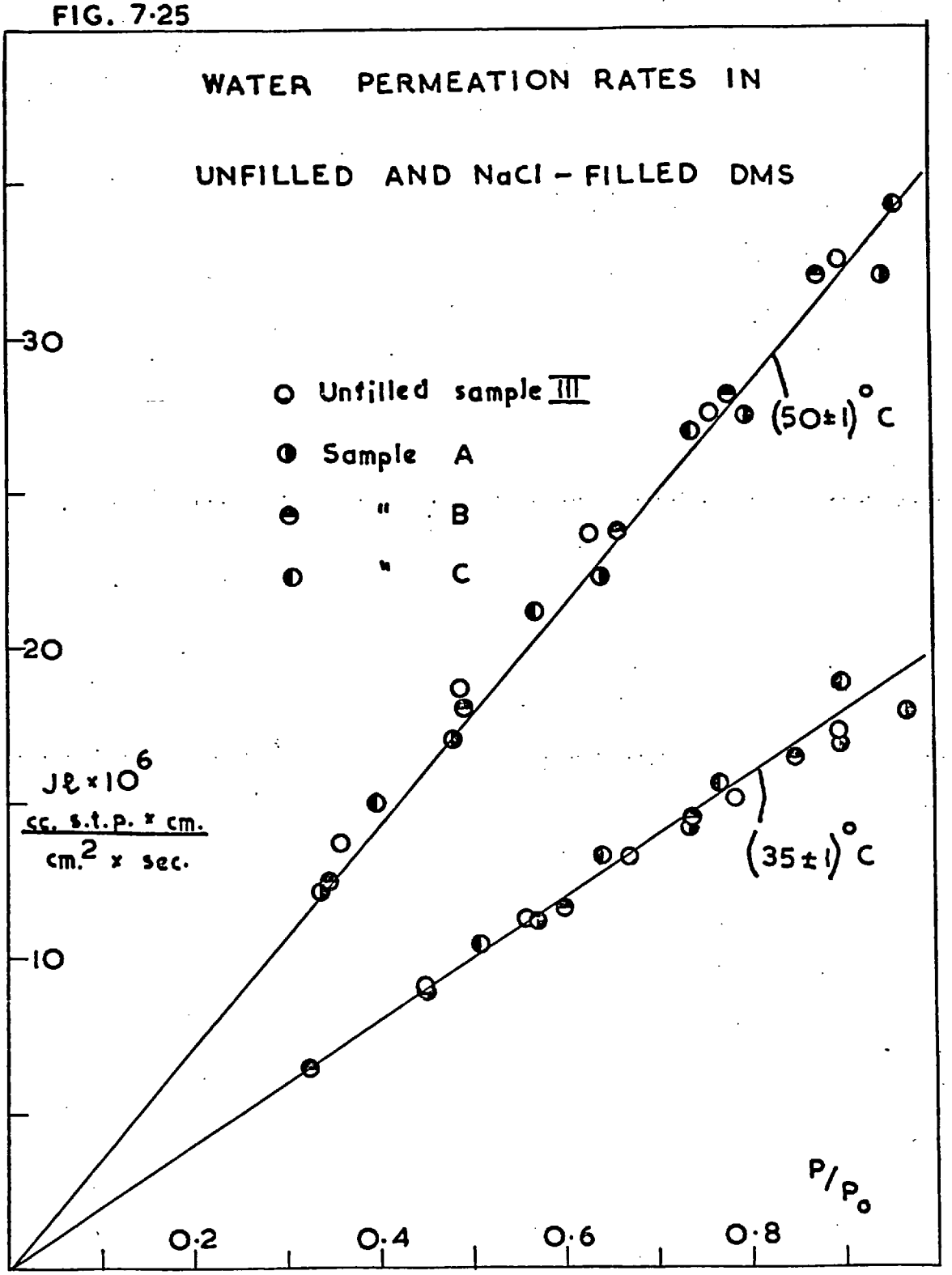
WATER PERMEATION RATES IN
UNFILLED AND NaCl - FILLED DMS
Unfilled sample III
Sample A
" B
" C
(50±1)° C
(35±1)° C
30
20
10
$J\ell \times 10^6$
cc. s.t.p. × cm.
cm.² × sec.
0·2
0·4
0·6
0·8
P/P₀

sufficient amount to increase appreciably the tortuosity of the diffusion paths through the polymer. Above ~ 0.75 relative humidity it appears surprising at first sight that J_1 should remain the same linear function of p/p_o since such large quantities of water are present that the membrane must swell. However the sorbed water does not swell the rubber in the same sense as would a penetrant which were a solvent for the rubber since the water remains associated with the salt.* In fact the water present in the pockets of salt solution can be regarded as being equivalent to clustered water, where the "clusters" are very large compared with those which form in the unfilled rubber.

TABLE 7-18

Permeability Coefficients P (cc.s.t.p.cm. $cm.^{-2}$ $sec.^{-1}$ $(cmHg)^{-1}$) For Water in Unfilled and Salt-Filled DMS

Sample of DMS	Temperature °C	P x 10^6
III	35.8	4.59
III	49.8	4.12
A	35.5	4.69
A	49.8	4.08
B	35.9	4.52
B	49.7	4.15
C	35.7	4.69
C	50.0	4.15

*Footnote: The author wishes to acknowledge the particularly helpful discussion of this point with Mr. A. G. Thomas and Mr. E. Southern.

Daynes[101] proposed that for rubbers containing water-soluble material, the diffusion of water is controlled by a gradient of osmotic pressure. The difference in the osmotic pressures of two solutions is proportional to the difference in the relative vapour pressures which would be in equilibrium with the two solutions so that

$$\partial c/\partial t = D^{\neq} \cdot \frac{\partial^2 (p/p_o)}{\partial x^2} \qquad \ldots.(7-4)$$

would then replace Fick's second law, where $D^{\neq}$ is a constant depending on the rubber. Equation (7-4) leads in fact to a linear $J\ell - p/p_o$ dependence since

$$J = -D^{\neq} \frac{\partial (p/p_o)}{\partial x} \qquad \ldots.(7-5)$$

Equation (7-5) applies above $\sim$ 0.75 relative humidity. At lower relative humidities, assuming diffusion of monomeric water only, $J = -D_1 \cdot \partial c_1/\partial x$ which can be re-written as

$$J = -D_1 \sigma_1 p_o \cdot \frac{\partial (p/p_o)}{\partial x} \qquad \ldots.(7-6)$$

if it is further assumed that the sorption of monomeric water follows Henry's law. Since the experimental results indicate that the $J\ell - p/p_o$ relation is linear over the whole range in relative humidity, the quantity $D^{\neq}$ for water in these salt-filled samples of DMS is given from equations (7-5)

and (7-6) by

$$D^{\neq} = D_1 \sigma_1 p_o \qquad \ldots\ldots(7\text{-}7\ ).$$

7.7 Diffusion Coefficients

Below ~0.7 relative humidity, diffusion coefficients for water calculated both from the steady state and from sorption rate measurements are compared in Table 7-19 with the corresponding values for water in unfilled DMS. The differences between the values of D in the salt-filled and unfilled samples are very small.

TABLE 7-19

Diffusion Coefficients D ($cm.^2$ $sec.^{-1}$) for Water in Unfilled and Salt-Filled DMS at low Relative Humidity

Sample of DMS	Temperature °C	Steady State $D \times 10^5$	Temperature °C	Transient State $D \times 10^5$
I	35.4	4.1	26.3	3.8
I	50.7	5.2	50.7	5.0
III	30.3	4.4	-	-
III	50.0	5.9	-	-
A	35.2	4.3	35.5	3.9
A	50.0	5.7	50.7	4.8
B	35.7	4.3	-	-
B	50.8	5.6	-	-
C	35.6	4.2	-	-

Above $\sim$ 0.75 relative humidity, D decreases extremely rapidly with increasing c. In this region the transport process depends both on the diffusion of water through the bulk rubber phase and on the equilibrium between water in the rubber and the pockets of salt solution. A reduced sorption curve measured at 35.6°C and for p/p_o = 0.81 for water in sample C is virtually linear initially, as shown in Figure 7-26, indicating that the system can be described by some sort of average diffusion coefficient. The curve yields $\bar{D}_s = \sim 7 \times 10^{-8}$ cm.^{2} sec.$^{-1}$ for c = 46 cc. s.t.p. cm.$^{-3}$. This value represents a decrease of almost three orders of magnitude from $D_{c=0}$. An approximate steady state analysis at the same value of c yields for the differential diffusion coefficient, $D(c) = \sim 2 \times 10^{-8}$ cm.^{2} sec.$^{-1}$. This value is at least in semiquantitative accord with that expected from the value of $\bar{D}_s$ since the latter would be expected to decrease by a factor less than the decrease in the differential D.

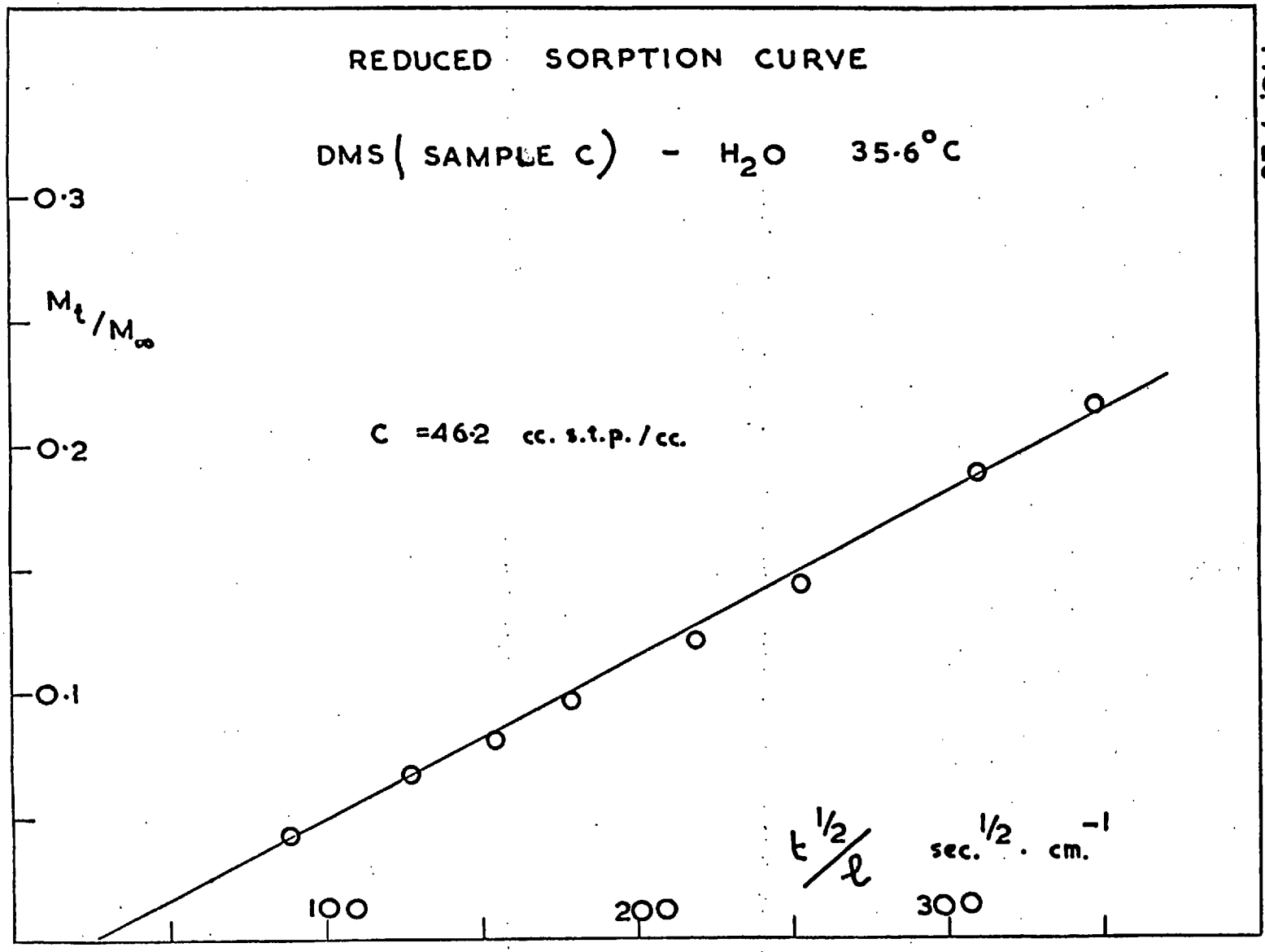
REDUCED SORPTION CURVE
DMS (SAMPLE C) - H_2O 35·6°C
0·3
M_t/M_∞
0·2
C =46·2 cc. s.t.p./cc.
0·1
100
200
300
$t^{1/2}/\ell$ sec.$^{1/2}$. cm.$^{-1}$

FIG. 7·26

C SILICA-FILLED SAMPLES OF DMS

7.8 Water Sorption by the Silica Filler

Difficulty was experienced in obtaining reproducible equilibrium sorption isotherms for water in the pure Aerosil. At first, water uptakes for a given relative humidity decreased with each successive isotherm determination regardless of the temperature of the sample. Eventually, after about seven or eight complete isotherm sorption-desorption cycles, more settled isotherms were obtained. However the scatter in the experimental points was still too great to establish with any certainty whether the sorbed water concentration for a given relative humidity increases or decreases with increasing temperature. These isotherms are illustrated in Figure 7-27 and appear to be of the BET type II classification with very slight "knees" at low relative humidities.

The variation in water uptake with the number of isotherm determinations is possibly associated with progressive aggregation of the very fine particles of silica. Presumably for the earlier isotherms the silica was still relatively loosely packed allowing more scope for inter-particle capillary condensation. Increasing the

FIG. 7·27

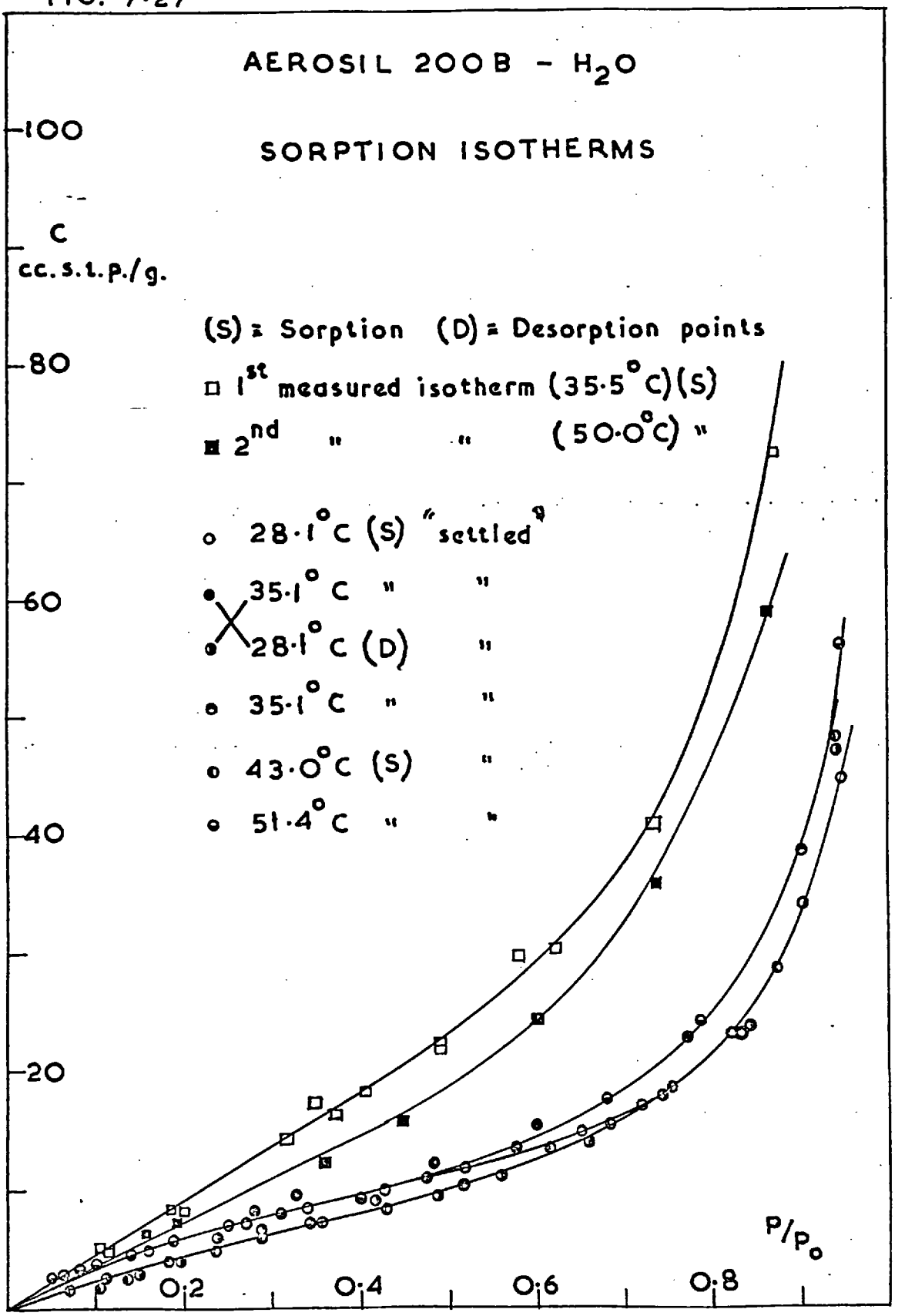
AEROSIL 200B - H_2O
SORPTION ISOTHERMS
100
C
cc.s.t.p./g.
80
60
40
20
(S) = Sorption (D) = Desorption points
□ 1st measured isotherm (35·5°C)(S)
■ 2nd " " (50·0°C) "
o 28·1°C (S) "settled"
• 35·1°C " "
28·1°C (D) "
o 35·1°C " "
o 43·0°C (S) "
o 51·4°C " "
P/Po
0·2
0·4
0·6
0·8

temperature of outgassing from room temperature up to $\sim 60^{\circ}C$ did not appear to have any marked influence on water sorption. In general the weights of the sample of Aerosil before and after an isotherm determination agreed to within 1-2% of the largest uptake of water observed for that isotherm. Hence the observed variations in uptake do not appear to have been caused by water being irreversibly sorbed on particularly active surface sites of the silica.

The Aerosil is porous and its bulk density is not readily determined with any precision, so that water concentrations in Figure 7-27 are expressed in cc.s.t.p. $g.^{-1}$. The conventional specific gravity bottle procedure yielded for the bulk density of the Aerosil,

$$\rho = 1.16,\ 1.10 \text{ g. cm.}^{-3} \text{ using water}$$

and $$\rho = 1.53,\ 1.53 \text{ g. cm}^{-3} \text{ using liquid paraffin.}$$

To explain the higher latter two values it is assumed that the degree of dispersion of the Aerosil particles was greater in the hydrocarbon than in water.

7.9 Equilibrium Sorption Results

Samples D, E and F contain 20, 30 and 40% by weight respectively of Aerosil. Equilibrium sorption isotherms for water in these samples are illustrated in

Figures 7-28 and 7-29. The experimental data used for their construction are presented in appendix 9.6.

"Integral" sorption experiments were carried out. For the first experimentally determined isotherm point the amount of water sorbed exceeded that which was desorbed again, i.e. a proportion of the water was apparently irreversibly sorbed. For the subsequent isotherm points, the difference between corresponding amounts of water sorbed and desorbed did not exceed $\sim 2\%$ of the total amounts sorbed.

7.9.1 Magnitudes of Water Sorption

The isotherms exhibit no linear region and, for very small c, could not be determined with sufficient accuracy to obtain values of $\sigma_{c=0}$.

Although the uptakes of water by samples D, E and F are considerably higher than the corresponding uptakes by the unfilled sample I of DMS (Figure 7-28), surprisingly little difference is observed at $\sim 35^{\circ}C$ between the samples D, E and F by themselves. A possible reason for this lies in the method of manufacture of the filled polymer sheets (J. Ross, Midland Silicones Ltd., private communication). The procedure yields two forms of Aerosil filler inside the polymer. One form is bound very strongly, through its surface

FIG. 7·28

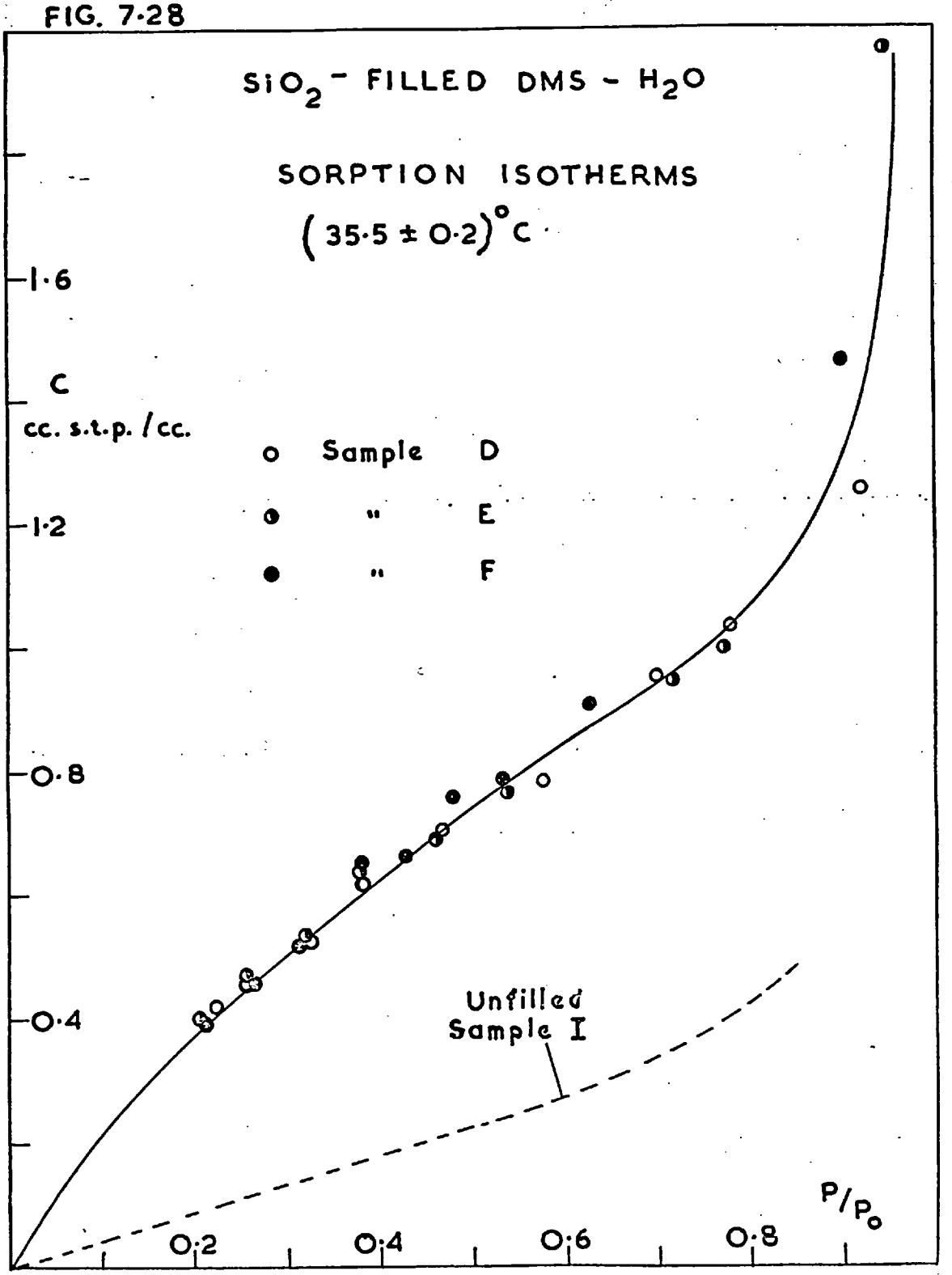
SiO2 - FILLED DMS - H2O
SORPTION ISOTHERMS
(35·5 ± 0·2)°C
C
cc. s.t.p. / cc.
Sample D
" E
" F
1·6
1·2
0·8
0·4
Unfilled
Sample I
0·2
0·4
0·6
0·8
P/Po

FIG. 7·29

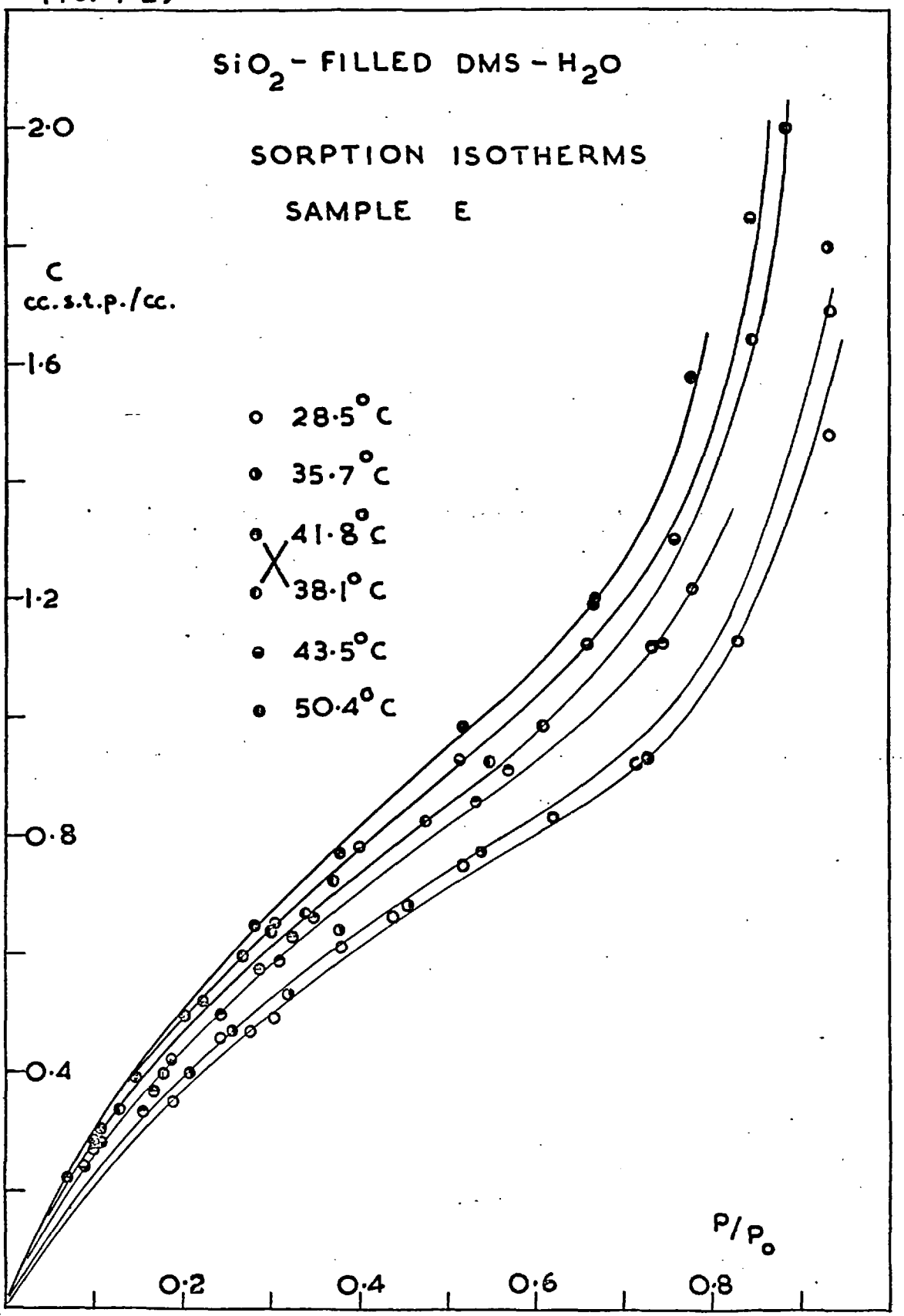
SiO2 - FILLED DMS - H2O
SORPTION ISOTHERMS
SAMPLE E
C
cc.s.t.p./cc.
2·0
1·6
1·2
0·8
0·4
28·5°C
35·7°C
41·8°C
38·1°C
43·5°C
50·4°C
P/Po
0·2
0·4
0·6
0·8

hydroxyl groups, to the polymer and the other is bound only through van der Waal's type interactions. For convenience these forms of silica are henceforth termed "bound" and "unbound" filler respectively. For optimum commercial properties of the rubbers, the unbound filler is not scaled up in the same ratio as that of the total filler but remains approximately constant. Unfortunately, no further information could be obtained regarding the exact nature of the two incorporated forms of silica or the ratio of the two forms in each sample.

If water is sorbed appreciably only by the unbound filler, then little variation in water uptake with the total filler content of the sample is to be expected. However, since the Aerosil is porous, the greater part of the internal surface of the bound silica would still be expected to be available to water, unless the entrances to the pores were blocked by polymer or unless water is contained "permanently" in the pores. That the latter may be so is suggested by the fact that a proportion of water appears to be irreversibly sorbed when a filled sample of DMS is first brought into contact with water vapour at the start of an isotherm determination. Presumably this water is desorbed again on prolonged outgassing between successive isotherm determinations.

7.9.2 Degree of Wetting of the Filler Surface

Degrees of wetting of the filler by polymer f_F, as defined by equation (3-12), were calculated for the Aerosil incorporated in samples D, E and F. Since the proportions of filler are known with accuracy only as weight fractions, the concentrations of sorbed water can be related by

$$\frac{c}{\rho} = \frac{c_B w_B}{\rho_B} + c_F w_F (1-f_F) \quad \ldots.(7\text{-}8\ )$$

where c, c_B and c_F are the concentrations of water in filled polymer (cc.s.t.p. $cm.^{-3}$) unfilled polymer (cc.s.t.p. $cm.^{-3}$) and pure filler (cc.s.t.p. $g.^{-1}$) respectively. ρ and w refer to density and weight fraction respectively. A rearrangement of equation (7-8) yields

$$f_F = 1 - \frac{c - \frac{\rho}{\rho_B} \cdot c_B w_B}{\rho c_F w_F} \quad \ldots.(7\text{-}9\ )$$

Values of f_F for the Aerosil in each sample at various relative humidities and calculated from equation (7-9) are given in Table 7-20.

The principal features are:

i) f_F increases with increasing relative humidity and sorbed water concentration.

ii) f_F increases with the overall filler content of the sample.

iii) f_F varies relatively little with temperature over the small range studied.

iv) Values for f_F are relatively high in all the samples.

TABLE 7-20

Degrees of Wetting of Aerosil Filler by DMS

Relative Humidity	f_F			
	Sample D 35°C	Sample E 35°C	Sample F 35°C	Sample E 50°C
0.1	0.67	0.77	0.84	0.85
0.2	0.71	0.80	0.85	0.84
0.3	0.73	0.82	0.86	0.83
0.4	0.75	0.83	0.87	0.83
0.5	0.77	0.85	0.88	0.84
0.6	0.80	0.87	0.90	0.86
0.7	0.83	0.89	0.91	0.88
0.8	0.86	0.91	0.92	0.88

The above features serve to illustrate the complexities involved in studies of heterophase solid systems such as filled polymers. This subject has been reviewed by Barrer[22], Holliday[145] and Corte[146] amongst others. At present there are no clear explanations of the features

listed above and it is stressed that the possibilities discussed below are purely speculative.

Three possible explanations for i) are:

a) If most of the initial water sorption were to occur on the internal surfaces of the Aerosil then the effect of the polymer blocking a proportion of the external surface sites would become increasingly important at higher water concentrations and f_F would increase with c.

b) If most of the water sorption were confined to the unbound filler and only the water sorbed on the most active sites were to disrupt van der Waal's interactions between the filler and the polymer then the polymer-filler interactions would assume increasing importance as sorption proceeded. Again therefore, f_F would increase with c.

c) If the effect of the sorbed water were to expand the aggregated structure of the filler then the physical presence of the polymer would tend to exert a greater retractive force or pressure on the filler and sorbed water at higher values of c and again f_F would increase with c.

If most of the sorption takes place on the unbound filler, the proportion of which remains approximately constant then the $\frac{\text{bound}}{\text{unbound}}$ ratio increases with the total filler content w_F and f_F would increase with w_F as observed in ii) above.

Little temperature dependence (point iii)) of f_F is perhaps to be expected over such a relatively small range. A decrease in the degree of filler-water interaction at higher temperatures would result in a smaller variation of f_F with p/p_o at higher temperatures if changes in the degree of filler-polymer interaction are neglected.

The point iv) is particularly difficult to interpret because the state of aggregation of the filler may have been appreciably different when incorporated in the polymer from that of the bulk powder. That the degree of aggregation affects the sorption of water is suggested by the variable results obtained initially for water in the pure Aerosil at various "degrees of aggregation" of the silica particles.

7.9.3 Isotherm Shapes

The isotherms are of the BET type II classification becoming convex to the pressure axis above ~ 0.6 relative humidity. This behaviour indicates that filled polymer-water

interactions are important initially with water-water interactions becoming more pronounced at higher sorbed water concentrations.

i) Clustering Functions

The clustering functions G_{AA}/v_A, $(1 + \phi_A G_{AA}/v_A)$, G_{AB}/v_A and $\phi_A G_{AB}/v_A$, henceforth termed Y, Z, Y' and Z' respectively for convenience, were calculated for water in samples D, E and F of DMS and are given in Table 7-21. At low relative humidities Y and Y' are both negative, Y becoming less negative and Y' more negative with increasing c. This behaviour indicates relatively strong filled polymer-water interactions which become less important as the sorbed water concentration is increased and is consistent with a mechanism involving the sorption of water on specific sites. Although the subscript B refers here to the filled polymer, the specific site sorption occurs almost entirely on the filler. Hence it is principally the filler-water interactions which decrease with increasing c.

At high relative humidities Y becomes positive as is illustrated by the typical plot of a_A/ϕ_A vs. a_A shown in Figure 7-30. For example, at 0.85 relative humidity Y for water in sample F at 35.5°C is +800 and Z is 1.9 indicating the strong tendency for water to cluster in this region.

TABLE 7-21

Clustering Functions for Water in Silica-Filled DMS

Sample of DMS	T°C	a_A = 0.3				a_A = 0.5			
		Y	Z	Y'	Z' x10^4	Y	Z	Y'	Z' x10^4
D	35.7	-600	0.79	-10	-3.0	-610	0.63	-22	-3.6
E	28.5	-680	0.72	-11	-2.8	-450	0.73	-24	-4.0
E	35.7	-730	0.69	-12	-2.8	-440	0.73	-25	-4.1
E	38.1	-670	0.68	-15	-3.1	-530	0.65	-29	-4.4
E	41.8	-640	0.70	-16	-3.4	-380	0.73	-35	-5.0
E	43.5	-530	0.74	-20	-4.0	-330	0.75	-41	-5.4
E	50.4	-500	0.73	-21	-3.9	-300	0.78	-44	-6.0
F	35.5	-610	0.75	-12	-3.0	-370	0.75	-29	-4.3

Sample of DMS	T°C	a_A = 0.7			
		Y	Z	Y'	Z' x10^4
D	35.7	- 57	0.93	-82	-6.7
E	28.5	-190	0.88	-43	-6.8
E	35.7	-160	0.90	-44	-7.1
E	38.1	-150	0.92	-47	-8.9
E	41.8	-120	0.89	-74	-8.1
E	43.5	-150	0.87	-74	-8.6
E	50.4	- 47	0.97	-66	-10
F	35.5	-140	0.93	-39	-7.8

FIG. 7·30

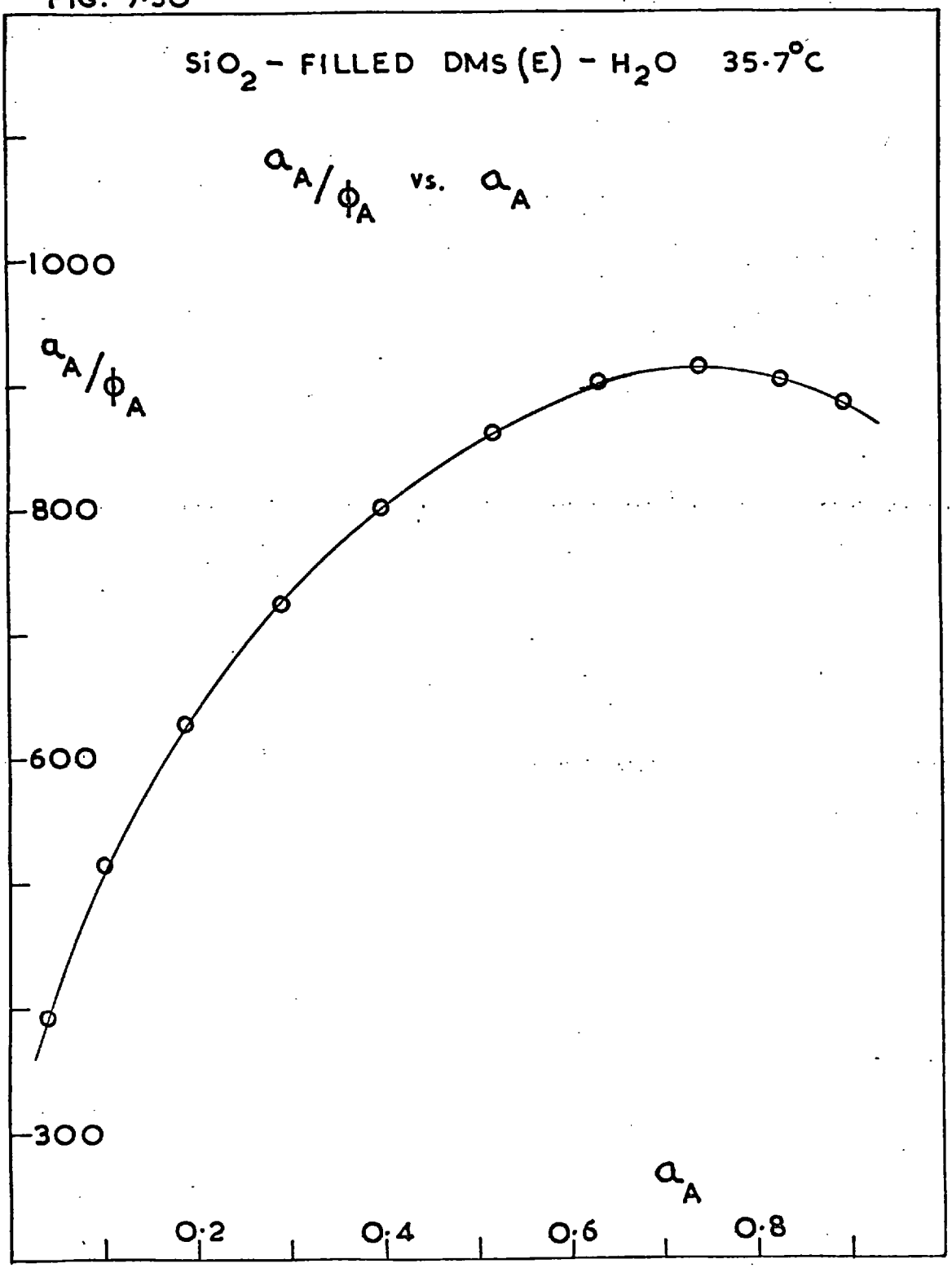
SiO2 - FILLED DMS (E) - H2O 35·7°C
aA/φA vs. aA
aA/φA
1000
800
600
300
aA
0·2
0·4
0·6
0·8

A comparison of samples D, E and F at $\sim 35^{\circ}C$ indicates no apparent trends in the clustering functions with w_F, although the experimental error involved is rather large. If water sorption occurs mainly on the unbound Aerosil then little difference is to be expected between the different samples.

ii) Comparison with Theory

In principle a theoretical isotherm equation for a model involving both clustering and specific site sorption could be constructed from a combination of equations such as (2-83) and (2-89). However, this would require the use of at least two adjustable parameters and a close fit to the experimental isotherm would not necessarily indicate the model to be a reasonable one. The physical interpretation of the adjustable parameters would tend to be somewhat difficult and no attempt is made here to derive an isotherm equation.

7.9.4 Temperature Dependence of Isotherms

Only for sample E was the water sorption measured at several temperatures. Despite an appreciable scatter in the results, Table 7-21 shows that Y at low relative humidities becomes less negative with increasing temperature.

This behaviour is to be expected because the effect in general of an increase in temperature is to disrupt interactions and filler -H_2O interactions are predominant at lower relative humidities.

Mean heats $\overline{\Delta\bar{H}}_A$ and entropies $\overline{\Delta\bar{S}}_A$ of dilution were calculated and are given in Table 7-22.

TABLE 7-22

Mean Heats $\overline{\Delta\bar{H}}_A$ (kcal.mole^{-1}) and Entropies $\overline{\Delta\bar{S}}_A$ (cal.deg.$^{-1}$ mole^{-1}) of Dilution for Water in Sample E of DMS

c cc.s.t.p. cm.$^{-3}$	$\overline{\Delta\bar{H}}_A$	$\overline{\Delta\bar{S}}_A$
0.25	+ 2.6	+ 13
0.50	3.4	14
0.75	3.6	13
1.00	3.2	11
1.25	2.6	9

Both $\overline{\Delta\bar{H}}_A$ and $\overline{\Delta\bar{S}}_A$ increase initially then decrease with increasing c. The initial increase in $\overline{\Delta\bar{H}}_A$ corresponds to the filling by water of the surface sites of the Aerosil in that $\overline{\Delta\bar{H}}_A$ becomes increasingly endothermic as the more active sites are used up or occupied. The Langmuir model[147] for sorption on specific sites predicts that the configurational

contribution to $\overline{\Delta\bar{S}}_A$ would decrease with increasing c. The initial increase observed for $\overline{\Delta\bar{S}}_A$ is probably due to experimental error although it may be partly a consequence of the variation in the thermal entropy with increasing coverage of the available sites for sorption.

At higher values of c, the decrease in $\overline{\Delta\bar{H}}_A$ and $\overline{\Delta\bar{S}}_A$ with increasing c are in accord with water clustering, as for the unfilled samples of DMS.

7.10 Steady State Permeability Results

The experimental data leading to the permeability results are presented in appendix 9.7.

7.10.1 Concentration Dependence of P

For water in each sample plots of $J\ell$ vs. p/p_o are linear right up to saturation at all temperatures. Once again therefore P is not a function of c. Values of P for water in samples D, E and F are given in Table 7-23 together with the corresponding values for the unfilled sample I.

The fact that P is constant suggests that neither clustered water nor water sorbed by the filler contribute appreciably to the diffusive flux, i.e. both forms are virtually immobilised.

TABLE 7-23

Permeability Coefficients P (cc.s.t.p. cm. $cm.^{-2}$ $sec.^{-1}$ $cmHg)^{-1}$) for Water in Unfilled and Silica-Filled DMS

Sample of DMS	$T^{o}C$	P x 10^{6}	Sample of DMS	$T^{o}C$	P x 10^{6}
I	35.7	4.34	E	50.2	2.93
I	50.2	3.79	E	28.1	3.67
			E	44.1	3.17
D	35.6	3.94			
D	50.0	3.28	F	36.2	3.05
			F	49.7	2.70
E	36.0	3.39			

7.10.2 Variation of P with Filler Content

Volume fractions ϕ_F of filler were calculated assuming a bulk density of 1.53 (section 7.8) for the Aerosil. P decreases approximately linearly with increasing ϕ_F as illustrated in Figure 7-31. Assuming that the water sorbed by the filler is immobile, then by equation (3-8) $P = \chi \phi_B P_B$. Values for the structure factor χ were calculated and are given in Table 7-24.

The values of χ are not particularly sensitive to changes in the value taken for the density of the Aerosil and may be considered fairly reliable. For all samples χ is

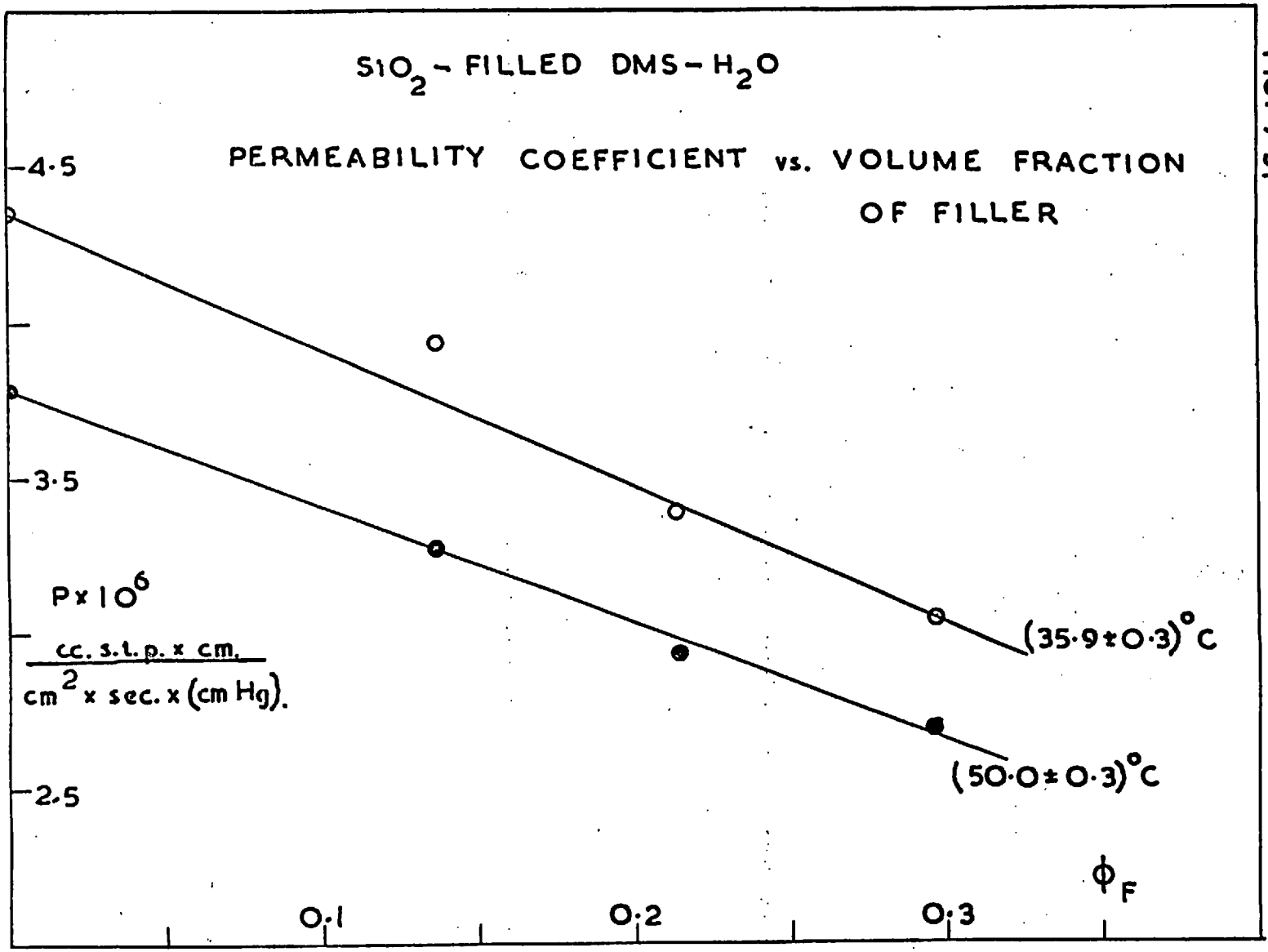
SiO_2 - FILLED DMS - H_2O
PERMEABILITY COEFFICIENT vs. VOLUME FRACTION OF FILLER
4·5
3·5
2·5
$P \times 10^6$
$\frac{cc.\ s.t.p. \times cm.}{cm^2 \times sec. \times (cm\ Hg).}$
(35·9±0·3)°C
(50·0±0·3)°C
ϕ_F
0·1
0·2
0·3

FIG. 7·31

TABLE 7-24

Values of the Structure Factor χ from Permeability Measurements

Temperature °C	Sample of DMS	ϕ_B	P/P_B	χ
50.0	D	0.86	0.91	1.05
"	E	0.79	0.78	0.99
"	F	0.70	0.70	1.00
35.9	D	0.86	0.86	1.00
"	E	0.79	0.77	0.98
"	F	0.70	0.71	1.01

close to unity which suggests that whereas P is reduced by a reduction in ϕ_B, the filler offers little if any geometric impedance to diffusion. This contrasts with the behaviour of some isomeric hydrocarbons in a similar series of filled samples[23] where χ decreases with increasing ϕ_F. A possible explanation in the case of water is that the external surfaces of the filler become covered by a monolayer or more of water and that some sort of exchange mechanism allows water transport round or between the filler particles and dispels the need for diffusion around an aggregate of filler particles. As water is apparently not sorbed appreciably by the bound filler (section 7.9.1), this

possibly suggests that some water is "permanently" incorporated in the pores of the bound filler. However, an alternative possibility is that air gaps exist around the filler particles.

7.10.3 Temperature Dependence of P

A plot of log P vs. 1/T for water in sample E is illustrated in Figure 7-32. From this it was calculated that E_p = -2.0 kcal.mole^{-1}, i.e. close to the value (-1.8) for unfilled DMS (sample I).

7.11 Diffusion Coefficients

7.11.1 Steady State Diffusion

Sorption isotherms were curve-fitted by expressing p/p_o as a polynomial in c. It was found that at least four term polynomials were necessary to fit accurately the isotherm data, i.e.

$$(p/p_o) = \alpha c + \beta c^2 + \gamma c^3 + \delta c^4 \quad \ldots.(7\text{-}10)$$

and $$D = D_{c=0}\,(1 + Ac + Bc^2 + Cc^3) \quad \ldots.(7\text{-}11)$$

A fit to an experimental isotherm using a four term polynomial is shown in Figure 7-33. Values of the polynomial coefficients for each system are given in Table 7-25. At low values of c where few experimental points were obtained

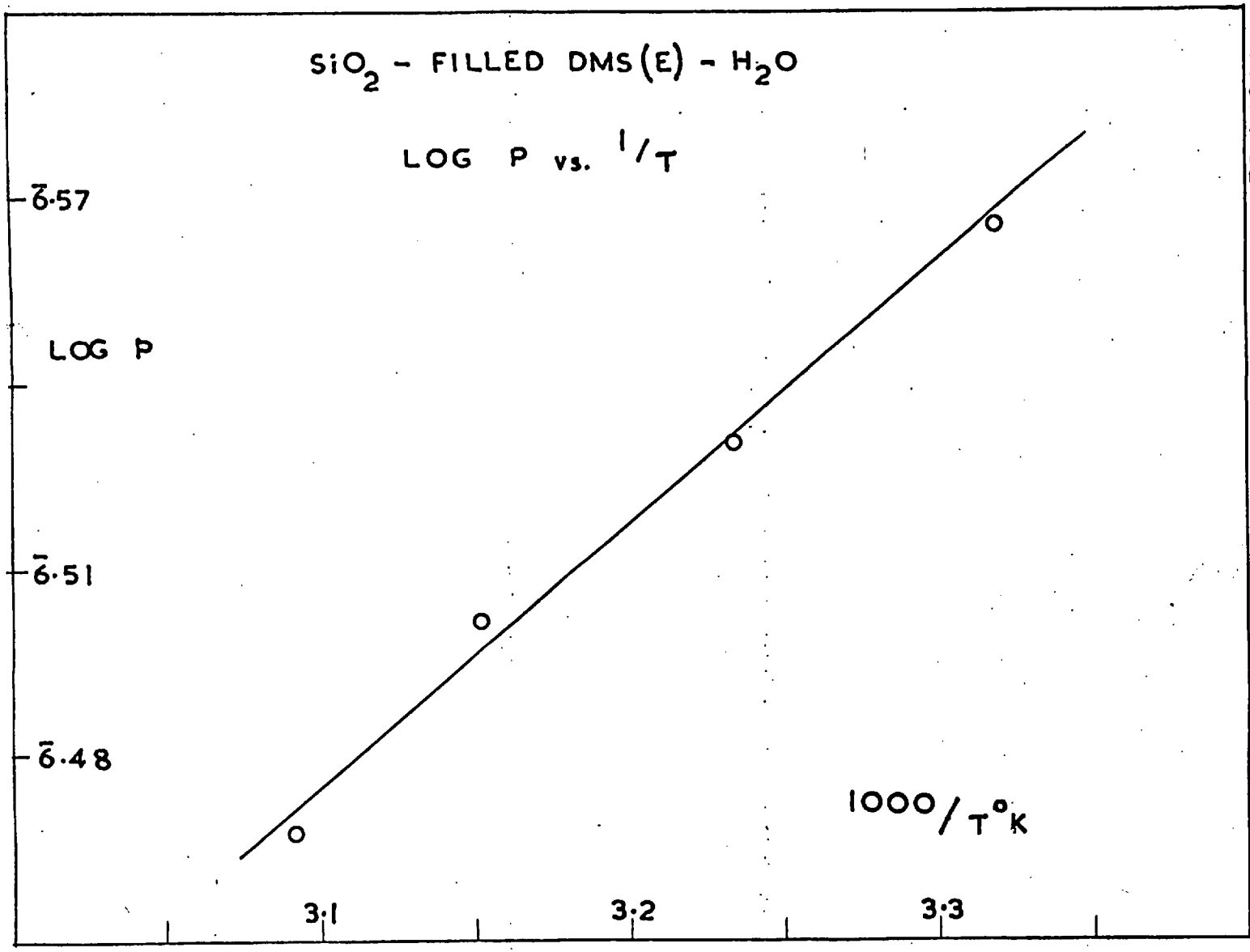
SiO2 - FILLED DMS(E) - H2O
LOG P vs. 1/T
LOG P
6·57
6·51
6·48
3·1
3·2
3·3
1000/T°K

FIG. 7.32

FIG. 7·33

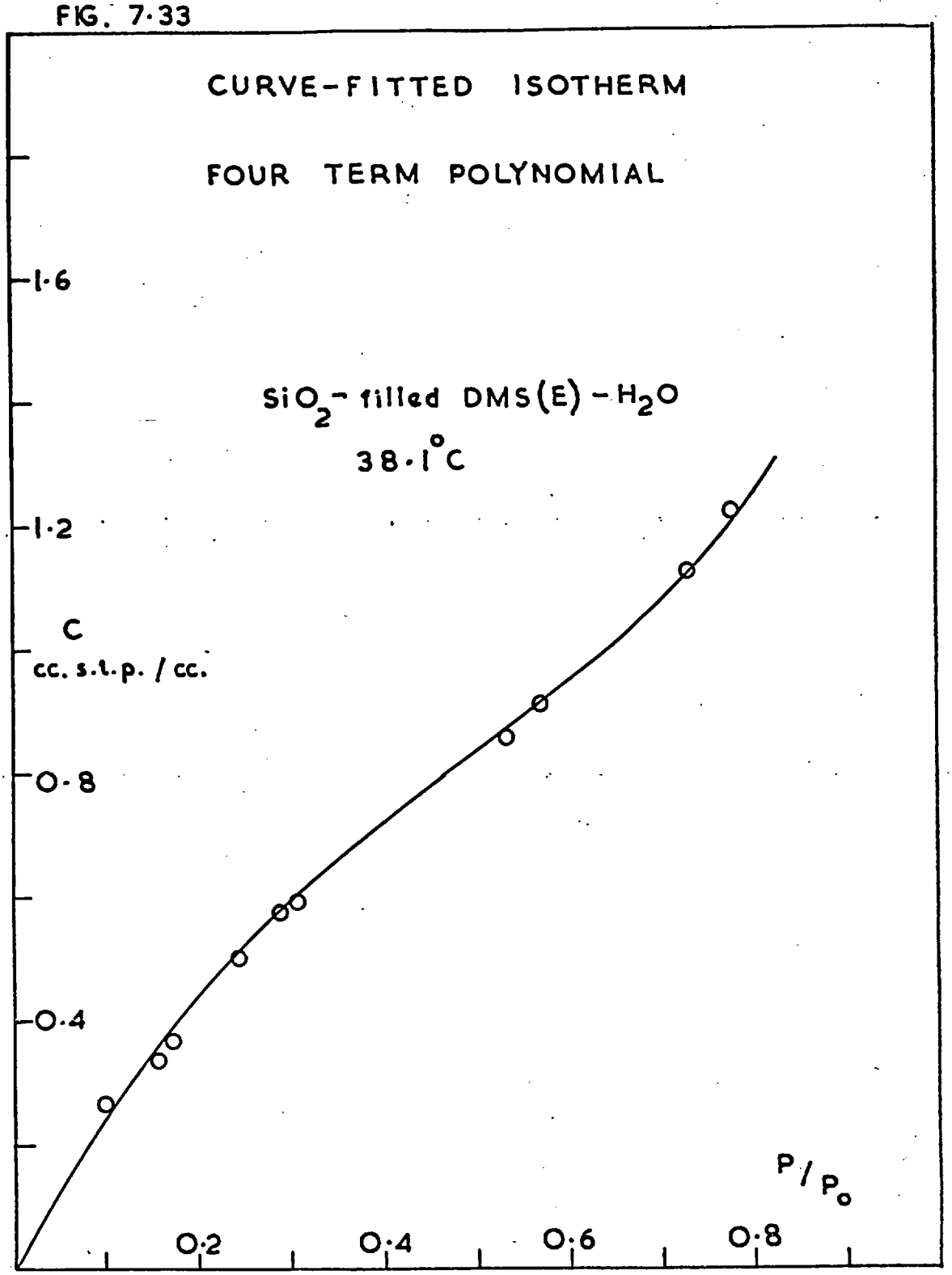
CURVE-FITTED ISOTHERM
FOUR TERM POLYNOMIAL
SiO2 - filled DMS(E) - H2O
38·1°C
1·6
1·2
C
cc. s.t.p. / cc.
0·8
0·4
P / Po
0·2
0·4
0·6
0·8

the use of the polynomials was rather dubious and D-c curves were extrapolated back graphically to obtain values for $D_{c=0}$.

TABLE 7-25

Values of Polynomial Coefficients for Curve-Fitting Isotherms. Equations (7-10) and (7-11)

Sample of DMS	T°C	α	β	γ	δ	$D_{c=0}$ x 10^6
D	35.7	0.468	-0.096	1.02	-0.623	8.06
E	28.5	0.301	0.692	-0.050	-0.179	3.15
E	35.7	0.202	0.958	-0.361	-0.060	3.07
E	38.1	0.408	-0.229	0.976	-0.515	6.79
E	41.8	0.293	0.257	0.266	-0.208	5.73
E	43.5	0.359	0.021	0.400	-0.218	7.54
E	50.4	0.294	0.183	0.203	-0.149	8.18
F	35.5	0.334	0.474	0.089	-0.197	4.58

Units : $D_{c=0}$ in $cm.^2$ $sec.^{-1}$, c in cc.s.t.p. $cm.^{-3}$

α in c^{-1}, β in c^{-2}, γ in c^{-3}, δ in c^{-4}.

i) Values of $D_{c=0}$

Values of $D_{c=0}$ are given in Table 7-26 together with the corresponding values for water in unfilled DMS (sample I).

TABLE 7-26

Values of $D_{c=0}$ ($cm.^2$ $sec.^{-1}$) for Water in Unfilled and Silica-Filled DMS

Sample of DMS	T^oC	$D_{c=0}$ x 10^6	Sample of DMS	T^oC	$D_{c=0}$ x 10^6
I	35.4	41	E	38.1	4.8
I	50.7	52	E	41.8	5.6
			E	43.5	6.4
D	35.7	5.4	E	50.4	8.1
E	28.5	3.2	F	35.5	3.9
E	35.7	4.2			

These values are not particularly accurate owing to the somewhat uncertain extrapolations which had to be employed. However, they are probably sufficiently accurate to indicate that $D_{c=0}$ decreases slightly with increasing filler content of the sample at $\sim 35^oC$. In addition, $D_{c=0}$ values for all the filled samples are about an order of magnitude lower than those for water in unfilled DMS. These lower values are to be expected because as $c \rightarrow 0$ an increasing fraction of the sorbed water is immobilised on the surface of the filler and consequently the overall mobility of water is relatively small and decreases with increasing filler content. However, since the decrease in $D_{c=0}$ observed on increasing the filler content from 20 to

40% by weight is very much less than that observed in going from 0 to 20% filler, it is again indicated that the unbound filler rather than the total filler provides most of the specific sites on which water is sorbed and immobilised.

ii) Concentration Dependence of D.

D for water in each filled sample increases initially with increasing c up to a maximum, at $p/p_o = \sim 0.5$, of 2-3 times its value at c=0 and then decreases with further increase in c. The concentration dependence of the relative diffusion coefficient $D' = D/D_{c=0}$ for each system is illustrated in Figures 7-34 and 7-35.

The shapes of the D'-c curves are qualitatively consistent with sorption of water occurring initially on specific sites and with water clustering becoming predominant at relatively high values of c. Thus initially a large proportion of the water is immobilised on specific sites and the sorbed water has a low overall D. As the more active sites become filled the proportion of strongly bound, i.e. immobilised, water decreases and D' increases with c. For higher values of c, water-water interactions begin to predominate so that clusters are formed and D' decreases with increasing c.

FIG. 7·34

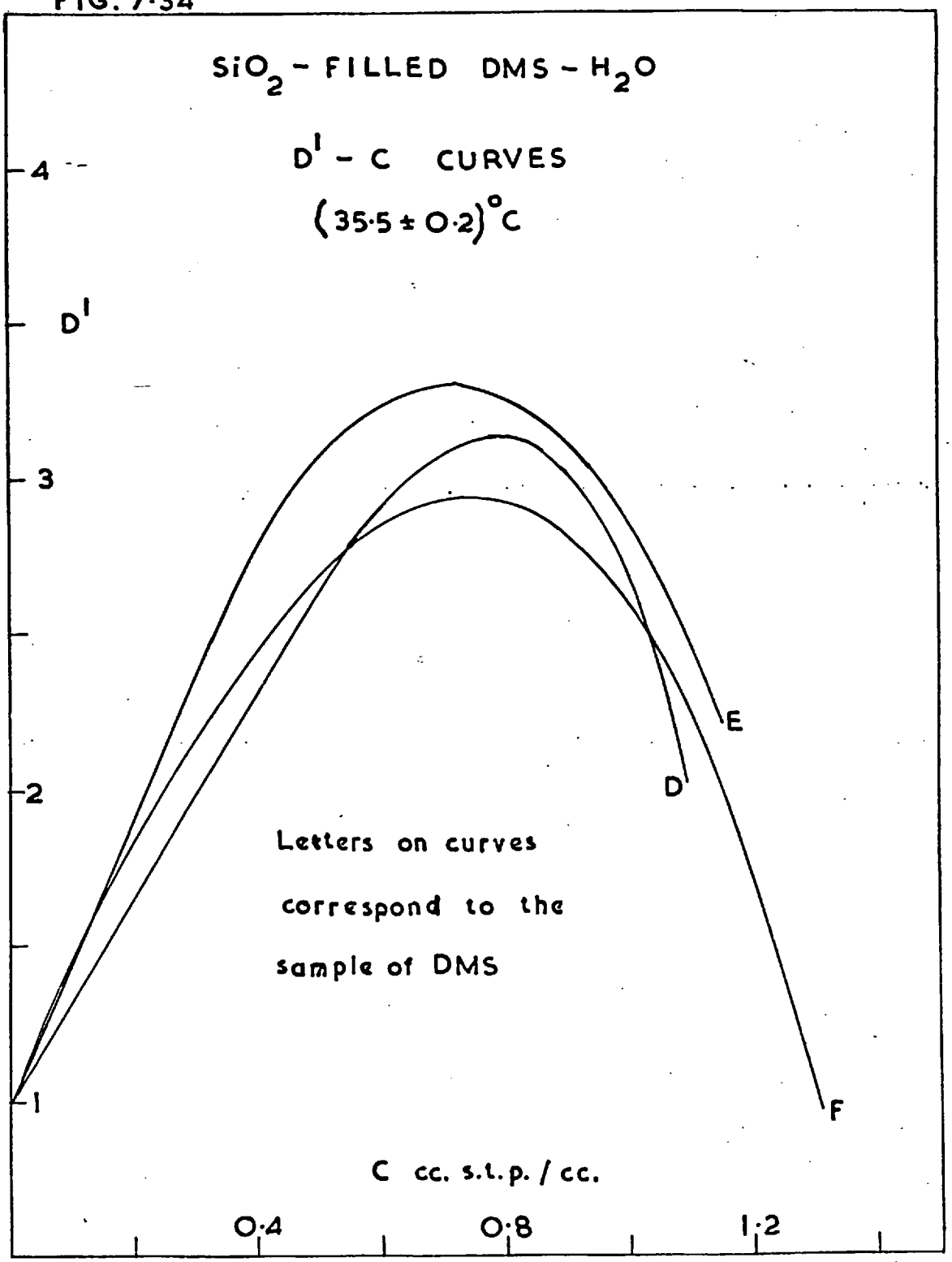
SiO2 - FILLED DMS - H2O
D' - C CURVES
(35·5 ± 0·2)°C
D'
4
3
2
1
E
D
F
Letters on curves correspond to the sample of DMS
C cc. s.t.p. / cc.
0·4
0·8
1·2

FIG. 7·35

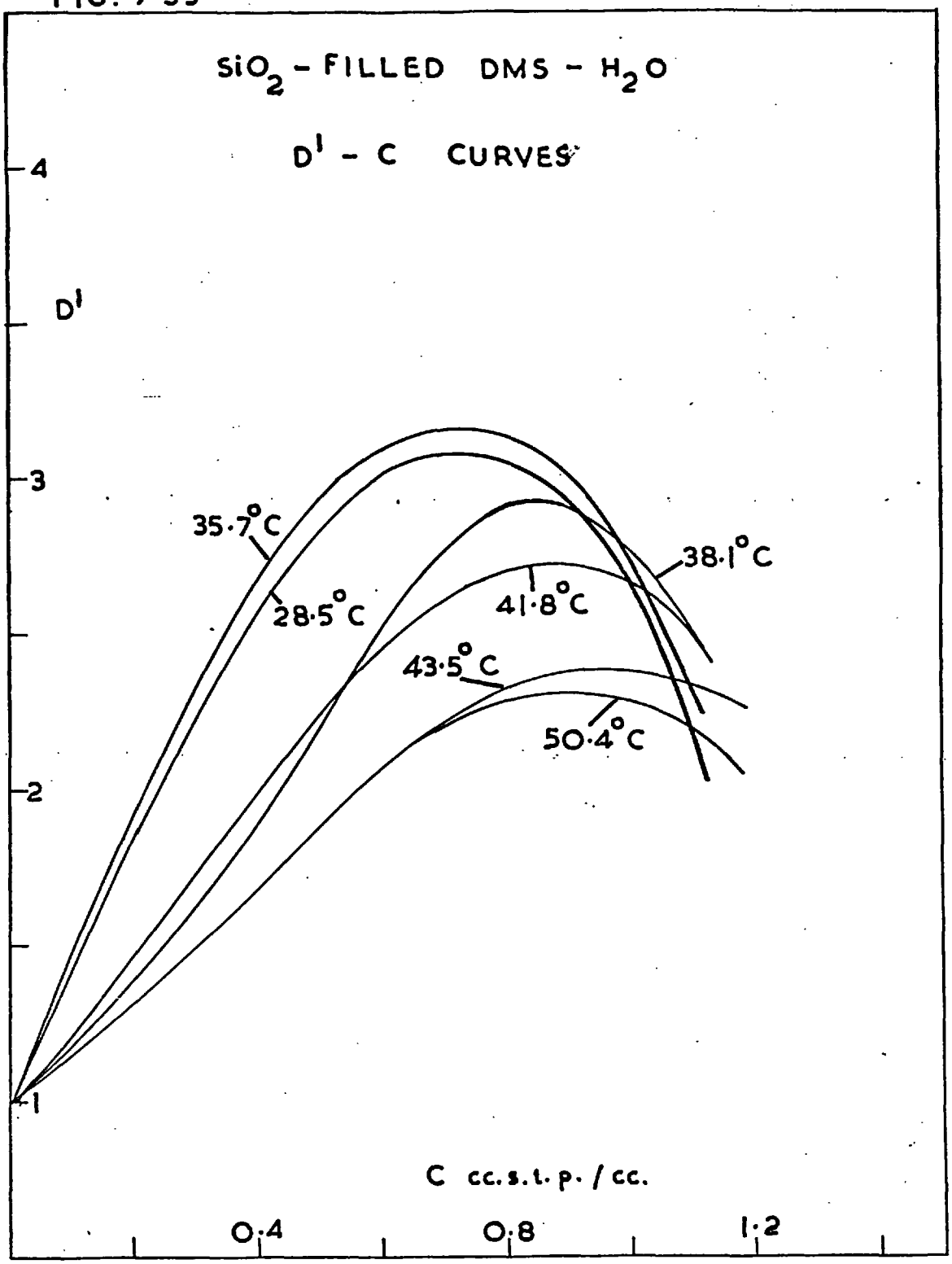
SiO2 - FILLED DMS - H2O
D' - C CURVES
D'
4
3
2
1
35·7°C
28·5°C
38·1°C
41·8°C
43·5°C
50·4°C
C cc.s.t.p./cc.
0·4
0·8
1·2

In principle the D'-c relationships could be compared with those expected from a theoretical model involving immobilisation both on specific sites and by cluster formation, involving equations such as (2-84) and (2-94). However, as for the sorption isotherm analysis this was not carried out because of the difficulty in interpreting the adjustable parameters involved.

7.11.2 Transient State Diffusion

Reduced sorption and desorption curves are initially linear becoming concave to the $t^{\frac{1}{2}}/\ell$ axis at longer times. On back extrapolation they did not pass through the origin but had positive intercepts for M_t/M_∞ at zero time. In general sorption curves lie above the conjugate desorption curves. A typical example of a conjugate pair of reduced curves is shown in Figure 7-36. As for the unfilled silicone rubbers, considerable error was involved in determining the initial slopes of reduced curves since only the latter stages of what appeared to be the linear regions of these curves were available for accurate measurement.

Values of I_s and I_d, and of $\bar{D}_s$ and $\bar{D}_d$ calculated from equation (2-30) are given in Table 7-27. Typical data from which the reduced curves were plotted are presented in appendix 9.8.

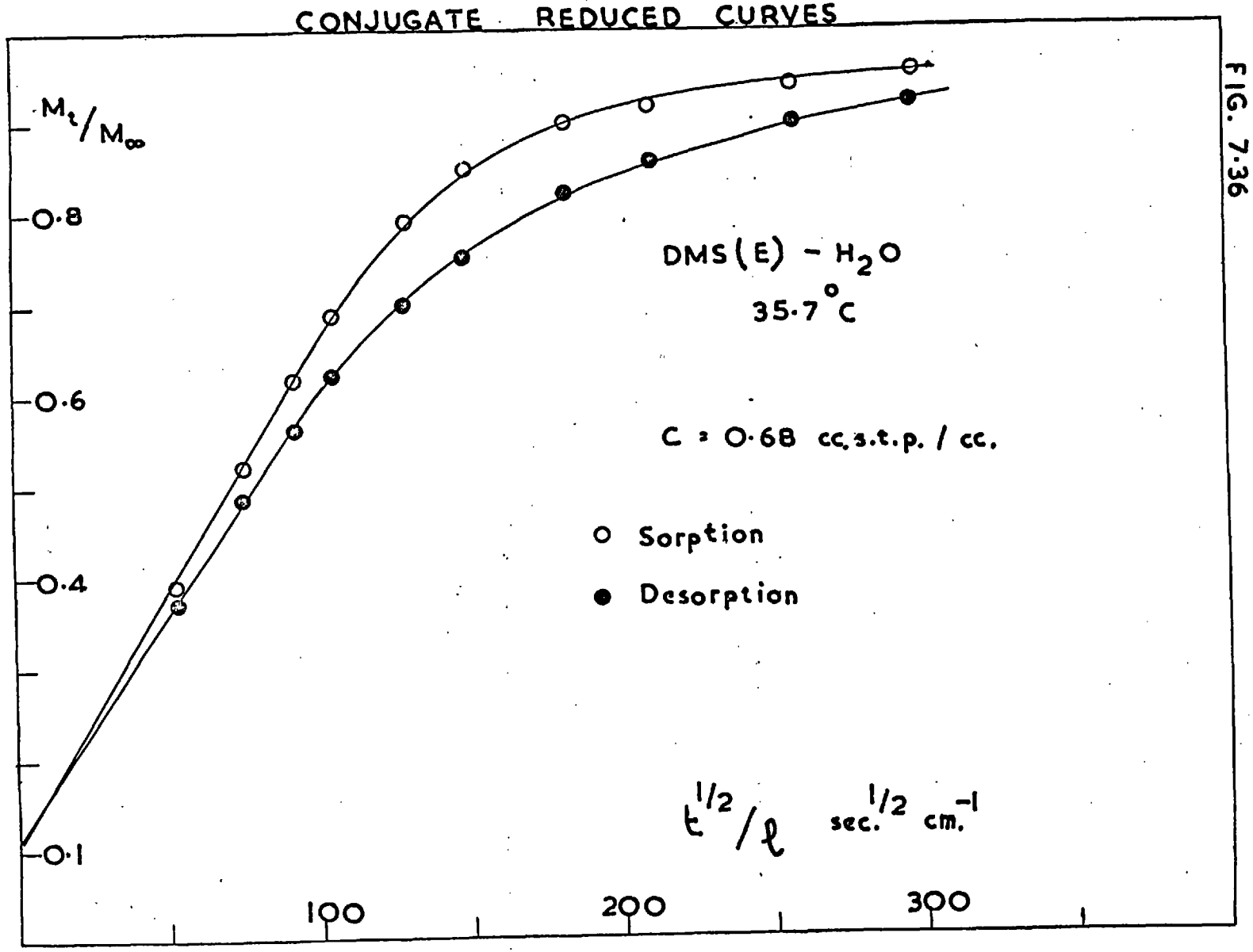
CONJUGATE REDUCED CURVES
M_t/M_∞
0·8
0·6
0·4
0·1
DMS (E) – H_2O
35·7 °C
C = 0·68 cc. s.t.p. / cc.
o Sorption
● Desorption
100
200
300
$t^{1/2}/l$ sec.$^{1/2}$ cm.$^{-1}$

FIG. 7·36

TABLE 7-27

Values of I_s, I_d ($cm.sec.^{-\frac{1}{2}}$) and $\bar{D}_s$, $\bar{D}_d$ ($cm^2\ sec.^{-1}$) for Water in Silica-Filled DMS

Sample of DMS	$T^{\circ}C$	c cc.stp cm^{-3}	$I_s \times 10^3$	$I_d \times 10^3$	$\bar{D}_s \times 10^6$	$\bar{D}_d \times 10^6$	$\bar{D}^{\#}_{AV} \times 10^6$
D	35.7	0.42	5.4	4.3	5.7	3.6	4.7
"	"	0.46	5.6	3.9	6.1	3.1	4.6
"	"	0.51	5.4	-	5.7	-	-
"	"	0.62	5.1	4.8	5.1	4.5	4.8
"	"	0.70	5.2	4.8	5.4	4.6	5.0
"	"	0.77	5.8	-	6.5	-	-
"	"	0.93	5.8	-	6.6	-	-
"	"	1.03	5.8	5.2	6.6	5.3	5.9
"	"	1.25	5.6	-	6.2	-	-
E	28.5	0.50	4.7	-	4.4	-	-
"	"	0.66	5.0	4.3	4.8	3.6	4.2
"	"	0.76	4.7	4.0	4.3	3.2	3.7
"	"	0.94	4.7	4.4	4.4	3.7	4.1
"	"	1.15	4.7	-	4.4	-	-
"	"	1.59*	3.7	4.2	2.6	3.4	3.0
"	35.7	0.41	5.4	4.4	5.8	3.9	4.8
"	"	0.46	5.3	4.4	5.6	3.9	4.7
"	"	0.51	5.2	-	5.2	-	-
"	"	0.62	5.4	4.5	5.8	4.0	4.9
"	"	0.68	5.7	4.7	6.4	4.3	5.4
"	"	0.76	5.4	-	5.7	-	-
"	"	0.94	5.1	4.2	5.1	3.5	4.2
"	"	0.99	5.4	4.0	5.7	3.1	4.4
"	"	1.80*	3.7	-	2.7	-	-
"	43.5	0.26	5.5	5.2	6.0	5.3	5.7
"	"	0.35	5.7	4.2	6.5	3.5	5.0
"	"	0.42	5.5	-	5.9	-	-
"	"	0.52	5.9	4.3	6.9	3.7	5.3
"	"	0.65	5.3	4.9	5.5	4.7	5.1
"	"	0.75	5.5	5.3	5.9	5.6	5.7
"	"	0.92	5.7	-	6.3	-	-
"	"	1.13	5.1	5.0	5.2	5.0	5.1
"	"	1.27	5.5	5.3	5.9	5.6	5.7
"	"	1.83*	4.1	-	3.4	-	-

TABLE 7-27 (cont.)

Sample of DMS	$T^{o}C$	c cc.stp cm^{-3}	$I_s \times 10^3$	$I_d \times 10^3$	$\bar{D}_s \times 10^6$	$\bar{D}_d \times 10^6$	$\bar{D}_{AV} \times 10^6$
E	50.4	0.22	6.2	5.7	7.5	6.4	6.8
"	"	0.28	6.1	5.5	7.3	5.9	6.6
"	"	0.48	5.9	-	6.7	-	-
"	"	0.63	6.1	-	7.3	-	-
"	"	0.99	5.8	5.3	6.6	5.6	6.1
"	"	1.19	6.3	-	7.9	-	-
"	"	1.56*	6.5	-	8.3	-	-
F	35.5	0.40	4.8	4.3	4.5	3.6	4.1
"	"	0.45	4.9	4.3	4.6	3.7	4.2
"	"	0.49	4.9	-	4.7	-	-
"	"	0.40	4.6	4.0	4.1	3.1	3.6
"	"	0.62	4.7	4.2	4.3	3.5	3.9
"	"	0.66	5.0	4.8	4.9	4.4	4.7
"	"	0.73	4.8	-	4.6	-	-
"	"	0.76	5.1	-	5.0	-	-
"	"	1.47*	4.3	-	3.6	-	-

$\bar{D}_{AV} = 1/2\ (\bar{D}_s + \bar{D}_d)$

i) Comparison with the Steady State

From the results in Table 7-27 no trend in the variation of $\bar{D}_s$ or $\bar{D}_d$ with c can be ascertained except that in general they both decrease with increasing c for the highest values (starred) of c. For this reason, values of $\bar{D}_s$ and $\bar{D}_{AV}$ (excluding those at the starred concentrations) were averaged. The averaged values of $\bar{D}_s$ and $\bar{D}_{AV}$ are

compared in Table 7-28 both with values of $1/c \int_0^c D\,dc$ and of $D_{c=0}$ obtained from the steady state results.

TABLE 7-28

Comparison of Diffusion Coefficients ($cm.^2$ $sec.^{-1}$) from Transient and Steady States : Silica-Filled DMS - H_2O

Sample of DMS	T°C	Transient State		Steady State	
		$\bar{D}_s \times 10^6$	$\bar{D}_{AV} \times 10^6$	$\bar{D}^* \times 10^6$	$D_{c=0} \times 10^6$
D	35.7	6.0	5.0	13	5.4
E	28.5	4.5	4.0	7.5	3.2
E	35.7	5.7	4.7	12	4.2
E	43.5	6.0	5.4	13	6.4
E	50.4	7.2	6.5	16	8.1
F	35.5	4.6	4.1	8.7	3.9

* $\bar{D} = 1/c \int_0^c D.dc$

The apparent lack of concentration dependence for the transient state $\bar{D}_s$ and $\bar{D}_{AV}$ is surprising and Table 7-28 indicates that these values are more in agreement with steady state values of $D_{c=0}$ than with $1/c \int_0^c D\,dc$ calculated from the steady state D-c relationships. Although the experimental errors involved, especially in the transient state measurements, were large, discrepancies of this magnitude were not expected. In addition, the fact that in general $\bar{D}_s$ exceeds $\bar{D}_d$ is qualitatively consistent with a D which increases with increasing c.

Comparisons of steady and transient states are complicated in systems such as these because the problem has to be considered in terms of diffusion with concurrent, reversible immobilisation on sites offered by the filler surface. Three possible situations arise and these are considered in turn:

a) Immobilisation is very rapid in comparison with diffusion. If this were the case then no discrepancy between the steady and transient state D-c dependences would be expected.

b) Immobilisation is very slow in comparison with diffusion. This would correspond to no immobilisation taking place in the initial stages of a sorption curve, i.e. immobilised water would contribute to M_∞ but not to M_t in this region. Hence for each sorption curve I_s is decreased by an amount ΔI_s from the value of I_s for the curve corresponding to infinitely rapid immobilisation. As c is increased, it follows from the shape of the equilibrium sorption isotherm that the relative decrease $\Delta I_s/I_s$ would become smaller. Hence the true concentration dependence of D would

be enhanced when determined from sorption rate measurements. However, Crank[94] has shown that the analysis of such systems by sorption rate measurements is further complicated because "shoulders" are exhibited in reduced sorption curves.

c) Immobilisation and diffusion occur at comparable rates. The argument still holds concerning the concentration dependence of D, which would be enhanced although to a lesser extent than in b). Depending on whether immobilisation were relatively slow or relatively rapid in comparison with diffusion, reduced sorption curves would exhibit shoulders or points of inflection respectively[94]. Relative rates of sorption and desorption would depend on the relative rates of immobilisation and of immobilised molecules breaking free from sites.

The comparison of steady and transient state D-c relationships reveals that situation a) cannot hold for these systems, so that some time-dependent process appears to be occurring in addition to diffusion.

Situations b) or c) then seem the more likely. The accuracy of the sorption rate measurements was such that the existence of shoulders, especially small shoulders, in the reduced sorption curves could not be ruled out with certainty. Small shoulders tend to occur when the forward rate constant for immobilisation (assuming a first order "reaction") is greater than the corresponding backward rate constant[94]. This would also be consistent with the observation that in general sorption is faster than desorption. The slow rates of immobilisation could perhaps arise if water has to diffuse slowly through the pores of the Aerosil to reach some of the active sites. Rates of desorption from sites would be even lower perhaps because water molecules become relatively "trapped" inside the pores of the filler, especially when sorbed on the more active or energetic sites. However, such an explanation can only be speculative at the present time and as yet the reason for the observed discrepancies between the steady and transient state results cannot be considered to be clear.

The point b) above is of general interest because, together with the treatment of section 6.3.2, it illustrates the fact that when immobilisation of penetrant is relatively slow, then whether D increases or decreases with c the

concentration dependence of D is enhanced, when determined from initial sorption rate measurements, compared with that measured in the steady state. This is the opposite situation to that where slow relaxation processes in the polymer exist and D increases with c, e.g. for the PEMA-MeOH system (section 6.3.2).

At high sorbed water concentrations the observed decrease in $\bar{D}_s$ and $\bar{D}_d$ from the averaged values at lower concentrations is consistent with water clustering and in a qualitative sense with the steady state results.

7.11.3 Temperature Dependence of D

Plots of log D vs. 1/T for water in sample E are shown in Figure 7-37. Values of E_D for various c are given in Table 7-29 and are compared with the value obtained from the transient state by plotting (Figure 7-37) log $\bar{D}_{AV}$ vs. 1/T, where $\bar{D}_{AV}$ refers to the averaged values given in Table 7-28. All these values of E_D are subject to appreciable uncertainty.

The initial decrease in E_D with increasing c is qualitatively consistent with a specific site mechanism for sorption in that extra energy is required for a water molecule to break free from a site and that the proportion of water sorbed on active sites decreases with increasing c.

FIG. 7·37

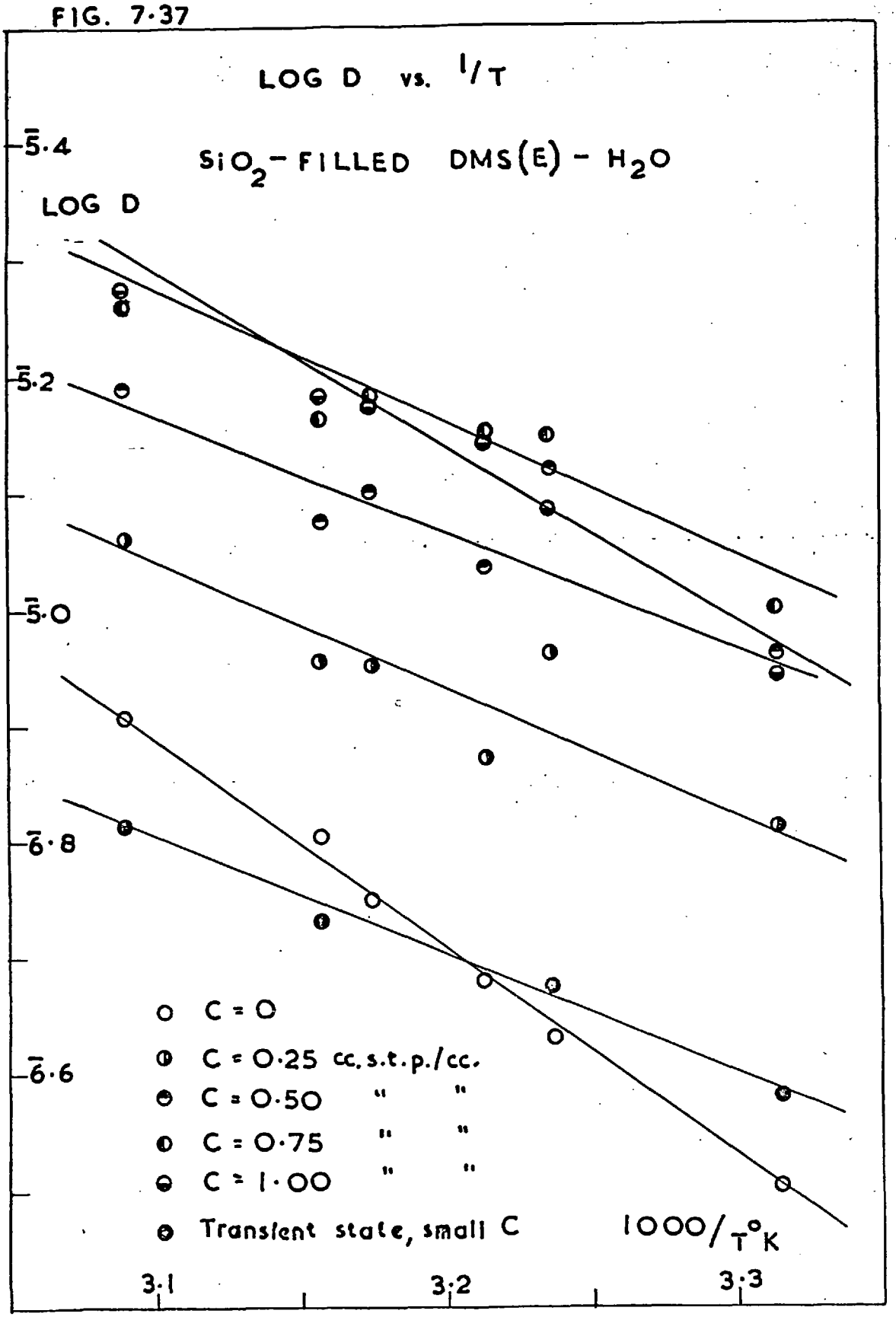
LOG D vs. 1/T
SiO2 - FILLED DMS(E) - H2O
LOG D
5̄·4
5̄·2
5̄·0
6̄·8
6̄·6
C = 0
C = 0·25 cc. s.t.p./cc.
C = 0·50 " "
C = 0·75 " "
C = 1·00 " "
Transient state, small C
1000/T°K
3·1
3·2
3·3

TABLE 7-29

E_D (kcal.mole^{-1}) for Water in Sample E of DMS

c cc.s.t.p. cm.$^{-3}$	E_D
0	$8._2$
0.25	$5._2$
0.50	$4._8$
0.75	$4._9$
1.00	$7._3$
Transient State (small c)	$4._7$

The increase in E_D with c for higher values of c is consistent with water clustering, as for water in the unfilled polymers.

The values of E_D for small c are appreciably higher than the corresponding values for unfilled DMS. This can be attributed to the change from diffusion to diffusion + immobilisation in going from unfilled to filled DMS. It seems unlikely that chain-stiffening by the incorporated Aerosil is significant as the measured T_g is similar for the filled as for the unfilled samples (Table 5-2).

CHAPTER 8

CONCLUSIONS

8.1 Summary and Reappraisal of Results

A number of interesting features concerning the sorption and diffusion of water in polymers has come to light during the course of this work and the principal points are discussed in this section.

8.1.1 Water Clustering and Immobilisation : Applicability of Simple Models for Clustering.

This investigation has clearly demonstrated further the tendency of water molecules to cluster inside a relatively hydrophobic polymer, particularly at relative vapour pressures close to saturation. Thus in this region the diffusion coefficient for water decreases with increasing sorbed water concentration for all of the water-polymer systems studied. In some respects the sorbed water seems to be well represented by considering it as comprised of a mobile fraction and an immobile fraction. The immobile fraction may be clustered water, water sorbed on sites or water present in "pockets" of salt solution.

The fact that P is constant for almost all the water-polymer systems studied suggests in addition that the mobile fraction of water has a constant diffusion coefficient

and is sorbed according to Henry's law. It seems that similar behaviour is exhibited by methanol and the fact that P increases with c for methanol in PEMA and FMS is attributed to plasticisation of the polymer. With water as penetrant the amount sorbed is usually so small that plasticisation is negligible. The slight increase in P with c observed for water in PMMA and PEMA occurs under conditions when the sorbed water concentration is highest so that some small degree of plasticisation may well be operative in these cases.

The difficulty of determining the effects of polymer structure on water clustering by comparing series of polymers has been illustrated. For example, harder and more crystalline polymers will tend to expand less readily to accommodate clusters (which may then tend to form in voids). However, the overall degree of perturbation required of a polymer matrix will depend on the overall sorbed water concentration which in turn will depend on the number and type of polar groups present in the polymer. Despite these difficulties, some progress has been made and it appears that for high relative vapour pressures the clustering tendency (G_{AA}/v_A) of water is in general higher the more hydrophobic and the more rubbery is the polymer. An exception is water in FMS at a relative vapour pressure of 0.7 in that G_{AA}/v_A

is higher than for water in DMS, which indicates that polar groups may in fact play some part in the initiation of clustering. In addition, the possibility that water clustering is initiated by polar impurities present in all the silicone rubbers studied cannot be ruled out.

The use of polycondensation theory for the description of water and methanol association in the polymers investigated has proved to be a useful reference model (except for PEMA-MeOH where plasticisation of polymer is the predominant feature) for explaining the shapes and temperature dependence of the equilibrium sorption isotherms and of the D-c curves, even though the quantitative agreement is rather poor in the case of water. It is hardly surprising that the random polycondensation model for water should fail to give quantitative agreement with experiment since such a strong co-operative effect is present for hydrogen bond formation in liquid water[32]. The nature of this co-operative effect is such that relevant statistical models would be complex and difficult to apply. The model applied here assumes a) that the co-operative effect is confined to the first shell, b) that a linear free energy relationship (equation (2-97)) exists and c) that the effect is sufficiently small to apply perturbation theory. Again, therefore, it is hardly surprising

that the agreement with experiment is only slightly improved on that obtained with the random model.

The assumption that a polymer approximates to an inert medium for water is an oversimplification and has been discussed several times in the thesis and by previous authors[42,43,50]. In particular, the investigation has illustrated the desirability and importance of obtaining the polymer free from even minute amounts of polar impurities, particularly if these are water-soluble. Unfortunately, it would be very difficult both to prepare such a "pure" polymer and to identify such a polymer when prepared.

An attempt to apply a more general clustering theory would almost certainly involve the use of further adjustable parameters, as would a model involving a combination of water clustering and sorption on specific sites inside a polymer. The accurate fitting of isotherm or D-c data would then be somewhat ambiguous unless the adjustable parameters could be interpreted physically. It would be useful to be able to use some other technique for investigating the association and structure of water sorbed inside a polymer. Unfortunately, for the polymers used in this investigation, sorbed water concentrations are so low

that conventional probe techniques such as infra-red or NMR spectroscopy would be difficult to apply.

The results indicate that the rate of immobilisation of water molecules by clustering or by the dilution of salt solution contained in the polymer is very rapid in comparison with the rate of the diffusion process. On the other hand it seems likely that the immobilisation of water on specific surface sites of the silica filler is a relatively slow process, although this can only be considered as a tentative explanation of the results at the present time.

8.1.2 Interpretation of Measurements on Silica-Filled Rubbers

There are several difficulties accompanying a study of transport in heterogeneous media which are comprised of one phase dispersed in another, and this point has been particularly illustrated in this investigation.

Firstly there is the inherent difficulty that the mathematics describing the transport process become complex when the dispersed particles are not sufficiently dilute for interactions between them to be neglected[22]. Filled rubbers often present additional difficulties. In this investigation the particle shape and the state of aggregation

of the Aerosil filler were not known, although the filler apparently offers little geometric impedance to water diffusion and it seems likely that some sort of interfacial transport mechanism is operative. A study of water sorption in filled polymers is additionally complicated because of the particular importance of the degree to which the filler surface is wetted by the polymer. A further complication with the silica-filled DMS samples of this investigation is the fact that the filler is present in two different bound forms.

It is not surprising therefore that an interpretation of some facets of the results has proved to be difficult, and as yet no general quantitative theory has been applied to systems such as these.

8.1.3 Practical Implications of the Results

In none of the series of samples studied is an increase in the sorptive capacity of the polymer for water associated with an increase in P. For the silicone rubbers this is of technical interest in a negative sense, i.e. in this sense it is perhaps disappointing that the increases in water solubility achieved through the addition of polar groups or fillers to DMS are compensated for by decreases

in D. Thus the polar, fluorine-containing groups are introduced as bulky side chains which reduce the segmental mobility (of FMS) in comparison with that of DMS. Again, the increased sorption gained by the polar Aerosil and the water-soluble sodium chloride fillers appears to be in the form of immobile water.

It seems unlikely then that a polysiloxane material could be prepared which would exhibit a permeability to water higher than that of pure DMS, unless a "continuum of clustered water" were to be created by the introduction of sufficient ionic groups.

8.1.4 New Aspects of the Determination of Concentration-Dependent Diffusion Coefficients

Incidental to this investigation (see appendix 9.2) is the numerical integration which was carried out to give practical value to the method of Lin Hwang[79] for obtaining the D-c relationship from the initial slopes of reduced sorption curves. For most systems in which D decreases with increasing c, this method is at least comparable with others such as the procedure of Crank[77] involving weighted mean diffusion coefficients. For D increasing with c the Lin Hwang procedure is of little use in general as it holds only for relatively small increases in D of the order of 50-100%.

This method was also used to examine the behaviour at low concentrations of the empirical weighting values 1.67 and 1.85, found by Crank[77] to apply to mean diffusion coefficients during sorption when D is respectively an increasing and a decreasing function of c. It turns out that the transition from 1.67 → 1.85 is not abrupt in the limit of zero concentration dependence of D but changes more gradually and depends on the precise mathematical form of the D-c relationship.

It has also been shown (appendix 9.5 and the accompanying published note) that if D decreases with increasing c then relatively small variations with concentration of measured "integral" quantities are to be expected, whether these are time lags or the initial slopes of reduced sorption curves. For systems in which D decreases with c therefore, measurements involving "integral" type experiments must be made with a correspondingly greater degree of accuracy. A similar analysis would also apply to steady state "integral" quantities, i.e. to the shapes of the J-c curves, although in this case the limiting factor is probably more often the degree of accuracy with which c can be measured. In the case of water vapour time lags a further complication arises through the possibility

of sorption on the glass walls of the receiving vessel, and it has been demonstrated[122] (appendix 9.4) that when, in addition, D decreases with c then very little variation in L with c may occur.

Finally, it has been pointed out that when immobilisation of penetrant molecules is relatively slow, then sorption kinetic measurements tend to enhance the "true" or steady state concentration dependence of D.

CHAPTER 9

APPENDIX

9.1 Weighting Values for Weighted Mean Diffusion Coefficients

The weighting values p for sorption and q for desorption are defined by equations (2-34) and (2-35) respectively as

$$\bar{D}_s = p\, c_o^{-p} \int_o^{c_o} c^{p-1} D(c)\, dc$$

and

$$\bar{D}_d = q\, c_o^{-q} \int_o^{c_o} (c_o - c)^{q-1} D(c)\, dc.$$

Crank[77] found that for D as several increasing functions of c, p = 1.67 and q = 1.85. The converse is expected when D is a decreasing function of c. This is most conveniently tested for sorption by determining p for D as various increasing and corresponding decreasing functions of c.

The following functions

(A) $D = D_{c=0}(1 + 0.009c^3)$ (A') $D = D_{c=0}(1 - 0.0009c^3)$

(B) $D = D_{c=0}(1 + 0.09c^2)$ (B') $D = D_{c=0}(1 - 0.009c^2)$

(C) $D = D_{c=0}(1 + 0.9c)$ (C') $D = D_{c=0}(1 - 0.09c)$

(D) $D = D_{c=0}(1+1.8c-0.09c^2)$ (D') $D = D_{c=0}(1-0.18c+0.009c^2)$

were used, where c is dimensionless and lies in the range 0-10.

For each of the above D-c functions, reduced sorption curves for various values of c_0 were constructed by the use of the explicit finite difference scheme outlined in section 2.3.4. Values of $\bar{D}_s$ were obtained from the initial slopes I_s of these curves using $\bar{D}_s = \pi I_s^2/16$. Graphs of $c \cdot d\bar{D}_s/dc$ vs. $D(c) - \bar{D}_s(c)$ were plotted and are illustrated in Figure 9-1. The slopes of these graphs equal p following equation (2-36). For D increasing with c the points corresponding to the functions (A) to (D) all fall close to a straight line as do those for functions (A') to (D') when D decreases with c. The slopes of these lines were obtained using the minimum mean squares deviation procedure and yielded p = 1.67 for the functions (A) to (D) and p = 1.84 for the functions (A') to (D'), i.e. very close to the values expected. It is therefore reasonable to suppose that a converse relationship exists for q.

9.2 Lin Hwang's Procedure for the Calculation of D

9.2.1 Calculation of the unknown Functions and Universal Constants

Lin Hwang obtained the solution to equation (2-37)

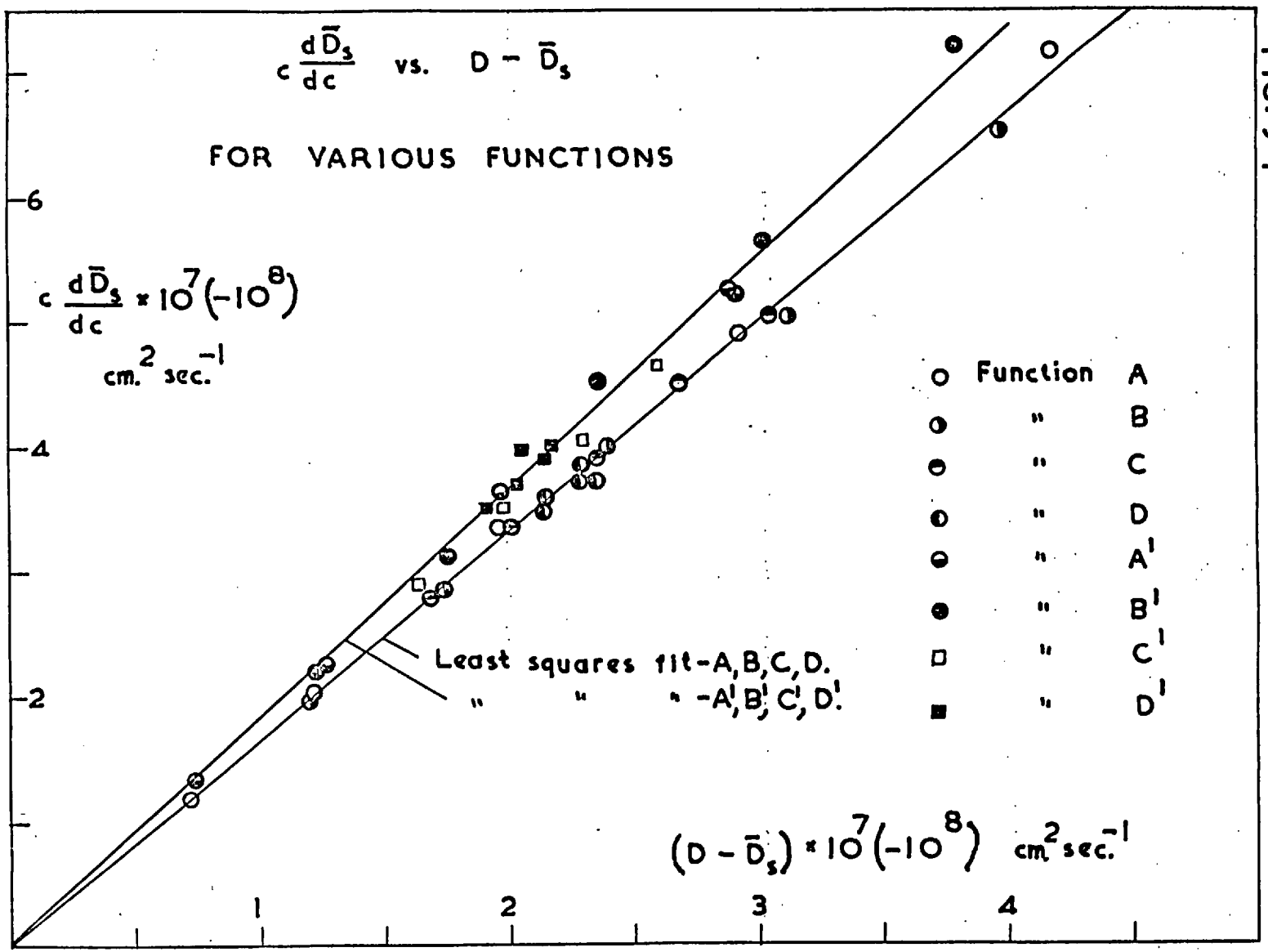
$c\frac{d\bar{D}_s}{dc}$ vs. $D-\bar{D}_s$
FOR VARIOUS FUNCTIONS
$c\frac{d\bar{D}_s}{dc}\times10^7(-10^8)$
cm.^{2} sec.$^{-1}$
6
4
2
1
2
3
4
Function A
" B
" C
" D
" A'
" B'
" C'
" D'
Least squares fit-A,B,C,D.
" " " -A',B',C',D'.
$(D-\bar{D}_s)\times10^7(-10^8)$ cm^{2}sec.$^{-1}$

FIG. 9.1

$$c(\eta) = c_0 \cdot \theta_1(\eta) + c_0^2 \cdot \theta_2(\eta) + c_0^3 \cdot \theta_3(\eta) + \ldots$$

in the form

$$\theta_1 = \text{erfc}\,(\eta), \qquad \theta_2 = \alpha \cdot \psi(\eta),$$

$$\theta_3 = \alpha^2 \cdot \chi_1(\eta) + \beta \cdot \chi_2(\eta),$$

$$\theta_4 = \alpha^3 \cdot \Omega_1(\eta) + \alpha\beta \cdot \Omega_2(\eta) + \gamma \cdot \Omega_3(\eta),$$

$$\theta_5 = \alpha^4 \cdot \epsilon_1(\eta) + \alpha^2 \beta \cdot \epsilon_2(\eta) + \alpha\gamma \cdot \epsilon_3(\eta) + \beta^2 \cdot \epsilon_4(\eta) + \delta \cdot \epsilon_5(\eta),$$

$$\theta_6 = \ldots\ldots\ldots\ldots \text{ etc},$$

where $\text{erfc}(\eta)$ is the error function complement of η given by $\text{erfc}(\eta) = 1 - \text{erf}(\eta) = 1 - (2/\pi^{\frac{1}{2}}) \cdot \int_0^{\eta} \exp(-\lambda^2)\, d\lambda$,

ψ is given by

$$\psi(\eta) = \left(\frac{\eta}{\pi^{\frac{1}{2}}} \cdot \exp(-\eta^2) + \frac{1}{\pi} + \frac{1}{2} \cdot \text{erf}(\eta)\right)(1 - \text{erf}(\eta)) - \frac{\exp(-2\eta^2)}{\pi} \qquad \ldots.(9\text{-}1)$$

and α, β etc. are the polynomial coefficients which are to be determined eventually. The remaining functions (χ_1 etc.) can all be expressed in the form

$$f(\eta) = -z \left\{ \int_0^{\eta} \exp(-\lambda^2) \int_0^{\lambda} f''(s) \exp(s^2)\, ds\, d\lambda - \text{erf}(\eta) \int_0^{\infty} \exp(-\lambda^2) \int_0^{\lambda} f''(s) \exp(s^2)\, ds\, d\lambda \right\} \qquad \ldots.(9\text{-}2)$$

where λ and s are dummy variables, $f''(s)$ represents the second derivative with respect to s of some function f(s) and z is a constant. These functions are summarised in Table 9-1. No functions beyond ϵ_5 were considered.

For some of the functions, $f''(s)\exp(s^2)$ is not given as an analytical function of s because the determination of such analytical functions would be exceedingly complicated. Instead, the same functions $f''(s)\exp(s^2)$ were obtained from tables of χ_1 vs. s, χ_2 vs. s, etc. For example, the function $\Omega_1(\eta)$ has

$$f(s) = (1-\mathrm{erf}(s)) \cdot \chi_1(s) + 1/2\,(\psi(s))^2$$

so that

$$f''(s) = \left(\frac{d\psi}{ds}\right)^2 + \psi(s) \cdot \frac{d^2\psi}{ds^2} - \frac{4}{\pi^{\frac{1}{2}}} \exp(-s^2) \cdot \frac{d\chi_1}{ds} + \frac{4s}{\pi} \exp(-s^2) \cdot \chi_1(s) + (1-\mathrm{erf}(s)) \cdot \frac{d^2\chi_1}{ds^2} \quad \ldots.(9\text{-}3)$$

By differentiation with respect to s of the appropriate equation (9-2) for $\chi_1(s)$ it follows that

$$\frac{d\chi_1}{ds} = -\left\{ \exp(-s^2) \int_0^s \frac{d^2[\psi(s)(1-\mathrm{erf}(s))]}{ds^2} \cdot \exp(s^2)ds - \frac{2}{\pi^{\frac{1}{2}}} \exp(-s^2) \int_0^\infty \frac{d^2[\psi(s)(1-\mathrm{erf}(s))]}{ds^2} \cdot \exp(s^2)ds \right\} \quad \ldots.(9\text{-}4)$$

TABLE 9-1

Constituents which make up the Lin Hwang Functions

$f(\eta)$	z	f (s)	$f''(s)\exp(s^2)$
χ_1	1	$\psi(s)\,(1-\mathrm{erf}(s))$	$\frac{4s}{\pi^{3/2}}\left[(2-2\pi)+3\pi\,\mathrm{erf}(s)\right]\left[1-\mathrm{erf}(s)\right]$ $+\frac{8s^2}{\pi}\exp(-s^2)(1-\mathrm{erf}(s))$ $+\frac{4s^3}{\pi^{\frac{1}{2}}}(1-\mathrm{erf}(s))^2$ $+\frac{4(2-3\pi)}{\pi^2}\exp(-s^2)$ $+\frac{16}{\pi}\exp(-s^2)\,\mathrm{erf}(s)$ $-\frac{12s}{\pi^{3/2}}\exp(-2s^2)$
χ_2	1/3	$(1-\mathrm{erf}(s))^3$	$\frac{12s}{\pi^{\frac{1}{2}}}(1-\mathrm{erf}(s))^2$ $+\frac{24}{\pi}\exp(-s^2).(1-\mathrm{erf}(s))$
Ω_1	1	$(1-\mathrm{erf}(s)).\chi_1(s)$ $+1/2\,(\psi(s))^2$	---
Ω_2	1	$(1-\mathrm{erf}(s)).\chi_2(s)$ $+(1-\mathrm{erf}(s))^2.\psi(s)$	---
Ω_3	1/4	$(1-\mathrm{erf}(s))^4$	$\frac{48}{\pi}\exp(-s^2)(1-\mathrm{erf}(s))^2$ $+\frac{16s}{\pi^{\frac{1}{2}}}(1-\mathrm{erf}(s))^3$
ϵ_1	1	$\mathrm{erf}(s)\,.\,\Omega_1(s)$ $+\psi(s)\,.\chi_1(s)$	---

TABLE 9-1 (cont.)

$f(\eta)$	z	f (s)	f'' (s) exp (s^2)
ϵ_2	1	$\text{erf}(s).\Omega_2(s) + (\text{erf}(s))^2.\chi_1(s) + \text{erf}(s).(\psi(s))^2 + \psi(s).\chi_2(s)$	---
ϵ_3	1	$\text{erf}(s).\Omega_3(s) + (\text{erf}(s))^3.\psi(s)$	---
ϵ_4	1	$(\text{erf}(s))^2.\chi_2(s)$	...
ϵ_5	1/5	$(1-\text{erf}(s))^5$	$\frac{80}{\pi}\exp(-s^2)(1-\text{erf}(s))^3 + \frac{20}{\pi^{\frac{1}{2}}}(1-\text{erf}(s))^4$

and

$$\frac{d^2\chi_1}{ds^2} = -\left\{-2s\exp(-s^2)\int_0^s \frac{d^2[\psi(s)(1-\text{erf}(s))]}{ds^2}\cdot\exp(s^2)ds + \frac{d^2[\psi(s)(1-\text{erf}(s))]}{ds^2} + \frac{4s}{\pi^{\frac{1}{2}}}\exp(-s^2)\int_0^\infty \frac{d^2[\psi(s)(1-\text{erf}(s))]}{ds^2}\exp(s^2)\,ds\right\} \quad ...(9\text{-}5)$$

Hence in the overall expression for $f''(s)\exp(s^2)$, which can be obtained from equation (9-3) and which has to be integrated in equation (9-2) to obtain $\Omega_1(\eta)$, every term can be expressed analytically except for the integral $S = \int_0^s \frac{d^2[\Psi(s)(1-\mathrm{erf}(s))]}{ds^2} \exp(s^2)\, ds$ which occurs in equations (9-4) and (9-5), and the function χ_1. S and χ_1 were therefore tabulated as subsidiary functions of s and the tables used in the course of the numerical integration involved in equation (9-2).

Hence, by the use of equation (9-2) together with equations equivalent to (9-3), (9-4) and (9-5), all the functions from $\chi_1(\eta)$ to $\epsilon_5(\eta)$ could be calculated. These, together with $\Psi(\eta)$ are plotted vs. η in Figure 9-2. The function $\mathrm{erfc}(\eta)$ has been tabulated extensively and is not given here.

The universal constants A, B, C_1, etc. of equation (2-39) could then be obtained by the infinite integration with respect to η of $\mathrm{erfc}(\eta)$, $\Psi(\eta)$, etc. i.e.

$$A = \int_0^\infty \mathrm{erfc}(\eta)\, d\eta, \quad B = \int_0^\infty \Psi(\eta)\, d\eta, \quad C_1 = \int_0^\infty \chi_1(\eta)\, d\eta$$

etc.

Lin Hwang himself lacked the computing facilities to calculate these constants, but the first twelve from

FIG. 9·2

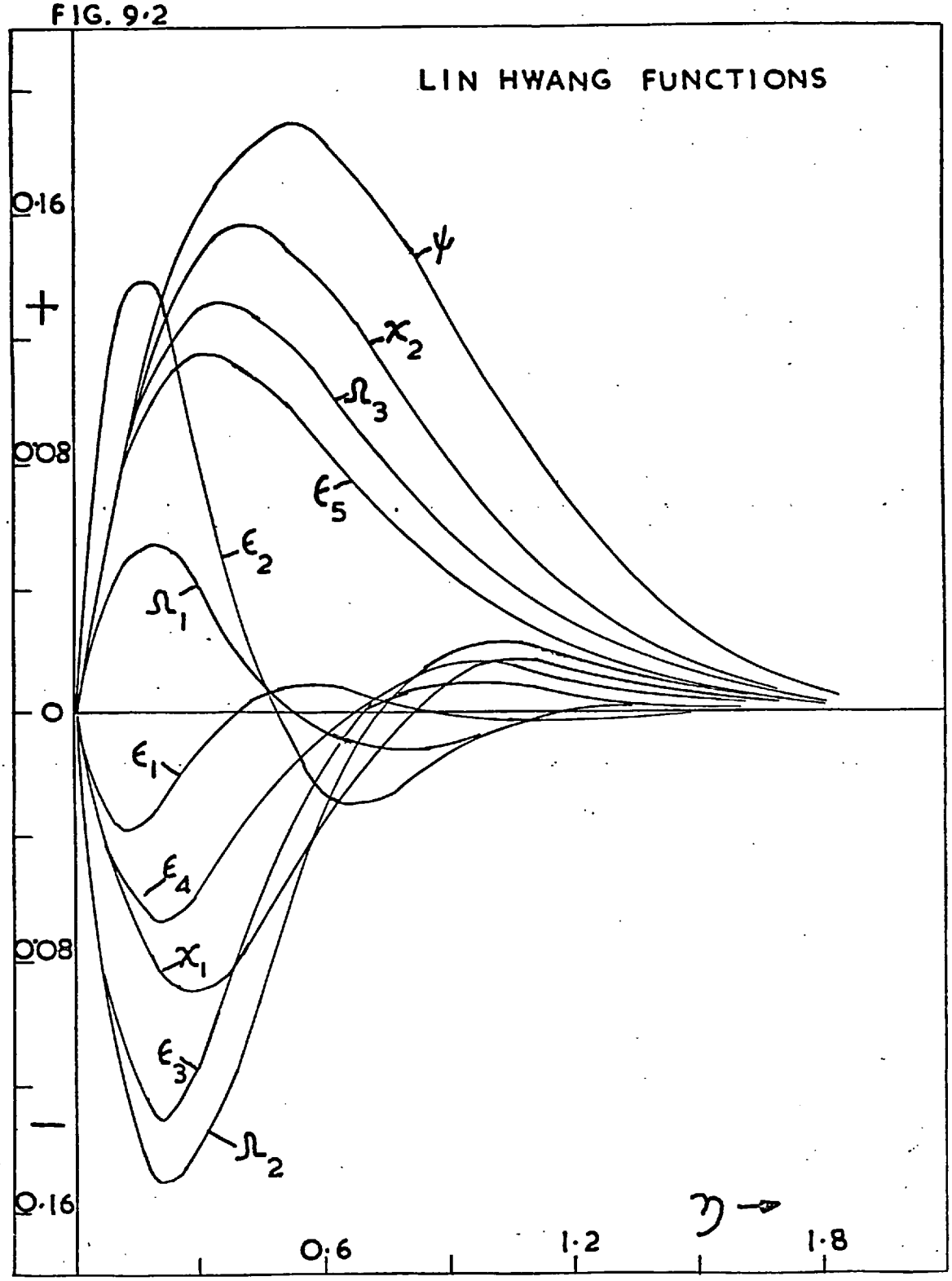
LIN HWANG FUNCTIONS
0·16
+
0·08
0
0·08
−
0·16
0·6
1·2
1·8
η →
ψ
χ2
Ω3
ε5
ε2
Ω1
ε1
ε4
χ1
ε3
Ω2

A to E_5 have now been determined using the University of London's Atlas Computer and are given in Table 9-2. The total computing time involved was about 1 hour.

TABLE 9-2

Lin Hwang's Procedure : Values of Universal Constants

Constant	Value	Constant	Value
A	0.5642 $(=\pi^{-\frac{1}{2}})$	D_3	0.1070
B	0.1796 $(=\pi^{-3/2})$	E_1	-0.006476
C_1	-0.03083	E_2	0.02908
C_2	0.1337	E_3	-0.03880
D_1	0.01168	E_4	-0.01888
D_2	-0.04763	E_5	0.08938

9.2.2 Determination of D-c relationships from the known Universal Constants

The series of simultaneous equations represented by equation (2-39) can be expressed in the form

$$(I_s)_n = a_n x_1 + b_n x_2 + c_n x_3 + \ldots + \ell_n x_{12} \qquad \ldots.(9\text{-}6)$$

where the subscript n refers to the n-th experimental measurement (of I_s and c_0). The unknowns x_1 - x_{12} to be calculated and the known coefficients a_n - ℓ_n, which include the universal constants, are listed in Table 9-3.

TABLE 9-3

Coefficients and Unknowns. Equation (9-6)

Unknown	Coefficient	Unknown	Coefficient
$x_1 = D^{\frac{1}{2}}_{c=0}$	$a_n = 2.257$	$x_7 = D^{\frac{1}{2}}_{c=0} \cdot \gamma$	$g_n = 0.4280(c_0)^3_n$
$x_2 = D^{\frac{1}{2}}_{c=0} \cdot \alpha$	$b_n = 0.7183(c_0)_n$	$x_8 = D^{\frac{1}{2}}_{c=0} \cdot \alpha^4$	$h_n = -0.0259(c_0)^4_n$
$x_3 = D^{\frac{1}{2}}_{c=0} \cdot \alpha^2$	$c_n = -0.1233(c_0)^2_n$	$x_9 = D^{\frac{1}{2}}_{c=0} \cdot \alpha^2\beta$	$i_n = 0.1163(c_0)^4_n$
$x_4 = D^{\frac{1}{2}}_{c=0} \cdot \beta$	$d_n = 0.5348(c_0)^2_n$	$x_{10} = D^{\frac{1}{2}}_{c=0} \cdot \alpha\gamma$	$j_n = -0.1552(c_0)^4_n$
$x_5 = D^{\frac{1}{2}}_{c=0} \cdot \alpha^3$	$e_n = 0.04673(c_0)^3_n$	$x_{11} = D^{\frac{1}{2}}_{c=0} \cdot \beta^2$	$k_n = -0.07552(c_0)^4_n$
$x_6 = D^{\frac{1}{2}}_{c=0} \cdot \alpha\beta$	$f_n = -0.1905(c_0)^3_n$	$x_{12} = D^{\frac{1}{2}}_{c=0} \cdot \delta$	$l_n = 0.3575(c_0)^4_n$

The simultaneous equations (9-6) cannot be solved directly using a 12 x 12 square matrix because a singular matrix would result. Instead, terms in $(c_0)^2_n$, $(c_0)^3_n$ and $(c_0)^4_n$ have to be combined to yield a 5 x 5 square matrix, the unknowns and coefficients of which are

$$X_1 = x_1, \quad X_2 = x_2, \quad X_3 = (-0.1233\ x_3 + 0.5348\ x_4),$$

$$X_4 = (0.04673\ x_5 - 0.1905\ x_6 + 0.4280\ x_7)$$

$$X_5 = (-0.02590\ x_8 + 0.1163\ x_9 - 0.1552\ x_{10} - 0.07552\ x_{11} + 0.3575\ x_{12})$$

and

$$A_n = a_n, \quad B_n = b_n, \quad C_n = (c_0)^2_n, \quad D_n = (c_0)^3_n, \quad E_0 = (c_0)^4_n$$

respectively.

If five sets of measurements only of I_s and c_0 are made then the matrix equation is

$$\begin{pmatrix} A_1 & B_1 & C_1 & D_1 & E_1 \\ \vdots & \vdots & \vdots & \vdots & \vdots \\ A_5 & B_5 & C_5 & D_5 & E_5 \end{pmatrix} \begin{pmatrix} X_1 \\ \vdots \\ X_5 \end{pmatrix} = \begin{pmatrix} (I_s)_1 \\ \vdots \\ (I_s)_5 \end{pmatrix} \qquad \ldots.(9\text{-}7)$$

However, it is preferable that many more than five sets of measurements should be made in order that the best I_s - c_0 relationship may be obtained from the minimum mean squares deviation technique. If m sets of measurements are made, or if m points are taken from the I_s - c_0 curve, then the matrix equation becomes

$$\begin{pmatrix} \sum_{n=1}^{m} A_n A_n & \sum_{n=1}^{m} B_n A_n & \sum_{n=1}^{m} C_n A_n & \sum_{n=1}^{m} D_n A_n & \sum_{n=1}^{m} E_n A_n \\ \vdots & \vdots & \vdots & \vdots & \vdots \\ \sum_{n=1}^{m} A_n E_n & \sum_{n=1}^{m} B_n E_n & \sum_{n=1}^{m} C_n E_n & \sum_{n=1}^{m} D_n E_n & \sum_{n=1}^{m} E_n E_n \end{pmatrix}$$

$$\begin{pmatrix} X_1 \\ \vdots \\ X_5 \end{pmatrix} = \begin{pmatrix} \sum_{n=1}^{m} (I_s)_n A_n \\ \vdots \\ \sum_{n=1}^{m} (I_s)_n E_n \end{pmatrix} \qquad \ldots.(9\text{-}8)$$

from which X_1 - X_5 are obtained.

Finally, the required values of $D_{c=0}$, α, β, etc. can be obtained from the equations

$$D_{c=0} = (X_1)^2, \qquad \alpha = X_2/X_1$$

$$\beta = \frac{X_3}{0.5348\ X_1} + \frac{0.1233\alpha^2}{0.5348},$$

$$\gamma = \frac{X_4}{0.4280\ X_1} + \frac{0.1905\alpha\beta}{0.4280} - \frac{0.04673\alpha^3}{0.4280},$$

and

$$\delta = \frac{X_5}{0.3575\ X_1} + \frac{0.02590\alpha^4}{0.3575} - \frac{0.1163\alpha^2\beta}{0.3575} + \frac{0.1552\alpha\gamma}{0.3575} + \frac{0.07552\beta^2}{0.3575}$$

so that the D-c relationship $D = D_{c=0}(1 + \alpha c + \beta c^2 + \gamma c^3 + \delta c^4)$ can be determined. An analogous procedure can be used if less than five polynomial terms are required.

9.2.3 Applicability of the Lin Hwang Procedure.

Equation (9-6) can be combined with $\bar{D}_s = \pi I_s^2/16$ to yield (dropping the subscript n)

$$\bar{D}_s = D_{c=0}\,(1 + 0.637\ (\alpha c_0) + 0.474\ (\beta c_0^2) + 0.379\ (\gamma c_0^3) + 0.317\ (\delta c_0^4) - 0.008\ (\alpha c_0)^2 + 0.007\ (\alpha c_0)^3 - 0.007(\alpha c_0)^4 - 0.018\ (\alpha c_0)\ (\beta c_0^2) + 0.023\ (\alpha c_0)^2\ (\beta c_0^2) - 0.011\ (\beta c_0^2)^2 - 0.017\ (\alpha c_0)\ (\gamma c_0^3) + ...) \qquad ....(9\text{-}9)$$

In order for the cross terms and the terms involving powers of (αc_0) etc. to become negligible or converge rapidly, it is obvious from equation (9-9) that (αc_0), (βc_0^2), etc. must remain small. Practically, for the D-c dependence to be established accurately using the first twelve of the universal constants, the individual values of (αc_0), (βc_0^2), etc. should certainly remain numerically less than unity and probably less than ~ 0.8. In addition, the values of the cross coefficients of equation (9-9) indicate that the sum $f(c_0) = (\alpha c_0) + (\beta c_0^2) + \ldots$, for $D = D_{c=0}\ (1 + f(c_0))$, should perhaps also remain numerically less than unity.

The latter condition implies that the Lin Hwang procedure would be more often useful for systems where D decreases with increasing c, for which $|f(c)| < 1$. To test this, the Lin Hwang procedure is compared in Table 9-4 with the procedure of Crank[77], involving weighted mean diffusion coefficients, for the functions (D) and (D') of section 9.1, i.e.

$$D = D_{c=0}\ (1 + 1.8c - 0.09\ c^2)$$

and $$D = D_{c=0}\ (1 - 0.18c + 0.009\ c^2)$$

respectively, starting from the computed values of I_s for various c. The D-c dependence obtained from each procedure

is also compared with the true D-c dependence which was calculated analytically.

TABLE 9-4

Comparison of Diffusion Coefficients from Weighted Mean (WM) and Lin Hwang (LH) Procedures

c	Function (D)			Function (D')		
	$D/D_{c=0}$ WM	$D/D_{c=0}$ LH*	True $D/D_{c=0}$	$D/D_{c=0}$ WM	$D/D_{c=0}$ LH#	True $D/D_{c=0}$
0	-	1.09	1.00	-	1.00	1.00
1	2.64	2.61	2.71	0.779	0.834	0.829
2	4.09	4.00	4.24	0.695	0.681	0.676
3	5.73	4.66	5.59	0.540	0.546	0.541
4	-	-	-	0.417	0.431	0.424
5	-	-	-	0.320	0.343	0.325
6	-	-	-	0.244	0.289	0.244

* 4 term polynomial # 5 term polynomial

Up to c=5 the LH procedure for the function (D') is at least as good as the WM procedure. However, for $c \geq 6$ the former begins to fail since the term $|\ 0.18c\ |$ becomes greater than unity. For the function (D) the LH procedure fails above c=1 since f(c) is already greater than unity. For the functions (A'), (B') and (C') of section 9.1, where D decreases with c, the LH procedure was found to be applicable up to c=8 or 9, but only over much smaller ranges for D as the corresponding increasing functions of c. Even for the function (A) (i.e. $D=D_{c=0}\ (1 + 0.009\ c^3)$) the method holds

only up to c=5, when f(c) = 1.1.

In general, therefore, the LH procedure will yield accurate D-c data only for the smallest concentration dependences of C. For such systems the WM procedure still yields quite a good approximation to the D-c dependence.

9.2.4 Determination of the Weighting Value p for Weighted Mean Diffusion Coefficients using the Lin Hwang Procedure

When D varies only slightly with c then the question arises as to whether the change from p = 1.67 to p = 1.85 is gradual as D changes from an increasing to a decreasing function of c or whether it is abrupt at the limit of zero concentration dependence. For D expressed as a polynomial in c, the LH procedure can throw some light on this. Thus equation (9-9) can be compared with equation (2-40) which is

$$\bar{D}_s = D_{c=0}\left(1 + \frac{p}{1+p}(\alpha c_0) + \frac{p}{2+p}(\beta c_0^2) + \frac{p}{3+p}(\gamma c_0^3) + \frac{p}{4+p}(\delta c_0^4) + \ldots.\right)$$

The comparison yields

$$0.637\,(\alpha c_0) + 0.474\,(\beta c_0)^2 + \ldots. = \frac{p}{1+p}(\alpha c_0) + \frac{p}{2+p}(\beta c_0^2) + \ldots \qquad \ldots.(9\text{-}10)$$

Dividing each side by αc_0 gives

$$0.637 \ (= 2/\pi) + 0.474 \ (\beta c_0/\alpha) + \ldots$$

$$= \frac{p}{1+p} + \frac{p}{2+p} \quad (\beta c_0/\alpha) + \ldots.$$

Hence for any polynomial in c_0 having α non-zero, as $c_0 \rightarrow 0$, so

$$\frac{p}{1+p} \rightarrow \frac{2}{\pi}$$

or $$p \rightarrow \frac{2}{\pi - 2} \quad \text{or} \quad 1.75.$$

This value is approximately the mean of 1.67 and 1.85, Crank's empirical values for D increasing and decreasing with c respectively. Similar comparisons can be carried out for special polynomials. For example, when $\alpha = 0$ then $p \rightarrow 1.80$ as $c_0 \rightarrow 0$, when $\alpha = \beta = 0$ then $p \rightarrow 1.83$ as $c_0 \rightarrow 0$ and when $\alpha = \beta = \gamma = 0$ then $p \rightarrow 1.85$ as $c_0 \rightarrow 0$. However, in most cases it is expected that α will be non-zero so that p will tend to 1.75 in general for $c_0 \rightarrow 0$.

Equation (9-10) can also be used to determine values for p for small (αc_0), (βc_0^2) etc., i.e. for non-zero c_0. This has been carried out and values of p for various values of (αc_0), (βc_0^2) and (γc_0^3) are given in Table 9-5.

TABLE 9-5

Values of Weighting Parameter p for various Polynomial Expressions and Concentration Ranges

αc_0	βc_0^2	γc_0^3	p
+ 0.5	0	0	1.73
- 0.5	0	0	1.80
+ 0.8	0	0	1.71
- 0.8	0	0	1.86
0	+ 0.5	0	1.76
0	- 0.5	0	1.84
+ 0.5	+ 0.5	0	1.74
- 0.5	- 0.5	0	1.88
+ 0.25	+ 0.25	+ 0.25	1.77*
- 0.25	- 0.25	- 0.25	1.84

In every case the value of p for D decreasing with c is higher than the corresponding value for D increasing with c. In addition it seems that p lies between $\lim_{c_0 \to 0}$ (p) and 1.67 for D increasing with c and between $\lim_{c_0 \to 0}$(p) and 1.85 for D decreasing with c. Thus the values of 1.86 and 1.88 obtained for p are possibly slightly inaccurate because in one case (αc_0) = -0.8 and in the other $f(c_0)$ = -1 so that these situations are such that the $\overline{D}_s$ - c_0 relationship is probably not expressed sufficiently accurately using only twelve of the universal constants. The (starred) value of 1.77 for p, which is outside the 1.75 - 1.67 range perhaps arises because no terms involving powers of (γc_0^3) are used.

More precise estimates of p would require the (very tedious) determination of a large number of the universal constants.

9.3 Random Polycondensation Model : Derivation of Expressions for $\overline{\overline{E}}_D$, $\overline{\overline{\Delta H}}_A$ and $\overline{\overline{\Delta S}}_A$.

9.3.1 $\overline{\overline{E}}_D$

Equations (2-121) to (2-124) are

$$E_D = E_{D(c=0)} - 3R\left(\frac{\partial \ln (k-K)}{\partial (1/T)}\right)_c - R\left(\frac{\partial \ln\left[\frac{8k}{k} - \frac{3(k-K)}{c}\right]}{\partial (1/T)}\right)_c \quad \ldots.(9\text{-}11),$$

$$\frac{\partial \ln K}{\partial (1/T)} = -\Delta H/R \quad \ldots.(9\text{-}12a),$$

$$\ln (K/K_0) = -\Delta H/R \quad (1/T - 1/T_0) \quad \ldots.(9\text{-}12b),$$

$$C = \frac{4c}{3K_0} \quad \ldots.(9\text{-}13)$$

and

$$k = K\left(1 + \frac{3K_0 C}{K}\right)^{\frac{1}{2}} \quad \ldots.(9\text{-}14)$$

If equation (9-14) is now written as

$$k = KX \quad \ldots.(9\text{-}15)$$

where

$$X = \left(1 + \frac{3K_0 C}{K}\right)^{\frac{1}{2}} = \left(1 + 3C \exp\left[\frac{\Delta H}{R}\left(\frac{1}{T} - \frac{1}{T_0}\right)\right]\right)^{\frac{1}{2}} \quad \ldots.(9\text{-}16)$$

then equation (9-11) becomes

$$\bar{E}_D = E_{D(c=0)} - 3R\left(\frac{\partial \ln K}{\partial (1/T)}\right) - 3R\left(\frac{\partial \ln (X-1)}{\partial (1/T)}\right)_C - R \cdot \left(\frac{\partial \left[\ln 8/X - \frac{4K(X-1)}{K_o C}\right]}{\partial (1/T)} \right)_C \quad \ldots.(9\text{-}17)$$

From equation (9-16), $\frac{K}{K_o} = \frac{3C}{X^2-1}$ so that equation (9-17) can be re-written in terms of ΔH and X only,

$$\bar{E}_D = E_{D(c=0)} + 3\Delta H - 3R\left(\frac{\partial \ln(X-1)}{\partial (1/T)}\right)_C - R\left(\frac{\partial \ln \left[8/X - \frac{12}{X+1}\right]}{\partial (1/T)}\right)_C$$

$$\text{or } \bar{E}_D = E_{D(c=0)} + 3\Delta H - 3R\left(\frac{\partial \ln(X-1)}{\partial (1/T)}\right)_C - R\left(\frac{\partial \ln \left[\frac{8-4X}{X(X+1)}\right]}{\partial (1/T)}\right)_C \quad \ldots.(9\text{-}18)$$

Removal of all the logarithmic expressions yields

$$\bar{E}_D = E_{D(c=0)} + 3\Delta H - \frac{3R}{(X-1)}\left(\frac{\partial (X-1)}{\partial (1/T)}\right)_C + \frac{R}{(2-X)}\left(\frac{\partial (X-2)}{\partial (1/T)}\right)_C + \frac{R}{X}\left(\frac{\partial X}{\partial (1/T)}\right)_C + \frac{R}{(X+1)}\left(\frac{\partial (X+1)}{\partial (1/T)}\right)_C .$$

But $\frac{\partial (X-1)}{\partial (1/T)} = \frac{\partial (X-2)}{\partial (1/T)} = \frac{\partial (X+1)}{\partial (1/T)} = \frac{\partial X}{\partial (1/T)}$

and from equation (9-16)

$$\frac{\partial X}{\partial (1/T)} = \frac{\Delta H}{2R} \cdot \frac{(X^2-1)}{X}, \text{ so that}$$

$$\bar{E}_D = E_{D(c=0)} + 3\Delta H + \frac{\Delta H}{2} \cdot \frac{(X^2-1)}{X}\left[\frac{-3}{(X-1)} + \frac{1}{(2-X)} + \frac{1}{X} + \frac{1}{(X+1)}\right] \quad \ldots.(9\text{-}19)$$

Finally, equation (9-19) can be re-arranged to yield

$$\bar{E}_D = E_{D(c=0)} + \Delta H \cdot \frac{(X-1)}{X}\left[2 + \frac{(X+1)}{X(2-X)}\right] \qquad ....(9\text{-}20)$$

9.3.2 $\overline{\Delta\bar{H}_A}$

Equation (2-127) is

$$\Delta\bar{H}_A = 4R\left(\frac{\partial \ln(k-K)}{\partial\,(1/T)}\right)_c - R\left(\frac{\partial \ln K}{\partial(1/T)}\right) \qquad ....(9\text{-}21)$$

From equations (9-13) to (9-16) this becomes

$$\overline{\Delta\bar{H}_A} = 3R\left(\frac{\partial \ln K}{\partial\,(1/T)}\right) + 4R\left(\frac{\partial \ln(X-1)}{\partial\,(1/T)}\right)_C \qquad ....(9\text{-}22)$$

Applying equation (9-12a) and removing the logarithmic term from equation (9-22) yields

$$\overline{\Delta\bar{H}_A} = -3\Delta H + \frac{4R}{(X-1)} \cdot \left(\frac{\partial X}{\partial(1/T)}\right)_C$$

As $\partial X/\partial(1/T) = \frac{\Delta H}{2R} \cdot \frac{(X^2-1)}{X}$, $\overline{\Delta\bar{H}_A}$ is given by

$$\overline{\Delta\bar{H}_A} = -3\Delta H + 2\Delta H \cdot \frac{(X+1)}{X}$$

or $$\overline{\Delta\bar{H}_A} = \Delta H \cdot \frac{(2-X)}{X} \qquad ....(9\text{-}23)$$

9.3.3 $\overline{\Delta\bar{S}_A}$

Equation (2-52) is

$$\Delta\bar{S}_A = -R\left(\ln(p/p_o) + \frac{\partial \ln(p/p_o)}{\partial \ln (T)}\right)_c \qquad ....(9\text{-}24)$$

Since $(p/p_o) = \frac{27(k-K)^4}{64\ Kc^3}$, equation (9-24) becomes

$$\Delta\bar{S}_A = -R\left\{\ln\left[\frac{27(k-K)^4}{64\ Kc^3}\right] - \frac{3}{T}\left(\frac{\partial \ln K}{\partial(1/T)}\right) - \frac{4}{T}\left(\frac{\partial \ln\left[(1+\frac{4c}{K})^{\frac{1}{2}} -1\right]}{\partial(1/T)}\right)_c\right\} \quad ....(9\text{-}25)$$

When equation (9-13) is applied, equation (9-25) becomes

$$\overline{\Delta\bar{S}}_A = -R\left\{3\ln(K/K_o) + 4\ln\left[(1+\frac{3K_oC}{K})^{\frac{1}{2}} -1\right] - 3\ln(C) - \frac{3}{T}\left(\frac{\partial \ln K}{\partial(1/T)}\right) - \frac{4}{T}\left(\frac{\partial \ln\left[(1+\frac{3K_oC}{K})^{\frac{1}{2}} -1\right]}{\partial(1/T)}\right)_C\right\}$$

Application of equations (9-12), (9-14), (9-15) and (9-16) then yields

$$\overline{\Delta\bar{S}}_A = -R\left(\frac{3\Delta H}{RT_o} + 4\ln(X-1) - 3\ln(C) - \frac{4}{T}\left(\frac{\partial \ln(X-1)}{\partial(1/T)}\right)_C\right) \quad ....(9\text{-}26)$$

Again, $$\frac{\partial \ln(X-1)}{\partial(1/T)} = \frac{1}{(X-1)}\cdot\left(\frac{\partial X}{\partial(1/T)}\right)$$

$$= \frac{1}{(X-1)}\cdot\frac{\Delta H}{2R}\cdot\frac{(X^2-1)}{X} = \frac{\Delta H}{2R}\cdot\frac{(X+1)}{X}$$

so that equation (9-26) becomes

$$\overline{\Delta\bar{S}}_A = \left(-\frac{3\Delta H}{T_o} + \frac{2\Delta H}{T}\cdot\frac{(X+1)}{X} - 4R\ln(X-1) + 3R\ln(C)\right) \quad ....(9\text{-}27)$$

9.4 The effect on the Time Lag of Water Sorption on the Glass Walls of the Receiving Vessel.

The data of Frank[120] and Barrett and Gauger[121] for the sorption of water by washed pyrex glass at 25°C in the relative humidity range (1-30) x 10^{-3} are well represented by

$$Q = 1.73 \times 10^{-4} \, p_e^{0.422} \qquad \ldots.(9\text{-}28)$$

where Q is the amount sorbed in cc.s.t.p. cm^{-2} at an equilibrium pressure p_e (mm.Hg).

To investigate the effect of equation (9-28) on time lags for water, the published data for the ethyl cellulose-water system[42,51] are considered. For a pressure increase from 0.02 to 0.40 mm.Hg, equation (9-28) indicates that appreciable sorption of water by the glass walls will occur as sorption proceeds. Further, sorption equilibrium is virtually attained in ~15 minutes[120], a time which is short compared with that taken to complete a permeation experiment[42].

Although D was observed to decrease with c for the ethylcellulose-water system, the following calculations treat D as constant (for convenience) and equal to 2.7 x 10^{-7} $cm.^2$ $sec.^{-1}$. The ingoing concentration c is in the range 0-80 cc.s.t.p. $cm.^{-3}$ and the membrane thickness (ℓ)

and cross-sectional area (G) are taken as 0.108 cm. and 0.3 cm^2 respectively. For no sorption of water vapour by the walls of the measuring section, the increase in the outgoing pressure p_1 with time is given by

$$p_1 = \frac{DxGx298.2x760}{V \times 273.2}\left(\frac{ct}{\ell} - \frac{c\ell}{6D}\sum_{n=1}^{\infty}\left[1+\frac{12(-1)^n}{\pi^2 n^2}\exp\left(\frac{-n^2\pi^2 Dt}{\ell^2}\right)\right]\right) \quad \ldots.(9\text{-}29)$$

where V is the volume (cc.) of the measuring section of the apparatus. The effect of sorption on the glass is to reduce the pressure p_1 at time t to some value p_2. As a rough approximation the amount of water sorbed by the walls at time t is taken as the amount in equilibrium with a pressure p_e^1, where p_e^1 is equated with the value of p_1 at a time (t-600) sec. From equation (9-28), the amount sorbed at time t is

$$1.73 \times 10^{-4} \cdot (p_e^1)^{0.422} \cdot A$$

where A is the surface area of the glass walls. This amount of sorption corresponds to a reduction in the pressure p_1 by an amount p' given by

$$p' = 1.73x10^{-4}.(p_e^1)^{0.422} \cdot A \cdot \frac{760 \times 298.2}{273.2 \times V} \text{ (mm.Hg)} \quad \ldots.(9\text{-}30)$$

As $p_2 = p_1 - p'$, the change in p_2 with time follows from equations (9-29) and (9-30). In the "pretreatment" technique[42] p_1 at zero time is ~ 0.02 mm.Hg so that the vapour pressure is now given by

$$p_3 = p_2 + p' + 0.02 - p'' = p_1 + 0.02 - p'' \quad \ldots\ldots(9\text{-}31)$$

as illustrated in Figure 9-3 by a typical example from the calculations.

Permeation curves of p_1, p_2 and p_3 vs. t were constructed for various c, assuming a spherical measuring section i.e. $A = 4.84\ V^{2/3}$. To attempt to simulate the experimental procedures used, two conditions were examined:

a) V was constant and equal to 1000 cm^3.

b) V increased with c according to $V=25\ c\ (cm^3)$ so that p_1 was confined to a given range regardless of c.

The effect of sorption on the variation of L with c is shown in Figure 9-4 and the effect on the steady state flux $\frac{d}{dt}(pV)$ is shown in Figure 9-5.

Clearly the sorption of water by the glass walls of the apparatus can have a marked effect on L for both the conditions a) and b). "Pretreatment" of the glass surface

FIG. 9-3

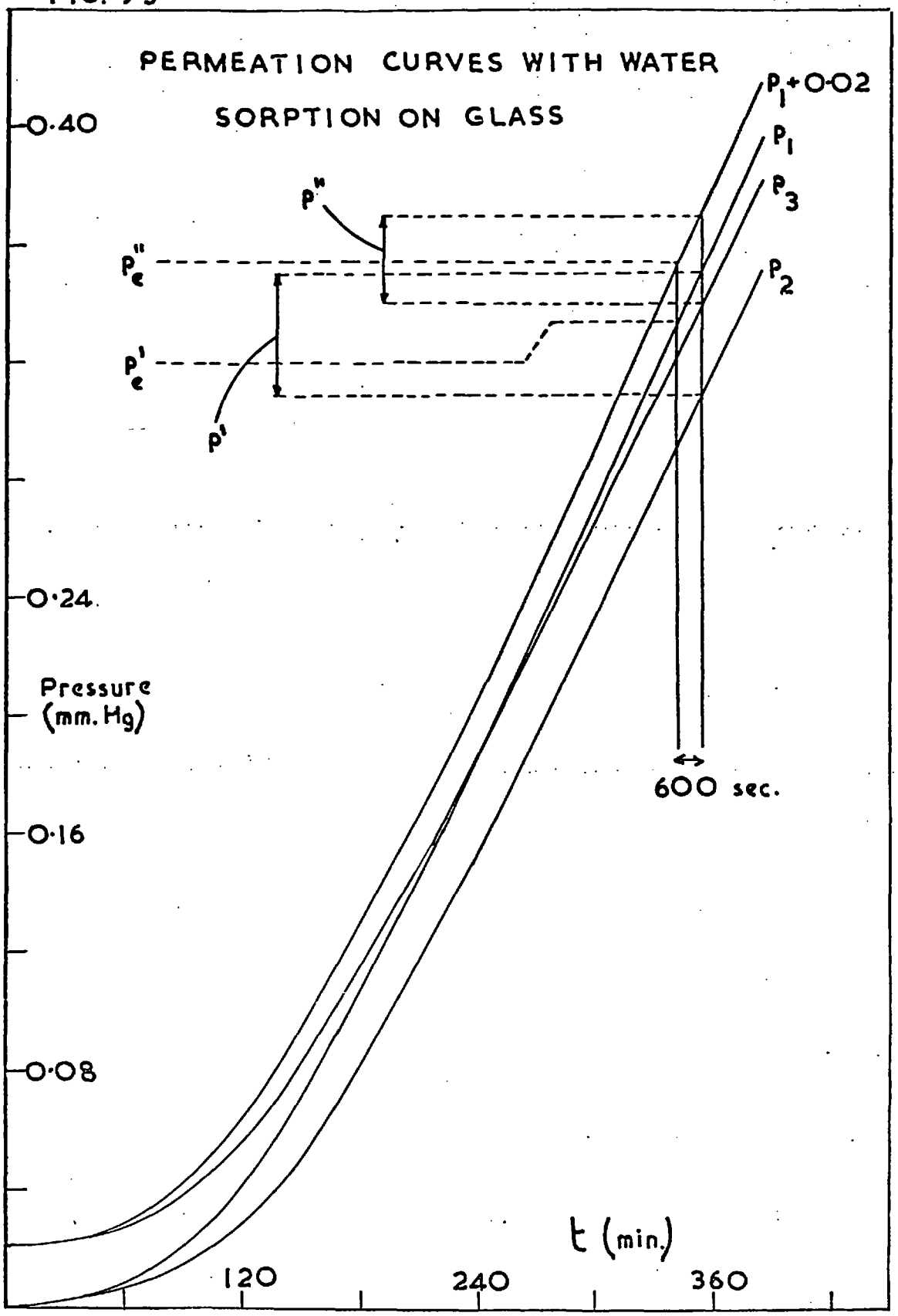
PERMEATION CURVES WITH WATER SORPTION ON GLASS
P1+0·02
P1
P3
P2
P''
P''e
P'e
P'
0·40
0·24
0·16
0·08
Pressure (mm. Hg)
600 sec.
t (min.)
120
240
360

reduces considerably this effect but does not eliminate it completely. As indicated previously the calculations are only approximate and in addition factors such as the nature, treatment, temperature and geometry of the glass surface will also affect the final result. For example, if A/V remains constant for condition b) then L will be independent of c but in error by a constant amount. In general, however, sorption by the glass in the region of low pressures will tend to cause L to decrease with increasing c.

9.5 Variation of I_s with c for various D-c Relationships

A number of D-c relationships for which D increases or decreases by one order of magnitude from its value at c=0 are considered. The functions of section 9.1 are employed with $D_{c=0} = 10^{-7}$ cm.^{2} sec.$^{-1}$, i.e.

(A) $D = 10^{-7}(1 + 0.009c^3)$ (A') $D = 10^{-7}(1 - 0.0009c^3)$

(B) $D = 10^{-7}(1 + 0.09c^2)$ (B') $D = 10^{-7}(1 - 0.009c^2)$

(C) $D = 10^{-7}(1 + 0.9c)$ (C') $D = 10^{-7}(1 - 0.09c)$

(D) $D = 10^{-7}(1+1.8c-0.09c^2)$ (D') $D = 10^{-7}(1-0.18c+0.009c^2)$

with c varying in the range 0-10. The explicit finite difference scheme, outlined in section 2.3.4, was used to calculate the I_s-c relationships which are shown in Figure 9-6.

FIG. 9·4

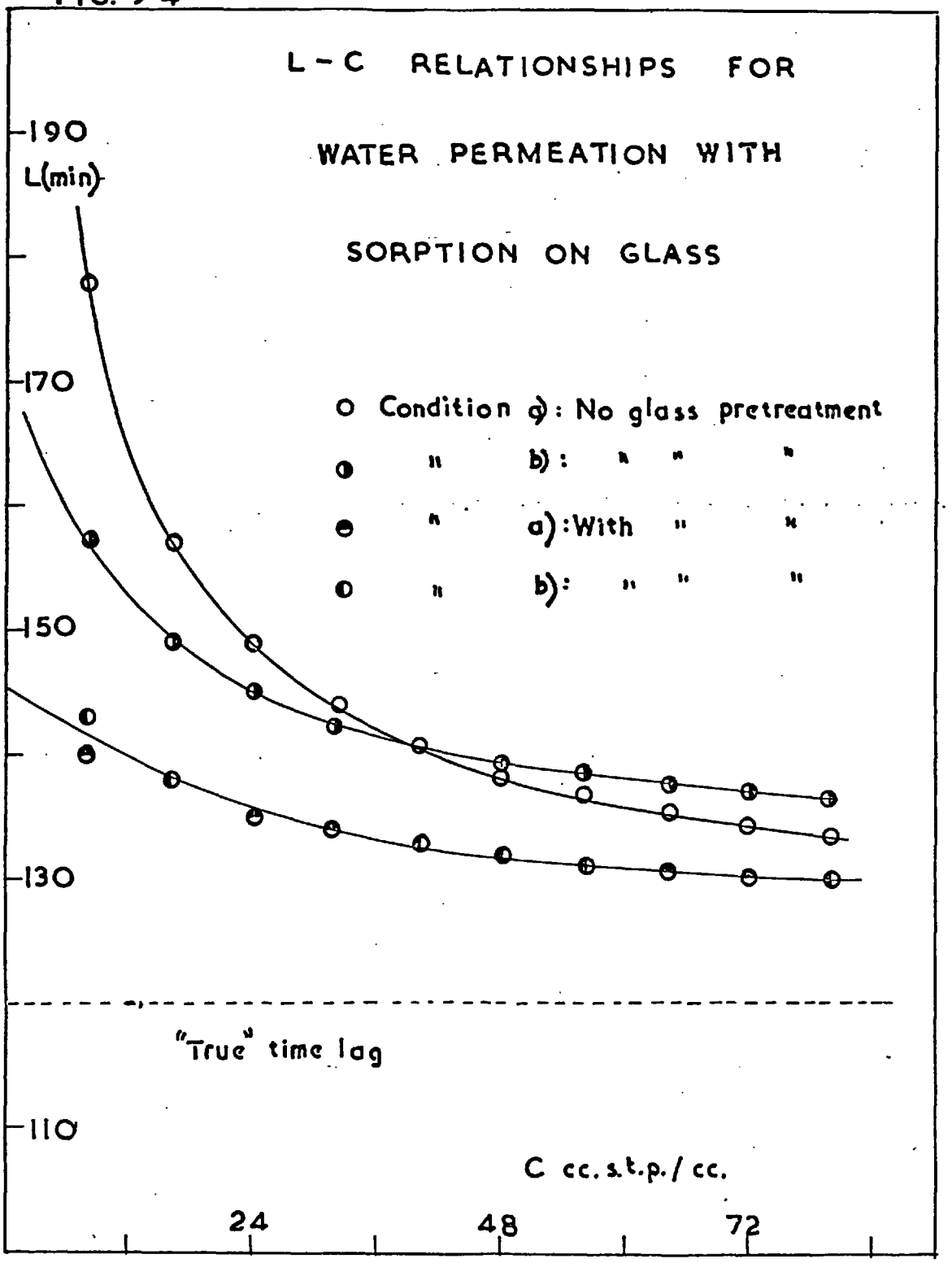
L - C RELATIONSHIPS FOR
WATER PERMEATION WITH
SORPTION ON GLASS
190
L(min)
170
150
130
110
O Condition a): No glass pretreatment
" b): " " "
" a): With " "
" b): " " "
"True" time lag
C cc. s.t.p./cc.
24
48
72

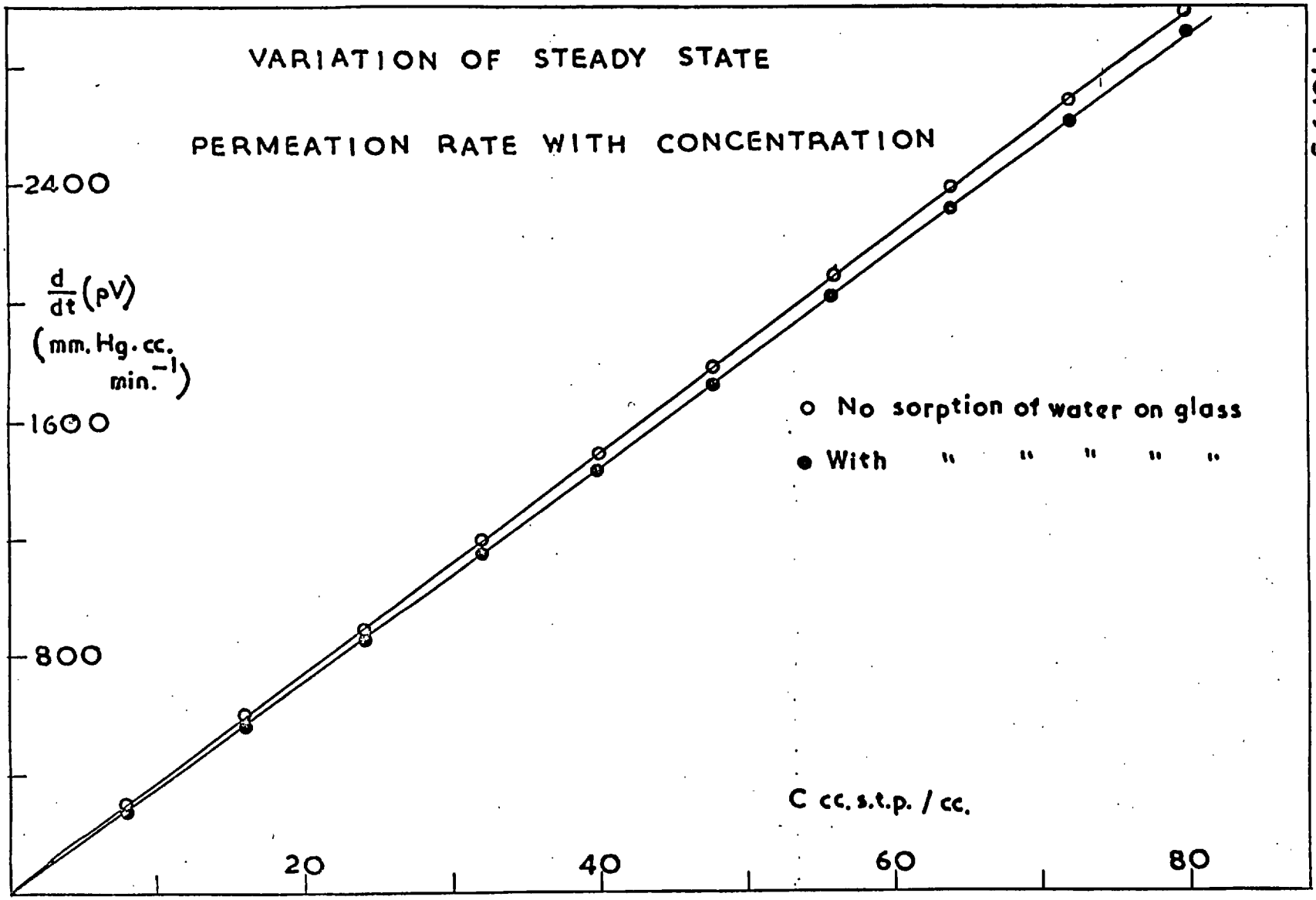
VARIATION OF STEADY STATE
PERMEATION RATE WITH CONCENTRATION
2400
1600
800
d/dt (pV)
(mm. Hg. cc. min.⁻¹)
o No sorption of water on glass
● With " " " " "
C cc. s.t.p. / cc.
20
40
60
80

FIG. 9.5

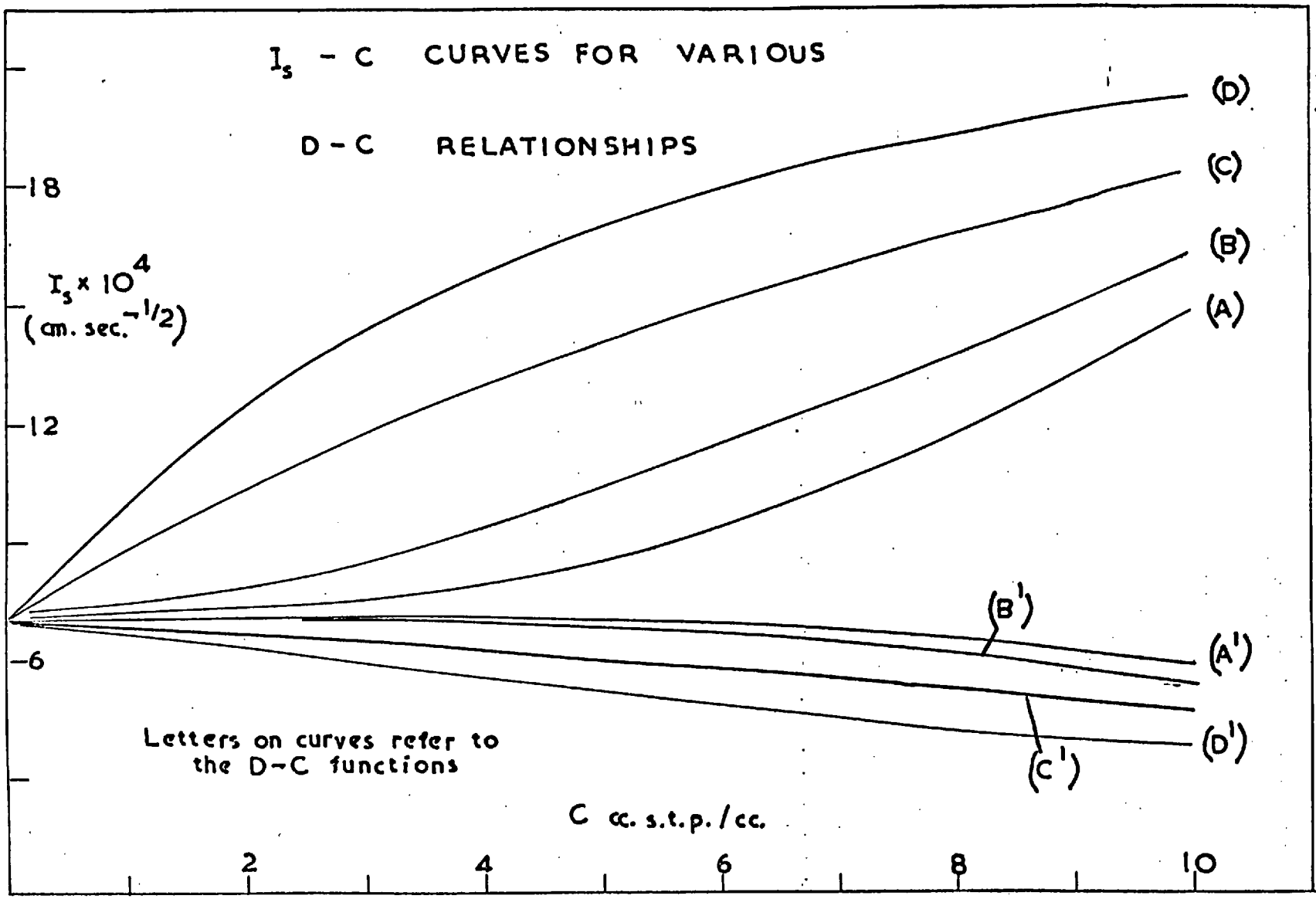
I_s - C CURVES FOR VARIOUS
D - C RELATIONSHIPS
18
12
6
$I_s \times 10^4$
(cm. sec.$^{-1/2}$)
(D)
(C)
(B)
(A)
(B')
(A')
(D')
(C')
Letters on curves refer to
the D-C functions
C cc. s.t.p./cc.
2
4
6
8
10

FIG. 9.6

It is obvious from Figure 9-6 that the relative variations in I_s with c are significantly less when D decreases with c than for the corresponding functions when D increases with c.

9.6 Equilibrium Sorption Data

Symbols used in Tables

k = sensitivity of quartz spiral ($cm.g.^{-1}$)

V = volume of polymer sample (cm^3)

c = concentration of water (methanol) ($cc.s.t.p.\ cm.^{-3}$)

p = vapour pressure (cm.Hg.)

p_o = saturation vapour pressure (cm.Hg)

$T_s\,^oC$ = temperature of sample

$T_b\,^oC$ = temperature of balance head (Sartorius)

All the values of c given in the following tables include buoyancy corrections and blank corrections when appropriate.

9.6.1 Polymethacrylates and PPA

The quartz spiral was used for PMMA, PEMA, PPMA and PBMA, and the Sartorius balance for PPA.

TABLE 9-6

PMMA - H_2O

k = 37.3 (37.8 for T_s=59.8°C) V = 0.482

T_s °C and p_o	c	p	c	p	c	p	c	p
T_s=40.5	1.6	0.59	4.4	1.65	8.2	2.67	14.2	4.03
p_o=5.68	19.2	4.82	13.6	3.86	2.9	1.02		
T_s=50.2	1.8	0.94	7.4	4.02	18.4	7.76	16.2	7.10
p_o=9.34	5.1	2.86						
T_s=59.8	2.1	1.85	3.7	3.31	6.8	5.85	10.9	8.72
p_o=14.8	15.1	10.7	17.6	11.9	14.9	10.1	5.4	3.75
	3.2	2.08						
T_s=70.0	1.6	2.28	3.2	4.67	11.6	14.3	19.0	19.6
p_o=23.4	14.2	16.4	4.9	6.65				

TABLE 9-7

PEMA - H_2O

k = 37.3 V = 0.493

T_s °C and p_o	c	p	c	p	c	p	c	p
T_s=30.0	1.4	0.44	2.1	0.76	3.3	1.19	5.0	1.66
p_o=3.17	7.8	2.23	11.7	2.76	10.2	2.59	7.3	2.06
	3.4	1.01						
T_s=39.9	1.0	0.47	1.7	1.06	2.9	1.66	4.6	2.32
p_o=5.50	6.9	3.38	9.1	4.20	13.0	5.29	11.7	4.96
	5.9	2.99	2.5	1.31				
T_s=49.5	0.9	0.97	1.9	1.66	3.4	2.81	5.3	4.18
p_o=9.03	7.3	5.34	10.7	6.96	13.6	8.05	10.0	6.64
	3.5	2.42	2.1	1.85				
T_s=60.2	1.1	1.50	2.6	3.56	4.1	5.19	6.3	7.71
p_o=15.1	7.8	8.90	10.9	11.2	14.9	13.7	14.4	13.6
	10.1	10.4	3.0	3.41	1.0	1.34	3.3	4.37
	7.1	8.42	12.9	12.8				
T_s=70.0	0.8	1.88	2.4	4.65	4.3	7.86	5.8	10.3
p_o=23.3	8.7	14.2	11.9	17.9	16.0	21.3	11.9	17.5
	9.8	15.2	5.8	10.2	1.7	3.38		
T_s=79.7	0.6	1.36	1.5	3.75	2.3	5.19	3.7	8.69
	5.6	12.7	7.2	15.8	8.7	18.0	10.5	21.1
p_o=35.1	16.1	29.2	17.4	30.5	14.4	27.1	9.5	20.1
	1.9	4.35						

TABLE 9-8

PPMA - H_2O

k = 37.3 V = 0.420

T_s °C and p_o	c	p	c	p	c	p	c	p
T_s=32.0	0.7	0.57	1.7	1.24	2.8	1.90	3.5	2.25
p_o=3.56	5.0	2.81	6.6	3.34	5.7	3.06	5.2	2.92
T_s=37.1	0.4	0.45	1.0	1.02	1.5	1.53	2.3	2.03
p_o=4.74	2.1	1.85	3.3	2.65	4.2	3.39	5.8	3.95
	6.8	4.27	4.3	3.18				
T_s=41.9	1.4	1.51	2.2	2.47	3.2	3.14	4.4	3.86
p_o=6.13	5.51	4.42	5.5	4.45	6.4	4.99	7.2	5.31
	3.7	3.48	3.1	2.79				
T_s=49.6	1.8	2.49	2.7	3.33	3.7	4.52	4.8	5.70
p_o=9.07	6.6	6.84	8.0	8.32	3.6	4.57	2.6	3.23
	1.3	1.71	4.9	5.78	5.8	6.60		
T_s=55.6	0.6	1.34	0.8	1.79	1.4	2.50	1.9	3.38
p_o=12.1	2.6	4.28	4.0	5.83	5.3	7.36	6.6	8.62
	8.3	9.79	8.8	10.0	9.5	10.2	2.6	4.07
	1.1	2.00						
T_s=64.4	0.7	1.85	1.7	4.22	2.6	5.66	3.3	6.99
	4.1	8.55	4.9	9.89	7.0	12.9	8.2	14.5
p_o=18.3	2.1	4.65						

TABLE 9-9

PBMA - H_2O

k = 37.3 V = 0.461

T_s °C and p_o	c	p	c	p	c	p	c	p
	0.4	0.40	1.0	0.79	2.1	1.16	2.4	1.34
T_s=27.0	3.0	1.66	3.7	1.92	5.0	2.25	6.1	2.32
	4.2	1.93	2.4	1.21	0.5	0.50	1.4	0.96
p_o=2.67	2.2	1.28	3.0	1.83	4.3	2.12	5.8	2.43
	4.5	2.27	2.7	1.75				
T_s=34.1	0.4	0.24	0.6	0.50	1.1	1.18	1.6	1.33
p_o=4.02	2.2	1.73	3.0	2.39	4.0	2.86	5.3	3.36
	3.0	2.37	1.5	1.28				
T_s=40.4	0.7	0.77	1.2	1.46	1.5	2.06	2.5	2.67
p_o=5.65	3.2	3.19	3.9	3.86	4.4	4.22	6.1	4.86
	3.3	3.58	2.7	2.69				
T_s=49.6	0.5	0.91	1.0	1.95	1.7	2.72	2.3	3.39
p_o=9.09	3.1	4.60	4.3	5.80	5.0	6.82	6.5	8.01
	2.0	3.33	1.5	2.35				
T_s=55.6	0.9	1.76	1.3	2.55	1.7	3.31	2.7	5.12
p_o=12.1	4.0	7.01	5.4	8.75	6.7	10.0	4.8	7.96
	2.3	4.27						

TABLE 9-10

PPA - H_2O

1 cc.s.t.p. ≡ 805μg. V = 0.306

T_s °C and p_o	c	p	c	p	c	p	c	p
T_s=48.9	0.73	0.65	2.04	1.61	1.78	1.52	3.71	2.98
p_o=8.76	3.20	2.60	6.57	4.75	9.85	6.41	10.6	6.71
	7.92	5.53	5.21	4.01	4.73	3.70	5.90	4.34

TABLE 9-11

PEMA - MeOH

k = 37.3 V = 0.493

T_s °C and p_o	c	p	c	p	c	p	c	p
T_s=29.8	5.8	2.77	10.5	4.62	15.8	6.13	24.3	8.00
p_o=15.8	46.4	12.1	69.9	13.8	54.0	12.6	30.9	9.22
	6.7	2.52						
T_s=40.6	4.0	2.79	5.0	3.53	6.6	4.47	14.2	9.08
p_o=26.6	12.0	7.86	18.2	11.2	23.3	13.6	47.6	19.4
	101	23.7	108	24.6	98.2	23.4	59.6	21.0
	33.7	16.6						

9.6.2 Unfilled Polysiloxanes and Salt-Filled DMS (below ~ 0.75 Relative Humidity)

The Sartorius balance was used for all systems except that of methanol in FMS.

TABLE 9-12

DMS (Sample I) - H_2O

1 cc. s.t.p. ≡ 805 μ g. V = 0.344

T_s °C and p_o	T_b °C and p_o	c	p	c	p	c	p
26.3°C	36.5°C	0.62	2.40	0.34	2.24	0.28	1.96
p_o=2.56	p_o=4.58	0.23	1.69	0.20	1.52	0.17	1.30
		0.15	1.14	0.14	1.04		
35.4°C	53°C	0.37	3.23	0.30	2.78	0.24	2.32
p_o=4.31	p_o=10.7	0.20	1.95	0.17	1.58	0.14	1.33
		0.11	1.09	0.095	0.92	0.076	0.69
44.7°C	59°C	1.44	5.90	0.44	5.13	0.37	0.38
		0.28	3.46	0.23	2.89	0.19	2.35
p_o=7.08	p_o=14.3	0.155	1.91	0.12	1.52	0.098	1.22
		0.078	0.91	0.064	0.76		
50.7°C	64°C	0.61	7.14	0.53	6.65	0.47	6.13
		0.35	4.84	0.27	3.67	0.20	2.72
p_o=9.59	p_o=17.9	0.15	2.03	0.11	1.48	0.083	1.08
		0.051	0.71				

TABLE 9-13

DMS (Sample II) - H_2O

1 cc.s.t.p. ≡ 805 μg. V = 0.509

T_s °C and p_o	T_b °C and p_o	c	p	c	p	c	p
		0.19	1.41	0.19	1.41	0.16	1.17
30.3°C	47.5°C	0.23	1.74	0.63	3.12	0.88	3.21
		0.48	2.92	0.38	2.60	0.32	2.29
p_o=3.24	p_o=8.17	0.28	2.04	0.25	1.84	0.21	1.58
		0.13	1.20	0.36	3.05	0.62	4.07
35.5°C	52°C	0.51	3.81	0.42	3.45	0.31	2.73
		0.27	2.46	0.24	2.14	0.21	1.90
p_o=4.33	p_o=10.2	0.18	1.64				
		0.13	1.33	0.17	1.73	0.70	5.44
40.7°C	53.5°C	0.56	5.14	0.44	4.37	0.35	3.58
p_o=5.74	p_o=11.0	0.29	3.06	0.24	2.55	0.20	2.15
		0.17	1.77				
		0.59	6.29	0.59	6.29	0.52	5.89
45.4°C	59.5°C	0.43	5.15	0.36	4.34	0.30	3.63
p_o=7.34	p_o=14.6	0.25	3.08	0.21	2.66	0.17	2.16
		0.14	1.72				
		0.13	1.75	0.16	2.23	0.20	2.86
50.0°C	55°C	0.25	3.61	0.32	4.50	0.39	5.53
p_o=9.25	p_o=11.8	0.50	6.85	0.56	7.45		

TABLE 9-14

DMS (Sample III) - H_2O

1 cc.s.t.p. ≡ 805 μg. V = 0.381

T_s °C and p_o	T_b °C and p_o	c	p	c	p	c	p
30.3°C	42°C	0.16	1.20	0.18	1.33	0.20	1.48
		0.22	1.64	0.26	1.92	0.31	2.26
p_o=3.24	p_o=6.15	0.35	2.38	0.38	2.57	0.50	2.92
50.0°C	63°C	0.096	1.46	0.21	2.86	0.37	5.38
		0.37	5.29	0.27	4.11	0.20	3.15
		0.15	2.32	0.11	1.67	0.43	6.15
p_o=9.25	p_o=17.2	0.49	6.99	0.57	7.68		

TABLE 9-15

DMS (Sample A) - H_2O

1 cc.s.t.p. ≡ 805 μ g. V = 0.445

T_s °C and p_o	T_b °C and p_o	c	p	c	p	c	p
35.2°C	52°C	0.18	1.55	0.20	1.81	0.25	2.23
		0.30	2.56	0.39	2.95	1.64	3.29
p_o=4.26	p_o=10.2	0.49	3.13	0.45	3.09	0.35	2.78
		0.28	2.43	0.23	2.04		
50.0°C	64°C	0.67	6.77	1.43	6.96	0.51	6.12
		0.36	4.85	0.27	3.76	0.20	2.81
p_o=9.25	p_o=17.9	0.58	6.45	0.42	5.47	0.30	4.23
		0.23	3.33	0.18	2.49	0.13	1.76

TABLE 9-16

DMS (Sample B) - H_2O

1 cc.s.t.p. ≡ 805 μg. V = 0.670

T_s °C and p_o	T_b °C and p_o	c	p	c	p	c	p
35.7°C	50°C	0.28	2.49	19.5	3.54	2.53	3.39
		0.57	3.27	0.37	2.99	0.34	2.87
p_o=4.38	p_o=9.25	0.30	2.69	0.24	2.24	0.20	1.87
		0.16	1.56	0.13	1.26		
50.8°C	64°C	0.12	1.60	0.15	2.21	0.21	2.98
		0.28	3.99	0.39	5.23	0.53	6.42
p_o=9.63	p_o=17.9	0.59	6.62	0.59	6.82		

TABLE 9-17

DMS (Sample C) - H_2O

1 cc. s.t.p. ≡ 805 μg. V = 0.671

T_s °C and p_o	T_b °C and p_o	c	p	c	p	c	p
35.6°C	50°C	1.37	3.28	0.41	3.10	0.35	2.90
		0.31	2.72	0.29	2.55	0.24	2.19
p_o=4.36	p_o=9.25	0.21	1.93	[illegible]	[illegible]	0.17	1.45
		0.15	1.29	0.135	1.18	0.12	1.01
		(46)	3.51	(140)	3.79		

TABLE 9-18

PMS - H_2O

1 cc. s.t.p. ≡ 805 μg. V = 0.389

T_s °C and p_o	T_b °C and p_o	c	p	c	p	c	p
25.9°C	34°C	0.75	2.33	0.38	2.19	0.31	1.87
p_o=2.50	p_o=3.99	0.26	1.62	0.21	1.37	0.18	1.16
		0.16	0.99	0.13	0.83		
31.2°C	39.5°C	0.64	3.00	0.39	2.73	0.33	2.39
p_o=3.41	p_o=5.38	0.27	2.04	0.22	1.66	0.18	1.37
		0.15	1.15	0.13	0.95	0.10	0.75
40.8°C	54.5°C	0.71	4.73	0.46	4.49	0.42	4.28
		0.33	3.46	0.26	2.72	0.21	2.16
p_o=5.78	p_o=11.5	0.16	1.72	0.13	1.32	0.10	1.03
		0.079	0.76				
48.8°C	62°C	0.53	6.75	0.50	6.39	0.38	5.04
		0.29	3.85	0.22	2.88	0.17	2.18
p_o=8.72	p_o=16.4	0.12	1.56	0.086	1.10	0.060	0.76

TABLE 9-19

FMS - H_2O

1 cc. s.t.p. ≡ 805 μ g. V = 0.347

T_s °C and p_o	T_b °C and p_o	c	p	c	p	c	p
20.4°C	40°C	0.25	1.03	0.42	1.32	0.54	1.49
		0.74	1.66	0.66	1.61	0.16	0.69
p_o=1.80	p_o=5.53	0.19	0.81	0.20	0.87	0.13	0.58
30.1°C	40°C	0.17	0.98	0.22	1.25	0.26	1.50
		0.31	1.80	0.41	2.20	0.64	2.61
p_o=3.20	p_o=5.53	0.56	2.42	0.28	1.59	0.34	1.97
		0.80	2.90	0.47	2.32		
41.1°C	49°C	0.14	1.04	0.17	1.32	0.21	1.58
		0.24	1.87	0.30	2.29	0.36	2.77
p_o=5.87	p_o=8.81	0.42	3.27	0.52	3.90	0.61	4.39
		0.76	4.78	0.87	5.02		
50.3°C	55°C	0.12	1.09	0.14	1.37	0.17	1.66
		0.21	2.04	0.26	2.48	0.30	2.92
		0.36	3.46	0.42	4.07	0.50	4.69
p_o=9.39	p_o=11.8	0.57	5.46	0.65	6.10	0.71	6.44
		0.96	7.29	1.12	7.64		

TABLE 9-20

FMS - MeOH

k = 37.3 V = 0.499

T_s °C and p_o	c	p	c	p	c	p	c	p
30°C	0.9	2.70	1.7	5.14	2.4	6.87	3.5	9.29
	4.7	10.9	7.7	14.0	12.5	15.6	8.1	14.0
p_o=15.9	5.9	12.8	2.5	7.64	1.1	3.39		
40.0°C	0.7	3.38	1.3	5.31	1.8	7.80	2.7	11.2
	3.5	13.2	5.5	17.5	7.9	19.9	11.8	23.3
p_o=25.8	6.2	18.0	4.4	15.2	1.8	7.81		

9.6.3 Silica-Filled DMS

For all these systems sorption measurements were made with the Sartorius balance.

TABLE 9-21

DMS (Sample D) - H_2O

1 cc. s.t.p. ≡ 805 μg. V = 0.306

T_s °C and p_o	T_b °C and p_o	c	p	c	p	c	p
35.7°C	50.°C	1.25	4.05	1.03	3.44	0.96	3.07
		0.78	2.54	0.70	2.06	0.62	1.68
p_o=4.38	p_o=9.25	0.52	1.41	0.46	1.16	0.42	0.97

TABLE 9-22

DMS (Sample F) - H_2O

1 cc. s.t.p. ≡ 805 μg. V = 0.342

T_s °C and p_o	T_b °C and p_o	c	p	c	p	c	p
35.5°C	50°C	1.47	3.90	0.90	2.72	0.78	2.33
		0.76	2.07	0.66	1.87	0.62	1.67
		0.39	0.93	0.51	1.35	0.45	1.12
p_o=4.33	p_o=9.25	0.40	0.93				

TABLE 9-23

DMS (Sample E) - H_2O

1 cc. s.t.p. ≡ 805 μg. V = 0.310

T_s °C and p_o	T_b °C and p_o	c	p	c	p	c	p
28.5°C	36°C	1.59	2.73	1.15	2.46	0.94	2.12
		0.83	1.81	0.76	1.52	0.66	1.27
p_o=2.92	p_o=4.45	0.61	1.09	0.47	0.79	0.50	0.87
		0.47	0.71	0.35	0.54		
35.7°C	50°C	1.80	4.10	0.99	3.42	0.94	3.14
p_o=4.38	p_o=9.25	0.78	2.38	0.68	2.06	0.62	1.66
		0.53	1.40	0.46	1.11	0.41	0.93
38.1°C	47.5°C	1.22	4.04	1.14	3.79	0.91	3.00
		0.86	2.81	0.66	1.81	0.58	1.63
p_o=4.99	p_o=8.17	0.63	1.56	0.57	1.41	0.51	1.16
		0.45	1.12	0.38	0.80	0.33	0.73
		2.01	5.37	1.64	5.20	1.13	4.51
41.8°C	54.5°C	1.08	4.37	0.99	3.70	0.93	3.33
		0.82	2.87	0.77	2.72	0.73	2.23
p_o=6.08	p_o=11.5	0.67	2.04	0.65	1.77	0.60	1.60
		0.41	1.05	0.34	0.75	0.28	0.57
43.5°C	54°C	1.86	5.57	1.27	5.02	1.13	4.38
		0.92	3.41	0.75	2.67	0.65	2.10
p_o=6.65	p_o=11.2	0.52	1.51	0.42	1.29	0.35	1.02
		0.29	0.73	0.23	0.59		
50.4°C	64.5°C	1.58	7.34	1.19	6.25	0.99	4.84
p_o=9.44	p_o=18.3	0.77	3.60	0.63	2.71	0.49	1.97
		0.38	1.44	0.28	1.02	0.22	0.68

9.7 Steady State Permeability Data

Symbols used in Tables

k = sensitivity of quartz spiral (cm.g.$^{-1}$)

ℓ = membrane thickness (cm)

A = exposed cross sectional area of membrane (cm^2)

p = vapour pressure (cm.Hg)

p_o = saturation vapour pressure (cm.Hg)

T°C = temperature of membrane

J = permeation flux (cc. s.t.p. cm.$^{-2}$ sec.$^{-1}$)

(1 cc. s.t.p. ≡ 8.05x10^{-4} g. H_2O ≡ 14.3x10^{-4}g. MeOH)

9.7.1 Polymethacrylates and PPA

TABLE 9-24

PMMA - H_2O

k = 32.7 ℓ = 0.015 A = 2.8

T°C	p_o	$J\ell \times 10^7$	p/p_o	$J\ell \times 10^7$	p/p_o	$J\ell \times 10^7$	p/p_o	$J\ell \times 10^7$	p/p_o
39.8	5.47	5.5	0.73	6.3	0.84	7.4	0.97		
50.0	9.25	8.5	0.64	10.6	0.80	12.1	0.90		
59.8	14.8	3.2	0.15	6.7	0.31	9.7	0.43	14.9	0.66
"	"	21.8	0.89						
70.7	24.0	14.7	0.38	22.3	0.58	34.2	0.89		

TABLE 9-25

PEMA - H_2O

k = 32.7 ℓ = 0.013 A = 2.8

T°C	p_o	$J\ell \times 10^7$	p/p_o	$J\ell \times 10^7$	p/p_o	$J\ell \times 10^7$	p/p_o	$J\ell \times 10^7$	p/p_o
30.9	3.35	11.6	0.69	14.0	0.82	16.4	0.96		
40.7	5.74	12.5	0.47	16.3	0.61	20.5	0.76	27.4	0.97
"	"	19.0	0.69						
51.0	9.73	10.7	0.25	15.1	0.36	23.7	0.54	40.5	0.93
60.7	15.4	10.7	0.16	17.1	0.26	31.9	0.48	50.9	0.76
70.7	24.0	12.4	0.12	21.5	0.21	39.1	0.38	70.3	0.64
80.6	36.4	12.9	0.09	23.1	0.15	42.0	0.28	136	0.89

TABLE 9-26(a)

PPMA - H_2O

k = 32.7 ℓ = 0.018 A = 2.8

T^oC	p_o	$J\ell \times 10^7$	p/p_o	$J\ell \times 10^7$	p/p_o	$J\ell \times 10^7$	p/p_o	$J\ell \times 10^7$	p/p_o
26.9	2.65	11.3	0.74	12.5	0.84	14.4	0.94	13.5	0.88
31.8	3.53	13.0	0.66	15.7	0.80	19.0	0.95	17.0	0.88
"	"	14.3	0.73						
37.1	4.73	11.5	0.45	14.2	0.55	17.1	0.66	19.4	0.75
"	"	24.9	0.94	22.4	0.85				
41.9	6.11	13.4	0.41	17.1	0.52	20.4	0.63	23.2	0.72
"	"	30.2	0.93	25.5	0.77				
49.6	9.05	12.6	0.32	17.3	0.45	22.4	0.55	26.9	0.65
"	"	30.7	0.73	40.2	0.93	35.1	0.83		
55.6	12.2	11.1	0.23	17.8	0.36	26.7	0.50	35.0	0.62
"	"	56.4	0.91	44.9	0.77	42.5	0.75	22.0	0.45
"	"	27.6	0.55	36.3	0.67	55.0	0.92		

TABLE 9-26(b)

PPMA - H_2O

k = 32.7 ℓ = 0.010 A = 2.8

T^oC	p_o	$J\ell \times 10^7$	p/p_o	$J\ell \times 10^7$	p/p_o	$J\ell \times 10^7$	p/p_o	$J\ell \times 10^7$	p/p_o
31.9	3.54	15.1	0.80	17.8	0.92	18.9	0.96		
37.4	4.81	16.5	0.63	21.4	0.81	25.0	0.95		
42.2	6.21	15.6	0.47	22.8	0.69	29.6	0.89		
49.8	9.16	15.2	0.32	25.0	0.53	43.7	0.91		

TABLE 9-27

PBMA - H_2O

k = 32.7 ℓ = 0.010 A = 2.8

T^oC	p_o	$J\ell \times 10^7$	p/p_o	$J\ell \times 10^7$	p/p_o	$J\ell \times 10^7$	p/p_o	$J\ell \times 10^7$	p/p_o
26.4	2.58	10.6	0.84	10.3	0.90	10.7	0.95	11.3	1.0
33.6	3.91	11.0	0.63	13.1	0.74	15.0	0.85	16.7	0.94
"	"	13.6	0.77						
40.5	5.68	11.8	0.45	15.9	0.59	21.0	0.77	26.5	0.96
47.5	8.19	12.7	0.32	16.8	0.41	22.9	0.55	30.2	0.74
55.5	12.1	13.9	0.22	23.5	0.37	38.0	0.60	57.6	0.90

TABLE 9-28

PPA - H_2O

k = 32.7 ℓ = 0.22 A = 2.0

T^oC	p_o	$J\ell x10^6$	p/p_o	$J\ell x10^6$	p/p_o	$J\ell x10^6$	p/p_o	$J\ell x10^6$	p/p_o
48.9	8.76	13.6	0.53	18.1	0.70	22.5	0.85	11.4	0.44

TABLE 9-29

PEMA-MeOH

k = 32.7 ℓ = 0.013 A = 2.8

T^oC	p_o	$J\ell x10^7$	p/p_o	$J\ell x10^7$	p/p_o	$J\ell x10^7$	p/p_o	$J\ell x10^7$	p/p_o
40.6	26.6	1.21	0.31	6.76	0.65	67.2	0.89	14.7	0.77
"	"	5.83	0.60	3.53	0.48	32.9	0.83	1.03	0.21
29.8	15.8	1.00	0.35	1.31	0.43	1.98	0.54	5.21	0.67
"	"	14.3	0.83	48.5	0.91	3.84	0.60	6.88	0.74

9.7.2 Unfilled Polysiloxanes

TABLE 9-30

DMS (I) - H_2O

k = 32.7 ℓ = 0.198 A = 2.3

T^oC	p_o	$J\ell x10^6$	p/p_o	$J\ell x10^6$	p/p_o	$J\ell x10^6$	p/p_o	$J\ell x10^6$	p/p_o
50.2	9.35	10.8	0.30	19.3	0.55	30.7	0.88		
35.7	4.38	4.63	0.24	13.3	0.71	17.5	0.92		
43.0	6.48	11.6	0.43	18.9	0.73	23.8	0.95		
26.0	2.52	8.05	0.70	10.3	0.86	12.0	1.00		

TABLE 9-31

DMS (II) - H_2O

k = 32.7 $\mathfrak{L}$ = 0.206 A = 2.8

T^oC	p_o	$J\mathfrak{L}x10^6$	p/p_o	$J\mathfrak{L}x10^6$	p/p_o	$J\mathfrak{L}x10^6$	p/p_o	$J\mathfrak{L}x10^6$	p/p_o
30.7	3.31	10.0	0.46	13.0	0.59	15.3	0.70	17.7	0.83
"	"	21.7	1.00						
50.1	9.30	14.2	0.32	20.2	0.47	27.3	0.61	34.7	0.77
"	"	41.7	0.92						
40.0	5.53	9.29	0.30	14.5	0.46	19.5	0.62	24.2	0.78
"	"	29.3	0.94						

TABLE 9-32

DMS (III) - H_2O

k = 32.7 $\mathfrak{L}$ = 0.250 A = 2.8

T^oC	p_o	$J\mathfrak{L}x10^6$	p/p_o	$J\mathfrak{L}x10^6$	p/p_o	$J\mathfrak{L}x10^6$	p/p_o	$J\mathfrak{L}x10^6$	p/p_o
49.8	9.16	13.7	0.36	18.7	0.49	23.6	0.63	28.0	0.76
"	"	32.6	0.90						
35.8	4.40	9.05	0.45	11.2	0.56	13.2	0.67	15.3	0.78
"	"	17.2	0.89						

TABLE 9-33

PMS - H_2O

k = 32.7 $\mathfrak{L}$ = 0.172 A = 2.8

T^oC	p_o	$J\mathfrak{L}x10^6$	p/p_o	$J\mathfrak{L}x10^6$	p/p_o	$J\mathfrak{L}x10^6$	p/p_o	$J\mathfrak{L}x10^6$	p/p_o
50.8	9.63	9.72	0.32	16.2	0.56	24.7	0.90		
40.9	5.80	4.69	0.23	10.9	0.55	16.0	0.88		
31.9	3.54	9.59	0.72	5.49	0.72	11.5	0.88		
22.8	2.08	4.44	0.50	6.33	0.72	7.95	0.93		

TABLE 9-34

FMS - H_2O

k = 32.7 ℓ = 0.153 A = 2.8

T°C	p_o	$J\ell \times 10^6$	p/p_o	$J\ell \times 10^6$	p/p_o	$J\ell \times 10^6$	p/p_o	$J\ell \times 10^6$	p/p_o
50.0	9.25	3.12	0.18	6.04	0.35	8.60	0.50	11.1	0.65
"	"	15.0	0.88	12.8	0.75				
40.0	5.53	3.27	0.31	5.50	0.51	7.76	0.71	8.78	0.82
"	"	9.98	0.93						
30.8	3.33	2.41	0.35	3.27	0.49	3.82	0.55	5.27	0.78
"	"	6.18	0.90						
20.4	1.80	2.97	0.75	3.70	0.83	3.55	0.91	3.93	1.00

TABLE 9-35

FMS - MeOH

k = 32.7 ℓ = 0.153 A = 2.8

T°C	p_o	$J\ell \times 10^6$	p/p_o	$J\ell \times 10^6$	p/p_o	$J\ell \times 10^6$	p/p_o	$J\ell \times 10^6$	p/p_o
30.8	16.6	6.21	0.41	7.96	0.51	10.4	0.64	14.0	0.79
"	"	17.9	0.92						
40.8	26.8	6.81	0.29	9.88	0.41	14.9	0.57	21.3	0.73
"	"	28.4	0.89						

9.7.3 Salt-Filled DMS

TABLE 9-36

DMS(A) - H_2O

k = 32.7 ℓ = 0.227 A = 2.3

T°C	p_o	$J\ell \times 10^6$	p/p_o	$J\ell \times 10^6$	p/p_o	$J\ell \times 10^6$	p/p_o	$J\ell \times 10^6$	p/p_o
49.8	9.16	12.2	0.34	17.0	0.48	27.6	0.80	22.2	0.64
"	"	31.7	0.94						
35.5	4.33	11.1	0.57	14.1	0.74	16.9	0.90	8.96	0.45
"	"	17.8	0.97						

TABLE 9-37

DMS (B) - H_2O

k = 32.7 ℓ = 0.35 A = 2.3

T^oC	p_o	$J_\ell \times 10^6$	p/p_o	$J_\ell \times 10^6$	p/p_o	$J_\ell \times 10^6$	p/p_o	$J_\ell \times 10^6$	p/p_o
49.7	9.12	12.5	0.34	23.8	0.66	32.0	0.88	18.1	0.49
		28.1	0.78						
35.9	4.43	6.46	0.32	11.7	0.60	16.4	0.85	14.4	0.74

TABLE 9-38

DMS (C) - H_2O

k = 32.7 ℓ = 0.367 A = 2.3

T^oC	p_o	$J_\ell \times 10^6$	p/p_o	$J_\ell \times 10^6$	p/p_o	$J_\ell \times 10^6$	p/p_o	$J_\ell \times 10^6$	p/p_o
50.0	9.25	15.1	0.40	21.2	0.57	27.0	0.74	34.3	0.96
35.7	4.38	10.5	0.51	13.2	0.64	15.7	0.78	18.8	0.90

9.7.4 Silica-Filled DMS

TABLE 9-39

DMS (D) - H_2O

k = 32.7 ℓ = 0.188 A = 2.3

T^oC	p_o	$J_\ell \times 10^6$	p/p_o	$J_\ell \times 10^6$	p/p_o	$J_\ell \times 10^6$	p/p_o	$J_\ell \times 10^6$	p/p_o
50.0	9.25	9.25	0.30	17.8	0.58	27.2	0.90	23.2	0.77
35.6	4.36	5.48	0.32	10.7	0.62	15.7	0.92	17.1	1.00

TABLE 9-40

DMS (E) - H_2O

k = 32.7 ℓ = 0.204 A = 2.3

T^oC	p_o	$J_\ell \times 10^6$	p/p_o	$J_\ell \times 10^6$	p/p_o	$J_\ell \times 10^6$	p/p_o	$J_\ell \times 10^6$	p/p_o
50.2	9.34	8.79	0.33	15.9	0.58	24.9	0.91	20.0	0.73
36.0	4.47	9.09	0.59	11.4	0.75	13.5	0.90		
44.1	6.86	6.46	0.30	13.7	0.63	19.8	0.91		
28.1	2.85	4.37	0.42	7.19	0.68	9.82	0.95		

TABLE 9-41

DMS (F) - H_2O

k = 32.7 ℓ = 0.194 A = 2.3

T^oC	p_o	$J\ell x10^6$	p/p_o	$J\ell x10^6$	p/p_o	$J\ell x10^6$	p/p_o	$J\ell x10^6$	p/p_o
49.7	9.12	8.36	0.34	14.8	0.60	22.6	0.91		
36.2	4.50	8.23	0.59	10.1	0.73	12.6	0.92		

9.8 Sorption and Desorption Kinetic Data

Symbols used in Tables

ℓ = membrane thickness (cm.)

V = volume of polymer sample (cm^3)

M_t = increase (decrease) in weight (μ g.) at time t. (sec.)

M_∞ = increase (decrease) in weight (μ g.) at equilibrium

E_t = spiral extension (cm.) at time t (sec.)

E_∞ = spiral extension (cm.) at equilibrium

T^oC = temperature of sample

B = buoyancy correction (μ g.)

All the values of M_t, M_∞, E_t and E_∞ include buoyancy corrections. Blank corrections are ignored.

9.8.1 Polymethacrylates and PPA

Measurements for the PEMA-MeOH system were made with the quartz spiral.

TABLE 9-42

PPA - H_2O (48.9°C)

ℓ = 0.41 V = 0.306 1 μg. = 1.24 x 10^{-3} cc.s.t.p.

B	M_∞	$t^{\frac{1}{2}}$	M_t/M_∞	$t^{\frac{1}{2}}$	M_t/M_∞	$t^{\frac{1}{2}}$	M_t/M_∞	$t^{\frac{1}{2}}$	M_t/M_∞
		5.3	0.053	7.5	0.078	9.2	0.096	10.6	0.11
		11.8	0.125	13.0	0.14	14.0	0.15	15.0	0.16
		16.8	0.18	18.4	0.19	19.8	0.21	21.2	0.22
		22.5	0.235	23.7	0.25	24.9	0.26	26.0	0.27
	181	28.1	0.29	30.0	0.31	31.8	0.33	33.5	0.34
1.5		35.2	0.36	36.7	0.37	38.2	0.39	39.7	0.40
	sorption	42.4	0.425	45.0	0.45	47.4	0.47	49.5	0.49
		53.9	0.525	57.9	0.56	61.7	0.59	65.2	0.61
		68.6	0.64	71.8	0.66	74.9	0.68	77.8	0.70
		80.6	0.72	83.4	0.74	88.6	0.77	93.6	0.79
		98.2	0.815	107	0.85	115	0.87		
		5.3	0.054	7.5	0.070	9.2	0.084	10.6	0.097
		11.8	0.11	13.0	0.12	14.0	0.13	15.0	0.14
		16.8	0.16	18.4	0.17	19.8	0.19	21.2	0.20
	181	22.5	0.21	23.7	0.22	24.9	0.23	26.0	0.24
1.5		28.1	0.265	30.0	0.28	31.8	0.30	33.5	0.32
	desorption	36.7	0.35	38.2	0.37	39.7	0.38	42.4	0.41
		45.0	0.44	47.4	0.46	48.7	0.47	53.1	0.51
		57.2	0.56	61.0	0.58	61.7	0.60	65.2	0.64
		68.6	0.67	71.8	0.70	74.9	0.73	77.8	0.75
		80.6	0.77	83.4	0.80	88.6	0.83	93.6	0.86
		98.2	0.89						
		5.3	0.053	7.5	0.078	9.2	0.096	10.6	0.11
		11.8	0.125	13.0	0.14	14.0	0.15	15.0	0.16
		16.8	0.18	18.4	0.19	19.8	0.21	21.2	0.22
		22.5	0.23	23.7	0.25	24.9	0.26	26.0	0.27
	470	28.1	0.29	30.0	0.31	31.8	0.325	33.5	0.34
3.7		35.2	0.36	36.7	0.37	38.2	0.385	39.7	0.40
	sorption	42.4	0.42	45.0	0.45	47.4	0.47	51.3	0.50
		55.5	0.54	59.4	0.57	63.1	0.60	66.6	0.63
		69.9	0.66	73.0	0.68	76.0	0.70	78.9	0.72
		81.7	0.74	84.4	0.76	89.6	0.79	94.5	0.82
		99.1	0.84	103	0.86	108	0.87	116	0.90

cont'd....

TABLE 9-42 (cont'd)

B	M_∞	$t^{\frac{1}{2}}$	M_t/M_∞	$t^{\frac{1}{2}}$	M_t/M_∞	$t^{\frac{1}{2}}$	M_t/M_∞	$t^{\frac{1}{2}}$	M_t/M_∞
		5.3	0.05	7.5	0.073	9.2	0.09	10.6	0.10
		11.8	0.11	13.0	0.12	14.0	0.13	15.0	0.14
		16.8	0.16	18.4	0.17	19.8	0.19	21.2	0.20
		22.5	0.21	23.7	0.23	24.9	0.24	26.0	0.25
	470	28.1	0.27	30.0	0.29	31.8	0.305	33.5	0.32
3.7		35.2	0.34	36.7	0.35	38.2	0.37	39.7	0.38
	desorption	42.4	0.41	45.0	0.43	47.4	0.46	49.7	0.48
		52.0	0.50	56.1	0.54	60.0	0.58	63.6	0.61
		67.1	0.64	70.4	0.66	73.5	0.69	76.5	0.71
		79.4	0.73	84.8	0.77	90.0	0.81	94.9	0.83
		99.5	0.86	104	0.88	108	0.90	116	0.94
		5.3	0.040	7.5	0.060	9.2	0.075	10.6	0.088
	870	11.8	0.10	13.0	0.11	14.0	0.12	15.0	0.13
6.6		16.8	0.145	18.4	0.16	19.8	0.17	21.2	0.19
	sorption	22.5	0.20	23.7	0.21	24.9	0.22	26.0	0.23
		28.1	0.25	30.0	0.27	31.8	0.29	33.5	0.30
		35.2	0.32	36.7	0.33	38.2	0.35	39.7	0.36
		42.4	0.39	45.0	0.41	47.4	0.43	49.7	0.45
		52.0	0.47	56.1	0.51	59.7	0.54	63.3	0.57
		66.8	0.60	70.1	0.63	73.2	0.66	76.2	0.68
		79.1	0.70	81.9	0.72	84.6	0.74	89.8	0.77
		94.7	0.80	99.3	0.82	104	0.85	112	0.88
		120	0.90						
		5.3	0.056	7.5	0.075	9.2	0.091	10.6	0.105
		11.8	0.12	13.0	0.13	14.0	0.14	15.0	0.15
		16.8	0.16	18.4	0.18	19.8	0.19	21.2	0.20
		22.5	0.22	23.7	0.23	24.9	0.24	26.0	0.25
	870	28.1	0.27	30.0	0.29	31.8	0.31	33.5	0.32
6.6		35.2	0.34	36.7	0.35	38.2	0.37	39.7	0.38
	desorption	42.4	0.41	45.0	0.43	47.4	0.455	49.7	0.48
		52.0	0.50	54.1	0.52	56.1	0.54	60.0	0.57
		61.1	0.58	64.7	0.61	68.0	0.645	71.3	0.67
		74.4	0.70	77.3	0.72	80.2	0.74	85.6	0.78
		90.7	0.82	95.6	0.85	100	0.875	109	0.92
		117	0.95						
		5.3	0.043	7.5	0.061	9.2	0.075	10.6	0.087
		11.8	0.10	13.0	0.11	14.0	0.12	15.0	0.13
		16.8	0.145	18.4	0.16	19.8	0.17	21.2	0.19
	1590	22.5	0.20	23.7	0.21	24.9	0.22	26.0	0.23
9.7		28.1	0.25	30.0	0.265	31.8	0.28	33.5	0.30
	sorption	35.2	0.31	36.7	0.325	38.2	0.335	39.7	0.35

TABLE 9-42 (cont'd)

B	M_∞	$t^{\frac{1}{2}}$	M_t/M_∞	$t^{\frac{1}{2}}$	M_t/M_∞	$t^{\frac{1}{2}}$	M_t/M_∞	$t^{\frac{1}{2}}$	M_t/M_∞
		42.4	0.38	45.0	0.40	47.4	0.42	49.7	0.44
	1590	52.0	0.46	56.1	0.50	60.0	0.53	63.6	0.56
9.7		65.9	0.58	69.2	0.61	72.4	0.63	75.5	0.66
	sorption	78.4	0.68	83.9	0.72	89.1	0.75	94.0	0.785
		98.7	0.81	103	0.84	107	0.87	115	0.89
		15.0	0.13	16.8	0.15	18.4	0.16	19.8	0.175
		21.2	0.19	22.5	0.20	23.7	0.21	24.9	0.22
		26.0	0.23	28.1	0.25	30.0	0.27	31.8	0.29
		33.5	0.31	35.2	0.32	36.7	0.34	38.2	0.35
	1590	39.7	0.37	42.4	0.39	45.0	0.42	47.4	0.44
9.7		49.7	0.47	52.0	0.49	55.4	0.52	59.3	0.56
	desorption	63.0	0.59	63.5	0.62	69.8	0.65	72.9	0.68
		76.0	0.70	78.9	0.73	81.7	0.75	87.0	0.785
		92.0	0.82	96.8	0.85	101	0.87	106	0.89
		114	0.93						
		5.3	0.036	7.5	0.054	9.2	0.068	10.6	0.080
		11.8	0.091	13.0	0.10	14.0	0.11	15.0	0.12
		16.8	0.13	18.4	0.145	19.8	0.16	21.2	0.17
		22.5	0.18	23.7	0.19	24.9	0.20	26.0	0.21
		28.1	0.225	30.0	0.24	31.8	0.26	33.5	0.27
	2360	35.2	0.28	36.7	0.30	38.2	0.31	39.7	0.32
14.7		42.4	0.34	45.0	0.37	46.8	0.38	49.2	0.40
	sorption	52.5	0.425	56.5	0.46	60.5	0.49	64.1	0.52
		67.5	0.55	70.7	0.57	73.9	0.60	76.8	0.62
		79.7	0.64	82.9	0.67	88.2	0.70	93.1	0.73
		97.8	0.75	102	0.78	111	0.82	119	0.85
		5.3	0.039	7.5	0.059	9.2	0.073	10.6	0.087
		11.8	0.10	13.0	0.11	14.0	0.12	15.0	0.13
	2360	16.8	0.14	18.4	0.16	19.8	0.17	21.2	0.18
14.7		22.5	0.20	23.7	0.21	24.9	0.22	26.0	0.23
	desorption	28.1	0.25	30.0	0.26	31.8	0.28	33.5	0.30
		35.2	0.31	36.7	0.32	38.2	0.34	39.7	0.35
		42.4	0.38	45.0	0.40	46.8	0.415	49.2	0.435
		52.5	0.46	56.5	0.50	60.5	0.53	64.1	0.57
		67.5	0.60	70.7	0.63	73.9	0.65	76.8	0.68
		79.7	0.70	82.9	0.73	88.2	0.76	93.1	0.79
		97.8	0.82	102	0.85	111	0.89	119	0.93

TABLE 9-43

PBMA - H_2O (39.8°C)

ℓ = 0.0255 V = 0.299 1 μg. ≡ 1.24×10^{-3} cc.s.t.p.

B	M_∞	$t^{\frac{1}{2}}$	M_t/M_∞	$t^{\frac{1}{2}}$	M_t/M_∞	$t^{\frac{1}{2}}$	M_t/M_∞	$t^{\frac{1}{2}}$	M_t/M_∞
		3.3	0.22	4.7	0.32	5.8	0.39	6.7	0.45
	185	8.2	0.54	9.8	.64	11.9	0.75	13.6	0.82
1.5		15.2	0.86	16.6	0.89	19.0	0.92	21.7	0.93
	sorption	24.2	0.955	28.4	0.97				
		3.3	0.23	4.7	0.32	5.8	0.39	6.7	0.45
	182	7.7	0.56	9.4	0.63	10.8	0.72	12.0	0.78
1.5		13.1	0.83	15.1	0.90	16.9	0.93	19.9	0.96
	desorption	24.0	0.98	32.0	0.995				
		2.4	0.14	3.3	0.19	4.7	0.27	5.8	0.33
	780	6.7	0.38	7.5	0.43	8.2	0.47	9.5	0.54
5.4		10.6	0.60	11.6	0.64	12.6	0.68	14.2	0.75
	sorption	15.2	0.78	16.1	0.80	17.8	0.84	19.3	0.86
		20.7	0.88	23.2	0.90	25.5	0.91	29.6	0.94
		2.4	0.145	3.3	0.21	4.7	0.29	5.8	0.36
	770	6.7	0.41	7.5	0.46	8.2	0.51	9.5	0.585
5.4		10.6	0.65	11.6	0.71	12.6	0.755	14.0	0.815
	desorption	14.9	0.85	15.8	0.88	17.5	0.92	19.1	0.94
		20.5	0.95	23.1	0.965	25.4	0.97	29.5	0.99
		2.4	0.11	3.3	0.17	4.7	0.24	5.8	0.30
	1130	6.7	0.35	7.5	0.39	8.2	0.42	9.5	0.48
7.1		10.6	0.53	11.6	0.57	12.5	0.61	13.9	0.66
	sorption	14.9	0.69	15.8	0.72	17.5	0.755	19.0	0.79
		20.5	0.81	23.1	0.85	25.4	0.88	29.5	0.92
		2.4	0.12	3.3	0.14	4.7	0.23	5.8	0.285
	1330	6.7	0.335	7.5	0.37	8.2	0.41	9.5	0.465
7.8		10.6	0.51	11.6	0.56	12.5	0.59	14.2	0.65
	sorption	15.9	0.70	17.6	0.74	19.1	0.77	20.5	0.80
		21.9	0.82	24.3	0.86	26.5	0.89	28.6	0.91
		2.4	0.13	3.3	0.18	4.7	0.25	5.8	0.305
	1140	6.7	0.35	7.5	0.38	9.5	0.49	10.6	0.54
7.0		11.6	0.58	13.4	0.65	15.1	0.71	16.9	0.755
	sorption	18.4	0.79	19.9	0.82	21.3	0.84	23.8	0.87
		26.0	0.91	30.0	0.94				

(cont'd)....

TABLE 9-43 (cont'd)

B	M_∞	$t^{\frac{1}{2}}$	M_t/M_∞	$t^{\frac{1}{2}}$	M_t/M_∞	$t^{\frac{1}{2}}$	M_t/M_∞	$t^{\frac{1}{2}}$	M_t/M_∞
		2.4	0.15	3.3	0.22	4.7	0.31	5.8	0.38
	232	6.7	0.44	7.5	0.49	8.2	0.54	9.5	0.62
2.0		10.6	0.68	12.1	0.75	14.3	0.83	16.1	0.87
	sorption	17.8	0.90	19.3	0.92	22.0	0.95	24.4	0.965
		28.7	0.975						
		2.4	0.16	3.3	0.225	4.7	0.32	5.8	0.39
	224	6.7	0.45	7.5	0.505	8.2	0.55	9.5	0.64
2.0		10.6	0.71	11.6	0.785	13.4	0.87	19.1	0.91
	desorption	21.8	0.94	24.3	0.96	28.5	0.99		
		2.4	0.14	3.3	0.21	4.7	0.30	5.8	0.36
	460	6.7	0.42	7.5	0.47	8.2	0.51	9.5	0.585
3.5		10.6	0.645	11.6	0.70	13.4	0.76	14.8	0.81
	sorption	16.6	0.855	18.2	0.88	19.7	0.90	21.1	0.915
		23.6	0.93	25.9	0.94	29.9	0.97		
		2.4	0.15	3.3	0.215	4.7	0.31	5.8	0.375
	450	6.7	0.43	7.5	0.485	8.2	0.53	9.5	0.61
3.5		10.6	0.68	11.6	0.74	12.7	0.79	14.8	0.86
	desorption	16.6	0.91	18.2	0.93	19.7	0.95	22.3	0.96
		24.7	0.97	28.9	0.99				
		2.4	0.14	3.3	0.20	4.7	0.285	5.8	0.35
	610	6.7	0.40	7.5	0.45	8.2	0.49	9.5	0.56
4.5		10.6	0.62	11.6	0.66	13.3	0.73	15.3	0.795
	sorption	17.0	0.84	18.6	0.865	20.0	0.88	22.7	0.905
		25.0	0.92	29.2	0.94				
		2.4	0.15	3.3	0.21	4.7	0.30	5.8	0.37
	600	6.7	0.43	7.5	0.48	8.2	0.43	9.5	0.61
4.5		10.6	0.67	11.6	0.73	14.4	0.84	16.2	0.89
	desorption	17.9	0.92	19.4	0.94	20.8	0.94	23.3	0.965
		25.6	0.975	29.7	0.995				
		2.4	0.14	3.3	0.20	4.7	0.29	5.8	0.35
	570	6.7	0.41	7.5	0.45	8.2	0.50	9.5	0.56
4.0		10.6	0.64	11.6	0.67	13.4	0.74	14.3	0.77
	sorption	16.1	0.82	17.8	0.86	19.3	0.89	20.7	0.91
		23.3	0.93	25.6	0.945	2?.6	0.97		

(cont'd)....

TABLE 9-43 (cont'd)

B	M_∞	$t^{\frac{1}{2}}$	M_t/M_∞	$t^{\frac{1}{2}}$	M_t/M_∞	$t^{\frac{1}{2}}$	M_t/M_∞	$t^{\frac{1}{2}}$	M_t/M_∞
		2.4	0.15	3.3	0.21	4.7	0.30	5.8	0.37
	560	6.7	0.43	7.5	0.48	8.2	0.53	9.5	0.61
4.0		10.6	0.67	11.6	0.73	13.4	0.80	15.4	0.87
	desorption	17.1	0.92	18.7	0.94	20.1	0.96	22.7	0.98
		25.1	0.98	29.2	0.99				
		2.4	0.15	3.3	0.215	4.7	0.305	5.8	0.37
	300	6.7	0.43	7.5	0.48	8.2	0.53	9.5	0.60
2.5		10.6	0.66	11.6	0.71	12.7	0.76	14.7	0.84
	sorption	16.5	0.89	18.2	0.92	19.7	0.95	22.3	0.98
		24.7	0.99	28.9	0.99				
		2.4	0.15	3.3	0.22	4.7	0.31	5.8	0.385
	290	6.7	0.44	7.5	0.50	8.2	0.545	9.5	0.63
2.5		10.6	0.70	11.6	0.75	13.0	0.81	15.0	0.88
	desorption	16.8	0.92	18.4	0.95	19.8	0.965	22.5	0.985
		24.9	0.99	29.0	0.99				
		2.4	0.15	3.3	0.21	4.7	0.30	5.8	0.37
	360	6.7	0.43	7.5	0.48	8.2	0.525	9.5	0.60
3.0		10.6	0.66	11.6	0.71	14.2	0.81	16.0	0.87
	sorption	17.7	0.90	19.2	0.93	20.6	0.94	23.2	0.96
		25.5	0.97	29.6	0.99				
		2.4	0.15	3.3	0.22	4.7	0.31	5.8	0.39
	350	6.7	0.44	7.5	0.50	8.2	0.55	9.5	0.63
3.0		10.6	0.77	11.6	0.75	13.0	0.815	15.0	0.89
	desorption	16.8	0.93	18.4	0.96	19.8	0.98	22.5	0.99
		24.9	0.99	29.0	0.995				
		2.4	0.14	3.3	0.205	4.7	0.29	5.8	0.36
	510	6.7	0.41	7.5	0.46	8.2	0.50	9.5	0.57
4.0		10.6	0.63	11.6	0.68	13.3	0.76	15.3	0.83
	sorption	17.0	0.87	18.6	0.89	20.1	0.91	22.7	0.93
		25.1	0.94	29.2	0.955				
		2.4	0.15	3.3	0.22	4.7	0.31	5.8	0.38
	500	6.7	0.43	7.5	0.49	8.2	0.535	9.5	0.615
4.0		10.6	0.68	11.6	0.74	13.0	0.80	15.0	0.87
	desorption	16.8	0.92	18.4	0.94	19.9	0.955	22.5	0.97
		24.9	0.98	29.1	0.99				

(cont'd)...

TABLE 9-43 (cont'd)

B	M_∞	$t^{\frac{1}{2}}$	M_t/M_∞	$t^{\frac{1}{2}}$	M_t/M_∞	$t^{\frac{1}{2}}$	M_t/M_∞	$t^{\frac{1}{2}}$	M_t/M_∞
		2.4	0.13	3.3	0.19	4.7	0.27	5.8	0.33
	840	6.7	0.38	7.5	0.42	8.2	0.46	9.5	0.53
6.0		10.6	0.59	11.6	0.64	13.3	0.71	15.3	0.78
	sorption	17.0	0.83	18.6	0.86	20.1	0.88	22.7	0.91
		25.1	0.92	29.2	-				
		2.4	0.14	3.3	0.20	4.7	0.29	5.8	0.36
	830	6.7	0.42	7.5	0.46	8.2	0.51	9.5	0.59
6.0		10.6	0.65	11.6	0.71	14.6	0.83	18.1	0.925
	desorption	20.9	0.96	23.5	0.98	25.7	0.99	29.8	0.99
		2.4	0.13	3.3	0.19	4.7	0.27	5.8	0.33
	790	6.7	0.38	7.5	0.43	8.2	0.47	9.5	0.53
5.0		10.6	0.59	11.6	0.64	13.8	0.73	17.4	0.84
	sorption	20.4	0.88	23.0	0.89	25.3	0.90	29.4	0.92
		2.4	0.145	3.3	0.21	4.7	0.295	5.8	0.36
	780	6.7	0.41	7.5	0.47	8.2	0.51	9.5	0.585
5.0		10.6	0.65	11.6	0.71	13.3	0.79	17.0	0.91
	desorption	20.1	0.95	22.7	0.97	25.0	0.98	29.2	0.99

TABLE 9-44

PEMA - MeOH (40.6°C)

ℓ = 0.025 V = 0.493 1 cm.extension ≡ 18.7 cc. s.t.p.

$t^{\frac{1}{2}}$	Values of E_∞ (s) = sorption (d) = desorption						
	.104(s)	.104(d)	.131(s)	.131(d)	.171(d)	.171(d)	.369(s)
	E_t/E_∞	E_t/E_∞	E_t/E_∞	E_t/E_∞	E_t/E_∞	E_t/E_∞	E_t/E_∞
17.3	0.14	0.14	0.14	0.14	0.15	0.16	0.15
24.5	0.21	0.22	0.21	0.20	0.21	0.22	0.22
34.6	0.29	0.31	0.30	0.30	0.32	0.30	0.32
45.8	0.41	0.39	0.41	0.39	0.40	0.39	0.43
54.8	0.48	0.47	0.50	0.45	0.48	0.48	0.51
64.8	0.57	0.53	0.56	0.53	0.56	0.56	0.58
88.3	0.69	0.68	0.69	0.67	0.70	0.68	-
107	0.78	0.75	0.80	0.75	0.79	0.77	0.80
136	0.87	0.84	0.89	0.85	0.88	0.86	0.89
161	-	-	-	0.89	0.93	0.90	0.94

(cont'd)....

TABLE 9-44 (cont'd)

$t^{\frac{1}{2}}$	Values of E_∞ (s) = sorption (d) = desorption						
	.369(d)	.311(s)	.311(d)	.474(s)	.474(d)	.608(s)	.608(d)
	E_t/E_∞	E_t/E_∞	E_t/E_∞	E_t/E_∞	E_t/E_∞	E_t/E_∞	E_t/E_∞
17.3	0.18	0.15	0.17	0.16	0.19	0.18	0.21
24.5	0.26	0.22	0.25	0.24	0.27	0.26	0.28
34.6	0.31	0.31	0.35	0.34	0.38	0.37	0.40
45.8	0.47	0.41	0.45	0.45	0.49	0.49	0.51
54.8	0.54	0.49	0.53	0.52	0.56	0.56	0.58
64.8	0.61	0.57	0.60	0.59	0.62	0.63	0.65
88.3	0.74	0.69	0.73	0.73	0.75	0.77	0.77
107	0.81	0.78	0.80	0.81	-	0.85	0.83
136	-	0.87	-	0.89	0.90	0.92	0.90
161	0.93	0.92	-	-	-	-	-

9.8.2 Polysiloxanes : Unfilled and Filled

Because such a large number of measurements, of relatively low accuracy, was made for these systems, data for the construction of one sorption curve or pair of conjugate curves only are presented here for each system.

TABLE 9-45

DMS (I) - H_2O (26.3°C)

ℓ = 0.198 V = 0.344 1 μ g. = 1.24×10^{-3} cc.s.t.p.

B	M_∞	$t^{\frac{1}{2}}$	M_t/M_∞ (s)
3.1	41	2.4	0.21
		3.3	0.31
		4.7	0.44
		5.8	0.53
		6.7	0.59
		8.2	0.69
		9.5	0.76
		10.6	0.83
		13.5	0.92

TABLE 9-46

DMS (II) - H_2O (35.5°C)

ℓ = 0.203 V = 0.509 1 μg. ≡ 1.24×10^{-3} cc.s.t.p.

B	M_∞	$t^{\frac{1}{2}}$	M_t/M_∞ (s)	M_t/M_∞ (d)
9.0	88	2.4	0.20	0.30
		3.3	0.30	0.40
		4.7	0.43	0.51
		5.8	0.51	0.58
		6.7	0.57	0.64
		8.2	0.66	0.73
		9.5	0.74	0.79
		12.1	0.85	0.89
		14.2	0.92	0.94

TABLE 9-47

DMS (A) - H_2O (35.5°C)

ℓ = 0.206 V = 0.445 1 μg. ≡ 1.24×10^{-3} cc.s.t.p.

B	M_∞	$t^{\frac{1}{2}}$	M_t/M_∞ (s)
7.7	90	2.4	0.16
		3.3	0.25
		4.7	0.36
		5.8	0.43
		6.7	0.49
		8.2	0.58
		9.5	0.65
		12.1	0.76
		14.2	0.84

TABLE 9-48

DMS (C) - H_2O (35.6°C)

ℓ = 0.335 V = 0.671 1 μg. ≡ 1.24×10^{-3} cc.s.t.p.

B	M_∞	$t^{\frac{1}{2}}$	M_t/M_∞ (s)
-	25,000	30.0	0.042
		42.5	0.065
		52.0	0.080
		60.1	0.095
		73.4	0.119
		84.8	0.143
		104	0.187
		116	0.217

TABLE 9-49

DMS (D) - H_2O (35.7°C)

ℓ = 0.197 V = 0.306 1 μg. = 1.24×10^{-3} cc.s.t.p.

B	M_∞	$t^{\frac{1}{2}}$	M_t/M_∞ (s)	M_t/M_∞ (d)
2.8	104	10.6	0.40	0.36
		15.0	0.53	0.45
		18.4	0.62	0.54
		21.2	0.69	0.59
		26.0	0.78	0.68
		30.0	0.83	0.74
		36.7	0.88	0.80
		42.4	0.91	0.85
		52.0	0.93	0.90
		60.0	0.94	0.92

TABLE 9-50

DMS (E) - H_2O (35.7°C)

ℓ = 0.203 V = 0.310 1 μg. ≡ 1.24×10^{-3} cc.s.t.p.

B	M_∞	$t^{\frac{1}{2}}$	M_t/M_∞ (s)	M_t/M_∞ (d)
2.7	111	10.6	0.36	0.35
		15.0	0.50	0.45
		18.4	0.58	0.52
		21.2	0.65	0.58
		26.0	0.75	0.66
		30.0	0.81	0.72
		36.7	0.87	0.79
		42.4	0.91	0.83
		52.0	0.94	0.88
		60.0	0.95	0.91

TABLE 9-51

DMS (F) - H_2O (35.5°C)

ℓ = 0.196 V = 0.342 1 μg. ≡ 1.24×10^{-3} cc.s.t.p.

B	M_∞	$t^{\frac{1}{2}}$	M_t/M_∞ (s)	M_t/M_∞ (d)
3.0	124	10.6	0.36	0.33
		15.0	0.47	0.43
		18.4	0.56	0.51
		21.2	0.62	0.57
		26.0	0.71	0.65
		30.0	0.78	0.71
		36.7	0.85	0.78
		42.4	0.89	0.82
		52.0	0.92	0.87
		60.0	0.94	0.90

TABLE 9-52

PMS - H_2O (31.2°C)

ℓ = 0.172 V = 0.389 1 μg $\equiv$ 1.24×10^{-3} cc.s.t.p.

B	M_∞	$t^{\frac{1}{2}}$	M_t/M_∞ (s)	M_t/M_∞ (d)
5.4	69	2.4	0.16	0.31
		3.3	0.25	0.41
		4.7	0.38	0.52
		5.8	0.47	0.59
		6.7	0.54	0.66
		8.2	0.65	0.75
		9.6	-	0.82
		12.2	-	0.92
		14.3	-	0.96

TABLE 9-53

FMS - H_2O (30.1°C)

ℓ = 0.143 V = 0.347 1 μg. $\equiv$ 1.24×10^{-3} cc.s.t.p.

B	M_∞	$t^{\frac{1}{2}}$	M_t/M_∞ (s)	$t^{\frac{1}{2}}$	M_t/M_∞ (d)
3.3	64	2.4	0.11	2.4	0.12
		3.3	0.15	3.3	0.20
		4.7	0.23	4.7	0.29
		5.8	0.29	5.8	0.35
		6.7	0.34	6.7	0.39
		8.2	0.42	8.2	0.47
		9.5	0.49	9.5	0.54
		11.6	0.60	10.5	0.59
		13.5	0.69	12.9	0.69
		15.4	0.78	14.9	0.77
		17.2	0.84	18.3	0.88
		20.2	0.92	21.1	0.93

9.9 Sample Calculations

9.9.1 Equilibrium Sorption

The following examples illustrate how a point on an equilibrium sorption isotherm is calculated from primary experimental measurements.

i) Quartz Spiral :- The system PEMA-H_2O

Temperature (T_s) of sample = 49.5°C

Volume (V) of sample = 0.493 cm^3

Observed spiral extension ($\Delta h'$) = 0.106 cm.

Transducer output = 3.18 mv.

Spiral calibration (k) = 37.3 $cm.g.^{-1}$

Transducer calibration = 1.68 $(cm.Hg).mv.^{-1}$

Molecular weight of H_2O = 18.02

Saturation vapour pressure (p_o) of water at 49.5°C[129]

= 9.03 cm.Hg

Volume of quartz spiral + platinum support (V')

= 0.12 $cm.^3$

Density of water vapour per unit pressure at 49.5°C

= 8.98×10^{-6} $g.cm.^{-3}(cmHg)^{-1}$

Vapour pressure p = 1.68 x 3.18 = 5.34 cm.Hg

Buoyancy correction to be added = $8.98 \times 10^{-6} \times p \times (V+V')g.$

= $8.98 \times 10^{-6} \times p \times (V+V') \times k$

= $8.98 \times 10^{-6} \times 5.34 \times 0.61 \times 37.3$ cm.

= 0.001 cm.

Hence true extension $\Delta h = \Delta h' + 0.001 = 0.107$ cm.

Amount of water sorbed(Q) $= \frac{\Delta h \times 22400}{k \times 18.02}$

$= \frac{0.107 \times 22400}{37.3 \times 18.02}$

$= 3.58$ cc.s.t.p.

Concentration (c) of sorbed water $= Q/V = \frac{3.58}{0.493}$

$= 7.3$ cc.s.t.p. cm^{-3}

Relative humidity $p/p_o = \frac{5.34}{9.03} = 0.59$

Hence the isotherm point $(c, p/p_o)$ is (7.3, 0.59)

ii) Sartorius Balance :- The system DMS (II) - H_2O

Temperature (T_s) of sample = 35.5°C

Temperature (T_b) of balance head = 52°C

Volume (V) of sample = 0.509 $cm.^3$

Observed weight increase (Δw) = 92 μg.

Transducer output = 2.03 mv.

Transducer calibration = 1.21 cm.Hg. $mv.^{-1}$

Molecular weight of H_2O = 18.02

Saturation vapour pressure (p_o) of water at

$35.5°C^{(129)} = 4.33$ cm.Hg.

Saturation vapour pressure ($(p_o)_b$) of water at

$52°C^{(129)} = 10.2$ cm.Hg.

Volume of platinum support for sample (V') = 0.004 cm^3

Volume of metal counterweight (V'') = 0.070 cm^3

Density of water vapour per unit pressure at 35.5°C

$= 9.40 \times 10^{-6}$ g. $cm.^{-3}(cm.Hg)^{-1}$

vapour pressure p = 1.21 x 2.03 = 2.46 cm.Hg

Buoyancy correction B to be added

$$= 9.40 \times p \times (V + V' - V'') = 9.40 \times 2.46 \times 0.443$$

$$= 10.3\ \mu g.$$

Relative vapour pressure at balance head

$$(p/p_o)_b = \frac{2.46}{10.2} = 0.24$$

From a pre-constructed isotherm (Figure 5-6), the blank correction B' to be added, which corresponds to 0.24 relative humidity = 11.2 μ g.

Hence total amount Q of water sorbed = $\Delta w + B + B'$

$$= 92 + 10.3 + 11.2 = 113\ \mu g.$$

$$= \frac{113 \times 10^{-6} \times 22400}{18.02} = 0.140 \text{ cc.s.t.p.}$$

Concentration (c) of sorbed water = $Q/V = \frac{0.140}{0.509}$

$$= 0.27 \text{ cc.s.t.p. cm.}^{-3}$$

Relative humidity $p/p_o = \frac{2.46}{4.33} = 0.57$

Hence the isotherm point $(c, p/p_o)$ is (0.27, 0.57)

9.9.2 Steady State Permeability

The following example illustrates how a point on a graph J_ℓ^g vs. p/p_o is calculated from primary experimental measurements.

The system DMS (E) - H_2O

Temperature of sample = 50.2°C

Temperature of water reservoir = 39.7°C

Membrane thickness (ℓ) = 0.204 cm.

Area of membrane (A) = 2.27 cm^2

Time of run = 24 h.

Spiral extension ($\Delta h'$) = 0.397 cm.

Spiral calibration (k) = 32.7 $cm.g.^{-1}$

Saturation vapour pressure (p_o) of water at

50.2°C (129) = 9.34 cm.Hg.

Saturation vapour pressure of water at

39.7°C (129) = 5.44 cm.Hg.

Calibrated change of length of spiral with

temperature = -0.0046 $cm.deg.^{-1}$

Initial room temperature = 20.8°C

Final room temperature = 22.1°C

Temperature correction to spiral extension

= -0.0046(20.8-22.1) = +1.3 x 0.0046 = 0.006 cm.

$\therefore$ Total extension $\Delta h = \Delta h' + 0.006 = 0.403$ cm.

Hence total amount of permeated water $Q = \frac{\Delta h \times 22400}{k \times 18.02}$

$= \frac{0.403 \times 22400}{32.7 \times 18.02} = 15.3$ cc.s.t.p.

Permeation rate $J = Q/At = \frac{15.3}{2.27 \times 24 \times 60 \times 60}$

$= 7.81 \times 10^{-5}$ cc.s.t.p. $cm.^{-2}$ $sec.^{-1}$

and $J\ell = 7.81 \times 10^{-5} \times 0.204 = 15.9 \times 10^{-6}$ cc.s.t.p.
cm. cm.$^{-2}$ sec.$^{-1}$

Ingoing vapour pressure p = s.v.p. at 39.7°C
= 5.44 cm.Hg.

Relative humidity $p/p_o = 5.44/9.34 = 0.58$

Hence the ($J\ell$, p/p_o) point is (15.9×10^{-6}, 0.58)

9.9.3 Sorption and Desorption Kinetics

A point on a reduced curve is calculated for each time t (sec.) by calculating the amount of water (or methanol) taken up by the polymer as a weight (M_t μg.) or spiral extension (E_t cm.) as shown in part 9.9.1 of this section (including the buoyancy but excluding the blank correction). The corresponding amounts M_∞ or E_∞ at equilibrium are likewise calculated, and with a knowledge of the membrane thickness (ℓ cm.) the required experimental point (M_t/M_∞ , $t^{\frac{1}{2}}/\ell$) or (E_t/E_∞ , $t^{\frac{1}{2}}/\ell$) is then obtained.

REFERENCES

1) "Diffusion in Polymers", J. Crank and G.S. Park eds., Academic Press (1968)

2) Rogers:- chapter 6 in "Physics and Chemistry of the Organic Solid State", D. Fox, M.M. Labes and A. Weissberger eds., Interscience, (1965).

3) Rogers:- chapter 9 in "Engineering Design for Plastics", E. Baer ed., Reinhold, (1964).

4) van Amerongen:- Rubber Chem. Technol., 37, 1065, (1964).

5) Fujita:- Fortschr. Hochpolym.-Forsch, 3, 1, (1961).

6) Rogers:- chapter 15 in "Surface Coatings related to Paper and Wood", Syracuse University Press, (1967).

7) Michaels:- Offic. Dig. J. Paint Technol. Eng., 37, 638,(1965).

8) Fick:- Ann. Phys. (Leipzig), 170, 59, (1855).

9) Stannett:- op. cit. ref. 1, chapter 2.

10) Fujita:- op. cit. ref.1, chapter 3.

11) Barrie:- op. cit. ref. 1, chapter 8.

12) Crank and Park:- op. cit. ref. 1, chapter 1.

13) Barrer, Barrie and Raman:- Polymer, 3, 595, (1962).

14) Aitken and Barrer:- Trans. Far. Soc., 51, 116, (1955).

15) Meares:- "Polymers : Structure and Bulk Properties", Van Nostrand, (1965). Chapter 12.

16) Newns:- Ph.d. Thesis, Univ. of London, (1961).

17) Long and Thompson:- J. Poly. Sci., 15, 413, (1955).

18) Newns and Park:- paper presented at the International Symposium on Macromolecular Chemistry, Brussels, (1965).

19) Park:- op. cit. ref.1, chapter 5.

20) Frisch:- J. Poly. Sci. B, 3, 13, (1965).

21) Furuya:- J. Poly. Sci., 17, 145, (1955).

22) Barrer:- op. cit. ref.1, chapter 6.

23) Barrer, Barrie and Raman:- Polymer, 3, 605, (1962).

24) Rogers, Stannett and Szwarc:- Ind. Eng. Chem., 49, 1933, (1957).

25) Rogers:- J. Poly. Sci. C10, 93, (1965).

26) Drost-Hansen:- Adv. Chem. Series, 67, 70, (1967).

27) Kavanau:- "Water and Solute-Water Interactions", Holden-Day, Inc., (1964).

28) Bernal and Fowler:- J. Chem. Phys., 1, 515, (1933).

29) Danford and Levy:- J. Am. Chem. Soc., 84, 3965, (1962).

30) Frank and Quist:- J. Chem. Phys., 34, 604, (1961).

31) Nemethy and Scheraga:- J. Chem. Phys., 36, 3382, (1962).

32) Frank and Wen:- Disc. Far. Soc., 24, 133, (1957).

33) Falk and Kell:- Science, 154, 1013, (1966).

34) Drost-Hansen:- "Anomalies in the Properties of Water", paper presented at the First International Symposium on Water Desalination, Washington,(1965).

35) Kumins, Rolle and Roteman:- J. Phys. Chem., 61, 1290, (1957).

36) Dorsey:- "Properties of Ordinary Water-Substance", Reinhold, (1950). p.54.

37) Asada and Onogi:- J. Coll. Sci., 18, 784, (1963).

38) Kawasaki and Sekita:- J. Poly. Sci. A, 2, 2437, (1964).

39) Hauser and McLaren:- Ind. Eng. Chem., 40, 112, (1948).

40) Myers, Meyer, Rogers, Stannett and Szwarc:- Tappi, 44, 58, (1961).

41) Meares:- European Poly. J., 2, 241, (1966).

42) Yasuda and Stannett:- J. Poly. Sci., 57, 907, (1962).

43) Barrie and Platt:- Polymer, 4, 303, (1963).

44) Brunauer:- "The Physical Adsorption of Gases and Vapours", Oxford University Press, (1945).

45) Lowry and Kohman:- J. Phys. Chem., 31, 23, (1927).

46) Taylor, Herrmann and Kemp:- Ind. Eng. Chem., 28, 1255, (1936).

47) Taylor and Kemp:- Ind. Eng. Chem., 30, 409, (1938).

48) Kishimoto, Maekawa and Fujita:- Bull. Soc. Chem. Japan, 33, 988, (1960).

49) Stannett and Williams:- J. Poly. Sci. C10, 45, (1965).

50) Barrer and Barrie:- J. Poly. Sci., 28, 377, (1958).

51) Wellons and Stannett:- J. Poly. Sci. A-1, 4, 593, (1966).

52) Wellons, Williams and Stannett:- J. Poly. Sci. A-1, 5, 1341, (1967).

53) Zimm:- J. Chem. Phys., 21, 934, (1953).

54) Zimm and Lundberg:- J. Phys. Chem., 6, 425, (1956).

55) Day:- Trans. Far. Soc., 59, 1218, (1963).

56) Vieth:- Kolloid-Zeit., 152, 36, (1957).

57) Gordon, Hope, Lean and Roe:- Proc. Roy. Soc., A258, 215, (1960).

58) Masterton and Gendrano:- J. Phys. Chem., 70, 2895,(1966).

59) Barrie:- J. Poly. Sci. A-1, 4, 3081, (1966).

60) Caldwell and Babb:- J. Phys. Chem., 59, 1113, (1955).

61) Starkweather:- J. Poly. Sci. B, 1, 133, (1963).

62) Rouse:- J. Am. Chem. Soc., 69, 1068, (1947).

63) Crank:- "The Mathematics of Diffusion", Oxford University Press, (1956). Chapter 11.

64) Hartley and Crank:- Trans. Far. Soc., 45, 801, (1949).

65) Bearman:- J. Phys. Chem., 65, 1961, (1961).

66) Mills:- J. Phys. Chem., 67, 600, (1963).

67) Crank:- op. cit. ref.63, chapter 4.

68) Daynes:- Proc. Roy. Soc., A97, 286, (1920).

69) Frisch:- J. Phys. Chem., 61, 93, (1957).

70) Rogers, Buritz and Alpert:- J. Appl. Phys., 25, 868, (1954).

71) Crank:- op. cit. ref. 63, chapter 10.

72) Ash, Baker and Barrer:- Proc. Roy. Soc., A304, 407, (1968).

73) Meares:- J. Appl. Poly. Sci., 9, 917, (1965).

74) Zhurkoff and Ryskin:- J. Tech. Phys. U.S.S.R., 24, 797, (1954).

75) Frensdorff:- J. Poly. Sci. A, 2, 341, (1964).

76) Crank and Park:- Trans. Far. Soc., 45, 240, (1949).

77) Crank:- Trans. Far. Soc., 51, 1632, (1955).

78) Kishimoto and Enda:- J. Poly. Sci. A, 1, 1799, (1963).

79) Lin Hwang:- J. Chem. Phys., 20, 1320, (1952).

80) Prager:- J. Chem. Phys., 19, 537, (1951).

81) Tyrrell:- "Diffusion and Heat Flow in Liquids", Butterworths, (1961). P.126.

82) Grun:- Experimentia, 3, 491, (1947).

83) Glasstone, Laidler and Eyring:- "The Theory of Rate Processes", McGraw-Hill, (1941).

84) Barrer:- Trans. Far. Soc., 39, 237, (1943).

85) Barrer:- J. Phys. Chem., 61, 178, (1957).

86) Kumins and Kwei:- op. cit. ref. 1, chapter 4.

87) Flory:- J. Chem. Phys., 10, 51, (1942).

88) Huggins:- Ann. N.Y. Acad. Sci., 43, 1, (1942).

89) Orr:- Trans. Far. Soc., 40, 320, (1944).

90) Guggenheim:- Proc. Roy. Soc., A183, 203, (1944).

91) Flory:- "Principles of Polymer Chemistry", Cornell,(1953). Chapter 12.

92) Flory and Rehner:- J. Chem. Phys., 11, 521, (1943).

93) Wilkens and Long:- Trans. Far. Soc., 53, 1146, (1957).

94) Crank:- op. cit. ref. 63, chapter 8.

95) Fujita:- Text. Res. J., 22, 195, 282, 823, (1952).

96) Flory:- op. cit. ref. 91, chapter 9.

97) Barrer and Skirrow:- J. Poly. Sci., 3, 549, (1948).

98) Standing, Warwicker and Willis:- J. Text. Inst., 38, T335, (1948).

99) Gordon and Scantlebury:- Trans. Far. Soc., 60, 604, (1964).

100) Michaels:- Ind. Eng. Chem., 57, 32, (1965)

101) Daynes:- Trans. Far. Soc., 33, 531, (1937).

102) Pethica:- Disc. Far. Soc., 21, 139, (1956).

103) Kuppers and Reid:- J. Appl. Poly. Sci., 4, 124, (1960)

104) Blanchard and Parkinson:- Ind. Eng. Chem., 44, 799,(1952).

105) Bueche:- J. Poly. Sci., 25, 139, (1957).

106) Warrick and Lauterbur:- End. Eng. Chem., 47, 486, (1955).

107) Barrer, Barrie and Rogers:- J. Poly. Sci. A, 1, 2665,(1963).

108) Barrer and Chio:- J. Poly. Sci. C10, 111, (1965).

109) Maxwell:- "Treatise on Electricity and Magnetism", Vol.1, Oxford University Press, (1873). p. 365.

110) Rayleigh: Phil. Mag., 34, 481, (1892).

111) Fricke:- Physics, 1, 106, (1931).

112) Runge:- Z. Tech. Phys., 6, 61, (1925).

113) Meredith and Tobias:- J. Appl. Phys., 32, 1271, (1960).

114) Nielsen:- J. Macromol. Sci., A1, 929, (1967).

115) Tester:- J. Poly. Sci., 19, 535, (1956).

116) Briggs, Edwards and Storey:- Rubber Chem. Technol., 36, 261, (1963).

117) Newns:- J. Text. Inst., 41, T269, (1950).

118) Wendisch and Plumer:- Plaste Kaut., 11, 654, (1966).

119) Barrie and Machin:- J. Appl. Poly. Sci. (paper accepted for publication).

120) Frank:- J. Phys. Chem. 33, 970, (1929).

121) Barrett and Gauger:- J. Phys. Chem., 37, 47, (1933).

122) Barrie and Machin:- J. Poly. Sci. A-2, 5, 1300, (1967).

123) Kishimoto and Kitahara:- J. Poly. Sci. A-1, 5, 2147,(1967).

124) e.g. Barrer, Barrie and Slater:- J. Poly. Sci., 27, 177, (1958).

125) McHaffie and Lenher:- J. Chem. Soc., 127, 1559, (1925).

126) Thomas and Williams:- Quart. Rev., 19, 231, (1965).

127) McBain and Bakr:- J. Am. Chem. Soc., 48, 690, (1926).

128) e.g. Day:- J. Sci. Instr., 3, 260, (1953).

129) Osborne and Meyers:- J. Res. Nat. Bur. Stand., 13, 1,(1934).

130) Stall:- Ind. Eng. Chem., 39, 517, (1947).

131) Bratt:- Ph.d. Thesis, Univ. of London, (1958).

132) e.g. Barrer:- Trans. Far. Soc., 35, 628, (1939).

133) Barrer, Barrie and Rogers:- Trans. Far. Soc., 58, 2473, (1962).

134) Michaels, Vieth and Barrie:- J. Appl. Phys., 34, 1, (1963).

135) Spirer:- Ministry of Aviation Contract PD/37/09/R1, "Permeability of Polymer Films to Water Vapour" Rept. No.3, (1964).

136) Krause, Gormley, Roman, Shetter and Watanabe:- J. Poly. Soi. A, 3, 3573, (1965).

137) Crank:- op. cit. ref.63, chapter 12.

138) Meares:- Trans. Far. Soc., 53, 101, (1957).

139) Kumins and Roteman:- J. Poly. Sci., 55, 683, (1961).

140) Freeman:- Adv. Sci., 60, 397, (1959).

141) Schneider, Dusablon, Spano, Hopfenberg and Votta:- J. Appl. Poly. Sci., 12, 527, (1968).

142) Alexopoulos, Barrie, Tye and Fredrickson:- Polymer, 9, 57, (1968).

143) Robb:- General Electric Int. Rept. No. 65-c-031, (1965).

144) "International Critical Tables", McGraw-Hill, (1928). Vol. 3, p.370.

145) Holliday:- Chem. Ind., 794, (1963).

146) Corte:- Consol. Paper Web., Trans. Cambridge Symp., 23, (1965).

147) Young and Crowell:- "Physical Adsorption of Gases", Butterworths, (1962). P.77-8.

7. K. H. Illers, *Makromol. Chem.*, **38**, 168 (1960).
8. E. Butta, V. Frosini, and P. L. Magagnini, *Chim. Ind.* (*Milan*), **46**, 209 (1964).

Mario Baccaredda
Enzo Butta
Vittorio Frosini
Silvano de Petris

Centro Nazionale di Chimica delle
Macromolecole del C.N.R., Sezione VI
Istituto di Chimica Industriale ed Applicata
dell'Università di Pisa
Pisa, Italy

Received February 1, 1967
Revised March 27, 1967

Concentration Dependence of the Time Lag for Diffusion

The permeation technique has been used extensively for measurement of the concentration dependence of vapor diffusion coefficients in polymer membranes. In this a pressure gradient is maintained across the membrane and the pressure on the outgoing side, which is usually effectively zero, obtained as a function of time until a steady state of flow has been established. From the slope of the linear portion of the plot the steady-state permeation rate is obtained and extrapolation back to the time axis gives an intercept L, the time lag for diffusion.[1,2]

To determine the concentration dependence of the diffusion coefficient D, the steady-state flux J per unit area and thickness of membrane is obtained as a function of the pressure on the ingoing side and the equilibrium sorption isotherm of the system is also measured. J as a function of the concentration C_1 in the ingoing face of the membrane follows and from Fick's law:

$$J = \int_0^{C_1} D dC \tag{1}$$

and

$$D_{C=C_1} = (dJ/dC)_{C=C_1} \tag{2}$$

so that the D versus C relationship may be determined.[3]

When D is a function of C only, Frisch[4] has shown that the dependence of the time lag L on the concentration is given by

$$L = \int_0^l x\, C(x)dx \Big/ \int_0^{C_1} D dC \tag{3}$$

$$= l^2 \int_0^{C_1} wD(w) \int_w^{C_1} D(u)du\,dw \Big/ \left\{\int_0^{C_1} D(u)du\right\}^2 \tag{4}$$

where l is the membrane thickness, $C(x)$ is the steady-state concentration at the point x, and u and w are dummy variables. When D is constant, eq. (4) reduces to $L = l^2/6D$. Thus if the D versus C or equivalent relationship is known from steady-state measurements then the variation of L with C may be predicted and compared with the observed dependence. For several vapor–polymer systems differences have been observed and are usually attributed to physical effects resulting in a time-dependent contribution to the diffusion coefficient which vanishes in the steady state.[5–8] It is the purpose of this communication to stress that when D varies with C, the relative variation of L with C over a finite concentration range is always considerably smaller than that of D with C. This is suggested by the form of eq. (4) in which D is always present as part of an integral. More specifically it has been shown[9,10] that when $\log \int_0^{ey} D(u)du$ is a convex function of y the time lag variation is governed by the inequality $1/6 \leqslant L(C_1) \int_0^{C_1} D(u)du/l^2C_1 \leqslant 1/2$. The smaller relative variation of L holds particularly when the diffusion coefficient decreases with increasing concentration and it is possible for the variation of L to be within experimental error even although D changes significantly with concentration. To illustrate this point the following calculations were made.

Several forms of the function $f(C)$ in the relation $D = D_{C=0}\, f(C)$ were chosen such that, in the range of C 0–10, the diffusion coefficient changed by an order of magnitude. The dependence of D and L on the concentration for the different forms of $f(C)$ are shown in Figures 1 and 2, respectively. The corresponding steady-state concentration distributions are shown in Figure 3. These results clearly illustrate that the relative variation of

L with C can be very much less than that of D. A comparison of curves E', D', and E, B of Figures 1 and 2 shows that it does not necessarily follow that the larger the departure of $D(C)$ from $D_{C=0}$ then the larger is the departure of $L(C)$ from $L_{C=0}$.

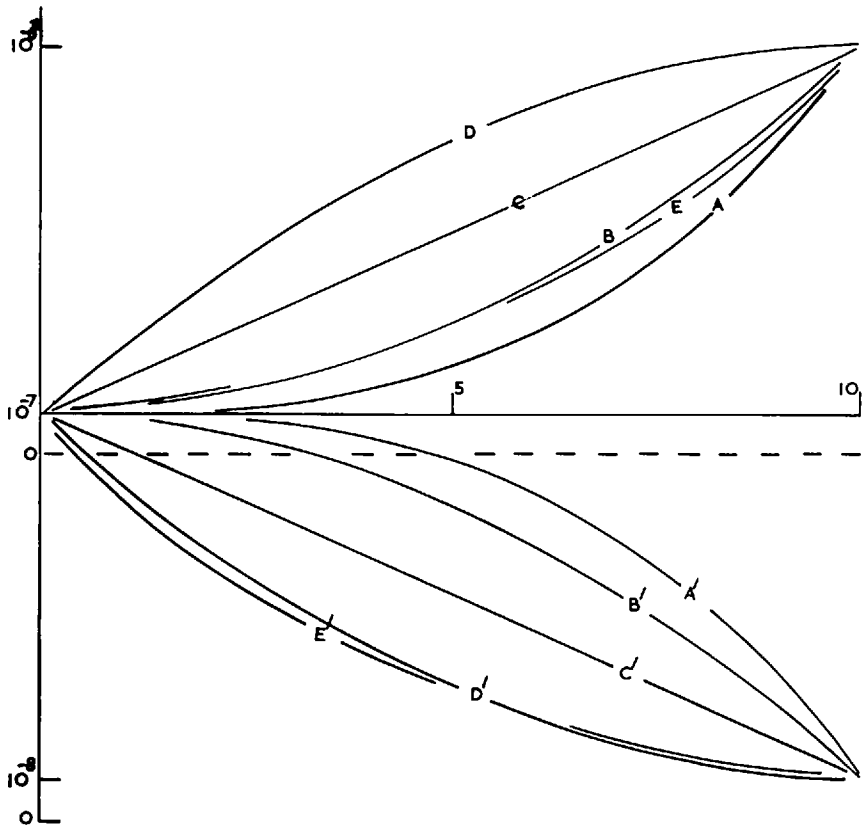

Fig. 1. D vs. C curves for various forms of $f(C)$: $(A)\ f(C) = 1 + 0.009C^2$; $(A')\ f(C) = 1 - 0.0009C^2$; $(B)\ f(C) = 1 + 0.09C^2$; $(B')\ f(C) = 1 - 0.009C^2$; $(C)\ f(C) = 1 + 0.9C$; $(C')\ f(C) = 1 - 0.09C$; $(D)\ f(C) = 1 + 1.8C - 0.09C^2$; $(D')\ f(C) = 1 - 0.18C + 0.009C^2$; $(E)\ f(C) = \exp\{0.2303C\}$; $(E')\ f(C) = \exp - \{0.2303C\}$. Ordinate: D, cm.^{2}/sec.; abscissa: C, arbitrary units. The dotted line represents the abscissa for curves (A)-(E).

In eq. (3) both the numerator and the denominator increase with concentration. The dominant factor in determining the concentration dependence of the time lag is the term $\int_0^{C_1} DdC$. For D increasing with C the percentage change in this term with C compared with the term $\int_0^{C_1} D_{C=0}dC$ is greater than that for a corresponding D which decreases with C (Fig. 1). When this term is similar (e.g., curves B and E of Fig. 1), then the difference in L–C relations is governed by the difference in the steady-state concentration profiles. On the basis of the term $\int_0^{C_1} DdC$ (Fig. 1), curve B may be expected to have the smaller

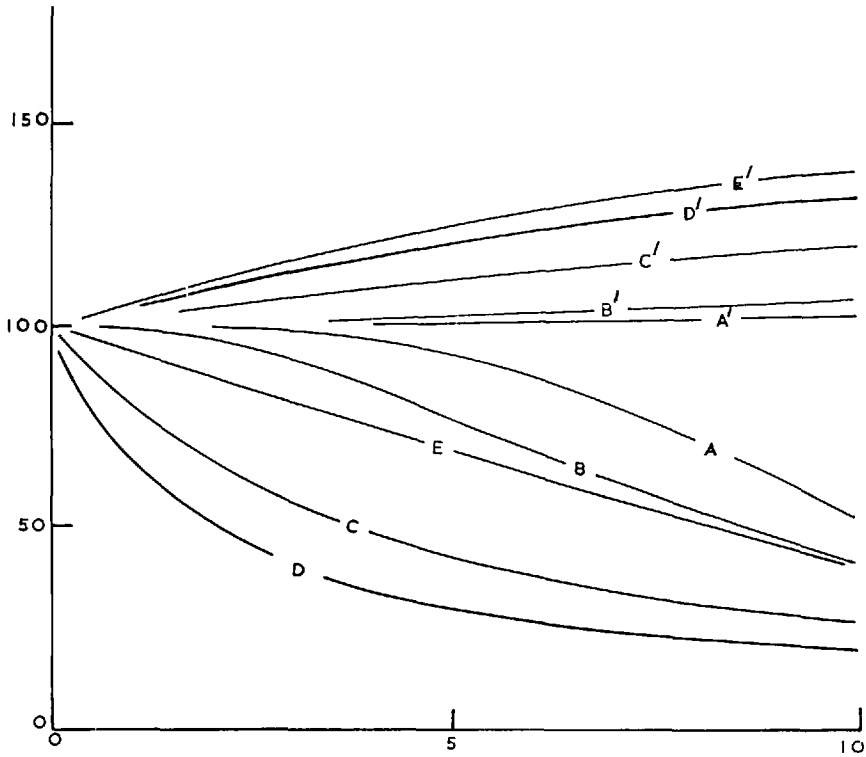

Fig. 2. L vs. C curves for various forms of $f(C)$. Ordinate: L, min.; abscissa: C units as in Figure 1. Membrane thickness = 0.06 cm. Labels as for Figure 1.

time lag, whereas Figure 2 shows the reverse is true. In this case the term $\int_0^l x\,C(x)dx$ (cf. Fig. 3) is larger for curve B than for curve E, and sufficiently so to counteract the effect of the denominator.

For an accurate comparison of steady-state and time-lag data it is necessary to know the D–C or equivalent relationship from zero concentration upwards with a high degree of precision. Usually D is measured as a function of C over a limited range of concentration followed by extrapolation to zero concentration which can introduce a not insignificant source of error unless measurements are made close to zero concentration. Similarly extrapolation of limited L–C date to give $L_{C=0}(=l^2/6D_{C=0})$ must also be treated with caution (e.g., curves A, C, and D of Fig. 2). More recently Ash et al. expressed eq. (3) in terms of permeation fluxes and solved for the L–C relation graphically.[11] This method has the advantage where accurate curve fitting of the J versus C_1 data is not possible, but, as before, extrapolation to zero concentration is necessary.

Finally, difficulties which may be encountered when comparing steady-state and time-lag data are illustrated with some examples taken from the literature. For several water–polymer systems it was found that the time lag was independent of concentration, suggesting that D was constant, whereas a steady-state analysis indicated that the diffusion coefficient decreased with concentration.[6–8] For example, by fitting a polynomial to the J–C_1 data of Stannett and Williams,[7] D was observed to decrease by a factor of $\sim$5 when the relative humidity increased from 0 to 0.85. From the Frisch equation it was calculated that the time lag should increase from 45 to 55.6 min. in this range. An arbi-

trary membrane thickness of 0.04 cm. was adopted in these calculations. The variation in L, although not large, should certainly be detectable. However, measurements with water vapor are complicated by sorption of the vapor on the glass walls of the apparatus. Although a procedure was adopted to minimize this effect it is questionable whether it was completely eliminated by the technique used.[7] Within experimental error the same J–C_1 data can be represented by a straight line up to a relative humidity of ~0.5. Because of the abrupt change in slope of the J–C_1 curve with this method of representation it was easier to use the graphical method[11] to calculate the L–C dependence. In this case the increase was from 58.2 to 60 min., which in practice would be difficult to detect. The

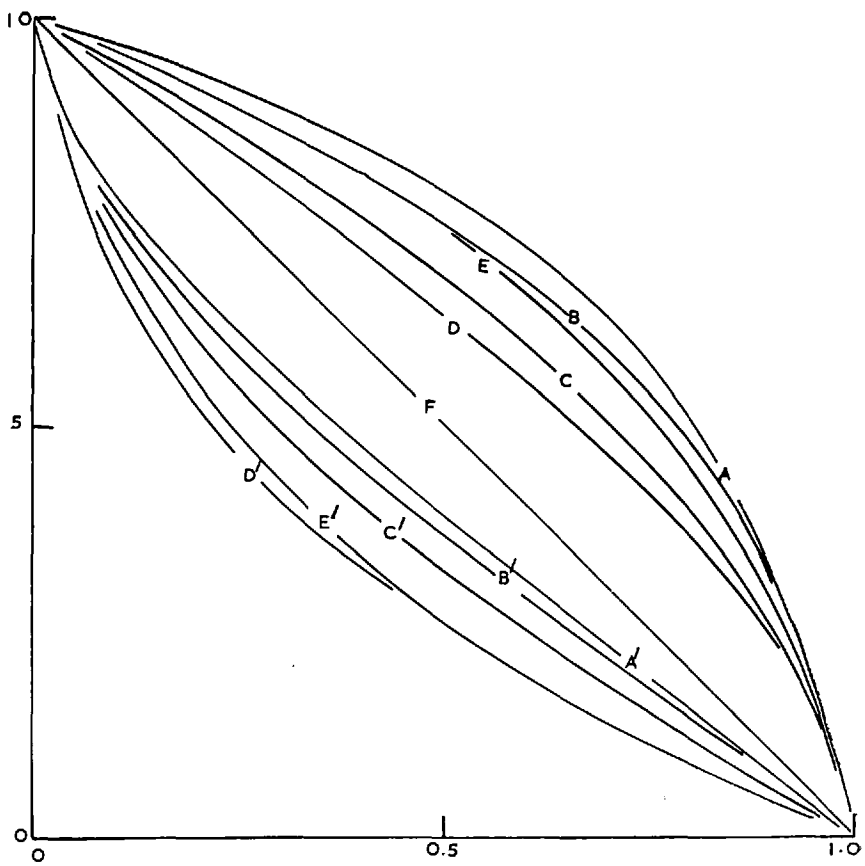

Fig. 3. Steady-state concentration profiles for various forms of $f(C)$. Ordinate: $C(x)$ units as in Figure 1; abscissa: x. Labels as for Figure 1. (F) constant D.

form of curve fitting can therefore be quite critical. However, it is perhaps unlikely that D should suddenly decrease at some nonzero concentration, and the polynomial method of representing the data is probably the better. A similar calculation with the water–rubber hydrochloride system[6] indicates that, in the relative humidity range of 0–0.8, D decreased by a factor of ~10 and the time lag should increase by about 30% (327 to 404 min. for a membrane thickness of 0.00622 cm.). A variation of this magnitude would seem to be outside experimental error even for water vapor time lags and it would appear for this system at least that a real discrepancy exists between steady-state and time-lag data.

In conclusion, for systems in which D decreases with C the variation of the time lag can be very much less than that of the diffusion coefficient. As a result the L–C dependence must be measured with an especially high degree of precision[9] if a successful comparison is to be made of steady-state and time-lag results.

This work is part of an investigation of water and similar vapors in polymer films. The paper is British Crown Copyright, reproduced with permission of the Controller, Her Britannic Majesty's Stationery Office.

References

1. H. Daynes, *Proc. Roy. Soc. (London)*, **A97**, 286 (1920).
2. R. M. Barrer, *Diffusion in and through Solids*, Cambridge Univ. Press, 1941.
3. P. E. Rouse, *J. Am. Chem. Soc.*, **69**, 1068 (1947).
4. H. L. Frisch, *J. Phys. Chem.*, **61**, 93 (1957).
5. R. M. Barrer and R. R. Ferguson, *Trans. Faraday Soc.*, **54**, 989 (1958).
6. H. Yasuda and V. Stannett, *J. Polymer Sci.*, **57**, 907 (1962).
7. V. Stannett and J. L. Williams, in *Transport Phenomena in Polymer Films* (*J. Polymer Sci. C*, **10**), C. A. Kumins, Ed., Interscience, New York, 1965, p. 45.
8. J. D. Wellons and V. Stannett, *J. Polymer Sci. A-1*, **4**, 593 (1966).
9. H. L. Frisch, *J. Phys. Chem.*, **62**, 401 (1958).
10. H. O. Pollak and H. L. Frisch, *J. Phys. Chem.*, **63**, 1022 (1959).
11. R. Ash, R. W. Baker, and R. M. Barrer, in press.

J. A. Barrie
D. Machin

Physical Chemistry Laboratories
Chemistry Department
Imperial College
London, England

Received February 21, 1967
Revised April 10, 1967